

Open Research Online

The Open University's repository of research publications
and other research outputs

Chromosome 1 Map, Sequence and Variation

Thesis

How to cite:

Gregory, Simon Gray (2003). Chromosome 1 Map, Sequence and Variation. PhD thesis The Open University.

For guidance on citations see [FAQs](#).

© 2003 Simon Gray Gregory

Version: Version of Record

Link(s) to article on publisher's website:

<http://dx.doi.org/doi:10.21954/ou.ro.0000f703>

Copyright and Moral Rights for the articles on this site are retained by the individual authors and/or other copyright owners. For more information on Open Research Online's data [policy](#) on reuse of materials please consult the policies page.

oro.open.ac.uk

**Chromosome 1 Map, Sequence
and Variation**

by

Simon Gray Gregory

**Thesis submitted for the
degree of Doctor of Philosophy**

The Open University

17th February 2003

The Wellcome Trust Sanger Institute

Wellcome Trust Genome Campus

Hinxton

Cambridge, UK

ProQuest Number: C813947

All rights reserved

INFORMATION TO ALL USERS

The quality of this reproduction is dependent upon the quality of the copy submitted.

In the unlikely event that the author did not send a complete manuscript and there are missing pages, these will be noted. Also, if material had to be removed, a note will indicate the deletion.



ProQuest C813947

Published by ProQuest LLC (2019). Copyright of the Dissertation is held by the Author.

All rights reserved.

This work is protected against unauthorized copying under Title 17, United States Code
Microform Edition © ProQuest LLC.

ProQuest LLC.
789 East Eisenhower Parkway
P.O. Box 1346
Ann Arbor, MI 48106 – 1346

*This thesis is dedicated to my wife, Deborah,
and my daughter, Olivia, for their unwavering
support, understanding, strength and love.*

*Also to my parents for their constant
encouragement and for instilling me
with a belief in my own abilities.*

Abstract

The construction of well characterised sequence-ready physical maps has been central to the generation of high quality genomic sequence by the Human Genome Project. The technological advances that made possible a clone based sequencing approach to large genomes have included the use of large insert bacterial clones and the development of high throughput fingerprinting techniques.

The first part of this thesis is devoted to development and application of these improvements in technology. The adaptation of fluorescent technologies and their application to existing fingerprinting methods described in this work has resulted in a fingerprinting technique which improves upon levels of data accuracy, increases throughput and incorporates of increased levels of safety and automation. The initial application of this and other restriction digest fingerprinting methods to the assembly of large insert P1-artificial chromosome clones (PACs) was also evaluated. PACs were used to construct a 1.4 Mb contig across a region of chromosome 13q12 that includes the breast cancer susceptibility gene *BRCA2*. These experimental and technical developments were then utilised within a hierarchical mapping strategy to construct a 13 Mb contig of human chromosome 1pcen – 1p13.

The finished sequence generated by the clone based sequencing strategy provides the basis for the elucidation of genic features and the motifs that influence their regulation within the human genome sequence. Detailed analysis of the finished genomic sequence from 1pcen – 1p13 is described. These analyses include the characterisation of base composition and

determination of repeat content within the region, as well as identification of known and novel genes by manual annotation.

The majority of differences between individuals can be attributed to allelic sequence variation. The characterisation of sequence differences and comprehension of how they may affect the expression and function of genes will be crucial for the study of molecular alterations in human disease. A subset of highly similar genes within 1pcen – 1p13, in addition to seven other genes of interest, were investigated by developing and assessing assays to determine sequence variation. The particular challenges of investigating gene families where sequences are nearly identical were explored, and enable better resolution of new and previously available data. The consequences that these sequence changes may have upon gene function is also discussed, and this provides an example of the ways in which knowledge of genomic sequence can be analysed to support new areas of structural and functional research.

Acknowledgements

I would like to thank my supervisor, David Bentley, for fulfilling a promise that he made more than 10 years ago, by seeing me through to the submission of my doctorate. I have appreciated your advice, friendship and tolerance, during not only my PhD but throughout our working relationship. I would also like to thank my second supervisor, Richard Wooster, for his guidance and many informal ‘thesis discussions’. Thanks are also extended to my long suffering office neighbour, Mark Ross, who has endured me barging into to his office with a multitude of questions and yet proffering an answer to *almost* every one.

Traditionally, a Sanger Institute PhD could not be completed without invaluable contributions from a multitude of individuals (all of whom I have aggravated at some stage). In particular, I wish to start by thanking Carol Scott for providing me with unflagging informatics support which extends beyond the work described in this thesis. I would also like to acknowledge Cordelia Langford, Nigel Carter, Laurent Baron, Andy Smith and Panos Deloukas for their help with the generation and assaying of the small insert library. Thanks to the awe-inspiring chromosome 1 sequencing team (Kirsten McLay, Becky Hall, Karen Barlow and the Sequencing Centre) for pushing my 1pcen – 1p13 clones through the sequencing pipeline and for carrying me on the C1 project! Assistance has also been gratefully received from Dave Beare, Stephen Keenan, James Gilbert, Jose Oliver and Jen Ashurst who helped me to analyse the 1pcen – 1p13 sequence. I have appreciated the help from Liz Sheridan, Jackie Bye and Liz Huckle with cDNA library screening and sequencing. Thanks also to the ExoSeq project (Andrew Bentley, Wilb Dunham, Sarah Hunt and Sarah Lindsay) for helping me to generate so much data so quickly. My thanks also go to Robert Steward, Jane Loveland and Tim Hubbard for opening my eyes to the wonderful world of proteins.

On a personal note, I would like to thank my many friends and colleagues at the Sanger whose help in large or small ways has made my molecular biological rites of passage more bearable. To Alison ‘Pod’ Coffey, Ian ‘Roo’ Barrett and Tamsin ‘Mate’ van de Ven thanks for all the proof reading, years of encouragement (Pod) and endless clichés to help me realise that I was *actually* making progress. To all the chromosome 1 mapping group members, past and present, many thanks for being a great bunch to work with and for allowing me to be a very ‘hands off’ group leader, particularly in the past 18 months. Thanks to Jane Rogers for your support, especially during the final stages of the thesis, and for accepting the same tired old excuses as to why the C1 project wasn’t progressing as quickly you’d hoped. Thanks Sean and Lisa for being good friends over the years. To Gareth, thanks for treading the long grass before me; without your calming influence, good humour and friendship I could have finished the thesis a lot earlier, but been the worse for it!

“He was calm; however, he had to be supported during the journey through the long corridors, since he planted his feet unsteadily, like a child who has just learned to walk, or as if he were about to fall through like a man who has dreamt that he is walking on water only to have a sudden doubt: but is this possible?” (Vladimir Nabokov; 1899–1977)

Thanks to my mother and father for equipping me with the tools to make this arduous journey and to my wife, Deborah, and daughter, Olivia, without whose confidence and support I would ever have arrived.

Table of Contents	page
Abstract	iii
Acknowledgements	v
Table of Contents	vii
List of Figures	xiii
List of Table	xvi
Glossary of Abbreviations	xviii
Publications	xxii
 Chapter 1: Introduction	 1
1.1 Mapping and sequencing model genomes	4
1.2 Mapping and sequencing the human genome	9
1.2.1 Cytogenetic mapping	9
1.2.2 Genetic mapping	11
1.2.3 Radiation hybrid mapping	12
1.2.4 Physical mapping	14
1.2.4.1 YAC Maps	14
1.2.4.2 Bacterial Clone Maps	15
1.3 Generating human genomic sequence	16
1.4 Interpreting the human genome landscape	18
1.4.1 Sequence composition	18
1.4.2 CpG island identification	19
1.4.3 Repeat content	20
1.5 Gene identification	21
1.6 Computational Genomics	25
1.6.1 <i>In silico</i> gene prediction	25
1.6.2 Sequence Analysis	27
1.7 Allelic variation	31
1.7.1 SNP discovery	32
1.7.2 Utilising SNPs	34
1.8 Chromosome 1	36
1.9 Aims of this thesis	41

Chapter 2: Materials and Methods	43
<u>Materials</u>	44
2.1 Chemical reagents	45
2.2 Enzymes and commercially prepared kits	45
2.3 Nucleotides	46
2.4 Solutions	46
2.4.1 Buffers	46
2.4.2 Electrophoresis and Filter preparation solutions	47
2.4.3 Media	48
2.4.4 DNA labelling and hybridisation solutions	49
2.4.5 General DNA preparation solutions	49
2.5 Size markers	50
2.6 Hybridisation membranes and X-ray and photographic film	50
2.7 Sources of genomic DNA	50
2.8 Bacterial clone libraries	51
2.8.1 Cosmid libraries	51
2.8.2 PAC and BAC libraries	51
2.8.3 cDNA libraries	51
2.9 Primer sequences	52
2.10 World Wide Web addresses	56
<u>Methods</u>	57
2.11 Isolation of bacterial clone DNA	57
2.11.1 Miniprep of cosmid	57
2.11.2 Microprep of cosmid, PAC and BAC DNA for restriction digest fingerprinting	58
2.11.3 Filterprep of PAC and BAC DNA for restriction digest fingerprinting	59
2.12 Bacterial clone fingerprinting	60
2.12.1 Radioactive fingerprinting	60
2.12.2 Fluorescent fingerprinting	61
2.12.3 <i>Hind</i> III fingerprinting	62

2.13	Marker preparation	63
	2.13.1 Radioactive fingerprinting	63
	2.13.2 Fluorescent fingerprinting	63
	2.13.3 <i>Hind</i> III fingerprinting	63
2.14	Gel preparation and electrophoresis	64
	2.14.1 Agarose gel preparation and electrophoresis	64
	2.14.2 Gel preparation and electrophoresis for radioactive fingerprinting	64
2.15	Construction of small insert library	65
	2.15.1 Library preparation	65
	2.15.2 Electroporation and library plating	65
2.16	Applications using the polymerase chain reaction	66
	2.16.1 Primer design	66
	2.16.2 Oligonucleotide preparation	66
	2.16.3 Amplification of genomic DNA by PCR	67
2.17	Radiolabelling of DNA probes	67
	2.17.1 Radiolabelling of PCR products	67
	2.17.2 Pre-reassociation of radiolabelled probes	68
2.18	Hybridisation of radiolabelled DNA probes	68
	2.18.1 Hybridisation of DNA probes derived from STSs	68
	2.18.2 Stripping radiolabelled probes from hybridisation filters	68
2.19	Restriction endonuclease digestion of cosmid DNA	69
2.20	Clone library screening	69
	2.20.1 cDNA library screening by PCR	69
	2.20.2 Vectorscreen PCR on cDNA	69
2.21	Exon Amplification	71
2.22	Mapping and sequence analysis software and databases	71
	2.22.1 IMAGE	71
	2.22.2 FPC	72
	2.22.3 1ace	73
	2.22.4 BLIXEM	74
	2.22.5 RepeatMasker	74

Chapter 3: Using large insert clones to construct contigs:**The development of fluorescent fingerprinting**

3.1	Introduction	76
3.2	Large insert clones	78
	3.2.1 Application of large insert clones to restriction enzyme fingerprinting	78
	3.2.2 Validation of PAC inserts	80
3.3	Fluorescent fingerprinting	84
	3.3.1 Fluorescent labelling of cosmid and lambda DNA	85
	3.3.2 Residual dye removal	87
	3.3.3 First position labelling	90
	3.3.4 One step reaction	92
	3.3.5 DNA prep modifications	94
	3.3.6 New size standard	96
	3.3.7 Data collection and processing	99
	3.3.8 Reproducibility	99
	3.3.9 Validation of fluorescent fingerprinting	101
3.4	Discussion	105

Chapter 4: Construction of a sequence-ready bacterial clone contig of 1pcen – 1p13 **108**

4.1	Introduction	109
4.2	Construction of sequence-ready map of 1pcen – 1p13	110
	4.2.1 Small insert library construction	112
	4.2.2 Hybrid mapping of SIL markers	115
	4.2.3 Bacterial clone contig construction	116
4.3	Evaluation of SIL marker distribution in chromosome 1	123
4.4	Comparisons of Published Maps	126
	4.4.1 Physical maps	126

4.4.2	Genetic map	127
4.4.3	Radiation hybrid map	128
4.4.4	A comparison of three maps	129
4.5	Discussion	131
Chapter 5: Sequence analysis of 1pcen – 1p13.2		134
5.1	Introduction	136
5.2	Sequence Composition Analysis	137
5.2.1	G-Banding	137
5.2.2	Isochores	140
5.2.3	Repeats	142
5.2.4	Low copy repeats	144
5.2.5	CpG Islands	148
5.2.6	Eponine	149
5.3	Gene Identification	149
5.3.1	Known genes	151
5.3.2	Novel genes	154
5.3.2.1	<i>Splicing ESTs support the structure of a gene</i>	159
5.3.2.2	<i>mRNA support of novel coding features</i>	162
5.3.3	Novel transcripts	165
5.3.4	Pseudogenes	166
5.4	Gene assessment	168
5.4.1	Alternative splicing	171
5.4.2	Genic features	173
5.4.2.1	<i>Putative bidirectional promoters</i>	174
5.4.2.2	<i>Overlapping genes</i>	175
5.5	Inferring function by protein homology	176
5.5.1	Identifying function through sequence homology	177
5.5.2	Identifying function by structural homology	179
5.6	Discussion	182
5.7	Appendix	187

Chapter 6: The identification and analysis of single nucleotide polymorphisms	192
6.1 Introduction	193
6.2 Gene Annotation	195
6.3 Identifying SNPs within Gene Families	195
6.4 Primer Design	199
6.5 DNA screening	201
6.6 Sequence Generation and Assembly	209
6.7 Exon coverage of sequence contigs	210
6.7.1 Validation and localisation of known SNPs	213
6.7.2 Identification of novel SNPs	215
6.8 SNP Analysis	216
6.8.1 Validating SNPs within highly homologous genes	217
6.8.2 Validating SNPs	219
6.8.2.1 <i>Known</i>	219
6.8.2.2 <i>Novel</i>	220
6.8.2.3 <i>Suspect candidate SNPs</i>	221
6.8.2.4 <i>Rejected candidate SNPs</i>	224
6.8.3 Effect of Sequence variation upon gene structure	225
6.9 Discussion	229
Chapter 7: Discussion	233
7.1 Genome Mapping and Sequencing	234
7.2 The determination of coding features	240
7.3 Assigning gene function	241
7.4 Sequence variation	245
7.5 Conclusion and future work	246
Chapter 8: References	250

List of figures:

Chapter 1	Figure 1.1 A plot of the increase in complexity of genomic sequencing.	8
	Figure 1.2 The alignment of syntenic region between human and mouse chromosomes 1.	40
Chapter 2		
Figure 2.1:	Strategy for vectorette PCR screening of cDNA libraries.	71
Chapter 3		
Figure 3.1:	A representation of the mapping of BRCA2 region.	79
Figure 3.2:	An agarose gel fingerprint of large insert bacterial clones in IMAGE.	82
Figure 3.3:	A comparison of <i>Hind</i> III fingerprint fragments and genomic sequence for the BRCA2 contig.	83
Figure 3.4:	The result of the first fluorescent fingerprinting experiment.	86
Figure 3.5:	Fluorescent fingerprint data collection using an extended run time.	87
Figure 3.6:	A comparison of labelled fragments when investigating removal.	89
Figure 3.7:	Labelling with spectrally distinct fluorophores.	91
Figure 3.8:	Testing one-step labelling.	93
Figure 3.9:	Testing one-step labelling and DNA prep protocols.	95
Figure 3.10:	A comparison of labelled lambda digest fragments using <i>Sau</i> 3A I, <i>Bsa</i> I and <i>Taq</i> α 1 restriction enzymes.	98
Figure 3.11:	An FPC display of band labelling uniformity.	100
Figure 3.12:	A comparison between fingerprinting methods of using 14 clones comprising a minimum tiling path.	103
Chapter 4		
Figure 4.1:	A representation of the two strategies used to construct a sequence-ready bacterial clone map of 1pc – 1p13.	111
Figure 4.2:	The construction of a chromosome 1 specific small insert library.	113
Figure 4.3:	Sequence length and frequency of SILs passing STS design stage.	115

Figure 4.4:	Generation of sequence ready bacterial coverage using the hierarchal strategy.	117
Figure 4.5:	The assimilation of PAC contigs into whole genome and chromosome specific fingerprint databases.	120
Figure 4.6:	A representation of PAC and BAC contig coverage of 1pcen – 1p13.	122
Figure 4.7:	Chromosomal distribution of flow sorted markers and comparison to of radiation hybrid and physical maps.	125
Figure 4.8:	The distribution of genetic mapped markers positioned within the 1pc – 1p13 contig by hybridisation.	128
Figure 4.9:	The distribution of radiation hybrid mapped markers positioned within the 1pc – 1p13 contig by hybridisation.	129
Figure 4.10:	A comparison of marker distribution between genetic, physical and radiation hybrid maps of 1pcen – 1p13.	130

Chapter 5

Figure 5.1	The genomic characterisation of human chromosome 1pc – 1p13.	141
Figure 5.2:	Low copy repeat detected within 1pc – 1p13.	146
Figure 5.3:	An ACeDB display of two annotated genes, including coding sequences, on opposite strands of DNA.	150
Figure 5.4:	Primer combinations used to validate putative gene structures.	155
Figure 5.5:	The annotation of a novel gene from <i>de novo</i> prediction and splicing EST alignment.	161
Figure 5.6:	The annotation of a novel gene from <i>de novo</i> prediction, splicing EST and homologous mRNA alignment.	164
Figure 5.7:	The characterisation of a processed pseudogene to 1p12, the original of which localised to 1p35.	167
Figure 5.8:	Incomplete polyA primed mRNA.	170
Figure 5.9:	Splice variants of adenosine monophosphate deaminase 2 (AMPD2).	173
Figure 5.10:	Genes in genomic context.	176
Figure 5.11:	Putative assignment of structure and function of a novel gene.	178
Figure 5.12:	Identification of putative functional domain of a novel protein.	181
Figure 5.13:	Generic structure of a gene.	185

Chapter 6

Figure 6.1:	An ACeDB display of GSTM 1 – 5 and a generic GSTM gene structure.	197
Figure 6.2	A genomic sequence alignment of GSTM 1 – 5:	232
Figure 6.3:	A CEPH pedigree.	202
Figure 6.4:	Screening of CEPH DNAs with exon specific primer pairs designed to GSTM4.	203
Figure 6.5	PCR products from exon primers using CEPH DNA as template.	206
Figure 6.6:	Assembly of <i>de novo</i> exon specific sequences shown in Gap4.	210
Figure 6.7:	A summary representation of the <i>de novo</i> sequence coverage of exons from the target genes.	211
Figure 6.8:	Identification of a known SNP which is within intron 3 of GSTM1.	214
Figure 6.9:	The identification of a known T/C SNP, dbSNP: 737497.	220
Figure 6.10:	A novel A/C SNP identified within intron 3 of GSTM2.	221
Figure 6.11	The alignment of GSTM 1 – 5 coding sequence.	223
Figure 6.12:	A 3-D representation within ICMLite of the homodimeric GST model, 3LJR.	227
Figure 6.13:	A vertical cross-sectional view of glutathione conjugating amino acid residues of 3LJR.	228

List of tables:**Chapter 1**

Table 1.1:	Comparison of G-bands and R-bands.	10
Table 1.2:	A comparison of marker content within genetic maps.	12
Table 1.3:	Genes in the human genome.	27
Table 1.4:	Prediction programs used to identify gene features.	27
Table 1.5:	Sequence queries available using BLAST alignment.	28
Table 1.6:	A list of the large scale comparative organisms sequencing projects.	30
Table 1.7:	SNP totals contained within or adjacent to coding features.	35
Table 1.8:	Diseases elucidated as a result of the Sanger Institute chromosome 1 mapping and sequencing project.	37
Table 1.9:	Disease loci mapping to 1pcen -1p13.	41

Chapter 2

Table 2.1:	Clones and appropriate antibiotics.	48
Table 2.2:	cDNA libraries used.	51
Table 2.3:	Vector-specific primer used in vectorette PCR.	52
Table 2.4:	STSs designed for cDNA screening and Link PCR product synthesis.	52
Table 2.5:	Exon specific primer pairs designed to pharmacogenomic gene targets.	54

Chapter 5

Table 5.1:	Fluorescence <i>in situ</i> hybridisation data of selected bacterial clones from 1pcen – p13.	138
Table 5.2:	The breakdown of repeat content within 1pcen – 1p13.2.	143
Table 5.3:	Known genes localising to 1pcen – 1p13.	152
Table 5.4:	cDNA primary pool and link PCR screening results.	156
Table 5.5:	Minimum tile path clones and accessions from the 1pcen – 1p13.2 contig (October 2002).	187
Table 5.6:	Primer pairs designed for the validation of predicted gene structures by cDNA library screening.	189

Chapter 6

Table 6.1:	A summary of the primers designed to the exons of 12 genes for the detection of coding polymorphisms.	200
Table 6.2:	A summary of the CEPH/Utah DNA used for the generation of exon sequence.	201
Table 6.3:	A summary of exon specific PCR reaction results using CEPH DNAs 1 – 8 as a template.	207
Table 6.4:	A summary of the known and novel SNPs associated with 12 target genes.	215
Table 6.5:	Expected occurrence of transitions and transversions in genomic sequence.	216
Table 6.6:	The observed number of transitions and transversions of known and novel SNPs within the 12 target genes.	216
Table 6.7:	Exonic SNP analysis.	217
Table 6.8:	Summary of categorised GSTM 1 – 5 SNPs.	218

Chapter 7

Table 7.1:	Organisms for which genome-wide fingerprint databases have or are being constructed.	240
------------	--	-----

Glossary of Abbreviations

1ace	1 chromosome version of ACeDB
ACeDB	<i>A. C. elegans</i> database
AMPD2	adenosone monophosphate deaminase 2
<i>Alu</i> -PCR	<i>Alu</i> -element-mediated polymerase chain reaction
ATP (dATP, ddATP)	adenosine 5'-triphosphate (deoxy-, dideoxy-)
BAC	bacterial artificial chromosome
BLAST	basic local alignment search tool
BLIXEM	BLAST In an X-windows Embedded Multiple Alignment
β-ME	β-mercaptoethanol
bp	base pair
BSA	bovine serum albumin
°C	degrees Celsius
CaM	calmodulin
cDNA	complementary deoxyribonucleic acid
chr	chromosome
CEPH	Centre d'Etude du Polymorphisme Humain
(c)M	(centi)Morgan
cm	centimetre
CDD	CONSERVED domain database
CpG	cytidyl phosphoguanosine dinucleotide
cR	centiRays
CTP (dCTP, ddCTP)	cytidine 5'-triphosphate (deoxy-, dideoxy-)
dbEST	database of expressed sequence tags
DNA	deoxyribonucleic acid
dNTP	2'-deoxyribonucleoside 5'-triphosphate
EDTA	ethylenediamine tetra-acetic acid
EMBL	European Molecular Biology Laboratory
EST	expressed sequence tag
FISH	fluorescence <i>in situ</i> hybridisation
FP	forward primer

FPC	FingerPrinted Contigs
g	gram
GDAP2	ganglioside-induced differentiation-associated protein 2
G banding	Geimsa banding
GDB	Genome Database
GSC	Genome Sequencing Centre, St Louis
GST (M)(T)(P)	glutathione S-transferase (mu) (theta) (pi)
GTP (dGTP, ddGTP)	guanine 5'-triphosphate (deoxy-, dideoxy-)
HapMap	haplotype block map
HGMP	Human Genome Mapping Resource Centre
HGNC	Human Genome Nomenclature Committee
HGP	Human Genome Project
H-W	Hardy-Weinberg
IHGSC	International Human Genome Sequencing Consortium
INSNPMWG	International SNP Map Working Group
kb	kilobase pairs
l	litre
LD	linkage disequilibrium
LINE	long interspersed nuclear element
LOH	loss of heterozygosity
M	molar
Mb	megabase pairs
MDS	myelodysplastic syndromes
μg	microgram
μl	microlitre
μM	micromolar
min(s)	minute(s)
mg	milligram
ml	millilitre
mm	millimetre
mM	millimolar
NCBI	National Centre for Biotechnology Information

NGFB	nerve growth factor – beta
NFE2L2	nuclear factor erythroid 2-like 2
NRAS	neuroblastoma RAS viral oncogene homolog
ng	nanogram
nm	nanometre
O/N	overnight
OD	optical density
OMIM	On-line Mendelian Inheritance in Man
ORF	open reading frame
PAC	P1-derived artificial chromosome
(e)PCR	(electronic) polymerase chain reaction
PDB	Protein Data Bank
PFAM	Protein Family
PFGE	pulsed-field gel electrophoresis
PNRC2	proline-rich nuclear receptor co-regulatory protein 2
poly(dT)	poly-deoxyribothymidyl oligonucleotide
R banding	Reverse Geimsa banding
RH	radiation hybrid
RFLP	restriction fragment length polymorphism
RNA (mRNA, rRNA, tRNA)	ribonucleic acid (messenger-, ribosomal-, transfer-)
RP	reverse primer
Rnase A	ribonuclease A
rpm	revolutions per minute
RT	room temperature
RT-PCR	reverse transcription polymerase chain reaction
SCL	stem cell leukaemia
SDS	sodium dodecyl sulphate
sec(s)	second(s)
seq	sequence
SIL	small insert library
SINE	short interspersed nuclear element
snoRNA	small nucleolar RNA

SNP	single nucleotide polymorphism
STS	sequence tagged site
TEMED	N,N,N',N'-tetramethylethylenediamine
TrEMBL	Translated EMBL
TSS	transcription start site
TSC	The SNP Consortium
TIGR	The Institute of Genome Research
Tris	tris(hydroxymethyl)aminomethane
U	unit
UCSC	University of California Santa Cruz
UNR	upstream of NRAS, gene
UTR	untranslated region
uv	ultraviolet
V	volt
v/v	volume/volume
VNTR	variable number of tandem repeats
W	watt
w/v	weight/volume
Wash U.	Washington University
WG(S)	whole genome (shotgun)
XLA	X-linked agammaglobulinaemia
YAC	yeast artificial chromosome

Publications:

Parts of the work presented in this thesis have appeared previously in the following publications which are bound at the back of this thesis:

Gregory, S.G., Howell, G.R. and Bentley, D.R. Genome Mapping by Fluorescent Fingerprinting. *Genome Research* (1997) 7: 1162-1168.

The International Human Genome Mapping Consortium. A physical map of the human genome *Nature*. 2001 Feb 15;409 (6822):934-41.

Bentley D.R., Deloukas P., Dunham A., French L., **Gregory S.G.**, Humphray S.J., Mungall A.J., Ross M.T., Carter N.P., Dunham I., *et al.* The physical maps for sequencing human chromosomes 1, 6, 9, 10, 13, 20 and X. *Nature*. 2001 Feb 15;409(6822):942-3.

Parts of the work presented in this thesis have appeared previously in the following publications which are not bound at the back of this thesis:

The International Human Genome Sequencing Consortium. Initial sequencing and analysis of the human genome. *Nature*. 2001 Feb 15;409, 860-921.

Chapter 1

Introduction

- 1.1 Mapping and sequencing model genomes**
- 1.2 Mapping and sequencing the human genome**
 - 1.2.1 Cytogenetic mapping
 - 1.2.2 Genetic mapping
 - 1.2.3 Radiation hybrid mapping
 - 1.2.4 Physical mapping
 - 1.2.4.1 YAC Maps*
 - 1.2.4.2 Bacterial Clone Maps*
- 1.3 Generating human genomic sequence**
- 1.4 Interpreting the human genome landscape**
 - 1.4.1 Sequence composition
 - 1.4.2 CpG island identification
 - 1.4.3 Repeat content
- 1.5 Gene identification**
- 1.6 Computational Genomics**
 - 1.6.1 *In silico* gene prediction
 - 1.6.2 Sequence Analysis
- 1.7 Allelic variation**
 - 1.7.1 SNP discovery
 - 1.7.2 Utilising SNPs
- 1.8 Chromosome 1**
- 1.9 Aims of this thesis**

In 1920, German botanist Hans Winkler first used the term 'genome', reputedly by the fusion of GENE and chromosOME, in order to describe the complex notion of the entire set of chromosomes and all the genes contained within an organism. A great deal of progress has since been made in the elucidation of the complex molecular interactions that underlie cellular functioning and the syntenic relationship between organisms at a nucleotide level.

The basis for these advances was the characterisation of the structure of DNA by Watson and Crick in 1953 (Watson *et al.*, 1953), and the realisation that DNA could be decoded to provide a guide to genetic inheritance. This underpinned the concept of genetics and gave scientists the possibility to explore and quantify the nature and extent of the biological information passed on from one generation to the next. The characterisation of biological inheritance permitted the elucidation of what it was that was being encoded and how it could determine biochemical function. Finally, extending from elucidation of the mechanisms behind inheritance of monogenic diseases, scientists are beginning to grasp how sequence is also involved in complex interactions, occasionally under the influence of environmental factors, to contribute to many (but still not all) diseases. Whilst the generation of the complete sequence of the human genome may provide the starting point for the characterisation of all human disease, clinical diagnosis and classification by specialists remains central to the appropriate treatment of individuals suffering genetic disease.

The speed at which the vast amount of human sequence data was generated can be attributed to the evolution of strategies and techniques developed to sequence organisms such, as bacteria (Kohara *et al.*, 1987), yeast (Olson *et al.*, 1986) and the nematode worm

(Coulson *et al.*, 1986). The availability of such an evolutionary diverse collection of sequences, with the addition of mouse (MGSC 2002) and other complex multi-cellular organisms, has also enabled comparisons to be made at a nucleotide level. These inter-species sequence comparisons, in conjunction with direct experimentation and computer based prediction programs, is facilitating the identification of evolutionarily conserved sequences, such as genes, and, to a lesser extent, the motifs that regulate them (Pennacchio *et al.*, 2001).

The elucidation of the molecular complexity of gene structure and determining their regulation is, however, only the first step in understanding the intricate networks in which genes interact. Though sequence analysis and homology matching may assist to define a gene on the nucleotide level, determining the structure of the gene's product, the protein, and its function, is a difficult paradigm to resolve. Whilst traditional methods, for example X-ray crystallography, are capable of characterising the structure of a protein their speed of application precludes them from large scale protein analysis. However, *in silico* modelling using previously determined domains or three dimensional structures may provide a means of inferring function and help characterise the networks in which they are involved (Skolnick *et al.*, 2000).

The identification of nucleotide differences (polymorphisms) between individuals, by comparison of high quality sequence, will assist our understanding of phenotypic variation. The localisation of single nucleotide polymorphisms (SNPs), particularly within functionally important sequences, such as genes, will contribute to our understanding of the aetiology and susceptibility to human disease and responsiveness to biochemical treatment. The identification of SNPs may also provide the opportunity to

partition the human genome into ancestral segments that have undergone minimal evolutionary recombination (haplotype blocks). Haplotype blocks, identified by linkage disequilibrium mapping, can then be used as a means of identifying multiple genes associated with complex phenotypes within unrelated individuals, where family-based studies are impossible because the complexity of the factors which contribute to the phenotype obscure any familial component. It is through approaches such as this that the true impact of the human genome sequence on human health and disease may bear the most fruit.

1.1 Mapping and sequencing model genomes

The first genomes that were characterised were relatively small by current standards, for example bacteriophage ϕ X174 (5 kb; Sanger *et al.*, 1977, Sanger *et al.*, 1978) and bacteriophage λ (48 kb; Sanger *et al.*, 1982), but they provided the underlying techniques and strategies that are being used for the more complex organisms currently being studied. Chain termination sequencing, developed by Sanger *et al* was a synthetic method, in which the nested sets of labelled fragments which constituted the sequence ladder were generated *in vitro* by a DNA polymerase reaction. The method was highly sensitive and robust. It was therefore amenable to biochemical optimisation to produce long, accurate sequence reads; and also to automation, which was necessary for large-scale application of the technique. In these respects it differed from the method of Maxam and Gilbert (1977), which necessitated production of all the labelled material prior to chemical degradation to form the sequence ladders of nested fragments. As a result, the synthetic method has remained the technique by which the majority of genomic sequence

from a variety of complex organisms is presently being generated, see figure 1.1. Neither method was capable of generating single reads of greater than 2-300 nucleotides, limited in part by the sequence ladder production itself, and partly by the ability to separate the sequence ladder by gel electrophoresis at single-base resolution (even today sequencing read-lengths approaching 1kb are rare). Assembly of larger tracts of DNA therefore required the development of methods to re-assemble a single sequence from multiple individual reads. Two approaches were adopted for this; first, the use of maps of restriction fragments, where multiple enzymes with sequence-specific cleavage activity are used, singly or in combination, to order and orientate segments of the sequence, which could be individually selected for sequencing; second, the use of the information gained from each individual sequence read to order and orient each segment relative to overlapping neighbours. This required the development of advanced computer programs to make the task possible on all but the smallest scale. In a further modification, the random shotgun strategy used by Anderson *et al.*, (1981a) to elucidate the mitochondrial genome involved using a random fragmentation process, by partial DNase I digestion (Anderson *et al.*, 1981b). This removed the dependence on sequence-specific restriction enzymes, while still relying on sequence-based assembly of contiguous tracts of overlapping reads.

The random shotgun approach provided the basis of the strategies used to assemble sequences of large inserts cloned in plasmids, lambda phage and cosmid vectors, and also the later bacterial artificial chromosome (BAC) and P1-derived artificial chromosome (PAC) clones. The same strategy was adopted to sequence the 1.8 Mb genome of the bacterium *Haemophilus influenzae* (*H. influenzae*) (Fleischmann *et al.*, 1995). Whilst the whole genome shotgun sequencing approach has proven itself to be a successful strategy

for the rapid assembly of smaller genomes, there are, however, doubts as to whether this strategy is suitable for assembling the sequence of complex organisms (as discussed in section 1.3).

The generation of a physical map, in which the genome is divided into bacterial clone units of 40 -200 kb and assembled into contiguous stretches (contigs) of overlapping clones, is a process analogous to the sequence contig assembly process. In contrast to sequence assembly, however, the information used to compare individual clones and identify overlaps, for the *C. elegans* (Coulson *et al.*, 1986) and *S. cerevisiae* (Olson *et al.*, 1986) genome projects, was a one-dimensional fingerprint, prepared by separating restriction fragments from a limited digest of each cloned DNA by electrophoresis. Overlaps between clones were detected on the basis of partially (or completely) shared fingerprint patterns. An alternative approach to identify overlapping relationships between clones was to test clones for the presence of characterised markers. Overlaps between clones could be identified on the basis that they shared a single copy sequence. The presence of the sequence was identified using a specific hybridisation probe or PCR assay.

Given a physical map of overlapping clones, individual clones can then be selected from the map to provide maximum genomic coverage with minimal redundancy. These clones permit specific regions to be targeted for further investigation, and in particular for determination of the complete DNA sequence separately from the other clones. Because the source of the genomic sequence is limited to an individual clone, problems encountered with sequence assemblies are greatly reduced compared to the corresponding whole genome assemblies.

At the time of their inception, the physical maps of the *Caenorhabditis elegans* (*C. elegans*) (Coulson *et al.*, 1986) and *Saccharomyces cerevisiae* (*S. cerevisiae*) (Olson *et al.*, 1986) genomes were constructed to enhance the molecular genetics of the respective organisms by facilitating the cloning of known genes and to serve as an archive for genomic information. However, the data associated with the construction of the clonal physical maps – even with good alignment to the genetic map – carried only a tiny proportion of information present within the genome. Consequently, a minimum tile path of the 30 kb cosmid and 15 kb lambda clones, used to build the physical maps of the *C. elegans* and *S. cerevisiae*, respectively, were subcloned into M13 phage vectors (1.3-2 kb insert size) and sequenced on a per clone basis. The physical maps of the two genomes, and subsequently of *Escherichia coli* (*E. coli*) (Kohara *et al.*, 1987), *Arabidopsis thaliana* (*A. thaliana*) (Arabidopsis Genome Initiative, The, 2000), *Drosophila melanogaster* (*D. melanogaster*) (Hoskins *et al.*, 2000) and human (McPherson *et al.*, 2000), used restriction enzyme fragments in various ways to overlap clonal units for the construction of genome wide physical maps.

For the *C. elegans* project, polyacrylamide gel electrophoresis was used to resolve DNA fragments that had been generated by digesting cosmid DNA with two restriction enzymes, *Hind* III and *Sau* 3AI. Restriction fragments, of which the *Hind* III ends had been labelled with a radioactive molecule, were then detected by exposure to autoradiograph film. Digitised cosmid specific ‘fingerprints’ were analysed by pair-wise comparison to establish contigs of overlapping bacterial clones within a seven fold genomic fingerprint data set (Coulson *et al.*, 1986). The mapping of *S. cerevisiae* used a similar contig construction strategy but alternatively, fingerprints were generated by a single restriction digest of lambda DNA and the clone fragments separated on an agarose

gel prior to reassembly into contigs (Olson *et al.*, 1986). Whilst both methods generated large tracts of genomic contig coverage, gaps remained in the physical maps. To compensate for the regions lacking cloned representation in the *C. elegans* map, fosmids, maintained as single copy within the host cell (Kim *et al.*, 1992), and large insert yeast artificial chromosome (YACs), (Burke *et al.*, 1987), were incorporated. Fosmids proved to be most useful generating bridging coverage in central, gene rich regions of chromosomes, whilst YACs tended to generate *de novo* map coverage on the more repeat-dense chromosome arms (A Coulson *pers comm.*).

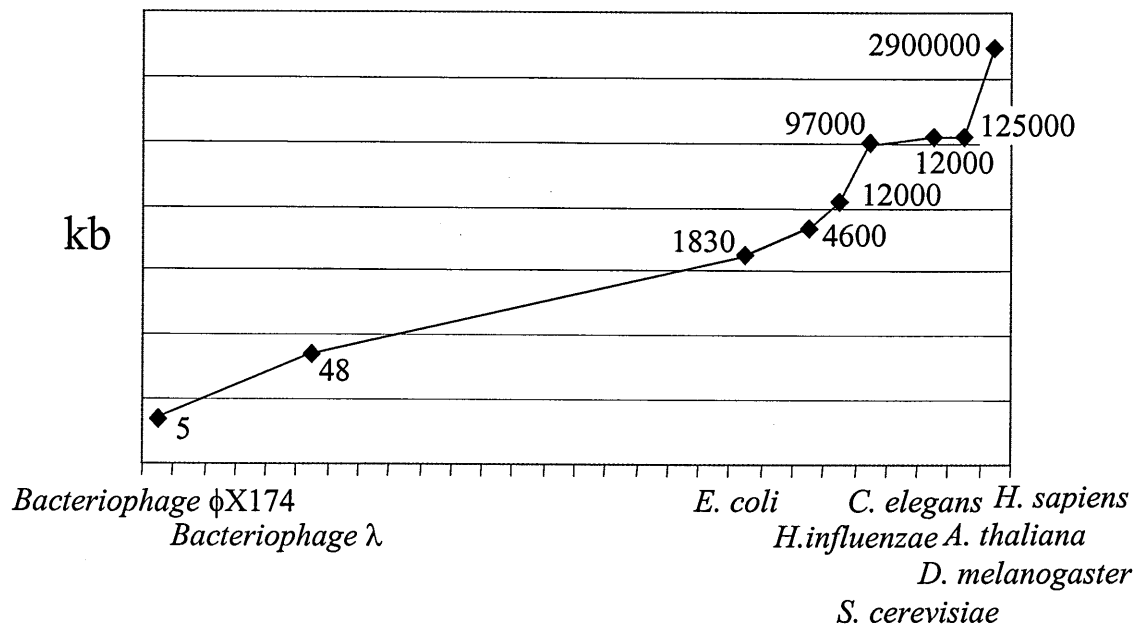


Figure 1.1 A plot of the near logarithmic increase in the complexity of genomic sequencing from the first full genomic sequence of Bacteriophage ϕ X174 in 1977 to the anticipated completion in the human genome in April 2003.

1.2 Mapping and sequencing the human genome

The human genome is contained within 22 autosomes (numbered from 1 – 22, largely according to size) and two sex chromosomes, X and Y (female XX and male XY).

Chromosomes are punctuated with centromere structures that are either located close to chromosome ends (acrocentric), towards a chromosome end (submetacentric) or centrally between ends (metacentric). The initial size estimate of the genome, 3200 Mb, was based largely upon cytometric measurements (Morton 1991) and has since been revised to 29000 Mb in light of the higher resolution human draft sequence analysis (IHGSC, 2001) supported by observed sizes of completed chromosome sequences, which suggested the earlier figures were over-estimates (Dunham *et al.*, 1999, Hattori *et al.*, 2000, Deloukas *et al.*, 2001). The construction of a map of the human genome was an important step towards understanding and characterising the sequence contained within it as it provided a means by which all the features could be ordered and partitioned, and the task of detailed characterisation and sequencing could be divided up into manageable segments.

1.2.1 Cytogenetic mapping

The treatment of metaphase chromosome spreads with trypsin digestion and Giemsa staining creates differential chromosome banding patterns. The generation of light (R-bands) and dark (G-bands) bands by Giemsa staining is reliant upon nucleotide content and the staining pattern therefore reflects the base composition and correlates other properties of the different regions (see table 1.1). However, the maximum genome-wide resolution was limited to an 850 banding pattern (Bickmore *et al.*, 1989). The recognition of characteristic banding patterns of chromosomal regions provided the basis for much of

the early characterisation of chromosome aberrations (duplications, deletions and translocations) which were associated with clinical phenotypes (Pinkel *et al.*, 1988, Tkachuk *et al.*, 1990, Dauwerse *et al.*, 1990).

The ability to hybridise labelled probes containing specific sequences and to detect their location on metaphase chromosome by autoradiographic or fluorescent detection techniques (fluorescence *in situ* hybridisation (FISH) (Pinkel *et al.*, 1986)) revolutionised cytogenetic mapping. Initially, the location of the probe relative to the metaphase banding pattern provided an approximate map position for the sequence represented by the probe. Pairs of markers, differentially labelled, could be simultaneously placed relative to the cytogenetic banding, and also ordered with respect to each other. The use of pairs of differentially labelled markers in combination with a third reference marker enabled FISH to be applied to chromosomal DNA in a less condensed state (in interphase nuclei). Although no banding pattern can be obtained in interphase DNA, the decondensed state of the chromatin relative to metaphase chromosomes means that increased levels of resolution could be obtained, as probes were better separated. An inter-probe distance of 1- 5 Mb can be resolved using metaphase FISH, 0.1 – 1.0 Mb by interphase FISH (Wilke *et al.*, 1994), and 5 kb by FISH using mechanical pre-treatment to extend DNA into fibres (Heiskanen *et al.*, 1994).

Table 1.1: Comparison of G-bands and R-bands

G-bands	R-bands
Dark staining Giemsa bands	Light Staining Giemsa bands
AT rich	GC rich
Late replicating	Early replicating
Early condensation	Late condensation
DNase insensitive	DNase sensitive
SINE poor, LINE rich	SINE rich, LINE poor
Gene poor	Gene rich
Less frequent recombination	More frequent recombination

Adapted from Bernardi (1989)

1.2.2 Genetic mapping

Genetics maps utilise the likelihood of recombination between adjacent markers during meiosis to calculate inter-marker genetic distances, and from this to infer a physical distance. The closer two landmarks are together on a chromosome, the less likelihood there is of a recombination event occurring between, with the opposite being true for markers that are further apart. The calculation of distance, and therefore the metric upon which the genetic map is based, is the length of the chromosomal segment that, on average, undergoes one exchange with a sister chromatid during meiosis, the Morgan (M). Therefore, a 1% recombination frequency is equivalent to 1 centimorgan (cM), and, since the human genome covers 3000 cM and contains approximately 30000 Mb, 1cM is approximately equivalent to 1 Mb. However, recombination is known to be non-random which can lead to a level of inaccuracy (Dib *et al.*, 1996) in inferring physical distances from measurements of genetic recombination.

The inherent limitation of primary genetic maps was the lack of availability of polymorphic markers between which genetic distances could be calculated. This was ameliorated in part by the suggested use of restriction fragment polymorphisms (RFLPs), identified by Kan and Dozy (1978), for the construction of a genome wide genetic linkage map (Botstein *et al.*, 1980). The first such map (Donis-Keller *et al.*, 1987) was limited in its usefulness, however, due to RFLPs having a maximum heterozygosity of 50% and the low level of resolution of the 403 characterised polymorphic markers, including 393 RFLPs, covering the genome. The identification of hypervariable regions, which showed multi-allelic variation (Wyman and White 1980), provided a new source of markers for genetic mapping. The variable regions contained short 11 to 60 bp variable

number tandem repeats which showed allelic variation. However, these minisatellite markers (Jeffreys *et al.*, 1985) and variable number tandem repeats (VNTRs) (Nakamura *et al.*, 1987) were shown to cluster at chromosome arms and were not inherently stable (Royle *et al.*, 1988). The identification of microsatellite markers (containing di-, tri- or tetra nucleotide repeats) greatly facilitated the generation of genetic maps. They were proven to be widely distributed throughout the genome, showed allelic variation (Litt and Luty 1989, Weber and May, 1989), were amenable to PCR amplification (Saiki *et al.*, 1988) by sequence-tagged-site screening (Olson *et al.*, 1989). In a relatively short period of time a number of genetic maps were published with increasing marker density and resolutions, culminating in the most recent deCODE genetic map which contains 5136 markers genotyped across 1257 meioses (Kong *et al.*, 2002), table 1.2.

Table 1.2: A comparison of marker content within genetic maps.

No. of Markers	Reference
100	Hudson <i>et al.</i> , 1992
813	Weissenbach <i>et al.</i> , 1992
2066	Gyapay <i>et al.</i> , 1994
5840	Murray <i>et al.</i> , 1994
5264	Dib <i>et al.</i> , 1996
5136	Kong <i>et al.</i> , 2002

1.2.3 Radiation hybrid mapping

The utilisation of somatic cell hybrids to maintain human genomic fragments, such as whole chromosomes or chromosomal regions, permits the generation of another form of mapping resource to be generated, the radiation hybrid map. The modification of a technique that fragmented human chromosomes by irradiation and which were then rescued by fusion to rodent cells (Goss and Harris 1975) prompted Cox *et al.*, (1990) to

propose that radiation hybrid (RH) mapping could be applied to the construction of long range maps of mammalian chromosomes.

The premise of the technique is similar to that of the genetic map, i.e. the more closely related two markers are related within the genome the less likelihood there is of a radiation induced break in between them in a reference panel of cell lines, and hence the less likely is their segregation to different chromosomal locations based on association of the markers to different sets of fragments. As the presence of two markers within a radiation fragment gives no indication to their physical distance a panel of radiation hybrids was required. By estimating the frequency of breakage, and thus the distance between two markers, it is possible to determine their order. The unit of map distance is the centiRay (cR) and represents 1% probability of breakage between two markers for given a radiation dose. Unlike the level of information garnered from a genetic marker, that may or may not be informative within a varying number of meioses, the radiation hybrid marker is either positive or negative for a DNA fragment, effectively digitising PCR results. Any amplifiable single copy sequence can therefore be placed in a radiation hybrid map. The radiation hybrid mapping technique has been used for the construction of high resolution gene maps (Schuler *et al.*, 1996, Deloukas *et al.*, 1998) and has also been used to supplement the construction of chromosome physical maps (Mungall *et al.*, 1996, Deloukas *et al.*, 2001, chapter 4).

1.2.4 Physical mapping

The generation of a physical map relies upon the construction of an ordered and orientated set of clone based contigs. The term “contig” was coined by Staden (Staden 1980) to refer to a contiguous set of overlapping segments which together represent a consensus region. These segments can be sequence, or clones, whose overlapping relationship is defined by information in common to each pair of overlapping segments. The overlaps are identified by performing a pair wise comparison of the dataset associated with each segment. Similarities that are statistically significant indicate the presence, and sometimes the extent, of overlap. Bacterial clone contigs are the most convenient route for the sequence generation of larger genomes. They presenting a means of coordinating physical mapping and, because of the way in which they are constructed, provide an optimal set of clones (the tile path) for sequencing.

1.2.4.1 YAC Maps

The main benefit of using YACs for the constructing of a physical map is that the insert size (up to 2 Mb) results in coverage of large regions of the genome with relatively few clones. Green and Olson (1990) utilised YACs to construct a physical map across the cystic fibrosis region on human chromosome 7 by overlapping YACs by STS content data. Chromosome specific (Chumakov *et al.*, 1992, Foote *et al.*, 1992) and genome wide YAC maps have also been published (Chumakov *et al.*, 1995, Hudson *et al.*, 1995). Though STS content mapping is the most frequent method used to generate YAC contigs, techniques such as repeat mediated fingerprinting, either by *Alu*-PCR (Coffey *et al.*, 1992) or by repeat content hybridisation (Cohen *et al.*, 1993), have also been used.

The advantages of using YACs are, however, offset by the relative difficulty of constructing YAC libraries and of analysing the cloned DNA, compared to the use of bacterial cloning systems. Many YAC clones have also been found to be chimeric, that is, to contain fragments derived from non-contiguous parts of genomic DNA being cloned (Green *et al.*, 1991, Bates *et al.*, 1992, Slim *et al.*, 1993). Rather than being used as a primary sequence resource, YACs became more generally used to support the construction of detailed landmark maps, and to underpin sequence ready bacterial clone maps (Collins *et al.*, 1995; Bouffard *et al.*, 1997). Recently, YACs have been used to facilitate gap closure in the bacterial clone maps by linking contigs (Coulson *et al.*, 1995). The links are identified by STS content mapping. In these cases the YACs have been sequenced directly.

1.2.4.2 Bacterial Clone Maps

In contrast to YACs, bacterial clone libraries are easier to make and the cloned DNA is more easily manipulated. Chimerism is low (Shizuya *et al.*, 1992, Ioannou *et al.*, 1994), and the supercoiled recombinant DNA can be purified readily from the host DNA. An important factor influencing the construction of bacterial clone contigs is the available genomic resources. Whilst the *C. elegans* and *S. cerevisiae* maps utilised total genomic 30 kb cosmid and 15 kb lambda libraries, in 7- and 5-fold coverage respectively, current bacterial clone contig construction utilises large insert P1-derived artificial chromosome (PAC) (Ioannou *et al.*, 1994) and bacterial artificial chromosome (BAC) (Shizuya *et al.*, 1992) libraries. Each BAC or PAC clone typically contains an insert of 100 – 300 kb and maps have been constructed from a >15 fold genomic clone coverage.

1.3 Generating human genomic sequence

The elucidation of the all genic and other features contained within the human genome is reliant upon the generation of high quality sequence. Two different strategies were adopted to produce human genomic sequence; the first, utilised by the International Human Genome Sequencing Consortium (IHGSC), is a hierarchical approach utilising bacterial clones from a well characterised sequence ready map as the basis for generating genomic sequence; the second strategy is a whole genome shotgun (WGS) approach, adopted by Celera, which relies upon the assembly of a consensus sequence from randomly derived genomic sequence reads (Venter *et al.*, 2001).

The IHGSC used an approach in which a sequence ready bacterial clone map was constructed by utilising high density panel of markers (15 markers / Mb) (Olson 1993, Bentley *et al.*, 2000) derived from genetic and radiation hybrid maps. Large insert bacterial clones, primarily PACs (Ioannou *et al.*, 1994) and BACs (Shizuya *et al.*, 1992), were identified by hybridisation and overlapped by restriction digest fingerprinting (Gregory *et al.*, 1997, Marra *et al.*, 1997), with STS content data (Olson *et al.*, 1989) supporting ambiguous overlaps. DNA generated from each one of a minimally overlapping set of clones from the physical map (tile path) was fragmented into 1.4 - 2.2 kb units, subcloned into M13 or plasmid vectors (Bankier *et al.*, 1987) and then sequenced by modified chain termination sequencing (see chapter 5). One of the benefits of generating sequence on a clone by clone basis is that if the consensus sequence generated by the shotgun phase is not contiguous, the bacterial clone from which the sequence was derived can be then used for directed finishing experiments. The production of finished sequence, which is >99.99% accurate and without the presence of

gaps, is one of the main differences between the WGS and hierarchical approaches.

Whilst the private WGS strategy was declared to be complete following the assembly of the shotgun sequence, the public hierarchical approach provided an initial draft covering 90% of the genome in 2000; and its production of highly accurate sequence, which will serve as a long-term reference, is now 87% done and due to be completed in April 2003. The results of the private WGS strategy were also announced in 2000 following the assembly of the shotgun sequence, incorporating a representative set of sequences from the public domain draft; however no subsequent finishing was undertaken on this product.

The elucidation of complete genomic sequence by the generation of whole genome shotgun data, as used by Celera, is a relatively simple approach that was first used for the characterisation of the mitochondrial genome (Anderson *et al.*, 1981). In 2001, Venter *et al.*, (2001) published their applied strategy to the elucidation of the human genome by assembling sequence data from complete inserts or ends of 1 – 2 kb and 50 kb subcloned plasmids, respectively, and by the incorporation of BAC end sequences. The publication of the human genome sequence in, on average, 100kb scaffolds proved that a considerable amount of human sequence could be generated and assembled in a relatively short period of time. However, some doubts remain as to the success of the approach as a sole means of assembling a complex genome (Waterston *et al.*, 2002, Myers *et al.*, 2002, Green *et al.*, 2002). Without the incorporation of the publicly available sequence data, and the inherent map information associated with it, highly repetitive motifs and low copy duplications introduce errors into the assembly of the sequence.

1.4 Interpreting the human genome landscape

The complete characterisation of the human genome will not be restricted to experimental or *in silico* identification of coding features and the elements affecting their expression. A full description of the long range sequence composition will be necessary to, amongst other things, facilitate an understanding of the coordinated regulation of genes, identify the underlying reasons for repeat mediated genomic rearrangements and to provide a basis for the identification of variation between populations.

1.4.1 Sequence composition

The human genome has previously been shown to contain considerable variation in its nucleotide composition. Separation of mammalian genomic DNA on caesium gradients indicated compositional heterogeneity (Thiery *et al.*, 1976) whilst fractionation of human DNA on $\text{Cs}_2\text{SO}_4\text{-Ag}^+$ gradients showed a broad range of GC based separation (Bernardi *et al.*, 1985). Regional partitioning of genomic sequence based on GC content can be used as a low resolution means of determining biological properties such as cytogenetic banding (Hurst and Eyre-Walker 2000), repeat composition and gene density (Zoubak *et al.*, 1996, Gardiner *et al.*, 1996) and structure (Oliver *et al.*, 1996). Analysis of the human draft sequence which, at the time of publication covered an estimated 94% of the genome, revealed GC content could vary by as much as 59.3% to 33%, from the genome average of 41%, within a 300 kb region (IHGSC, 2001). It was also estimated that 98% of large insert clones mapping to the darkest Giemsa staining bands contained below average GC content, whilst 80% of the clones mapping to light bands contained higher than average GC content.

The fractionation of human DNA on $\text{Cs}_2\text{SO}_4\text{-Ag}^+$ led Bernardi *et al.*, (1985) to suggest that DNA fractions could be classified based on their relatively homogeneous GC content (isochores). GC-poor isochore family members, L1 and L2, contained <38% and 38-42%, GC respectively, whilst heavy (GC rich) family members, H1, H2 and H3, contain 42-47%, 47-52% and >52%, GC respectively. However, the debate continues as to whether isochores provide a useful means of partitioning the sequence contained within the human genome (IHGSC, 2001, Oliver <http://genomebiology.com/>)

1.4.2 CpG island identification

CpG islands are short stretches of hypomethylated DNA that are rich in GC nucleotides and have a CpG:GpC ratio approaching or exceeding 1:1. Their occurrence within human genomic sequence is one fifth of the expected 4% frequency, by multiplying the relative fractions of G's and C's within the genome (0.21×0.21) (IHGSC, 2001) due to the spontaneous deamination of the methyl-C residue which give rise to a thymine (Coulondre *et al.*, 1978). By contrast, deamination of non-methylated cytosine produces uracil residues which are recognised and repaired as cytosine by the cell. The identification of CpG islands within human sequence is significant because they are often associated with the 5' ends of genes (Bird *et al.*, 1986, Gardiner-Garden and Frommer 1987). It has been estimated that 56% of human genes are associated with CpG islands (Antequera and Bird 1993), including constitutively expressed genes, and approximately 40% of genes with tissue specific patterns of expression (Larsen *et al.*, 1992). Analysis of the draft human sequence identified 28,890 putative CpG islands (putative as no information on the methylation status was obtained) within sequence from which repeats had been removed by RepeatMasker (Smit and Green, unpublished) (IHGSC, 2001).

Whilst variation in the length (up to 36,619 bp), and density (2.9 - 22 CpG islands / Mb) of putative CpG islands was observed, their estimated number closely matched previous estimates (Antequera and Bird 1993).

1.4.3 Repeat content

Analysis of the human draft sequence revealed that repetitive motifs account for at least 50% of the genomic content (IHGSC, 2001). These repeat motifs can be roughly divided into five different classes,

- 1) transposon-derived (interspersed) repeats
- 2) inactive retroposed copies of genes (processed pseudogenes)
- 3) simple sequence repeats (e.g. (A)_n, (CA)_n, (CGG)_n)
- 4) segmental duplications (10 – 300 kb duplicated within the genome)
- 5) tandemly repeated sequences (centromeres / telomeres / RNA gene clusters).

The transposon-derived interspersed repeats account for more than 90% of all repeats currently identified (IHGSC, 2001). This class of repeats, which includes short-interspersed-elements (SINES), long interspersed elements (LINES), LTR retrotransposons and DNA transposons, accounts for 13%, 20%, 8% and 3% of the draft sequence, respectively. In general the SINE and LINE elements, as has previously been reported (Soriano *et al.*, 1983), show an inversely proportional distribution by genomic GC content. LINE elements are found at a higher density in AT-rich, GC-poor, regions whilst SINEs are found in AT-poor, GC-rich regions. The prevalence of LINE elements in AT-rich regions, where gene density is lower, is logical from the perspective that these genomic parasites would not present a mutational burden to their host. Whereas SINES,

that utilise LINE transposon machinery for replication (Jurka *et al.*, 1997), do not co-localise with LINEs and are in fact found in GC-rich regions at a four fold higher density than in GC-poor region. It has been proposed that SINEs may somehow target GC-rich regions for insertion or that they are co-distributed similarly to LINEs, in gene-poor regions, but their distribution is subsequently reshaped by evolutionary forces (IHGSC, 2001) or that they are randomly integrated but are then fixed preferentially in GC-rich DNA (Smit *et al.*, 1999).

1.5 Gene identification

It is estimated that 5% of the human genome contains coding sequence (IHGSC, 2001), with as little 1 – 2% encoding for protein (Green *et al.*, 2001). It is therefore important that the structures of genes are clearly and accurately defined above the background of apparent non-coding and repetitive sequence. It is known that human genes encode RNAs that, for example, facilitate the expression of protein-coding genes by the excision of introns by the spliceosome (small nuclear ribonucleoproteins -snRNA), participate in translational machinery (ribosomal RNA - rRNA and transfer RNA - tRNA), or act as the template for the transcription of messenger RNA (mRNA) which is subsequently translated into a protein product. The majority of the protein-coding genes will most likely be identified within human genomic sequence by *in silico* gene prediction with the support of cDNA and EST sequence alignment. However, techniques that were developed to identify genes from the transcript rather than the sequence will be central to the elucidation of human genes that are difficult to characterise, and to assist

identification of genes within other organisms for which large amounts of sequence data will not be available.

Prior to the availability of large tracts of human genomic sequence, the identification of protein-coding genes was largely reliant upon the isolation of a transcript from tissue specific mRNA or cDNA clones. These early studies used mRNA enrichment coupled with biological assays of *in vitro* translated products, or cDNAs library hybridisation, using plasmids containing coding fragments, or oligonucleotide mixtures based on peptide sequence, to obtain clones for sequencing to characterise the genes of interest. This highly targeted approach has successfully identified a number of genes, including the rabbit (Rabbitts *et al.*, 1976) and human α - β - γ - globins (Little *et al.*, 1978), human interferon, IFN (Taniguchi *et al.*, 1980) and factor IX (Choo *et al.*, 1982).

Genomic fragments, in the form of cloned DNA (cosmids and YACs), have also been used to identify cDNA clones by direct screening of cDNA libraries. This technique proved successful for the identification of the neurofibromatosis type 1 (Wallace *et al.*, 1990) and Menkes genes (Chelly *et al.*, 1993). Whilst the identification of candidate genes by genomic fragment hybridisation is successful, it relies upon the correct hybridisation kinetics between the exons in the genomic DNA and transcribed sequence. Therefore, genomic hybridisation may not be the most productive method of identifying the gene of interest where the gene or exons may be very short in the genomic sequence.

Direct selection, which can be used to enrich cDNA libraries for genes encoded by large genomic regions, can result in a 1000-fold amplification of target cDNAs. The technique has successfully been applied to the characterisation of genes within a 300 kb region around the G6PD on Xq28 (Sedlacek *et al.*, 1993) and a 6.5 Mb region on Xq21, which

led to the identification of the X-linked agammaglobulinemia gene (XLA) (Vetrie *et al.*, 1993).

Another technique of gene discovery, which utilises the genomic sequence of a gene is exon trapping. Though the technique has successfully been used in several positional cloning projects (Walker *et al.*, 1993, Trofatter *et al.*, 1993, The Huntington's Disease Collaborative Research Group 1993) its technical complexity precludes it from large-scale application.

The technique of amplifying multiple genes by oligo dT priming (Verma *et al.*, 1972, Wickens *et al.*, 1978) or with anchored oligo(dT) priming (Khan *et al.*, 1991), together with advances in sequencing technologies, led to the development of a strategy to generate single pass sequence of all human cDNAs. It was suggested that this approach would obviate the need to map and sequence the entire genome (Brenner *et al.*, 1990). Large-scale sequencing projects were initiated to generate gene fragments by single pass sequencing from the 5' and 3' ends of cDNA clones (Adams *et al.*, 1991, Okubo *et al.*, 1992, Adams *et al.*, 1993, Sudo *et al.*, 1994, Hillier *et al.*, 1996). One of the difficulties encountered with this strategy was the representation of genes by multiple expressed sequence tags (ESTs). Consequently, a database (UniGene) was established that rationalised EST data by clustering the sequences into a non-redundant data set (Boguski and Schuler 1995, Schuler *et al.*, 1996) (<http://www.ncbi.nlm.nih.gov/UniGene/clust.cgi?ORG=Hs>). UniGene currently contains (31st October 2002) 3,911,348 EST sequences which have been condensed into 110743 clusters. Almost half of the clusters, 50476, contain a single EST entry, whilst the average cluster contains 5 – 8 ESTs, with the largest cluster containing 16385-32768

ESTs. Another problem encountered with the generation of EST sequence was the contamination of the cDNA libraries with genomic DNA. Poly(A) sequences within the genomic DNA act as templates for the oligo(dT) primer and false cDNA sequence is generated. Additionally, some transcripts have proven to be incomplete, for example, large transcripts that are sometimes not represented if reverse transcription of the mRNA has terminated prematurely. A further problem with the cDNA based approach is that some transcripts may be absent if the gene is not expressed in the tissues used to construct any of the cDNA libraries used for EST sequencing.

Whilst the integration of ESTs within existing radiation hybrid and genetic maps has facilitated the identification of putative candidates for a number of diseases by positional cloning (APOE; Pericak-Vance *et al.*, 1991, Strittmatter *et al.*, 1993, RET; Mulligan *et al.*, 1993) it is their localisation within the human genome sequence that ESTs will prove their greatest worth. Alignment of ESTs to genomic sequence have facilitated the correct annotation of gene structure by assisting to define exon – intron boundaries and helped to identify splice variants, which are present in at least 35% of all human genes (IHGSC, 2001).

Detailed sequence analysis of previously characterised genes has permitted conclusions to be drawn their about generalised genomic structure. Regulatory elements, such as those residing at the 5' ends of genes, which act as a template upon which transcription factors assemble prior to the initiation of RNA synthesis, have been inherently difficult to identify. This is due to the absence of consistently shared motifs within the genomic sequence. However, the combined occurrence of specific elements, CpG islands and TATA boxes flanked by regions of C-G, permits *in silico* prediction of at least a fraction

of the core promoter region to be made. Whilst Eponine (Down and Hubbard 2002) and PromoterInspector (Scherf *et al.*, 2000) currently have approximately 50% sensitivity (detecting known TSSs) and 75% specificity (predictions supported by known TSSs) their accuracy is likely to increase when trained upon larger data sets of elucidated promoters.

Unlike prokaryotic organisms, in which genes are located as a single tract of DNA, complex organisms, from yeast onwards, contain genes that are usually segmented by introns of non-coding sequence (Tilghman *et al.*, 1978; Gilbert *et al.*, 1978). The spliceosome recognises sequence motifs within the intron which leads to their excision, usually a GT di-nucleotide at the 5' end of an intron (splice donor), an AG di-nucleotide at the 3' end (splice acceptor) and an internal branch point (Moor and Sharp 1993).

Localising the site of translation initiation within genomic sequence, unlike the TSS, has been facilitated by the identification of a consensus motif within the genomic sequence. The translation start site, usually an ATG, is typically found in a consensus, GCC^A/_GCCATGG, which includes the two bases which exert the strongest effect, a G at the first base after the translation start, ATG, and a purine (preferably an A) which is located three nucleotides upstream (Kozak *et al.*, 1987). The identification of stop codons (TGA, TAA or TAG) and polyadenylation signals (Kessler *et al.*, 1986), most commonly as AATAAA (Beaudoing *et al.*, 2000), have helped define the 3' ends of genes within genomic sequence.

1.6 Computational Genomics

1.6.1 *In silico* gene prediction

The *in silico* prediction of genes within genomic sequence utilises characteristic sequence motifs associated with genes mentioned above. Whilst initial computer programs were developed to identify single exons, for example GRAIL (Uberbacher *et al.*, 1996), and HEXON (Solovyev *et al.*, 1994), more recently developed programs attempt to identify complete gene structures. These programs, GENSCAN (Burge *et al.*, 1997) and FGENESH (Solovyev *et al.*, 1995) predict individual exons based on codon usage and sequence signals and assemble these putative exons into candidate gene structures. The greatest problem associated with using *in silico* gene prediction programs to identify coding structures within genomic sequence is the number of over predictions that are generated. Whilst all genes may be identified by setting low prediction thresholds, the gene structures will be generated with low specificity. Guigo *et al* (Guigo *et al.*, 2000) assayed the accuracy of gene prediction methods using an artificially generated data set. They found that GENSCAN accurately predicted 90% of coding nucleotides with 70% of the exons being predicted correctly. However, there was also significant over prediction of 30% based upon predictions in simulated intergenic sequences. The study concluded that it is not currently viable to use computational methods alone to accurately identify the exonic structure of every gene in the human genome (Guigo *et al.*, 2000).

The estimated total number of genes contained within the human genome has varied considerably according to the technique that was used to evaluate it and the data that was available at the time. Estimates have been variously based upon average genome and

gene size, the number of observed CpG islands (and the proportion associated with genes), redundant and non-redundant EST sequences and, latterly, upon chromosome specific totals, comparative analyse and genome-wide sequence analysis (table 1.3).

Table 1.3: Genes in the human genome

Data set	Gene Number	Date	Reference or source
Hypothetical	100,000	1992	Gilbert <i>et al.</i> , 1992
CpG Islands	80,000	1993	Antequera <i>et al.</i> , 1993
EST clusters	60,000-70,000	1994	Fields <i>et al.</i> , 1994
Unigene clusters	92,000	1996	Schuler <i>et al.</i> , 1996
Gene sequences	140,000	1999	*IncyteGenomics
Chr. 22 sequence	43,000-61,000	1999	Dunham <i>et al.</i> , 1999
Chrs 22, 21 sequence	44,000	2000	Hattori <i>et al.</i> , 2000
Tetraodon seq.	28,000-34,000	2000	Roest-Crolius <i>et al.</i> , 2000
ESTs in dbEST	120,000	2000	Liang <i>et al.</i> , 2000
EST and mRNA	35,000	2000	Ewing, B., <i>et al.</i> , 2000
Draft Sequence	31,000	2001	IHGSC, 2001

*press release available at <http://incyte.com/company/news/1999/genes.shtml>

1.6.2 Sequence Analysis

Whilst computer programs have been written to predict a number of features associated with coding sequences (table 1.4) the alignment of experimental data is critical to the validation of predicted structures.

Table 1.4: Prediction programs used to identify gene features

Program	Description	Reference
RepeatMasker	Repeat Sequence prediction	Smit and Green, unpublished
CPGFIND	CpG island prediction	Micklem, unpublished
PromoterInspector	Promoter Prediction	Scherf <i>et al.</i> , 2000
Eponine	TSS prediction	Down and Hubbard, 2002
Hexon	Exon prediction	Solovyev <i>et al.</i> , 1994
Grail	Exon prediction	Ueberbacher <i>et al.</i> , 1991
GENSCAN	Gene prediction	Burge <i>et al.</i> , 1997
FGENESH	Gene prediction	Solovyev <i>et al.</i> , 1995

Programs such as CLUSTALW (Thompson *et al.*, 1994), which is used to align multiple nucleotide or protein sequences, and DOTTER, which utilises pair-wise local sequence alignment strategy (Sonnhammer *et al.*, 1995), are useful for inferring structural and functional conservation by sequence homology. Sequence homology searching can also be performed using SSAHA (Ning *et al.*, 2001), Exonerate (Slater, unpublished) and BLAT (Kent *et al.*, 2002) which permits homology sequences to be identified within gigabases of DNA. BLAST (Basic Local Alignment Search Tool), which measures the local similarity between two sequences (Altschul *et al.*, 1990, 1997), is the primary method for identifying protein and DNA sequence similarities prior to incorporation of the features into project specific ACeDB databases (Durbin and Thierry-Mieg 1994) (<http://www.acedb.org/>) or genome browsers. One of the major advantages of using BLAST for sequence alignment is the flexibility with which nucleotide and amino acid sequences can be aligned (table 1.5)

Table 1.5: Sequence queries available using BLAST alignment

Program	Query	Database	Comparison
blastn	DNA	DNA	DNA level
blastp	Protein	Protein	Protein level
blastx	DNA	Protein	Protein level
tblastn	Protein	DNA	Protein level
tblastx	DNA	DNA	Protein level

From Brenner (1998)

Whilst BLAST alignment of human mRNA, EST and protein sequences to predicted coding structures provides a primary level of support, predicted features can also be supported by alignments with sequence from other organisms for comparison (comparative sequence analysis). The identification of sequences that are conserved between species is important because sequences that contain elements that are potentially

functional are more likely to retain their sequence than non-functional segments, under the constraints of natural selection during evolution. The evolutionary distance between species is an important consideration. Sequence comparisons between closely related species may facilitate the identification of gene structures and regulatory elements but, if the evolutionary distance between the species is relatively small, these sequences may be obscured by non-functional sequence conservation. Therefore a variety of species, including more distantly related species may be required to identify potential functional sequences using the comparative approach.

The identification of conserved sequences by comparative analysis has focused on the identification of non-coding regions (Hardison *et al.*, 1993; Koop *et al.*, 1994; *et al.*, 1997; Hardison *et al.*, 1997) and protein coding regions (Makalowski *et al.*, 1996; Ansari-Lari *et al.*, 1998; Jang *et al.*, 1999) between human and mouse genomes. The alignment of sequence from multiple organisms has also been used to identify upstream regions that may affect gene expression. Gottgens *et al* (Gottgens *et al.*, 2000) used the alignment of human, mouse and chicken sequences to identify a novel neural enhancer element in their elucidation of the human stem cell leukaemia (SCL) gene region. Whilst comparative sequence analysis may not identify all control regions associated with a gene, conserved regions may be identified that would be candidates for further experimental investigation (Pennacchio *et al.*, 2001). Large scale sequencing and comparative analyses is progressing on a number of different organisms (table 1.6).

Table 1.6: A list of the large scale comparative organisms sequencing projects

Organism	Genome Size (Mb)	Reference
<i>E. coli</i>	4.6	Blattner <i>et al.</i> , 1997
<i>S cerevisiae</i>	12	Goffeau <i>et al.</i> , 1996
<i>C. elegans</i>	97	The C. elegans sequencing consortium, 1998
<i>D. melanogaster</i>	120	Adams <i>et al.</i> , 2000
<i>M. musculus</i>	2600	The Mouse Genome Sequencing Consortium, 2002*
<i>D. rerio</i>	1600	on going
<i>F. rubripes</i>	400	on going
<i>R. rattus</i>	2800	on going
<i>T. nigroviridis</i>	350	on going

* draft sequence publication

The availability of large tracts of human genomic sequence has necessitated the development of databases (genome browsers) that provide a framework upon which the enormous amount of data associated with the human genome can be stored and displayed. The two main databases, Ensembl, developed at the Sanger Institute and the European Bioinformatics Institute (http://www.ensembl.org/Homo_sapiens/), and the University of California Santa Cruz (UCSC) genome browser. (<http://genome.cse.ucsc.edu/>) contain information pertaining to physical maps, chromosome specific sequence assemblies, aligned mRNAs and ESTs, cross species homologies, SNPs and repeat elements. The development of generic genome browsers, as such as those hosted by Ensembl, makes possible the rapid identification of homologous sequences between comparative organisms and in doing so assist to identify conserved features that may be of some functional significance.

1.7 Allelic variation

Most differences between individuals, at the nucleotide level, can be attributed to allelic sequence variation. The characterisation of sequence differences and comprehension of how these genomic variations affect the expression and function of genes will be crucial for the study of molecular alterations in human disease. Whilst sequence variation has previously been used for genome-wide linkage and positional cloning studies (leading to the identification of many disease causing genes (see 1.2.2)), the association of single nucleotide polymorphisms (SNPs) with genes, either by mapping or as causal sequence variants, promises to be a valuable method in the future for identifying genes involved in complex diseases.

Approximately 90% of the allelic differences existing within the human genome can be attributed to SNPs, the remainder being insertions or deletions (Collins 1998b). A comparison of any two diploid genomes is estimated to identify one SNP per 1.3 kb which has an allele frequency of $> 1\%$ (ISNPMWG, 2001). The prevalence of SNPs in the genome, their existence as bi-allelic variants and their stability through inheritance makes them amenable to large-scale high through-put analyses. SNPs will, therefore, be applied to several research areas, including 1) large-scale genome analysis of linkage disequilibrium and haplotype patterns, 2) genetic analysis of simple and complex disease states, and 3) genetics and diversity of human populations.

1.7.1 SNP discovery

De novo candidate SNPs were initially identified by the alignment of STSs and ESTs to available genomic sequence (Wang *et al.*, 1998, Picoult-Newberg *et al.*, 1999, Irizarry *et al.*, 2000, Deutsch *et al.*, 2001). The clone based strategy used by the Human Genome Project for the large-scale production of human genomic sequence contributed to a dramatic increase in the SNP numbers by allowing identification of novel SNPs within sequence overlaps between minimum tile path clones (Taillon-Miller *et al.*, 1998, Dawson *et al.*, 2001). A directed approach to SNP discovery was initiated by sequencing DNA from population specific individuals (Mullikin *et al.*, 2000, Altshuler *et al.*, 2000). Two to five fold redundant shotgun sequence coverage was generated from 1.5 kb small insert library clones and the resultant sequences were aligned to each other in clusters. As the Human Genome Project progressed, these assemblies and additional shotgun sequence data were aligned to available genomic sequence to identify more SNPs. The total number of SNPs identified using the strategies outlined above culminated in the International SNP Map Working Group (ISNPMWG) constructing a SNP map of the human genome which contained 1.42 million candidate SNPs (ISNPMWG 2001). A proportion of the candidate SNPs were validated experimentally during the project, confirming that >90% were real SNPs. The SNPs identified by The SNP Consortium (TSC) (<http://snp.cshl.org>, Marshall *et al.*, 1999) and the HGP had generated a SNP density of 1 SNP per ~1.9 kb of available sequence.

Akin to the rationalisation that was required to establish a unique set of ESTs, a database was established to generate a non-redundant collection of candidate SNPs (dbSNP) (Sherry *et al.*, 2001, <http://www.ncbi.nlm.nih.gov/SNP/index.html>). dbSNP currently

contains 4.8 million entries which have been condensed into a non-redundant set of 3.0 million SNPs, 522,072 of which have been validated to date (build 110, 13th January 2003). Localisation of these unique SNPs within a recent the human sequence assembly (build 30) yields a SNP density of 1 per 1.2 kb. Additional validation of SNPs was carried out on a subset of TSC and HGP candidate SNPs by Marth *et al.*, (2001) by screening 1200 SNPs across 30 individuals from 3 difference populations. Results indicated that 80% of the SNPs were polymorphic in the populations tested, and that 50% had allele frequencies of greater than 20%. Data generated by Kruglyak and Nickerson (Kruglyak and Nickerson 2001) suggests that the number of non-redundant SNPs currently present within dbSNP, in which the minor allele is present in > 1%, comprise 11 - 12% of all single nucleotide sequence variants. The identification of >95% of available SNPs will require analysis of 96 haploid genomes, many more than the number from which the candidate SNPs have been derived so far.

There are many different platforms that have been developed for SNP analysis but which are based upon four basic allele-specific assays types, 1) hybridisation with allele-specific probes, 2) oligonucleotide ligation, 3) single nucleotide primer extension and 4) enzymatic cleavage. Many of the techniques have been developed further and automated in commercial systems. The range of formats used include colorimetric microtitre-plate based assays (Taqman by Applied BioSystems or Invader assay by Third Wave Technologies) or fluorometric methods of detecting SNP alleles that have been separated by gel electrophoresis (Applied Biosystems), fluorometric assay of target hybridised to oligonucleotides immobilised in a microarray chip format (Affymetrix), or immobilised via beads on the ends of arrays light sensing glass fibres (Illumina).

1.7.2 Utilising SNPs

SNPs may be utilised for population genetic studies in order to identify an association between a SNP allele and a specific phenotype. Ultimately the goal of such a study is to identify the causal variant, the mechanism by which the variant has its functional effect. The functional variant will have maximal predictive value in future individual tests, and the gene involved may encode a target protein or mRNA for possible therapeutic intervention. Functional variants may be assayed for using two approaches. The direct approach requires prior availability of a candidate functional variant (e.g. a SNP which alters the encoded protein sequence in a non-conservative way, thus affecting function). The variant is then tested by genotyping a population of defined phenotype and comparing the frequency of one allele with the frequency in a population of matched controls (a case-control study). In the absence of a candidate functional variant, the indirect approach can be taken, in which available SNPs within specific genes (candidate gene association studies) or throughout the genome (genome-wide association studies) can be used to test the same populations.

An aid to the indirect approach is the identification of allele specific sequence variants and generation of a map of common combinations of specific alleles (or haplotype patterns) that have been largely conserved during the recent population expansions. Among other factors, it is believed that the regions of conserved local haplotype patterns have been maintained by the absence of ancestral recombination within each region. Identification of these conserved segments is facilitated by the availability of SNPs identified by the ISNPMWG. Pairs of alleles can be statistically quantified to determine whether recombination has occurred between them, in which case they are said to be in

equilibrium, or if the alleles share evolutionary co-segregation and are therefore in linkage disequilibrium (LD). The generation of an LD map does not require the analysis of related individuals (by comparison to the genetic map), only that they share a common evolutionary history (although inclusion of pedigrees allows direct determination of the phase between SNP alleles and facilitates definition of long range haplotypes). It is hoped that the generation of a map of common haplotype patterns (HapMap) will facilitate the identification of common diseases by indirect association studies as described above (Couzin *et al.*, 2002, Harris *et al.*, 2002).

The availability of genome sequence with annotated gene structures provides the means to search for candidate functional variants. Build 110 in dbSNP (13th January 2003) contains 60541 SNPs that have been localised to exons, untranslated regions or non-coding regions adjacent to genes (introns or flanking sequence), table 1.7.

Table 1.7: SNP totals contained within or adjacent to coding features.

SNP Count	FUNCTIONAL CLASSIFICATION
20851	Gene region
5228	Synonymous
5220	Non-synonymous
13462	untranslated region
15651	Intron
129	Splice site

SNPS localising within coding a feature (cSNPs) have the greatest potential to affect the structure and function of the gene. The characterisation of allelic variants enables conclusions to be drawn as to whether a specific allele may have an effect upon the amino acid sequence. Slightly more than half of the SNPs localising to coding sequences result in a synonymous change (no change in the amino acid sequence because of codon redundancy) whilst the remaining SNPs result in a non-synonymous change. Non-

synonymous changes are further classified as to whether the resultant amino acid has similar biological properties to the 'normal' allele, in which case the change is conservative, or if the biological properties of the amino acid are different, then the change is non-conservative. Whilst the molecular significance cSNPs have upon protein structure and function has previously been reported (Chasman *et al.*, 2001, Sunyaev *et al.*, 2001, Wang and Moulton 2001), the effects that SNPs have in non-coding sequence such as splice junctions (Pan *et al.*, 2002, Khan *et al.*, 2002), folding of mRNAs (Shen *et al.*, 1999) and promoter function (Knight *et al.*, 1999, Hijikata *et al.*, 2000) have also been described.

The identification of SNPs that show an allelic influence on the functioning of proteins, particularly of drug metabolising enzymes, promises a bright future for the optimisation of clinical therapeutics. Associating inherited variations with pharmacological responsiveness provides a basis for the possible development of personalised medicine which will improve the efficacy of drug treatments and decrease the side effects experienced by the individual (Roses *et al.*, 2000, 2002, Pfohl *et al.*, 2000).

1.8 Chromosome 1

Chromosome 1, the largest human chromosome, is estimated to be 263 Mb in length (Morton 1991), which represents 8% of a 3200 Mb human genome. The chromosome is submetacentric and contains a large block of heterochromatin adjacent to the centromere on the long arm which, together with tandemly repeat sequences contained within the centromere and telomeres, reduces the euchromatic size of the chromosome to 214 Mb

(IHGSC, 2001). The chromosome has an average GC content of 43%, compared to the genome average of 41%, with the 40 Mb telomeric region of the short arm containing 47.1% GC (IHGSC, 2001). Draft sequence analysis indicates that chromosome 1 contains slightly more (~11 / Mb) than the genome average of 10.5 CpG islands / Mb, whilst the estimated gene content is noticeably higher (~15 genes / Mb) when compared to the genome average of ~ 11.5 genes / Mb (IHGSC, 2001).

A hierarchical strategy was used to map and sequence chromosome 1, as outlined in section 1.3. To date (15th of February 2003), the sequence ready map of chromosome 1 is contained within 9 bacterial clone contigs from which 2244 minimum tile path clones have been selected for sequencing (including 5 cosmids and 4 YACs). Currently, 95% of the chromosome is contained within finished sequence clones. The chromosome 1 mapping and sequencing project has directly facilitated the elucidation of a number of genetic disease genes, table 1.8.

Table 1.8: Genes that are associated with disease that have been elucidated as a result of the Sanger Institute chromosome 1 mapping and sequencing project.

Gene	Disease	Publication
CACP	Camptodactyly-arthropathy-coxa vara-pericarditis	Marcelino <i>et al.</i> , 1999
SLC19A2	Thiamine-responsive megaloblastic anaemia	Labay <i>et al.</i> , 1999
HPC1	Prostate cancer	Carpten <i>et al.</i> , 2002
LMNA	Partial lipodystrophy	Shackleton <i>et al.</i> , 2000
CIAS1	Muckle-Wells syndrome	Hoffman <i>et al.</i> , 2001
IRF6	Van der Woude syndrome	Kondo <i>et al.</i> , 2002
TBCE	HRD/Autosomal recessive Kenny–Caffey syndrome	Parvari <i>et al et al.</i> , 2002

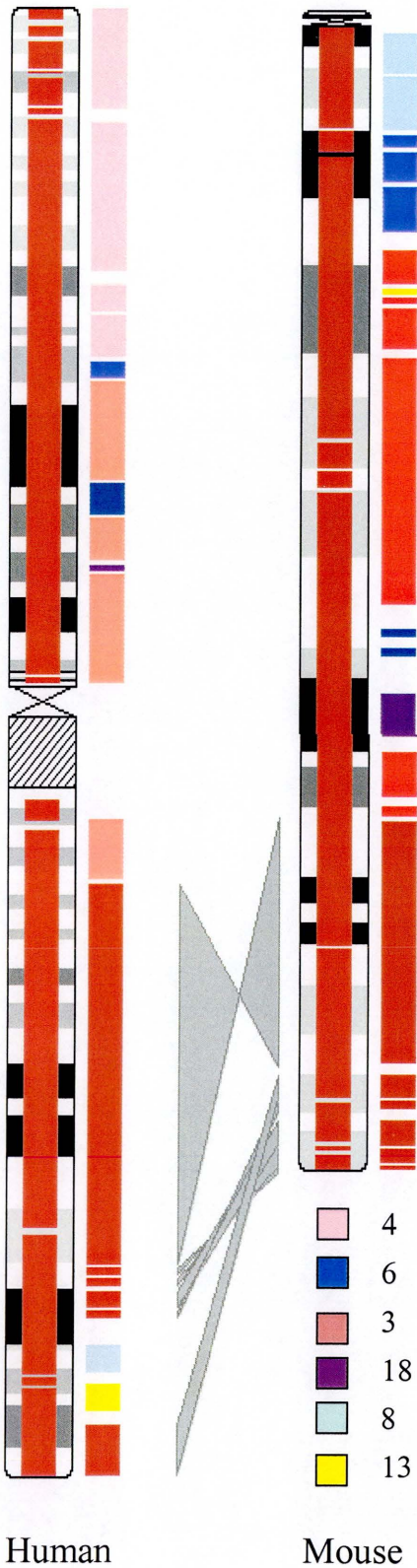
Included among the 157 genetic diseases localised to chromosome 1 within OMIM (<http://www.ncbi.nlm.nih.gov/entrez/query.fcgi?db=OMIM>) (16th of January 2003) are: Alzheimer disease-4 (Levy-Lahad *et al.*, 1995), Chediak-Higashi syndrome (Kritzler *et*

al., 1964), Fanconi anemia (Loetscher *et al.*, 1987), Gaucher disease (Hsia *et al.*, 1959) and Usher syndrome, type 2 (Kimberling *et al.*, 1990)

Alterations of chromosome 1 are amongst the most common chromosomal abnormalities in human neoplasia. These abnormalities include translocations and other structural rearrangements involving chromosome 1 and other regions of the genome, as well as region specific deletions and amplifications. In general, regions on 1p (the short arm) seem to be most frequently lost, indicating the possible presence of tumour suppressor genes, whereas regions on 1q (the long arm) are more often amplified. Loss of 1p has been detected in meningiomas and oligodendrogliomas (Bello *et al.*, 2000, 2002), endometrial hyperplasia (Kiechle *et al.*, 2000) and primary gastrointestinal tumors (El-Rifai *et al.*, 2000). Gains of 1q have previously been implicated in neoplasia such as, hepatoblastoma (Nagata *et al.*, 1999), lymphoma (Rao *et al.*, 1999) and sarcoma (Forus *et al.*, 1995).

The generation of continuous stretches of genomic sequence has permitted higher resolution synteny maps to be drawn than those based on mapping of orthologous genes or genetic markers. The construction of a physical map (Gregory *et al.*, 2002) and the draft sequence (MGSC 2002) has enabled accurate localisation of syntenic boundaries between mouse and human genomes. The availability of more genomic sequence from a broader range of organisms will improve upon our understanding of chromosomal evolution. Figure 1.2 is a representation of the alignment of human and mouse chromosome 1 (also shown are the mouse syntenic blocks contained within human chromosome 1).

A number of physical maps have previously been constructed on chromosome 1. The clones used in their construction have evolved with the availability of new cloning systems, i.e. earlier physical maps were constructed using YACs and cosmids whilst later maps have utilised PACs and BACs. Comprehensive lists of chromosome 1 physical maps have been published within chromosome 1 workshop reviews (Gregory *et al.*, 1998, White *et al.*, 1999, Schutte *et al.*, 2001). Though constructed primarily for the elucidation of disease genes maps have also been generated in difficult to clone regions, such as the telomere on 1q (Xiang *et al.*, 2001).



(From Gregory *et al.*, 2002)

Figure 1.2 The alignment of syntenic region between human and mouse chromosomes 1. Bacterial clone coverage on each chromosome is represented by red boxes on the ideograms of each chromosome, whilst chromosomes syntenic to human and mouse chromosome 1 are individually coloured and listed.

1.9 Aims of this thesis

The construction of physical maps, prior to the commencement of this thesis, primarily relied upon the assembly of YAC contigs by STS content hybridisation and, to a lesser extent, cosmid assembly into contigs by radioactive restriction digest fingerprinting. If the goal to generate sequence of the human genome was to be realised, techniques would require development that would enable physical maps to be constructed rapidly and safely. The first part of this thesis describes the development of a fluorescence based restriction digest fingerprinting technique that could be applied to the generation of sequence ready maps. The second aim of this thesis was to apply this fingerprinting, in combination with large-insert bacterial clone library screening, to the generation of a 12 Mb contig within 1pcen – 1p13. Minimum tile path clones from the contig would then selected for sequencing and to assist in elucidating disease causing genes that had been localised to the interval (table 1.9)

Table 1.9: Disease loci mapping to 1pcen -1p13

Disease	Reference	Localisation
Radiation induced meningioma	Zattara-Cannoni <i>et al.</i> , 2001	1p11
Autosomal recessive tachycardia	Lahat <i>et al.</i> , 2001	1p11 - 1p13.3
Acute megakaryoblastic leukaemia	Mercher <i>et al.</i> , 2001	1p13
Hypothyroidism	Dracopoli <i>et al.</i> , 1986	1p13
Achromatopsia	Kohl <i>et al.</i> , 2002	1p13
Adrenal Hyperplasia II	Zachmann <i>et al.</i> , 1979	1p13.1
Colorectal Cancer	Nitta <i>et al.</i> , 1987	1p13.2

The third aim was to use the sequence data generated from the first two sections to characterise the genomic landscape of the interval and to identify as many coding features as possible by *in silico* prediction and experimental support. A family of genes, annotated during the course of this section, and seven other genes of medical interest, form the basis for the final part of the thesis.

The aim was to assemble exon specific sequences from 47 unrelated individuals, of the 12 target genes, to confirm the presence of known, or identify novel, single nucleotide polymorphisms. SNPs identified by this strategy would then be categorised according to their occurrence in coding sequence and, where found, further analysis carried out to predict what possible affect they may have upon the structure and function of the resultant protein.

Chapter 2

Materials and Methods

Materials

- 2.1 Chemical reagents**
- 2.2 Enzymes and commercially prepared kits**
- 2.3 Nucleotides**
- 2.4 Solutions**
 - 2.4.1 Buffers
 - 2.4.2 Electrophoresis and Filter preparation solutions
 - 2.4.3 Media
 - 2.4.4 DNA labelling and hybridisation solutions
 - 2.4.5 General DNA preparation solutions
- 2.5 Size markers**
- 2.6 Hybridisation membranes and X-ray and photographic film**
- 2.7 Sources of genomic DNA**
- 2.8 Bacterial clone libraries**
 - 2.8.1 Cosmid libraries
 - 2.8.2 PAC and BAC libraries
 - 2.8.3 cDNA libraries
- 2.9 Primer sequences**
- 2.10 World Wide Web addresses**

Methods

- 2.11 Isolation of bacterial clone DNA**
 - 2.11.1 Miniprep of cosmid
 - 2.11.2 Microprep of cosmid, PAC and BAC DNA for restriction digest fingerprinting
 - 2.11.3 Filterprep of PAC and BAC DNA for restriction digest fingerprinting
- 2.12 Bacterial clone fingerprinting**
 - 2.12.1 Radioactive fingerprinting
 - 2.12.2 Fluorescent fingerprinting
 - 2.12.3 Hind III fingerprinting

2.13 Marker preparation

2.13.1 Radioactive fingerprinting

2.13.2 Fluorescent fingerprinting

2.13.3 Hind III fingerprinting**2.14 Gel preparation and electrophoresis**

2.14.1 Agarose gel preparation and electrophoresis

2.14.2 Gel preparation and electrophoresis for radioactive fingerprinting

2.15 Construction of small insert library

2.15.1 Library preparation

2.15.2 Electroporation and library plating

2.16 Applications using the polymerase chain reaction

2.16.1 Primer design

2.16.2 Oligonucleotide preparation

2.16.3 Amplification of genomic DNA by PCR

2.17 Radiolabelling of DNA probes

2.17.2 Radiolabelling of PCR products

2.17.3 Pre-reassociation of radiolabelled probes

2.18 Hybridisation of radiolabelled DNA probes

2.18.1 Hybridisation of DNA probes derived from STSs

2.18.2 Stripping radiolabelled probes from hybridisation filters

2.19 Restriction endonuclease digestion of cosmid DNA**2.20 Clone library screening**

2.20.1 Bacterial clone library screening

2.20.2 cDNA library screening by PCR

2.20.4 Vectorette PCR on cDNA

2.21 Exon Amplification**2.22 Mapping and sequence analysis software and databases**

2.22.1 IMAGE

2.22.2 FPC

2.22.3 lace

2.22.4 BLIXEM

2.22.5 RepeatMasker

Materials

2.1 Chemical reagents

All common chemicals were purchased from Sigma Chemical Co., BDH Chemical Ltd., and Difco Laboratories unless specified below or in the text.

Amersham Pharmacia Biotech	Dextran sulphate, Na ⁺ salt
Bio-Rad Laboratories	β-mercaptoethanol
Gibco BRL Life Technologies	Foetal bovine serum
	ultraPURE™ Ammonium sulphate, enzyme grade
	ultraPURE™ agarose
Roche Applied Science	Restriction Buffer B
Stratagene®	Perfect Match® (1 U/μl)
	Taq Extender

2.2 Enzymes and commercially prepared kits

All restriction endonucleases were purchased from New England Biolabs, unless listed.

Amersham Pharmacia Biotech	T4 DNA ligase (1 U/μl)
	<i>Sau3A1</i>
Bio101Inc	GeneClean II
Gibco BRL Life Technologies	M-MLV reverse transcriptase
New England Biolabs	T4 DNA ligase
PE Applied Biosystems	Amplitaq™
	Sequenase
	TaqFS
Qiagen	DNA gel purification
Roche Applied Science	Klenow enzyme (sequencing grade, 5 U/μl)
	T4 Polynucleotide kinase
Sigma	Ribonuclease A
USB	Shrimp Alkaline Phosphatase
	Exonuclease I

2.3 Nucleotides

Amersham Pharmacia Biotech	Redivue™[α - 32 P]-dCTP (AA 005) aqueous solution (370 Mbq/ml, 10 mCi/ml)
	Redivue™[γ - 32 P]-dATP (AG 1001) aqueous solution (370 Mbq/ml, 10 mCi/ml)
	[α - 35 S]-dATP (Q11135) (370 Mbq/ml, 400 Ci/mmol)
PE Applied Biosystems	Fluorescently labelled (TET, HEX, NED) dideoxyadenosine triphosphate (ddA)
	Fluorescently labelled (ROX) dideoxythymidine triphosphate (ddT)
Amersham Pharmacia Biotech	2'-deoxynucleoside 5'-triphosphates (dATP, dTTP, dGTP, dCTP)
	dideoxyguanine 5'-triphosphate (ddGTP)
	Random hexanucleotides pd(N) ₆ , 5'-PO ₄ , Na ⁺ salt

2.4 Solutions

Solutions used in the present study are listed below, alphabetically within each section. Final concentrations of reagents are given for most solutions. Amounts and/or volumes used in preparing solutions are given in some cases. Unless otherwise specified, solutions were made up in autoclaved nanopure water.

2.4.1 Buffers

10x Ligase buffer	500 mM Tris-HCl (pH 7.4)
	100 mM dithiothreitol
	100 mM MgCl ₂
10x PCR buffer	670 mM Tris-HCl (pH7.4)
	166 mM (NH ₄) ₂ SO ₄
	67 mM MgCl ₂
1x TE	10 mM Tris-HCl (pH 7.4)
	1 mM EDTA

1x T _{0.1} E	10 mM Tris-HCl (pH 8.0) 0.1 mM EDTA
-----------------------	--

SAP reaction buffer	20 mM Tris-HCl (pH 8.0) 10 mM MgCl ₂
---------------------	--

2.4.2 Electrophoresis and hybridisation solutions

6x Buffer II	0.25% bromophenol blue 0.25% xylene cyanol 15% ficoll
--------------	---

Denaturation solution	0.5 M NaOH 1.5 M NaCl
-----------------------	--------------------------

Formamide dyes	80% v/v deionised formamide 0.1% w/v bromophenol blue 0.1% w/v xylene cyanol 1 mM EDTA 50 mM Tris-borate (pH 8.3) (<i>i.e</i> 0.56x TBE)
----------------	---

Formamide dyes mix	0.0075% w/v SDS 3.75 mM EDTA 1.6x formamide dyes
--------------------	--

6x Glycerol dyes	30% v/v glycerol 0.1% w/v bromophenol blue 0.1% w/v xylene cyanol 5 mM EDTA (pH 7.5)
------------------	---

Neutralisation solution	1.5 M NaCl 1 M Tris-HCl (pH 7.4)
-------------------------	-------------------------------------

20x SSC	3 M NaCl 0.3 M Trisodium citrate
---------	-------------------------------------

10x TAE
400 mM Tris-acetate
20 mM EDTA (pH8.0)

10x TBE
890 mM Tris base
890 mM Borate
20 mM EDTA (pH 8.0)

2.4.3 Media

All media were made up in nanopure water and either autoclaved or filter-sterilised prior to use.

For agar used for bacterial growth 15 mg/ml bacto-agar was added to the appropriate media. Antibiotics were added to media as appropriate (see Table 2.1) to the following final concentrations: Ampicillin (sodium salt dissolved in 1 M sodium bicarbonate, stored at -20°C), 100 µg/ml; Kanamycin (purchased as a solution, stored at 4 °C), 30 µg/ml; Chloramphenicol (stored at 4 °C), 12.5 µg/ml (all supplied by Sigma).

Table 2.1: Clones and appropriate antibiotics.

Clone type	Library	Antibiotic
Cosmid	LL22NC01	Kanamycin
PAC	RPCI1,3,4,5, 6	Kanamycin
BAC	RPCI-11, 13	Chloramphenicol
SIL clones	FS library	Ampicillin

LB
10 mg/ml bacto-tryptone
5 mg/ml yeast extract
10 mg/ml NaCl
(pH 7.4)

2X TY
15 mg/ml bacto-tryptone
10 mg/ml yeast extract
5 mg/ml NaCl
(pH 7.4)

2.4.4 DNA labelling and hybridisation solutions

100x Denhardt's	20 mg/ml Ficoll 400-DL 20 mg/ml polyvinylpyrrolidone 40 20 mg/ml BSA (pentax fraction V)
Hybridisation buffer	6x SSC 1% w/v N-lauroyl-sarcosine 10x Denhardt's 50 mM Tris-HCl (pH 7.4) 10% w/v dextran sulphate
OLB3	240 mM Tris-HCl (pH 8.0) 75 mM β -mercaptoethanol 0.1 mM dATP 0.1 mM dGTP 0.1 mM dTTP 1 M HEPES (pH 6.6) 0.1 mg/ml hexadeoxyribonucleotides (2.1 OD units/ml)

2.4.5 General DNA preparation solutions

GTE	50 mM glucose 1 mM EDTA 25 mM Tris-HCl (pH 8.0)
3 M K ⁺ /5 M Ac ⁻	300 mM potassium acetate (pH 4.8) 11.5 ml glacial acetic acid 28.5 ml H ₂ O

2.5 Size markers

1 kb ladder (1 mg/ml) (Gibco BRL Life Technologies)

Contains 1 to 12 repeats of a 1,018 bp fragment and vector fragments from 75 to 1,636 bp to produce the following sized fragments in bp: 75, 142, 154, 200, 220, 298, 344, 394, 516/506, 1,018, 1,635, 2,036, 3,054, 4,072, 5,090, 6,108, 7,125, 8,144, 9,162, 10,180, 11,198, 12,216.

Lambda DNA/*Hind* III (Gibco BRL Life Technologies)

Contains *Hind* III restricted dsDNA fragments of the following sizes (kb): 23.13, 9.416, 6.557, 4.361, 2.322, 2.027, 0.564, 0.125

Analytical marker DNA wide range (Promega)

Provides an evenly spaced distribution of DNA fragments from 0.702 kb to 29.95 kb

DNA molecular weight marker V (Boehringer - Mannheim)

2.6 Hybridisation membranes and X-ray and photographic film

Amersham	Hybond-N™ Nylon (78 mm x 119 mm) (used for high-density clone gridding)
----------	--

Polaroid	Polaroid 667 Professional film
----------	--------------------------------

X-ray film	Fuji RX medical X-ray film
------------	----------------------------

2.7 Sources of genomic DNA

Human placental DNA for pre-reassociation (ready-sheared) was purchased from Sigma Chemical Co. Human placental DNA for PCR was purchased from Sigma Chemical Co. DNA from whole chromosome 1 hybrid cell line, GM13139, and chromosome 1p specific cell line, GM11526A, was kindly provided by Richard Wooster

2.8 Bacterial clone libraries

2.8.1 Cosmid libraries

Cosmid clones used for the development of the fluorescent fingerprinting were from the Lawrence Livermore flow-sorted 22 chromosome cosmid library (LL22NC01) (prefixed 'cE') were kindly provided by Ian Dunham and the chromosome 22 mapping group.

2.8.2 PAC and BAC libraries

The RPCI-1, RPCI-3, RPCI-4, RPCI-5 (prefixed 'dJ'), and the RPCI-11 (prefixed 'bA') BAC libraries were used as a source of human derived PAC clones and BAC clones respectively in this thesis. These libraries were all kindly provided by Pieter de Jong and Joe Catanese (see <http://bacpac.med.buffalo.edu/>), and imported and maintained by the Sanger Institute Mapping Core Group.

2.8.3 cDNA libraries

A range of up to 9 different cDNA libraries were used in this study (see Table 2.2). cDNA libraries were imported and maintained by Jacqueline Bye and Susan Rhodes. Each library contains 500,000 cDNA clones, divided into 25 pools of 20,000 clones. Five pools were combined to form a superpool containing 100,000 clones. Prior to their use in PCR, each superpool was diluted 1:100 and 1:1000 in $T_{0.1}E$.

Table 2.2: cDNA libraries used.

cDNA lib. code	cDNA library description	Vector	Source/ Reference
1. U*	(Monocyte NOT activated-from a patient with promonocytic leukaemia) (U937+)	pCDM8	Simmons (1993)
2. AK	Adult kidney	pcDNA3.1	Invitrogen
3. AB	Adult brain	pcDNA3.1-Uni	Invitrogen
4. HeLa	Cervical carcinoma cell	pcDNA3.1-Uni	Invitrogen
5. SK	Neuroblastoma cells	pCDNA1	Invitrogen
6. T	Testis	pCDM8	Clontech
7. FLU	Fetal lung	pCDNA1	Invitrogen
8. HPB*	T cell from a patient with acute lymphocytic leukaemia (HPBALL)	pH3M	Simmons (1993)
9. AH	Adult heart	pcDNA3-Uni	Invitrogen

* Generously provided by Dr Simmons, Oxford (Simmons, D., et al., 1993).

2.9 Primer sequences

All primers were synthesised in house by Dave Fraser or externally by Genset. Table 2.3 lists the universal primer. Tables 2.4 and 2.5 list the primer pairs used in this thesis for cDNA library screening and exon amplification, the sequence and size in base pairs (bp) of each PCR product. The 110 STSs used to screen large insert bacterial clone libraries (and the resultant 878 positive PAC clones) can be found in 1ace within STS pools pool_1pc-1p13_STS1 – 5. Where appropriate, the clones, or genes from which the STSs were derived are also listed.

Table 2.3: Vector-specific primer used in vectorette PCR.

Primer Name	Primer Sequence
224*	CGAATCGTAACCGTTCGTACGAGAATCGCT
BPHI*	CAAGGAGAGGACGCTGTCTGTCGAAGGTAAGGAACGGACGACAG AAGGGAGAG
BPHII*	CTCTCCCTTCTCGAATCGTAACCGTTCGTACGAGAATCGCTGTCCT CTCCTTG

* (Riley, J., et al., 1990)

Table 2.4: STSs designed for cDNA screening and Link PCR product synthesis. S=Sense, A=Anti-sense; a 60°C annealing temperature was used for all PCR reactions. stSG # corresponds EMBL accession numbers assigned to individual STSs.

Gene	Exon	stSG #	Primer 1 (S)	Primer 2 (A)	bp
bA483I13.C1.1.mRNA	e2	452926	GGTATCTGCCGACCCTTTGT	GAGTAGGCAGTAGCTTGAGT	147
bA483I13.C1.3.mRNA	e2	452927	GCAGTCTGGAGATTGGTGGA	TGCATCATGACTTTCAAGCG	102
	e5	452928	GGGATTATTGATTGTGGCAA	CGGCATAAGGTACAATGCCT	100
	e7	452929	GGTTTCACCTCAAACATCAT	ACATCTCTTTATAACACAGG	164
bA475E11.C1.2.mRNA	e1 5'UTR	452930	TGACGGCTGAAGAAACAGTG	CTCCAGGGCCAGCATACTAA	104
	e4	452931	GCTTTTGACTTTGCCTCGTC	GCTTCCTATCAGCAGGGATG	128
	e7	452932	CAGCACTCAACCAGCAATGT	TCCAGGATTACGAGGAGTGC	149
	e10	452933	ATGAGACTCCTAAGCAGCCG	GGGCAGCACTTTGACGTATT	137
	e12	452934	ATACCTGGAGTGGCTGGATG	GTTGTGCCAACAAACACGAAC	100
	e14 3'UTR	452935	CGAAGAGGCCCTTATTACC	GGAGTGCACACCAACAACCTG	166
bA475E11.C1.1	e1 5'UTR	452936	AGGCTATGCATAGTGAGACT	GCTTGACTTAGAAGCGTCTC	155
	e5	452937	ACTGCAGGGACACCTTGAAC	CCAACGATTGTTGATTCGTG	105
	e6	452938	TTGGAGATGCTGCTTGAAGA	AGAGAAGGTGGAGGCCAAGT	117
	e10	452939	GAAGCAAAACGTGGAGAAAA	TTGAATCTGAGTGTGGTGCC	92
	e13	452940	CTTCCAAATCCAGCCCTACA	ATGGGTTGCTACCAACTTGC	127
bA297O4.C1.1.mRNA	e1 5'UTR	452941	GCCACTATTGGGAGACCAAG	GTAGAGCCAGAGGTTTCGACG	124
dJ831G13.C1.1.mRNA	e1	452942	CTTTGCTATTTTCGCCTTCG	CTGAAGGGATAGCCAAATGC	123
	e3	452943	CCTTCACCTTCTTCTGGCTG	CTTCCTCTCCATGGCACACT	120
	e4	452944	GCTCAGTGCTTCTTGTGCAG	TGGCTGCTAGGAACCAGTCT	146
bA180N18A.C1.2.mRNA	e1	452945	CCCCTGATCGTGAACAACA	CTCTGAGTCTTTGCGCTGGT	154
dJ773N10.C1.1.mRNA	e2	452946	CAGCCTGCATCTTCTCTTT	AGACCTTCTCCAGCTCCTCC	125
dJ1003J2.C1.1	e2	452947	CCCTGAATGAGAAGGAGCTG	CACGGACTCAGTGACATGCT	148

	e4	452948	CTGTCTCTTTGTGGGGCTGT	ACAGGACATTCACTCCAGGG	102
	e7	452949	ACCCAGGTCTTCTTTGCCTT	GCCAACACTGACGTGAAGAA	134
	e9	452950	CCTTCATCGCCTTCACTGAG	GTGAACATCTCCTTGGGCAC	169
	e12	452951	CGCTACCTGTATTTCCTCAA	CCCTTCTTGTAGGACACGGA	149
bA470L19.C1.2.mRNA	e1	452952	CACCAAGCATTCCATACGTG	GAACCCAATGGGGATTCTTT	150
bA284N8.C1.2/3	e2	452953	ATGCTCGGCTGTCTTCAAGT	AATGGTGAGTCATTCTGGGC	128
bA165H20.C1.3.mRNA	e3	452954	TGTTACTTCACCAACTGGGC	TGGTGATCTCGTTGTTCTGC	127
	e5	452955	TTCCACTCCTGAGAACCACC	CTGCACCAGGACAGTGAAGA	151
	e7	452956	CTATGACCTCCATGGCTCCT	ACATTGAGGTAGGCGTTGCT	96
	e10	452957	AACAACCTTGGAGGTGCCAT	TTGTACTCTGCAGGCCCAGA	124
dJ1125M8.C1.1mRNA	e2	452958	GCGGATAACTACCCTTTTGG	AAATAACACCCAGGCCCTCT	128
	e4	452959	ATGCAGGCAGGTACCAGAAA	TTCTTAAATCGAGGCACCAA	91
	e6 3'UTR	452960	ACGTTACTGTGGCCCTCTTG	ACAGAAACCCACAGACCCAG	154
dJ1125M8.C1.2	e1	452961	GAATGGAGGAGCAGGGTGTA	TCCAGGTAGTTGGTGAAGGG	121
	e3	452962	ACAACAGGTTCAATCCAGC	TGTCATAGCCCAGGAACACA	105
	e5	452963	ACCCGCCAGTATTGTGGAGA	GGCAATCTGCCAGTACAGTT	107
	e8	452964	AACAATGGCTACTGCAGGCT	CTAGGCAGAGAAGGCCAAAGC	153
bA552M11.C1.4.1/2	e2 .2	452965	ACCACGTGGGATTGTATGTT	GGATGCCAAATTAAGAGCCA	137
	e3/4 .1	452966	CCTTTTGTGCTGGGGTTCTA	GCTGGAGGATCTGAGTGAGG	121
	e5	452967	TGAGGCTTGAATCCATTTCC	CTCTGGCCAGGAAAAGACTG	175
bA552M11.C1.5	e1/2	452968	TGCTTCCTCCAGTCATGTG	TGGTCAGGCAGGACATAGTG	120
	e3/4	452969	CAGGCAACAAAACCAGAAGC	CCCAAACCCGTGATCAGTAT	103
	e5	452970	ATCATTTGCAGCCAGGTAGC	GTCCCCAATCCAGATTCTCC	154
dJ836N10.C1.1	e2/3	452971	GGAAGAACAAGGAAAAGGGC	CTCAATGCTTCCCCTCACTG	176
	e4	452972	AAAAGCCAGAGCTTCTGAC	TGTGGTCCCTTTCTTCTTGT	120
dJ1073O3.C1.3	e1	452973	CTGGGCTGAAAACGTCTTG	GTTGGGCTCAAGAAGTCCAT	134
	e3	452974	GACCTGGTGTGCTCAGGATT	TTCCCATTGATCATACCCGT	144
dJ1037B23.C1.1.mRNA	e2	452975	TCCCTCTCTGCTAATCCCC	ACCTCAGCTGGGATATCTGG	122
	e4	452976	AGCGTGGACTTGGGAGAGAT	GTGATGTCCATCGCCTTGAG	107
	e6	452977	TAGGAGTCTGTCGTGTGGGG	TTACCTCCACCAAGGAGTGC	114
	e8 3'UTR	452978	AAACAGTGTTGTGCAGTCGC	CATCACCTTGGGAGACACAA	144
dJ1156J9.C1.1	e1 5'UTR	452979	ACCTTGGAGCGGGATCTTAT	TGCCAGGGAATTGTTGTATG	127
dJ929G5.C1.1.mRNA	e2	452980	TCCTGTTGAAGAGTGGCTCC	TCCAGAATAAGTGGATTCCG	157
	e4	452981	GTTTGTGTTTCGTGCCCTTT	TATTGCACAATGCCCTGGTA	120
	e6	452982	CAGTAACAATGCCACTGGCC	CTTCTTTACTCGCCGTTTCT	118
	e8	452983	GCAATATGACAAGGACCGCT	TACGAGGCTGAAGTCCAAGC	121
bA12L8.C1.1.mRNA	e2	452984	CATCCTCATTGCACTGGTTG	TGCACGTGCTTATGGATCTC	159
dJ655J12.C1.2.mRNA	e1	452985	AAGACAAGGAAGAGCACCTG	GAGTCCTTGAAGTGGTCGGA	120
	e2	452986	GCTCTGTTCAAGGAAAATGCC	TGATCATCAGTGAGCCAAGC	165
dJ655J12.C1.3.mRNA	e2	452987	AGTCCTCCCTGAACTGTTGC	TGGGCATGAGATAAAACACG	106
dJ686J16.C1.1.mRNA	e1/2	452988	GGGCAGTGTCCAATTTATGG	GGAAGGAGGACTGATGGTGA	116
bA39H13.C1.1.mRNA	e1	452989	AAAAACCCAGCTGGACAATG	TCAGCAAGATTCTCGGTCT	142
	e2	452990	ATCTGGAAGCAGAGCCAGTA	CCATTTCAGAGCTTCTGTGC	90
bA42I21.C1.1.mRNA	e1	452991	CACATGCGTCGGCTTAAATG	CCTCCACGATCGATGTTTCT	95
	e2	452992	CCCTCGCTGGGAAAGACATA	TGCTGGGGGAAAAGATTACT	139
dJ776P7.C1.1	e1	452993	GGCACTCTATTCGCACGTCT	CTCCATCATCCCAGGACACT	99
	e1/2	452994	GCTGAGAGGATTATGGAGGC	CTGAACTCTGCCCCTTACCA	101
	e4	452995	CTGTCCTCCCACTGGAATGT	TTCCGAGGTGAAGGAGAAAG	145
dJ832K2.C1.1.mRNA	e1	452996	AAAAACTCCAGGACCTCCGT	ACCTGCAGCCTCAGTTTCAC	171
	e6/7	452997	CCGCATAATACCACCCTTTT	CAGCTGTTTCGTTTGCATCT	131
dJ832K2.C1.2.mRNA	e2	452998	CCTCCAAACACAGGCTCTCT	CATGATGTACCTGCCAGCTC	126
dJ832K2.C1.3.mRNA	e2	452999	CCTTCAAGAAGCCCATAGC	CAACATTGGAGTGGAGAGCA	146

	e5	453000	AGGCAAGGATAACGCAGAGA	CTTAGGTTCTGGTTGGTGGG	133
	e8	453001	ATCCCTTCAGCACTCACTCC	TCTTTGGGTTTTCTTTGCC	98
bA224F24.C1.1.mRNA	e1	453002	TTAGAGGCCAATGCTTCTCC	AGCGAGGGTTCATATCTT	95
	e4	453003	ACGGCAGCAAAAGCAATTAT	TTCTTTTCATTTTCCCGTCG	125
	e6	453004	GGGCTTTAACAATCTCAGC	CTGGTTAACTGCTGCCAGGT	124
	e8	453005	TTGCCTGCTTGATGTATGAC	CTCTGAAGTTGGCATGGCTT	131
	e11	453006	AAGAAGATCTCGTCCCACCC	GACAGAGTGAGGGCAGAAGG	105
	e15	453007	AGCAACCGAGAACCTTCAGA	AGAGACTCATGTTGGGGCTG	149
dJ794L19.C1.1.mRNA	e1	453008	GGCGGCTAAAATGAGTGAAA	ATAGACAGGTCCAGCCCCTT	141
	e3	453009	AGGATGTTTCTGCCATGAG	TTTTATTGTCCACAGGCACA	94
	e5	453010	CTCGAGTTCATGTGATTCGC	AGGCCGTAACGTGGTGAAC	123
	e8	453011	TACCAACTCCTCCCTCGTTG	CATGTGTGGTGATGAGGAGC	137
dJ834N19.C1.1.mRNA	e1	453012	TACCGTCCAGACTCCAGGTC	AGGTCCTCTCTTTGCCCTCC	93
	e3	453013	CAGTAACTGAGGAGGGCCAC	GGCTGCGATAGAAAGCAAAAG	143
dJ834N19.C1.2.mRNA	e2	453014	AGACGAGGTCTTGCCACATT	GCATGGTGGCTTATGCTGTA	108
dJ599G15.C1.5.mRNA	e1	453015	TCGTAGCCATTATCCAACC	CCTGTCCTTGTAGTGGGCAT	129
dJ599G15.C1.6.mRNA	e1	453016	ACTTTCAGGAGCCACATGC	TCTACTGGAAGAGCACCAGC	95
dJ1042I8.C1.4.mRNA	e2	453017	ATGCTGGCCACAATCTACCT	GATCACTCCCCACAGCACTT	127
	e3	453018	TGGTCCAGTGAGAAAGCAGA	CCGGCCATTTGAGTTACAAG	125
	e5	453019	GGAACGAGAGCTGATCCAGT	AGCTGTTCTCGGAAGTCCTG	138
	e7	453020	GGAGGAATGTGCCATCACTT	GAGCATCCTGCCATTCTCT	152
	e9	453021	AGGAAGCTGCAGGAGTCTGA	CCAAGAAAGTGCCTTCACAA	124

Table 2.5: Exon specific primer pairs designed to pharmacogenomic gene targets. An annealing temperature of 60°C was used for PCR reactions except where listed in chapter 6.

Target	Chr	Exon	stSG #	Primer 1	Primer 2	bp
GSTM4	1	1	452701	TCCGGACCTTGCTCCCTGAA	CCTAGTCTACACTGCACTGC	528
		2	452702	TTCCCTCCTTAGGGCTATCT	TGTCATAGTCAGGAGCTGCC	724
		3/4	452703	TCACTTCTTCTTCCCCACGG	ACACAGACTCACTCTGAGCAT	566
		5	452704	TGGCTGGATTGGGGTGCTAT	GGTGCTATTACATCCCACTACA	527
		6/7	452705	GTGTAATAAATGCTGGTATG	AGGACTGACCCCTCATTCAA	701
		8	452706	CCTCAGCACTTGAGCCCACG	AGCAAATAAGACAAGACTAT	689
GSTM2	1	1	452707	AGCCCCATGAGCGCGCTCCA	GGGGAGCCCCATCTCCTCCT	408
		2	452708	GCGGTGGGACGGGGGTGCGT	CCCATCATAATTACCCAGAC	534
		3/4	452709	GCCCCGTCTGGGTAATTAT	CGCATCTTGCAACCAAATCT	719
		5	452710	TCGGCTTGCTGGGCTGTGAG	TGTATTTTCTTTCACTCGTCA	614
		6/7	452711	CAGCTGGGGCCATGCACAAA	GGCGTGAGCCACCGCACATG	508
GSTM1	1	1	452712	CCTGGGAGGCGGGAGGAAGT	GACTTTGTCTGCACCAGGGA	448
		2	452713	TGGGACGAGGGCGCAGGGGA	AAGCCCTGAGGGACACCCGT	535
		3	452714	GCCCCCTGTCTAATTGGGAC	TCACATGAACGAATGCAGGT	484
		4/5	452715	TGTCCACCTGCATTCTGTTCA	AGATGCAGCTCACTGGGGAC	468
		6/7	452716	CTCTGCCTTCTGATCAGTTT	GATAATTCTGTTACCTTACT	709
GSTM5	1	1	452717	ACTGGGAGGCGGGAGGGGGC	GACTTTCTCTGCACCAGGCC	448
		2	452718	TAAGCGAGGGTCTCTGGTG	AACCCAATTAGACAGGGTGT	548
		3/4	452719	CTGGGGCGGGATGCTGGACA	TGACCAGCTCCATGTGGTTA	878

		5	452720	AATGTGCGGGGGGAAGGTGA	GGTAGCAGATCATGACCAGT	409
		6/7	452721	GAAGAGCATCTCATTCTGAT	GTATAATGTGCTGGGCATGA	663
		8	452722	GCCTGCAGCAAAGCTACTTG	ACAGTCCTGAGTCAAGGGAG	621
GSTM3	1	1	452723	CGGCCCTGTGGAGCCGCGGA	CAGCGGTTCAAGCGACTGCGC	520
		2/3	452724	CCCCGGGCCGGGGAACGTTA	GCAAGGATGGATATACTTGAA	622
		4/5	452725	TGTTCACTGCCCTGCAAGTGT	GCAGCAGAATGGAACAGAGA	463
		6/7	452726	GTGCTGGTGCCTCTTCTTTC	CCCATTAGGCAAAAGCCGGG	567
		8	452727	GGTTGGGGTCGTTATAAGAT	TCTCCTACCCCGTGGTCACA	748
GSTP1	11	1	158595	GGTCCTCTCCTGCTGTCTG	CCCCTGAAAGCCGCTAAC	465
		2	158596	GTTAGCGGCTTTCAGGGG	GAGGGAACAGGGAAACAGGT	384
		3	158597	GCCCCAGTGTTGTGTGAAAT	AGGTCTCCGTCCTGGAAGCTT	385
		3/4	158591	TCTCGTACTTCTCCCTCCCC	GATTTAAACAAAAGGGCTCCG	399
		5	158592	ACATCCTCTTCCCCTCCTCC	AGGTTGTGTCTTGTCCCAGG	399
		6	158593	AAGGATGGACAGGCAGAATG	CATCCCCTAGGTCTGCTCTG	399
		7	158594	GCTTCCAGATGGACACAGGT	TGCTGGAGGAGCTGTTTTCT	498
GSTT1	22	1	140015	CTCAAACCAGACCAGCAAT	CTAAAGAGTGTCCCAGGCGT	348
		2	140017	TGGAATAGCAGGAAGGCAAG	GTCTTTGCCAACCAGGAGTG	351
		3	452728	GACTATGTATGAAATACCCA	CTGGTGCCTGAACACCTTTG	276
		4	452729	GCTCAGCATCACTAATCATT	GATTTGGGGACCACAGATCT	406
		5	140020	GGGGGTTGTCTTTTGCATAG	CCTGCTTATGCTGCCACAC	659
CYP1A1	15	1a	452730	CTGACACTCTAGATATTGGCT	GTCAGAGGCAATGGAGAAAC	556
		1b	452731	ATGGTCAGAGCATGTCCTTC	CCCAGGCCCTGATGCCATCT	533
		2/3/4	452732	CCTGTGGACTTTCCCTACCT	CAGTGGCTCCATGGGGCCTT	564
		5/6	452733	TTGCCCTGAGCCTGACTGAG	GGTAGACAGAGTCTAGGCCT	637
		3' UTRa	452734	TTGAGAGCCCTGAGGCCTAG	CAGGACAGCAATAAGGGTCT	620
		3' UTRb	452735	CAGCAAGTTAGAACTAGCCA	GGCTACACCTCTTCACTGCT	697
CYP1A2	15	1a	452736	ATCTCAACCCTCAGCCTGGT	CTCATCGCTACTCTCAGGGA	700
		1b	452737	GCCCTCAACACCTTCTCCAT	TCTGAGGTGTCCAGAGCCTT	536
		2/3	452738	ACCTTGGAAGTGCCAGAGGT	TCAAGGCTTCTCCTGGCTAT	753
		4	452739	GACAGTCTTACATAAGAGTG	CAATAGGGTCATGCTTGTGA	511
		5	452740	TGCTGAAGTTAAAGAACAGG	GATTATAGGCTTGAGCCACT	484
		6	452741	CCATCTCCTCTGTTCCCTCTT	GCCTCCTAAAATGCTGGGAT	464
CYP2A6	19	½	452742	GGCAGTATAAAGGCAAACCA	GAACACTGAGACCTTCGTGT	722
		¾	452743	TGTCTCCATTCCCGCGTTCA	GCAGTTGGCAGGTTGTGGTA	626
		5	452744	CAGCCTCGTTTAAATACCTG	GGATTACAGGCTGTTAGCCA	588
		6	452745	GAGCGAGTCTGGTAGATCTA	CCTGTCTCTGGACAGCAAGT	404
		7	452746	TGGCACAACCTGGTTAACAG	CAGGGTCTAGAAAGCTTCTA	467
		8	452747	CCTGTTTCAGAGATGTGAAC	GGTAGATTCTAACAGGAAGT	443
		9	452748	TGCACTGAGAGTGGGCTTCA	ATTAGGTGAGCGTGCAATGG	538
CYP3A4	7	1	452755	ACTGCAGGCAGAGCACAGGT	GGCATGATCTCAGCTCACTG	613
		2	452756	GACCATGAAGACTTCAGCTG	GAGGTTCTGAGAGTTAGCA	519
		3	452757	GACATCAGAAAGACAAAGAG	TCCATTGCAATACTCTACA	510
		4	452758	CATATGAAGACTTGAGTGGC	GCACATAAAGCTGGTGAAAT	549
		5/6	452759	CCTCCACAACCTGATGTAGGA	GGAATATCAGCTCCATGGCA	589
		7	452760	AGTGTCTCCATCACACCCAG	ATGATGACAGGGTTTGTGAC	592

		8	452761	GTCATAGAAGGAATGGCTTC	GCTGTCTCTGACTCATTCTC	476
		9	452762	CCATCTCACATGATAGCCAG	TCTAGCATGCCAGGTTTGCT	512
		10	452763	GCCCACATTCTCGAAGACCT	TTCAGAGCCTTCTACATAG	523
		11	452764	ACATCTCAGTGGGCCACTGA	GGACATAACTGATGACCTTC	654
		12	452765	CAGCCCACAAAAGTATCCTG	GGCCTAATTGATTCTTTGGC	419
		13a	452766	CCTCAACACTGAAGGAGTGT	GTGCAGGAAAGCATCTGATA	669
		13b	452767	CACATGTTTTCTCTGGAGTA	GTGCTTTTAGGCTTATTGCT	791
NFE2L2	2	1	452768	AGAGCGCTGCCCTTATTTGC	TCCTGGCTCTGGCCAGACGT	589
		2	452769	CACTTCCCACCATCAACAGT	GTGTTTCCTTAAACCTGCCA	419
		3	452770	GTGCATCAAAGTGATCTCTG	CTTCGTTTATTGCCAGCTG	577
		4	452771	GGGTCATGACTGGTTAGTAA	TCAGAGTTCAGATCAGAC	527
		5a	452772	GAGATAAGCCTGAAGATAAT	TCTTCCACTTCAGAATCACT	649
		5b	452773	TGTGGCATCACCAGAACACT	GCTGCAGGGAGTATTCATA	695
		3' UTR	452774	GCATGCTACGTGATGAAGAT	TTATTTCTCTGTAACCCTGG	756

2.10 World Wide Web addresses

ACeDB	http://www.acedb.org/
ACT	http://www.sanger.ac.uk/Software/ACT
Baylor College of Medicine Search Launcher	http://searchlauncher.bcm.tmc.edu/
British Columbia Genome Sequence Centre	http://www.bcgsc.bc.ca/
Chromosome 1 Mapping Project - Sanger Institute	http://www.sanger.ac.uk/HGP/Chr1/
CHLC	http://chlc.org/
Coriell	http://locus.umdj.edu/ccr
dbSNP	http://www.ncbi.nlm.nih.gov/SNP/index.html
DOTTER	www.cgr.ki.se/cgr/groups/sonn/Dotter.html
EMBL	http://www.ebi.ac.uk/
Ensembl	http://www.ensembl.org/
GDB	http://gdbwww.gdb.org/
Généthon	http://www.genethon.fr/php/index.php
HGNC	http://www.gene.ucl.ac.uk/nomenclature/
INTERPRO	http://www.ebi.ac.uk/interpro/scan.html
Incyte	http://incyte.com/company/news/1999/genes.shtml
Locus Link	http://www.ncbi.nlm.nih.gov/LocusLink/
National Centre for Biotechnology Information	http://www.ncbi.nlm.nih.gov/

OMIM	http://www3.ncbi.nlm.nih.gov/Omim/
Primer 3	http://www.sanger.ac.uk/cgi-bin/primer3.cgi
PIX	http://www.hgmp.mrc.ac.uk/Registered/Webapp/pix/
PSI-BLAST	http://www.ncbi.nlm.nih.gov/BLAST/
RepeatMasker	http://ftp.genome.washington.edu/RM/webrepeatmaskerhelp.html
The Institute for Genome Research	http://www.tigr.org/
The SNP Consortium	http://snp.cshl.org
The Wellcome Trust Sanger Institute	http://www.sanger.ac.uk/
Unigene	http://www.ncbi.nlm.nih.gov/UniGene/
University of California, Santa Cruz genome browser	http://genome.cse.ucsc.edu/
Washington University Center Genome Sequencing Center	http://genome.wustl.edu/
Whitehead Institute	http://www-genome.wi.mit.edu/

Methods

2.11 Isolation of bacterial clone DNA

2.11.1 Miniprep of cosmid

1. Ten ml of 2 X TY containing 30 µg/ml of appropriate antibiotic (kanamycin for cosmids and PACs, chloramphenicol for BACs) were inoculated with a scraping from the frozen glycerol stock of the chosen bacterial clone and incubated overnight at 37°C with shaking.
2. The cells were collected by centrifugation at 4,000 rpm for 10 minutes at room temperature in a Beckman J6-MC, re-suspended in 200 µl of GTE in a 1.5 ml eppendorf tube, and left on ice for 5 minutes.
3. 400 µl of freshly prepared 0.2 M NaOH/1% SDS were added to the cells, mixed by gentle inversion, and the sample left on ice for another 5 minutes.
4. 300 µl of 3 M K⁺/5 M Ac⁻ (pH 4.8) were added, mixed by gentle inversion and left on ice for 10 minutes. The sample was centrifuged for 10 minutes at 14,000 rpm in an eppendorf microfuge.

5. The supernatant was transferred to a fresh tube and mixed with 600 μl of cold isopropanol and left on ice for at least 10 minutes. The tube was subjected to centrifugation for 15 minutes at 14,000 rpm in an Eppendorf microfuge at 4°C to pellet the DNA, the supernatant removed and the pellet re-suspended in 200 μl of $T_{0.1}\text{E}$.
6. 200 μl of 50:50 (v/v) phenol/chloroform were added to the sample, which was vortexed and briefly centrifuged. 20 μl of 3 M sodium acetate (pH 5.2) and 200 μl of isopropanol were added to the aqueous layer, and the sample placed at -20°C for at least 10 minutes. The tube was subjected to centrifugation at 14,000 rpm in an Eppendorf microfuge for 15 minutes at 4°C to pellet the DNA. The pellet was washed with 70% ethanol and re-suspended in 50 μl of $T_{0.1}\text{E}$.
7. 1 μl of 10 mg/ml RNase was added and the sample incubated at 37°C for 1 hour prior to storage at -20°C.

2.11.2 Microprep of cosmid, PAC and BAC DNA for restriction digest fingerprinting

1. 500 μl of 2 X TY containing 30 $\mu\text{g}/\text{ml}$ of appropriate antibiotic (kanamycin for cosmids and PACs, chloramphenicol for BACs) were added to a 96-well deep-well microtitre plate (COSTAR).
2. Each well was inoculated from a glycerol stock with either a 96-well inoculating tool, or a sterile cocktail stick. A plate sealer (Dyntax) was placed on top of the plate to seal the wells, and the cultures grown for 18 hours at 37°C with gentle shaking.
3. For each well, 250 μl of the overnight growth were transferred to a clean microtitre plate. The cells were collected by centrifugation (Sorvall RT7, Du Pont Company Sorvall, Delaware US) at 1550 g for 4 minutes.
4. For each well, the supernatant was removed and the pellet re-suspended in 25 μl of GTE, by vortexing gently (a cocktail stick was used for resuspending pellets still attached to the plate).
5. 25 μl of GTE were added to each well and gently mixed. 25 μl of freshly prepared 0.2 M NaOH/1% SDS were added, mixed and left to stand for 5 minutes at RT.
6. 25 μl of 3 M K^+ /5 M Ac^- (pH5.0) were added, mixed and left at RT for 5 minutes. A plate sealer was placed on top of the plate and the plate was vortexed gently for 10 seconds, prior to centrifugation of the samples in a microtitre plate in a Sorvall RT7 centrifuge at 1800 g for 10 minutes at 4°C (Sorvall RT7, Du Pont Company Sorvall, Delaware US).

7. 75 μ l of the supernatant from each well were transferred to a fresh microtitre plate containing 150 μ l of 96% ethanol (or 100 μ l of isopropanol) and left at -20 °C for 30 minutes.
8. The microtitre plate containing the samples was centrifuged at 1800 g in a Sorvall RT7 centrifuge for 10 minutes at 4°C. The supernatant was discarded and the samples drained on a tissue.
9. 25 μ l of ddH₂O were added to each well and the pellet resuspended by tapping or with a sterile toothpick. 25 μ l of 4.4 M lithium chloride were then added to each well mixed by tapping and left for 60 minutes at 4°C.
10. After centrifuging the samples in a Sorvall RT7 centrifuge at 1800 g for 10 minutes at 4°C, the supernatant from each well was added to 100 μ l of 96% ethanol in a fresh plate and left for 60 minutes. The samples were then spun in a Sorvall RT7 at 1800g for 10 minutes at 4°C, the supernatant discarded and 200 μ l of 70% ethanol added. The pellets were then air dried until transparent.
11. 10 μ l of T_{0.1}E were added to each well and mixed by careful pipetting up and down. The resuspended DNA was then used directly for fingerprinting or stored at -20 °C.

2.11.3 Filterprep of cosmid, PAC and BAC DNA for restriction digest fingerprinting

1. Steps 1 – 6 from the microprep procedure (2.11.2) were followed before progressing to step 2 of the filterprep procedure.
2. A microtitre plate containing 100 μ l of isopropanol was taped to the bottom of 2 μ m filter-bottomed plate (Millipore cat. no. MAGVN2250). The total well volume of the sample was transferred to the filter-bottomed plate and the sample was filtered by centrifugation in a Sorvall RT7 at 1550 g for 2 minutes at 20°C.
3. The filter-bottomed plate was removed and the microtitre plate was left at RT for 30 minutes, before samples were centrifuged in a Sorvall RT7 at 1500g for 20 minutes at 20°C.
4. The supernatant was tipped from the microtitre plate and the DNA dried by inverting the plate and placing it on clean tissue paper, ensuring no disruption of the pellet.
5. 100 μ l of 70% ethanol were added to the dried DNA to wash the pellet, mixed gently, and the DNA precipitated by centrifugation in a Sorvall RT7 at 1500g for 10 minutes at 20°C. For restriction digest fingerprinting the wash was repeated.
6. 5 μ l of freshly prepared T_{0.1}E / 1 μ g/ml RNase were added and mixed gently to resuspend the DNA. Samples were stored at -20°C.

2.12 Bacterial clone fingerprinting

2.12.1 Radioactive fingerprinting

1. For each well of a 96-well microtitre plate of sample DNA, a premix containing 1x NEB2 buffer (as supplied by New England Biolabs), 0.72 U *Hind* III, 1.3 U *Sau*3AI, 0.4 U Reverse Transcriptase, 0.07 μ l [α -³²P]dATP (3000Ci/mmol), 0.04 μ l 10 mM ddG was prepared in a 1.5 ml microfuge tube.
2. 2 μ l of premix were added to the sample DNA using a Hamilton repeat dispenser. The reaction was mixed by gentle agitation and the samples were centrifuged in a Sorvall RT7 at 150 g for 10 seconds.
3. The reaction was incubated for 1 hour at 37°C. The reaction was then stopped by the addition of 2 μ l formamide dye.
4. The sample DNA was denatured at 80°C for 10 minutes and loaded in groups of 6 onto a 4% polyacrylamide gel, leaving the first well and every subsequent seventh well of empty (see Section 2.14.2). Marker DNA (see Section 2.13.1) was denatured by boiling for 5 minutes and 2 μ l were loaded in the first well and every seventh well. Fragments were resolved by running the gel at 74 W for 1.5 hours (or until the bromophenol blue dye front reached the bottom of the gel).
5. Following electrophoresis, the back plate was removed and the gel was fixed in a 10 % glacial acetic acid solution for 10 minutes then washed in water for 25 minutes. The gel was dried onto the front plate by incubation at 80°C for 45 minutes in an oven. Autoradiography was for 72 hours at RT.
6. The autoradiograph was scanned using a flat bed scanner (Amersham) and the digitised version imported to IMAGE.

2.12.2 Fluorescent fingerprinting

1. For one 96-well microtitre plate of sample DNAs, three digest premixes were prepared, one for each fluorescent label, in three 1.5 ml microfuge tubes labelled TET, HEX and NED. Each premix contained 25.5 μ l $T_{0.1}E$, 24.5 μ l NEB2 buffer, 5.0 μ l *Hind* III (20 U/ μ L), 8.0 μ l Taq FS, (32 U/ μ l) and 3.0 μ l *Sau*3AI (30 U/ μ l) and 4.0 μ l of the appropriate ddA-dye. Each premix was mixed prior to being aliquoted.
2. 2 μ l of the TET premix were added to wells A1-H4 of the microtitre plate containing sample DNAs using a Hamilton repeat dispenser. Similarly, 2 μ l of the HEX premix were added to wells A5-H8 and 2 μ l of the NED premix were added to wells A9-H12. The plate was covered with a plate sealer, the reaction mixed by gentle agitation on a vortex. In order to ensure the sample was in the bottom of the wells the plate was centrifuged at 150 g for 10 seconds (Sorvall RT7, Du Pont Company Sorvall, Delaware US).
3. The reaction was incubated for 1 hour at 37°C.
4. To precipitate the DNA, 7 μ l of 0.3 M sodium acetate (pH 5.2) and 40 μ l 96% ethanol were added to each well. For multiplexing the samples, rows 5 and 9 were added to row 1, rows 6 and 10 were added to row 2, rows 7 and 11 were added to row 3, and rows 8 and 12 were added to row 4 respectively, using a multichannel pipette.
5. The samples were incubated at RT for 30 minutes in the dark.
6. The samples in the microtitre plate were centrifuged in a Sorvall RT7 at 1550 g for 20 minutes at 20°C to pellet the DNA.
7. The supernatants were discarded and the pellets dried by tapping the plate face down onto tissue paper.
8. The pellets were washed by adding 100 μ l of 70% ethanol to each well, mixed gently tapping the plate, and the samples centrifuged in a Sorvall RT7 at 1550 g for 10 minutes at 20°C.
9. The supernatants were discarded and the pellet dried as in step 7.
10. The fingerprinted DNAs were re-suspended in 5 μ L $T_{0.1}E$.
11. Prior to loading, 2 μ l of the marker DNA (see Section 2.13.2) were added to each sample using a Hamilton repeat dispenser. The samples were denatured for 10 minutes at 80°C. 1.25 μ l of each sample were loaded on a 5% denaturing acrylamide gel and resolved on an ABI377 Automated DNA sequencer using a 0.2 mm, 12 cm well-to-read 4.5% denaturing polyacrylamide gel (prepared by Sanger Institute Gel Production Team). Data were collected using the ABI Prism Collection Software v1.1.
12. After data collection, the gel image was transferred to a UNIX workstation for entry into IMAGE.

2.12.3 *Hind* III and *Eco* RI fingerprinting

1. For one 96-well microtitre plate of sample DNA, a premix containing 231 μl H_2O , 99 μl Boehringer buffer B (50 mM NaCl, 10 mM Tris-HCl, 10 mM MgCl_2 , 1 mM DTE, pH 7.5), 55 μl *Hind* III 10U/ μl (or *Eco* RI 10U/ μl), was prepared in a 1.5 ml microfuge tube, and mixed using a vortex. 4 μl of the premix were added to each well of a 96-well microtitre plate containing previously prepared DNA (see Section 2.11.2), and the plate covered with a plate sealer (Dynex).
2. The reactions were mixed gently on a vortex and incubated at 37 °C for 2 hours.
3. The reactions were terminated by the addition of 2 μl of buffer II and either loaded straight away or stored at 4 °C.
4. 0.8 μl of the marker (see Section 2.13.3) were added to the first well and then every sixth well of a freshly prepared 1% agarose/1x TAE gel (see Section 2.14.1 for preparation). 1 μl of each sample was loaded (i.e. wells 2-5, 7-10 *etc.*) between the marker lanes. Fragments were resolved by electrophoresis through the gel at 4 °C in a cold room for 15 hours at 90 volts.
5. Following electrophoresis, the gel was cut down so the length was 19-20 cm and stained in Vista Green (mix 5 ml 1 M Tris HCL, 0.5 ml 0.1 M EDTA, 50 μl Vista Green, make up to 500 ml with H_2O) for 30-45 minutes on a shaker. The gel was washed with dd H_2O to remove excessive stain.
6. The gels were scanned on a FluorImager SI. The parameters were set to 530 nm for emission filter, the pixel size was 100 microns, detection sensitivity was normal, digital resolution was at 16 bits, dye was single label, excitation filter was 488 nm, Em filter 1530 nm and PMT voltage was 800.
7. The gel image was transferred to a UNIX workstation for entry into IMAGE.

2.13 Marker preparation

2.13.1 Radioactive fingerprinting marker

1. 171 μl of $T_{0.1}\text{E}$, 25 μl of 10 X NEB2 buffer (as supplied by New England Biolabs), 16.5 μl of lambda DNA (500 $\mu\text{g}/\text{ml}$) and 5 μl of *Sau3AI* (50 U/ μl) was added to a 1.5 ml Eppendorf microfuge tube and incubated at 37°C for 1 hour
2. To a 43.5 μl aliquot of digested lambda DNA (from step 1) in a 1.5 ml Eppendorf microfuge tube was added 2.0 μl 10 mM dGTP, 2.0 μl 10 mM ddTTP, 4.0 μl [α - ^{35}S] dATP (3000Ci/mmol), 1.0 μl AMV reverse transcriptase (10 U/ μl) and incubated at 37°C for 1 hour.
3. The reaction was stopped by the addition of 53 μl of 1:15 dilution of formamide dye.
4. The marker was stored at -20°C.

2.13.2 Fluorescent fingerprinting marker

1. 70 μl $T_{0.1}\text{E}$, 10 μl NEB2, 6 μl lambda DNA (500 ng/ μl), 6 μl *BsaI* 1 (2.5 U/ μl), 4 μl TaqFS (32 U/ μl), 4 μl of 10 mM ddC-ROX were added to a 1.5 ml microfuge tube and incubated for 1 hour at 60°C.
2. 100 μl of 0.3 M sodium acetate (pH 5.2) and 400 μl 96% ethanol were added to the reaction mix and incubated at RT in the dark for 15 minutes, then at -20°C for 20 minutes. The Eppendorf microfuge tube was subjected to centrifugation in a bench top centrifuge at maximum speed for 20 minutes to pellet the DNA.
3. The supernatant was discarded and the DNA pellet dried by tapping the tube gently onto tissue paper. The pellet was washed by adding 200 μl 70% ethanol and spun in a bench top centrifuge at maximum speed for 5 minutes, the supernatant discarded and the pellet dried as described in step 2.
4. The DNA was re-suspended in 120 μl $T_{0.1}\text{E}$ and 120 μl blue dextran formamide dye.
5. The marker was stored at -20°C.

2.13.3 For *Hind III* fingerprinting

1. 19.2 μl $T_{0.1}\text{E}$, 1.5 μl Analytical Marker DNA wide range, 0.2 μl Molecular Weight Marker V and 4.2 μl 6x loading dye were added to a 1.5 ml microfuge tube.
2. The marker was stored at -20°C.

2.14 Gel preparation and electrophoresis

2.14.1 Agarose gel preparation and electrophoresis

1. Agarose gels were prepared in 1x TBE (or 1x TAE, for *Hind* III fingerprinting) containing 250 ng/μl ethidium bromide and the appropriate percentage of agarose according to the size of fragments being separated: 2.5 % agarose gels were used for electrophoresis of fragments below 1 kb; 1.0% agarose gels were used for analysis of larger fragments. Electrophoresis was performed at 50 - 90 V for 15 - 45 minutes depending on the separation required.

2.14.2 Polyacrylamide gel preparation for radioactive fingerprinting

1. 42.0 g of urea were dissolved in 10 ml 10x TBE and 35 ml ddH₂O by warming to 37°C, and stirring.
2. A large glass plate (back plate – Gibco BRL) was washed on both sides and one side was treated with 2 % dimethyldichlorosilane, and left to dry.
3. A small glass plate (front plate – Gibco BRL) was washed on both sides with detergent and water and one side was treated with freshly prepared bonding solution (3 ml 96 % ethanol, 50 μl 10 % Acetic acid, 5 μl methacryloxypropyl-trimethoxysilane; Sigma-Aldrich) and left to dry.
4. The front and back plates were taped together along three edges (treated sides facing inwards) separated by 4 mm spacers.
5. 10 ml 40% acrylamide, 800 μl 10 % ammonium persulphate and 80 μl TEMED (KODAK) were added to the dissolved urea solution, mixed and poured in between the glass plates using a 50 ml syringe. A 4 mm, 60 well comb (IBI) was placed in the top of the gel (the edge not taped) and the glass plates clamped with bulldog clips. The gel was left to set for up to 3 hours.

2.15 Construction of small insert library

2.15.1 Library preparation

1. 1 μ l 4 mg/ml PMSF was added per every 100 μ l of flow-sorted chromosome preparations (previously treated with Proteinase K and sarkosyl) for a 40 μ g/ml final concentration and incubated at room temperature for 40 minutes.
2. 20 μ l 5 M NaCl was added to a concentration of 0.2 M. Two volumes of absolute ethanol were added, and the DNA precipitated overnight at -20°C.
3. DNA was pelleted in a microfuge at maximum speed (14,000 rpm) at RT for 15 minutes.
4. The supernatant was removed with a P1000 Gilson pipette and the remainder removed with Gilson P200 pipette, avoiding the pellet. 1 ml 70% ethanol was added and the eppendorf tube centrifuged again at maximum speed for 7 minutes and the supernatant removed as before. Pellets were air-dried for approximately 10 minutes.
5. 17.0 μ l of sterile TE were added directly to the pellet to give approximately 8.0 ng / μ l of flow sorted DNA. DNA was mixed by very gentle flicking and allowed to dissolve for at least 2 hours.
6. 2.0 μ l 10x buffer 2 (as supplied by New England Biolabs), 1.0 μ l HindIII (20 U/ μ l) and 2.0 μ l ddH₂O were added to 15 μ l of flow-sorted DNA which was digested for 3 hours at 37°C.
7. The *Hind* III was inactivated by incubation of the digest at 65°C for 20 minutes.
8. 2.5 μ l (15 ng) of digested flow-sorted DNA, 1 μ l (5 ng) of phosphatased pBluescript II (SK+) vector DNA (5 ng/ μ l) (kindly supplied by Dr. Mark T. Ross), 1 μ l of 10x ligase buffer (NEB), 0.5 μ l of T4 DNA ligase (NEB; 400 U/ μ l) and 6.5 μ l of water (a total reaction volume of 10 μ l) were incubated for 16 hours at 16°C
9. The ligase was inactivated by incubation at 65°C for 10 minutes.
10. 10 μ l of TE were added and the ligation stored at -70°C.
11. 1 μ l of each of the samples were electroporated into *E. coli* XL1-blue electrocompetent cells (see 2.15.2)

2.15.2 Electroporation and library plating.

1. LB agar plates (containing 50 μ g/ml ampicillin) were poured and left to dry before 40 μ l of Xgal and 4 μ l of 200 mg/ml of IPTG were spread on the surface of the plates and left for 2 hours at 37°C to dry.

2. 40 μ l of XL1 blue cells (previously thawed at room temperature and stored on ice) and 1 μ l of *Hind* III digested DNA were added to a 0.1 cm cuvette and mixed. After cells were electroporated at 25 μ FD, 1.8 KV and 200 Ω , 1ml of LB media was added, mixed then the whole sample added to a 50 ml Falcon tube and incubated in a shaking incubator for 45 minutes. at 37°C.
3. 50 μ l were plated on the previously prepared selection agar plates and grown overnight at 37°C and then stored at 4°C for 1 hour to accentuate the blue non-recombinant cells. Recombinant cells were picked into flat bottom microtitre plates containing 150 μ l LB broth containing 50 μ g/ml ampicillin and grown overnight at 37°C . Glycerol was added to the cultures to a final concentration of 7.5% v/v, aliquotted and then stored at -70 °C.

2.16 Applications using the polymerase chain reaction

2.16.1 Primer design

Primers were designed manually using the following guidelines:

1. Primer 3 (<http://www.sanger.ac.uk/cgi-bin/primer3.cgi>) was used to design primers sequences that were 20 bp in length, were possible beginning and ending with a C or G, and with an optimal annealing temperature of 60°C.
2. Where possible sequences were chosen to avoid areas of simple sequence showing non-representative use of the bases and obvious repetitive sequence i.e., runs of single nucleotide (e.g. TTTT) or double nucleotide (CGCGC) motifs.
3. Sequences were chosen to exclude palindromes which will form inhibitory secondary structure, especially at the 3' ends (e.g. GACGTC).
4. As far as possible, sequences were chosen with a GC content of at least 50%.
5. Sequences were chosen to avoid complementarity between pairs of primers, especially at the 3' end, which could result in primers annealing to each other and forming primer dimers.
6. If possible, sequences were chosen which would generate products of at least 100 bp in length.

216.2 Oligonucleotide preparation

All oligonucleotides used were synthesised in house by David Fraser or supplied as working dilutions from Genset. The concentration of the primer in ng/ μ l was determined by measuring the absorbance at 260 nm (Abs_{260}) and multiplying this by 33 and any necessary dilution factor.

2.16.3 Amplification of DNA by PCR

1. 1-3 ng/ μ l of genomic DNA were amplified in a reaction volume of 15 to 50 μ l as required. Reactions contained approximately 1.3 μ M of each oligonucleotide primer, 67 mM Tris-HCl (pH 8.8), 16.6 mM $(NH_4)_2SO_4$, 6.7 mM $MgCl_2$, 0.5 mM of each deoxyribonucleoside triphosphate (dATP, dCTP, dGTP, dTTP), 1.5 U of AmplitaqTM (Cetus Inc.); 10 mM β -mercaptoethanol and 170 μ g/ml of BSA (Sigma Chemical Co., A-4628) were added to the reactions from freshly made stock solutions as the reactions were set up.
2. Unless specified otherwise, cycling conditions were as follows: all reactions were preceeded by an initial denaturing step of 5 minutes at 94°C, followed by 35 cycles of: 94°C for 30 seconds, (primer-specific annealing temperature) for 30 seconds, 60°C for 30 seconds, 72°C for 30; followed by a final extension step of 5 minutes at 72°C. Primer-specific annealing temperatures are given for each primer pair in the text or in Tables 2.3 – 2.9.
3. PCR products were separated on 2.5% agarose minigels as described in Section 2.14.1 and visualised by ethidium bromide staining.

2.17 Radiolabelling of DNA probes

2.17.1 Radiolabelling of PCR products by PCR

PCR products were radiolabelled essentially as described in Bentley et al. (1992).

1. 5 - 10 μ l of PCR product were separated on a 2.5% agarose minigel and visualised by ethidium bromide staining.
2. The gel was rinsed in deionised water to remove excess buffer. The desired band was excised from the gel and placed in 100 μ l of $T_{0.1}E$ at 4°C overnight.

3. 2 µl of the T_{0.1}E were used as template in the PCR-labelling reaction containing 40 ng of each primer, 1 µl of 10x PCR buffer, 0.5 µl of [α -³²P]-dCTP (3,000 Ci/mmol), 0.5 U of *Taq* polymerase (Cetus) and 0.375 mM each of dATP, dTTP and dGTP. Reactions were performed in a 0.5 ml microfuge tube and overlaid with mineral oil (Sigma) in a DNA thermal cycler (Perkin Elmer, USA).
4. PCR cycling conditions were as follows: 94°C for 5 minutes; followed by 20 cycles of: 93°C for 30 seconds, 55°C for 30 seconds, and 72°C for 30 seconds; followed by 72°C for 5 minutes.
5. Probes were pre-reassociated (as described in Section 2.17.2) prior to use if necessary. All probes were boiled for 5 minutes and snap-chilled on ice prior to use.

2.17.2 Pre-reassociation of radiolabelled probes

1. Radiolabelled probe was mixed with 125 µl of 20x SSC and 250 µl of the sheared 10 mg/ml human placental DNA (Sigma) in a final volume of 500 µl.
2. The mix was boiled for 5 minutes, snap-chilled in ice-water, and then added directly to the hybridisation reaction.

2.18 Hybridisation of radiolabelled DNA probes

2.18.1 Hybridisation of DNA probes derived from STSs

1. Filters were prehybridised flat in sandwich boxes for 3 hours in 10-25 ml of hybridisation buffer at 65°C with gentle shaking.
2. Radiolabelled probe was added and hybridised to the filters.
3. Filters were washed twice at RT in 2x SSC for 5 minutes, twice at 65°C in 0.5 x SSC, 1.0% Sarkosyl for 30 minutes. Filters were rinsed at RT in 0.2x SSC prior to draining the excess liquid, wrapping in Saran Wrap (Dow Chemical Co.) and exposing to autoradiograph film.

2.18.2 Stripping radiolabelled probes from hybridisation filters

1. Filters were washed in 0.4 M NaOH for 30 minutes at 42°C followed by 30 minutes in 0.2 M Tris-HCl (pH 7.4), 0.1x SSC, and 1.0% w/v Sarkosyl at 42°C with gentle shaking. Successful removal of radiolabelled probe was assessed by autoradiography.

2.19 Restriction endonuclease digestion

1. 4 µl (approximately 150 ng) of prepared cosmid DNA (described in Section 2.11.1) were digested with *Hind* III using commercial buffers according to manufacturers' instructions in a final volume of 10 µl.
2. 5 µl of each digest were checked for complete digestion by electrophoresis on a 1% agarose minigel and visualised by ethidium bromide staining.

2.20 Clone library screening

2.20.1 cDNA library screening by PCR

The strategy used to screen the cDNA libraries by PCR is illustrated in Figure 2.1.

1. Nine different cDNA libraries were subdivided into 25 subpools of 20,000 clones, which were then combined to produce 5 superpools of 100,000 clones by J. Bye and S. Rhodes. Details of the cDNA libraries are given in Table 2.2.
2. Aliquots of the superpools of each library were arranged in a microtitre plate to facilitate subsequent manipulations with a multi-channel pipetting device.
3. In the primary screen, 5 µl of each superpool were used as template in a 15 µl final volume PCR using buffer and PCR conditions as described in Section 2.16.3.
4. PCR products were loaded on 20 cm x 20 cm 2.5% agarose horizontal slab gels using an 8-way multi-channel pipetting device, separated by electrophoresis and visualised by ethidium bromide staining.
5. In the secondary screen, 5 µl of each of the 5 subpools of 20,000 clones corresponding to the superpool that were positive in the first round, were screened by PCR with the same primer pair as used in step 2. PCR products were separated by electrophoresis through 2.5% agarose minigels and visualised by ethidium bromide staining.

2.20.2 Vectorette PCR on cDNA libraries

1. Vectorette PCR was performed on the superpools of the cDNA libraries (figure 2.1). PCR was performed using 5 µl of the diluted superpools as template in a 15 µl final volume using buffer conditions as described in Section 2.16.3. Primer combinations were as follows: 224 and specific primer A, 224 and specific primer B.
2. PCR was performed in a DNA thermocycle (Omingene) using hot start. Cycling conditions were as follows: an initial denaturation step of 5 minutes at 95°C, followed by 17 cycles of: 94°C for 5 seconds, 65°C for 30 seconds and 72°C for 3 minutes, followed by 18 cycles of: 94°C for 5 seconds, 65°C for 30 seconds and 72°C for 3 minutes, followed by 72°C for 5 minutes. The PCR was paused after 4 minutes of the initial denaturation and 2 µl of Taq premix (containing 0.12 µl Amplitaq, 0.12 µl TaqExtender, 0.12 µl Perfect Match, 0.5 µl 40% sucrose + cresol red, 1.14 µl T_{0.1}E) were added to each reaction (pipetting underneath the oil).
3. Products were separated by electrophoresis through 2.5% agarose gels and visualised by ethidium bromide staining. Products were gel-purified using gel extraction kits and following manufacturer's instructions from either GeneClean™ or Qiagen™ prior to sequencing directly.

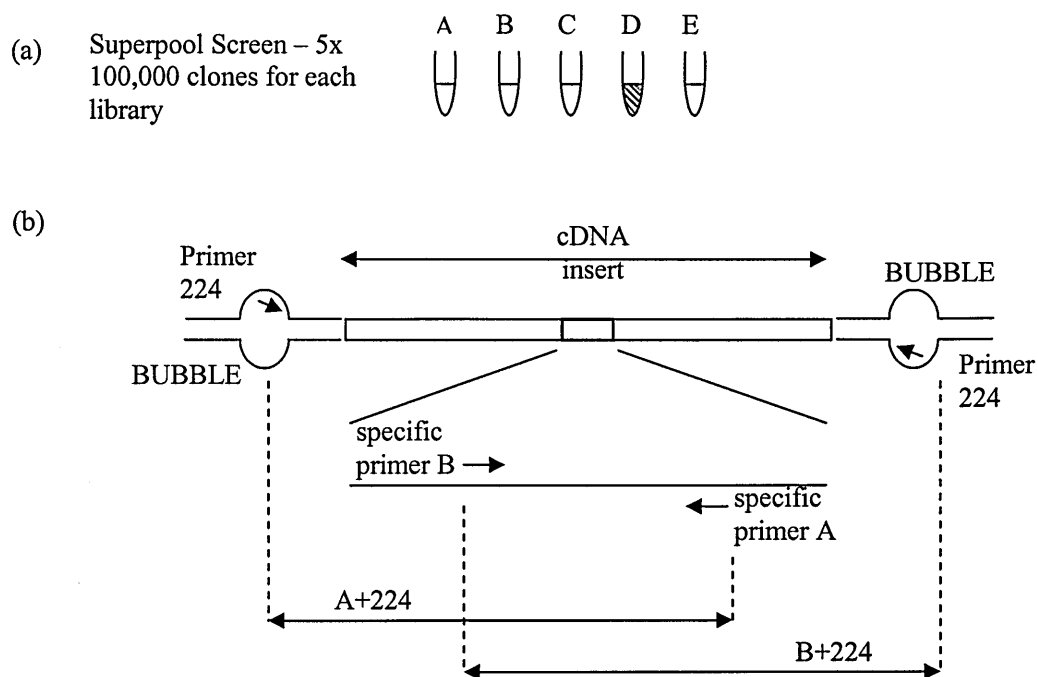


Figure 2.1: Strategy for vectorette PCR screening of cDNA libraries. a) Superpools representing 100,000 clones (A-E) were screened by PCR and positive super pools recorded (e.g. D, shown in red). (b) Rescue of the insert of the cDNA of interest by vectorette PCR. Insert of cDNA is shown as white rectangle; ligated ‘bubble’ is shown in yellow. Original position of primers for pool screening is indicated by a red rectangle. A combination of the ‘bubble’ primer (224) and insert specific primers (e.g A and B) were to generate two products (e.g. 224+A, 224+B) representing the entire insert of the cDNA of interest.

2.21 Exon Amplification

1. Exon-specific primers were diluted from 1 mg / ml to a stock 100 ng / μ l and a working dilution of 8 ng / μ l in T_{0.1}E.
2. 1 μ l 10 X NEB buffer, 1 μ l dNTPs (5mM), 0.33 μ l BSA, 0.14 μ l β ME, 0.12 Amplitaq and 1.41 μ l of T_{0.1}E were added to 1 μ l of individual CEPH DNA (5 ng / μ l) aliquotted in a 384-well PCR plate.
3. Following PCR samples were separated on an agarose gel as described in 2.14.3.
4. Residual primers and dNTPs were removed by the addition of 2 μ l of a premix containing 0.66 μ l of shrimp alkaline phosphatase, 0.66 μ l of reaction buffer, 0.66 μ l of double distilled H₂O and 0.066 μ l of exonuclease I. The 384-well microtitre plate

containing the exon amplified PCR products was incubated at 37°C for 30 minutes, and then 80°C for 15 minutes.

5. Exon specific PCR products were then sequenced by the Research and Development Group or The Sanger Institute Sequencing facility.

2.22 Mapping and sequence analysis software and databases

2.22.1 IMAGE

Gel images from radioactive, fluorescent and *Hind* III gels were processed using IMAGE. Band patterns for each lane were extracted and the data manually edited and normalised by marker locking prior to data entry into another program, fingerprinted contigs (FPC) (Soderlund *et al.*, 1997), for analysis. Within IMAGE several procedures were run on each gel in turn:

Lane tracking – a grid was superimposed and manually edited on each gel image to ensure it exactly matched the lanes on the gel.

Band calling – an analysis module then identified labelled restriction digest fragments within each lane. Manual editing ensured the correct bands are chosen.

Marker locking – A set of DNA fragments of known length or migration distance was loaded as a marker to facilitate normalisation of restriction fragments and permit accurate clone to clone comparisons to be made (see Section 2.13 for specific marker patterns for each method of fingerprinting used). Manual editing of each marker lane ensured the observed experimental marker matched the previously established standard marker pattern.

Normalisation – once marker lanes were locked onto standard marker positions, the bands within the sample lanes were normalised to account for differences in gel to gel run conditions. IMAGE finally generated a 'Bands' file for each gel containing normalised migration distances for all selected bands in each clone lane.

2.22.2 FPC

FPC, which was used for all contig construction described in this thesis, utilises the bands file output from IMAGE as the digitised set restriction fragments for each clones. Fingerprint patterns for each clone were compared to those of all clones in the database. The relationship between two clones was reported as a probability of coincidence, i.e. the probability that bands

in common between two clones overlap by chance. Two variables can be set to filter the reported overlaps:

Cut off – a match between two clones will only be reported if the probability of coincidence is less than or equal to the cut off. When analysing matches between larger insert PAC and BAC clones the tolerance was $1e-08$.

Tolerance – two bands of equal size are considered as their migration distances differ by less than tolerance. For the analysis carried out in this thesis the tolerance was set to 7.

Overlapping clones were identified by automatic analysis and contigs were constructed manually using the available editing tools within FPC. Clones were overlapped by iterative pair-wise analysis by determining the number of bands in common between clones. Subsequent clones were added positioned within the initial clone assembly based on the number of bands they shared with the existing clones in the contig. Marker data was imported from 1ace and integrated into the FPC contigs to identify clone overlaps that could not be identified using pre-determined analysis parameters. A minimum set of clones for sequencing was chosen based on a combination of shared bands and shared marker data.

Contig Sizing – one unit in the contig display represents one fingerprint band which permits for estimates to be made for contig sizes. For each fingerprinting method, a kilobase/band figure was derived. For radioactive cosmid fingerprinting, one band was the equivalent of 3.3 kb, based on the fact the average number of fingerprint bands for bacterial clones in comparison to finished sequence. For fluorescent fingerprinting of PACs and BACs an average figure for each clone type, based on the number of bands observed in clones that had generated finished sequence, was 4.0 kb/band. For *Hind III* fingerprinting of PACs and BACs, 4.4 kb/band was used based on the length of finished genomic sequence.

2.22.3 1ace

All mapping and sequencing data generated in this thesis were stored in 1ace, a chromosome-specific implementation of ACeDB (Richard Durbin and Jean Thierry-Mieg, 1991).

ACeDB uses a flat file format with data being accessed using a series of windows to represent various data types. All windows are linked in a hypertext fashion, so that clicking on an object will display further information about that object. For example, clicking on a region of a chromosome map will highlight landmarks mapping to that part of the chromosome; clicking on a landmark will display information about that landmark including landmark-clone associations, etc.

All PAC, BAC and cosmid library filters and polygrids are represented graphically in 1ace and data were entered directly. Data were then saved in the database establishing landmark-to-clone associations which can be displayed as text windows relating to either the landmark or the clone. Data can also be entered via text windows or via an internal web page. PCR library pool screening and colony PCR results were entered via the text windows.

In addition to the data generated by the 1 chromosome mapping group, 1ace also contains displays published 1 chromosome maps, which have been used as part of the project. This greatly facilitates integration of maps from different sources. Genomic sequence data is also displayed in ACeDB along with the collated results from the computational sequence analysis performed by the Sanger Institute Human Sequence Analysis Group. 1ace can be accessed by following the instructions at <http://www.sanger.ac.uk/HGP/Chr1>.

2.22.4 Blixem

Individual matches identified as a result of similarity searches using the BLAST algorithm, or matches between sequences of cDNA clones or PCR products amplified from genomic DNA generated as part of the project, were viewed in more detail using Blixem. Blixem, (Blast matches In an X-windows Embedded Multiple alignment) is an interactive browser of pairwise Blast matches displayed as a multiple alignment. Either protein or DNA matches can be viewed in this way at either the amino acid or nucleotide level. Blixem contains two main displays: the bottom display panel shows the actual alignment of the matches to the genomic DNA sequence, and the top display shows the relative position of the sequence being viewed within the context of the larger region of genomic DNA. A program “pfetch” retrieves the record from an external database (*e.g.* EMBL, SWISSPROT).

2.22.5 RepeatMasker

Human repeat sequences were masked using RepeatMasker, a program that screens DNA sequence for interspersed repeats and low complexity DNA sequence (Smit, AFA & Green, P RepeatMasker at <http://ftp.genome.washington.edu/RM/RepeatMasker.html>). The output of the program is a detailed annotation of the repeats that are present in the query sequence. Sequence comparisons are performed by the program cross_match, an implementation of the Smith-Waterman-Gotoh algorithm developed by P. Green. The interspersed repeat databases screened by RepeatMasker are based on the repeat databases (Repbase Update) copyrighted by the Genetic Information Research Institute.

Chapter 3

Using large insert clones to construct contigs:

The development of fluorescent fingerprinting

3.1 Introduction

3.2 Large insert clones

3.2.1 Application of large insert clones to restriction enzyme fingerprinting

3.2.2 Validation of PAC inserts

3.3 Fluorescent fingerprinting

3.3.1 Fluorescent labelling of cosmid and lambda DNA

3.3.2 Residual dye removal

3.3.3 First position labelling

3.3.4 One step reaction

3.3.5 DNA prep modifications

3.3.6 New size standard

3.3.7 Data collection and processing

3.3.8 Reproducibility

3.3.9 Validation of fluorescent fingerprinting

3.4 Discussion

3.1 Introduction

The construction of sequence-ready maps of overlapping sets of bacterial clones has been one of the central components of large-scale genomic sequencing. Map construction is reliant upon techniques that are able to accurately assemble bacterial clone contigs at a depth that will facilitate the identification of a set of minimally overlapping clones.

Restriction digest fingerprinting has proved to be a robust method that can be used as a means of producing accurate fragment patterns to allow the overlapping relationship between genomic clones to be determined accurately, as well being a technique that is amenable to increases in scale and speed for generation of clone data.

The approach of overlapping sets of random cloned DNA was first used to assemble contigs of cosmids or bacteriophage lambda clones of the *Caenorhabditis elegans* (Coulson *et al.*, 1986) and *Saccharomyces cerevisiae* (Olson *et al.*, 1986, Riles *et al.*, 1993) genomes, respectively. The basic premise of these projects was to generate overlaps between clones that share a statistically significant number of restriction fragments, where the shared fragments representing the region of overlap. Restriction digest fingerprinting has also been applied to the construction of sequence-ready maps within regions of the human genome (Carrano *et al.*, 1989, Heding *et al.*, 1992, Taylor *et al.*, 1996). The inception of large insert bacterial clones has greatly facilitated the construction of maps of larger chromosomes and genomes. Large insert clones BACs and PACs are maintained in single to low copy number, (like fosmids), which means that a smaller percentage of the clones are likely to be unstable or to lose any cloned material. Additionally, a smaller

fraction of the genome is likely to be unstable in the host *E. coli*. PAC and BAC clones can be manipulated in the same way as cosmids and fosmids and, because of their larger insert size, generate genomic coverage more rapidly. As sequencing projects increase in scale (e.g. from *C. elegans* to human) there is a need to adapt existing fingerprinting techniques to the analyses of genome scale clone resources, to improve upon through-put and to incorporate increased levels of safety and automation.

This chapter outlines the evaluation of the first application of restriction digest fingerprinting to large insert clones by the construction of a 1.4 Mb contig across a region of chromosome 13q12 that includes the breast cancer susceptibility gene *BRCA2*. The chapter also details the development and testing of fluorescent fingerprinting, describes an assessment of the technique in comparison to other fingerprinting methods and discusses its application to the large scale generation of sequence-ready bacterial clone maps.

3.2 Large insert clones

3.2.1 Application of restriction enzyme fingerprinting to large insert clones

Linkage analysis in a series of breast cancer families localised the putative BRCA2 gene to a 3cM interval on 13q12-13. The work described in this chapter therefore contributed to the search for the BRCA2 gene, as well as providing a first opportunity to test the suitability of large insert bacterial clones (specifically PACs) as a resource for map assembly. The clones were identified from a whole genomic library by hybridising the *Alu*-PCR products of five yeast artificial chromosomes (YACs) (Burke *et al.*, 1987) from a suggested CEPH YAC tiling path (Cohen *et al.*, 1993) (figure 3.1a) and nine genetic markers (from the region) to a total genomic PAC library (see chapter 2.8.2) (initial library screening was done in collaboration with Richard Wooster). All clones were restriction digest fingerprinted (Coulson *et al.*, 1986) using the established radioactive *Hind* III/*Sau*3A I procedure and assembled into contigs using image editing (<http://www.sanger.ac.uk/Software/Image>) and data manipulation and analysis programs (Soderlund *et al.*, 1997). Two separate walking procedures were employed to confirm overlaps within contigs and to bridge the remaining five gaps (in conjunction with Richard Wooster). Clones at the ends of contigs were used either as a template for SP6 or T7 primers vector specific primers (Ragoussis and Olavesen, 1997) or for the production of inter-*Alu* PCR fragments which were hybridised back to the library and to clones previously identified. The identification of new overlaps and the extent of overlap between clones by restriction fingerprinting was confirmed by the hybridisation results. Figure 3.1

displays the complete contig of the critical region containing 49 PACs and the SP6/T7 and *Alu*-PCR hybridisation probes and results. A minimum set of fourteen clones was chosen from the contig, representing the central region D13S260 to sls234, based on hybridisation and fingerprinting overlaps. The absolute size of the region represented by this minimum clone set was later determined to be 1.4 Mb based on complete genomic sequence data

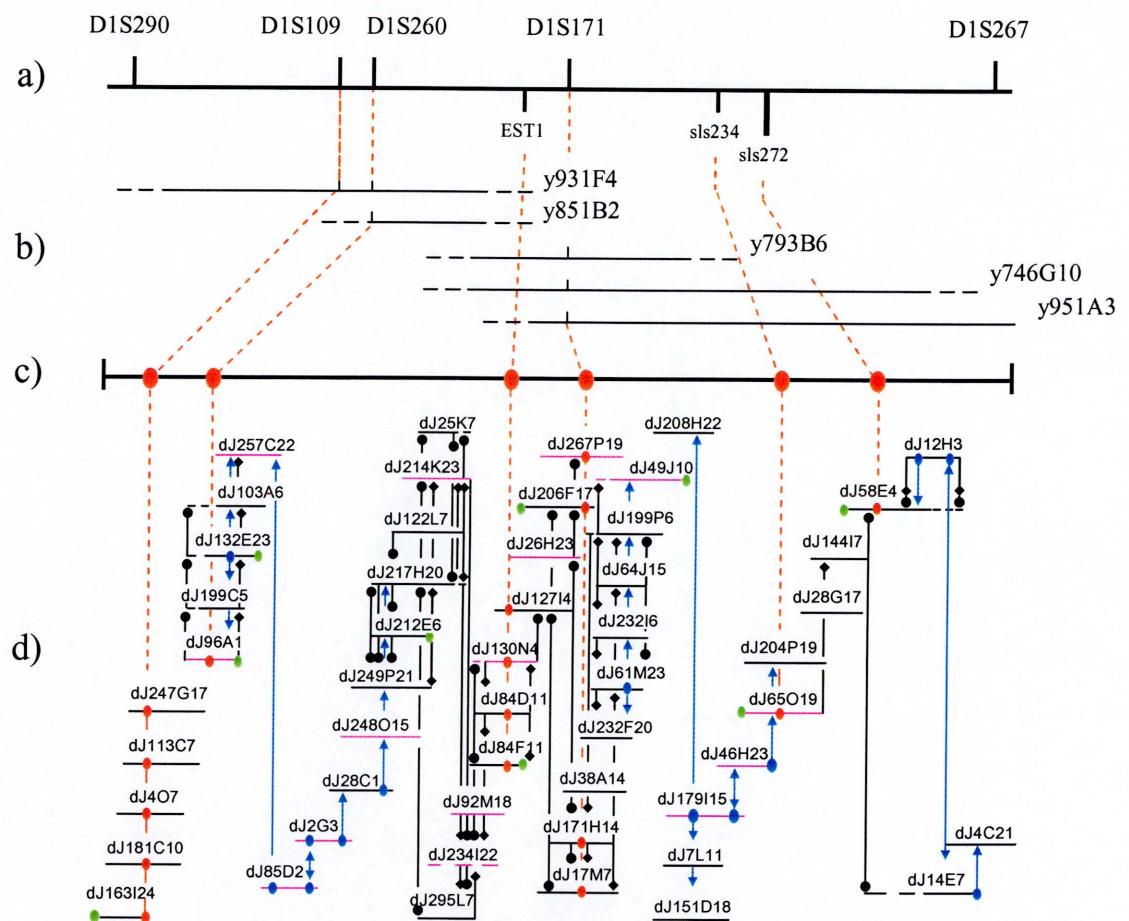


Figure 3.1: A representation of the mapping of BRCA2 region.

a) Genetic markers used in the identification of the putative region; b) YAC minimum set; c) Extent of PAC contig coverage; d) Fingerprint contig across the BRCA2 region; clones isolated by • *Alu*-PCR hybridisation; ◐ clones fluorescent *in situ* hybridised; ↓ T7 ⚡ SP6 end probes; — sequencing minimum set (234I22 sequenced as a PCR product)

3.2.2 Validation of PAC inserts

Given that the PACs were a new cloning system it was important to examine the integrity of the large insert PAC clones. Contiguous sequence from the 1.4 Mb contig provided an opportunity to compare the fingerprint patterns obtained empirically with those expected from the finished sequence. An additional check was possible by cross-comparison of fingerprints of regions in common between overlapping clones. Four hundred and ninety two ordered *Hind* III fragments were produced from a 'virtual' digestion of the 1.4 Mb of submitted sequence. The virtual fragments were compared to corresponding bands of the *Hind* III fingerprints from 37 clones completely overlapping the chosen minimum set (figure 3.2, for example). The resolution of agarose gels limited the accurate sizing of bands to those over 500 bases (figure 3.2b). Occasionally bands of similar size, migrating in the same position of the gel, were not distinguishable. Figure 3.3 displays the band content of the *BRCA2* clones from the contig as compared to the virtual bands derived from the sequence. Bands of less than 500 bp, for which the size could not be accurately determined, accounted for 17% (82/492) of sequence fragments whilst missing bands (see

figure 3.3, red boxes) accounted for 2% (22/1091) of all fingerprint bands. These missing bands do not indicate the presence of large rearrangements within the PACs as no additional bands that could have resulted from the rearrangement were observed in overlapping clones. The absence of bands at the same location of overlapping clones (blue arrow in figure 3.3) may indicate a genuine restriction fragment length polymorphism within the PAC library. The missing bands within 199C5, 257C22 and 103A6 were large enough to be accurately sized on the agarose gel and were contained within overlapping clones.

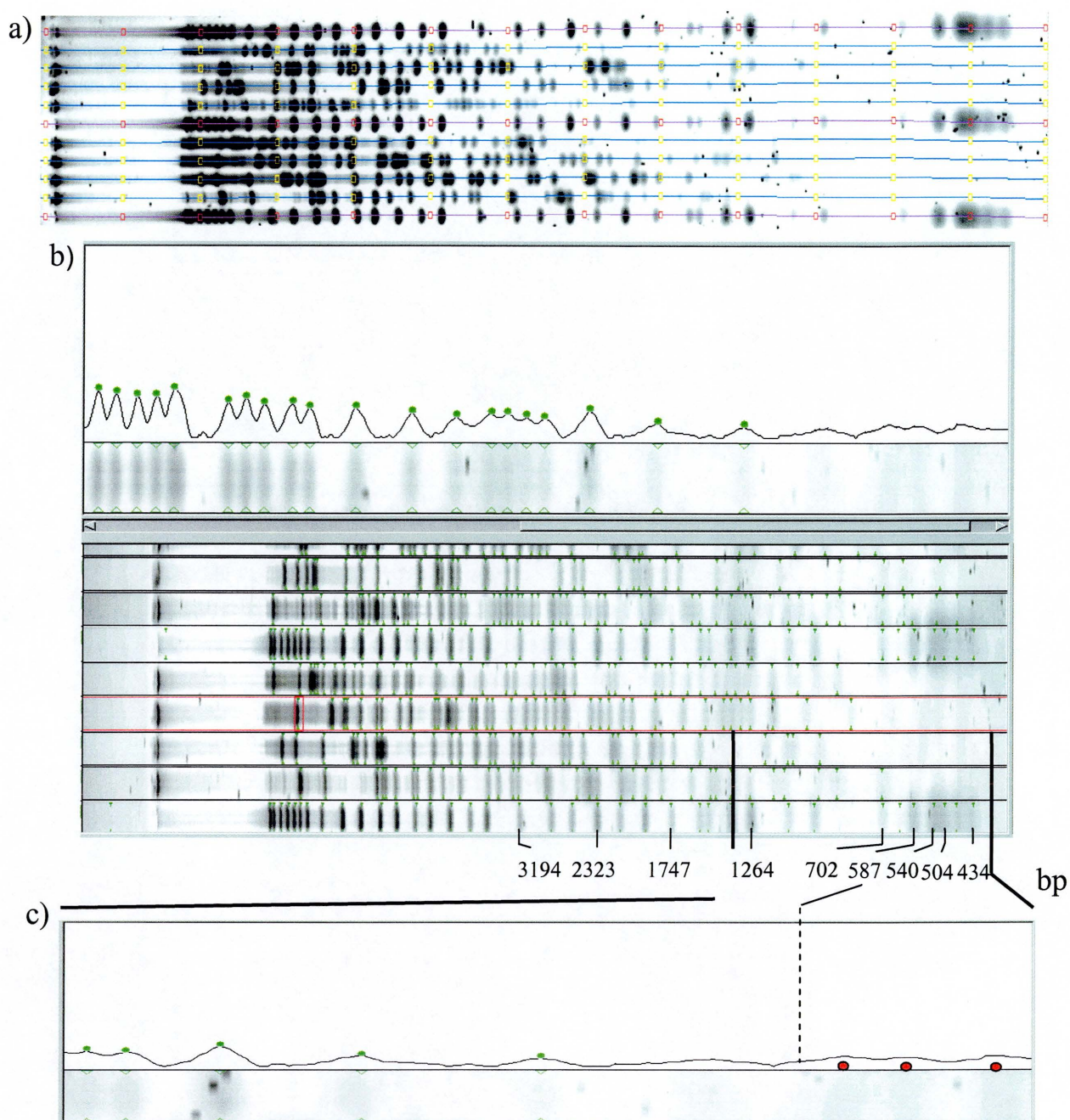


Figure 3.2: An agarose gel fingerprint of large insert bacterial clones in IMAGE. a) depiction of lane lock of 8 clones (yellow boxes) and 3 marker lanes (red boxes). b) data entry phase with edited bands indicated by green pips, also represented are marker lanes with a sub-set of sized fragments in base pairs. c) zoomed region of clone 3 indicating restriction fragments below 500 bp in size (red dots).

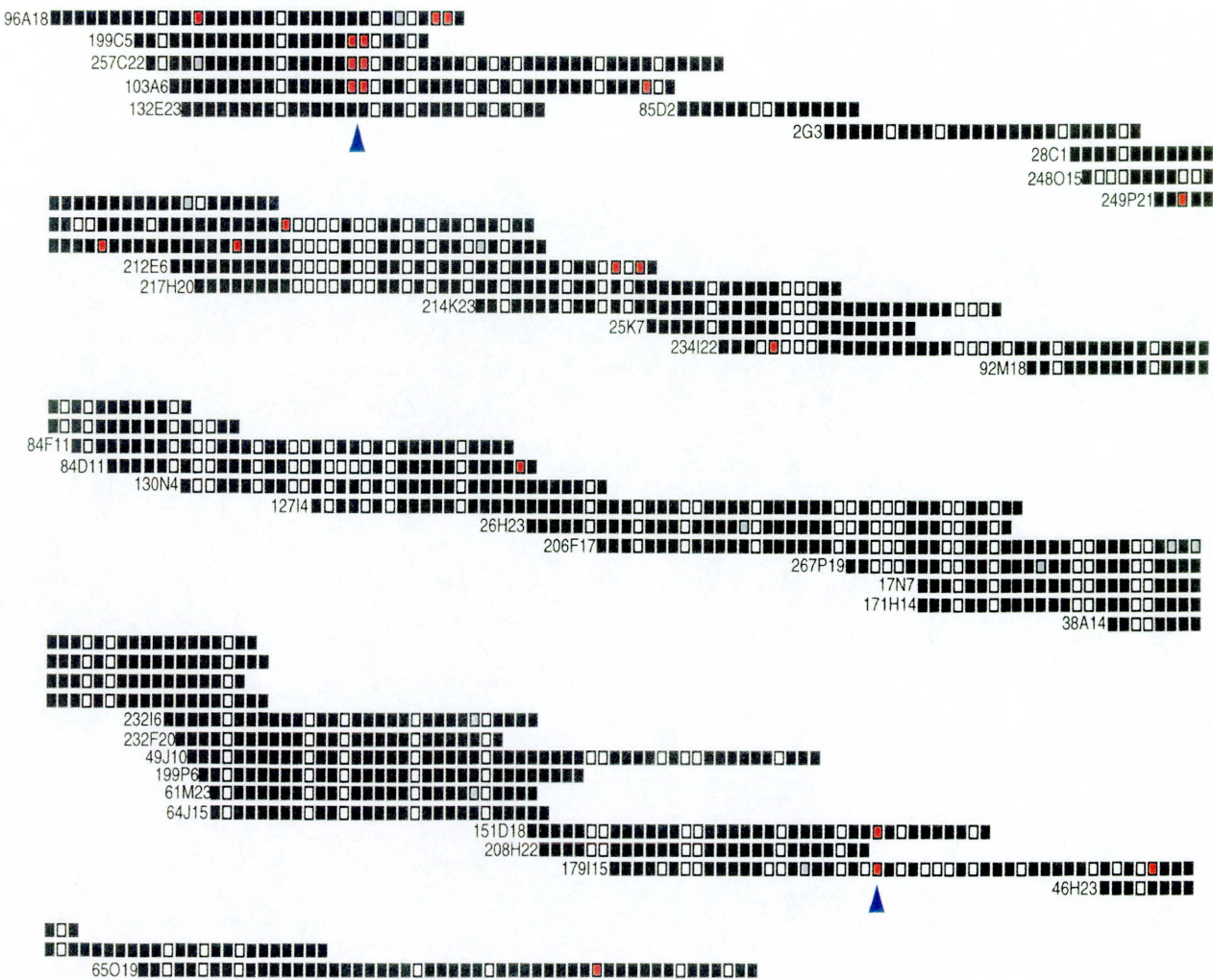


Figure 3.3: A comparison of *Hind* III fingerprint fragments and genomic sequence for the BRCA2 contig, top left to bottom right. Black boxes indicate when a band contained within the genomic sequence is accounted for by a fingerprint band, grey boxes where a band is ambiguous on the agarose gel, clear boxes where a band derived from the sequence falls outside of the resolution of the agarose gel, red boxes where the band was absent from the restriction fingerprint. The blue arrow indicates a possible restriction fragment length polymorphism.

3.3 Fluorescent fingerprinting

The development of a hierarchical clone by clone approach by the Human Genome Project (HGP) for the large-scale generation of human genomic sequence (see chapter 4) required the development of a restriction fingerprinting technique that was high throughput, accurate and safe. For these reasons the application of fluorescent sequencing technologies to restriction fingerprinting was investigated.

The first experiments utilized fluorescent dideoxy molecules, used in terminator sequencing, to end label fingerprint fragments. The aim was to emulate the dual restriction digest and end labelling technique developed by Coulson *et al.*, (1986) for the construction of a physical map of the *C. elegans* genome. In this technique, a radioactive reporter molecule, [α -³²P] deoxy-adenosine-tri-phosphate (dATP), is complementarily conjugated via a DNA polymerase (AMV RT) with the first base in the 5' overhang of *Hind* III restriction digest. A dideoxy guanine-tri-phosphate (ddGTP) is then incorporated at the second base to ensure irreversible completion of the labelling reaction, prior to a second restriction digest with *Sau*3A I. Fingerprint fragments were resolved on a denaturing polyacrylamide gel and migration values of the fragments determined by comparison to a known marker run interposed between fingerprints on the gel. The marker is produced by digesting lambda DNA with *Sau*3A I, filling the first position of the 5' overhang with dGTP, labelling with radioactive [α -³³S] dATP and utilizing ddTTP to prevent exonuclease removal of the reporter molecule.

3.3.1 Fluorescent labelling of cosmid DNA

The first fluorescent fingerprint experiment was designed to mimic the radioactive protocol. DNA minipreps of two chromosome 22 cosmid clones (see chapter 2.4.3) were digested with *HindIII* and Sequenase used to incorporate the unlabelled dATP and fluorophore conjugated ddGTP. A phenol/chloroform extraction step was introduced to remove latent fluorescent dye (soluble in phenol) from the labelling mix prior to gel running and data capture on an ABI 373 using ABI Prism sequencing software. The results from this initial experiment showed a stochastic relationship between DNA concentration and signal strength of the fingerprint fragment peaks. Though the data collected from the gel run identified only smaller restriction fragments it determined that fragments had been successfully labelled and identified a noticeable salt front and a large peak corresponding with unincorporated dye (figure 3.4).

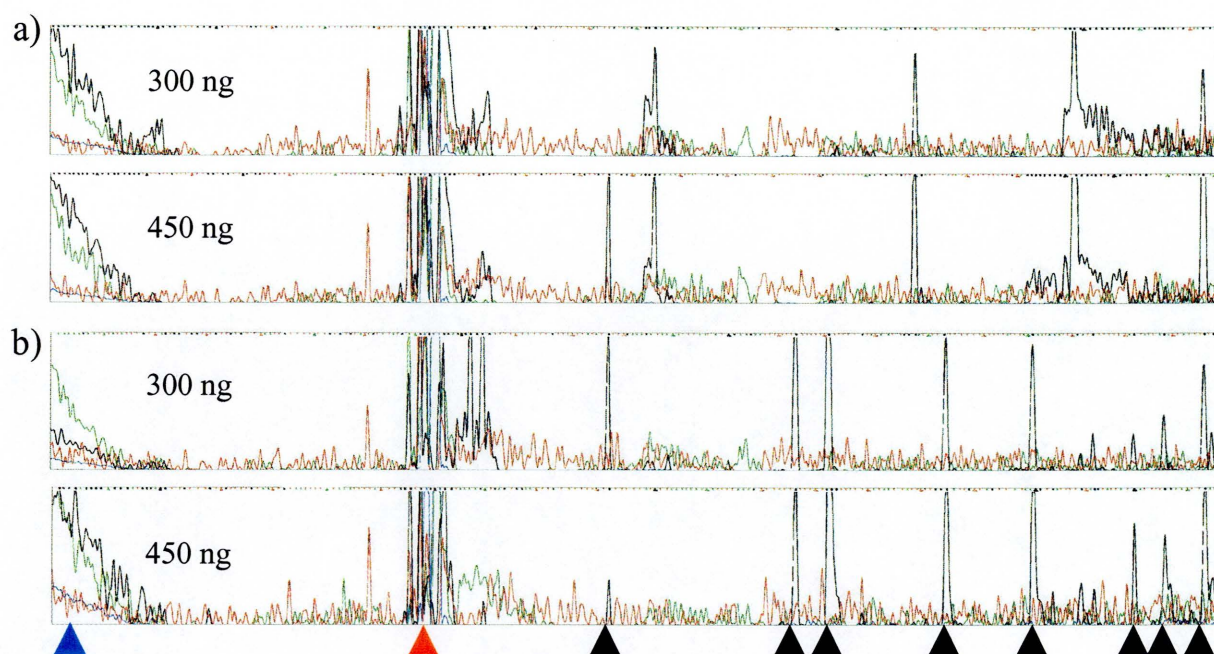


Figure 3.4: The result of the first fluorescent fingerprinting experiment. Two cosmid clones (a and b) of known concentration (shown), were digested with *Hind*III and *Sau*3A, labelled with ddGTP dye-terminator run on an ABI 373 sequencing machine. Labelled fragments of different DNA concentrations were collected using Prism sequencing software. The blue arrow denotes salt/buffer front, the red arrow denotes latent dye-terminator present in fingerprint reaction and black arrows identify labelled restriction fragments.

Having proven that it was possible to generate and detect fluorescently labelled fingerprint fragments, the next aim was to repeat the cosmid labelling experiment and to replicate the labelling of the radioactive lambda marker which would enable a comparison to the radioactive cosmid fingerprint to be made and therefore determine if all cosmid restriction

fragments were being collected (figure 3.5). Lambda DNA was digested with *Sau3A* I and labelled by filling the 5' overhangs with dATP, dGTP and fluorescent dideoxy thymine-tri-phosphate (ddTTP) using Sequenase. This protocol necessitated incorporation of the labelled dNTP at the third position of the 5' overhang which would be spectrally distinct to nucleotides used to label cosmids in the first and second positions.

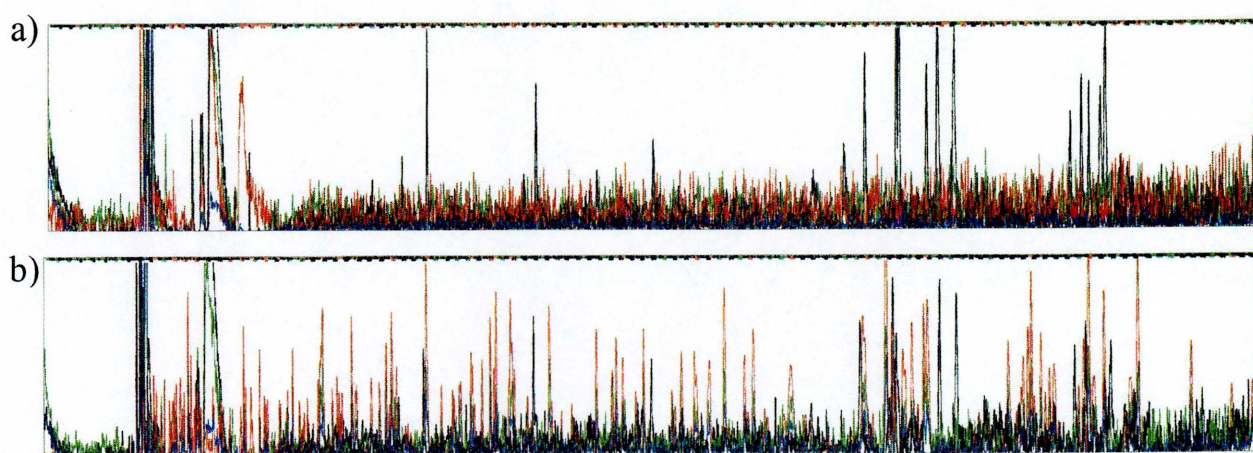


Figure 3.5: Fluorescent fingerprint data collection using an extended run time. a)

fragments were labelled as previously but the run time was extended. b) Replications of the labelling of radioactive lambda marker using a spectrally distinct fluorophore to label a *Sau3A* I digest of lambda DNA.

3.3.2 Residual dye removal

A transition was made to ABI Genescan software which would allow us to separate fingerprint and marker traces from within a single lane on the gel. The presence of latent dye remaining in the fingerprint reaction could affect data production. Small fingerprint

fragments migrating adjacent to the dye front may be masked by dye signal or the dye may affect the resolution of separating fragments. Comparisons were made between techniques to remove the unincorporated dye, namely phenol/chloroform extraction, molecular sieving using Sepharose beads (figure 3.6a and b) and ammonium acetate/ethanol precipitation (figure 3.6c). It was noted that all dye removal techniques resulted in a reduction of fragment signal. Phenol/chloroform extraction resulted in the largest loss of signal (60-70%), ammonium acetate (30-40%) and P10 Sepharose beads (20-30%). Though the P10 beads resulted in the least amount of signal loss, ammonium acetate extraction could more easily be incorporated into the fingerprinting procedure without the introduction of an additional extraction step.

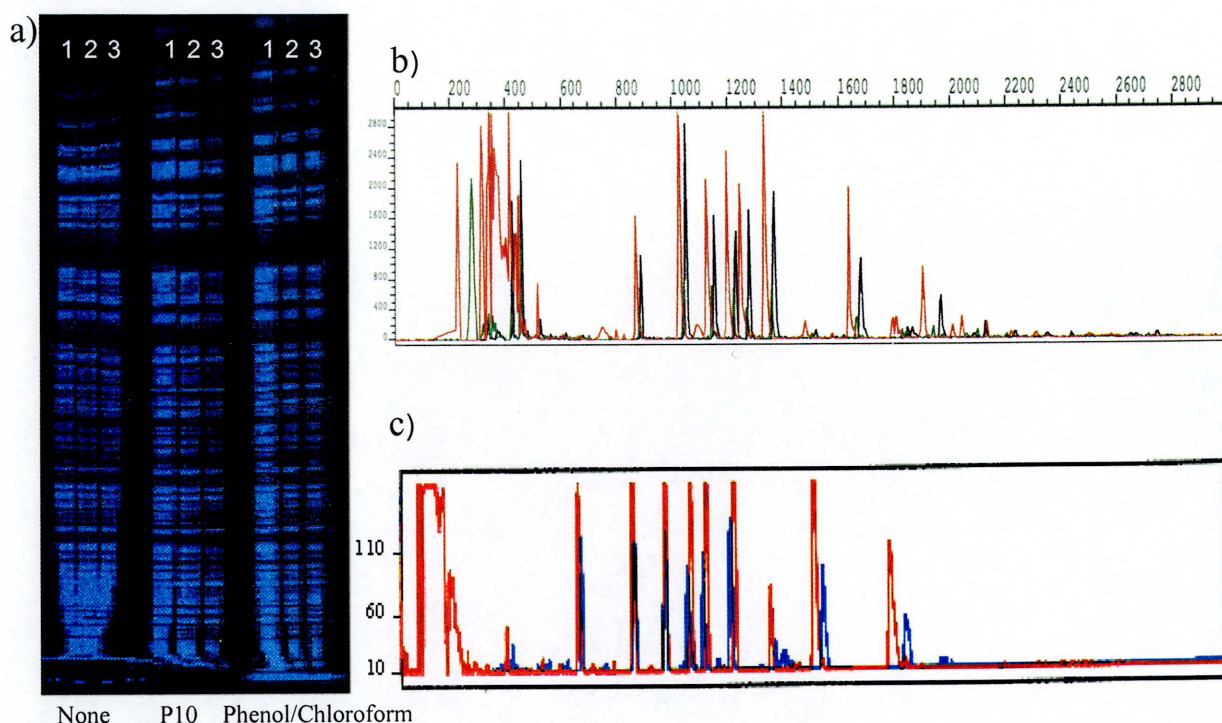


Figure 3.6: A comparison of labelled fragments when investigating removal. a) *Sau3A* I digest of 100 ng (1), 200 ng (2), and 500 ng (3) of lambda DNA. DNA digested with *Sau3A* I was labelled with ddTTP dye-terminator and data displayed and analysed using Genscan software. b) signal intensities of 500ng sample tracks displaying differences between dye removal techniques. Red traces correspond to fingerprint reaction with no dye removal, black traces using P10 Sepharose beads and green traces phenol/chloroform extraction. c) a comparison of ammonium acetate dye extraction (blue) and fingerprint reaction from which no dye was removed (red).

3.3.3 First Position Labelling

Previously, it was shown that fluorophore labelled dNTPs could be incorporated in positions 1 and 2 of *Sau3A* I digested lambda and position 2 of a *Hind* III restriction digests of cosmid DNA (figure 3.7a). However, incorporation of a dideoxy-nucleotide reporter molecule in the first position of bacterial clone fingerprints would negate the effect of poor fragment labelling through incomplete dinucleotide incorporation which would prevent efficient labelling with a dideoxy-nucleotide in 2nd or 3rd positions. To test the efficiency of first position labelling, lambda DNA at different concentrations was digested with *Hind* III and labelled with fluorescent ddATP, figure 3.7. The labelling of restriction fragments with a fluorophore conjugated ddA in the first position of *Hind* III digest, without the requirement of deoxy-nucleotides, means that DNA could be digested in parallel with *Sau3A* I without these fragments being labelled (figure 3.8a). Results indicated that labelling of relatively low concentrations of DNA with very low background could be achieved using first position labelling. Custom synthesis of ddATP spectrally distinct derivatives, on which one of three differently fluorescing fluorophores were attached (figure 3.7c), permitted multiplexing of three different fingerprint samples within one lane on a gel (yellow, blue and green). Identical sizes of the conjugated fluorophores meant no correction was required during data collection to permit fragment comparison. Lambda DNA digested with *Hind* III/*Sau3A* I was again used as the control for testing the efficiency of the three ddATP fluorophores.

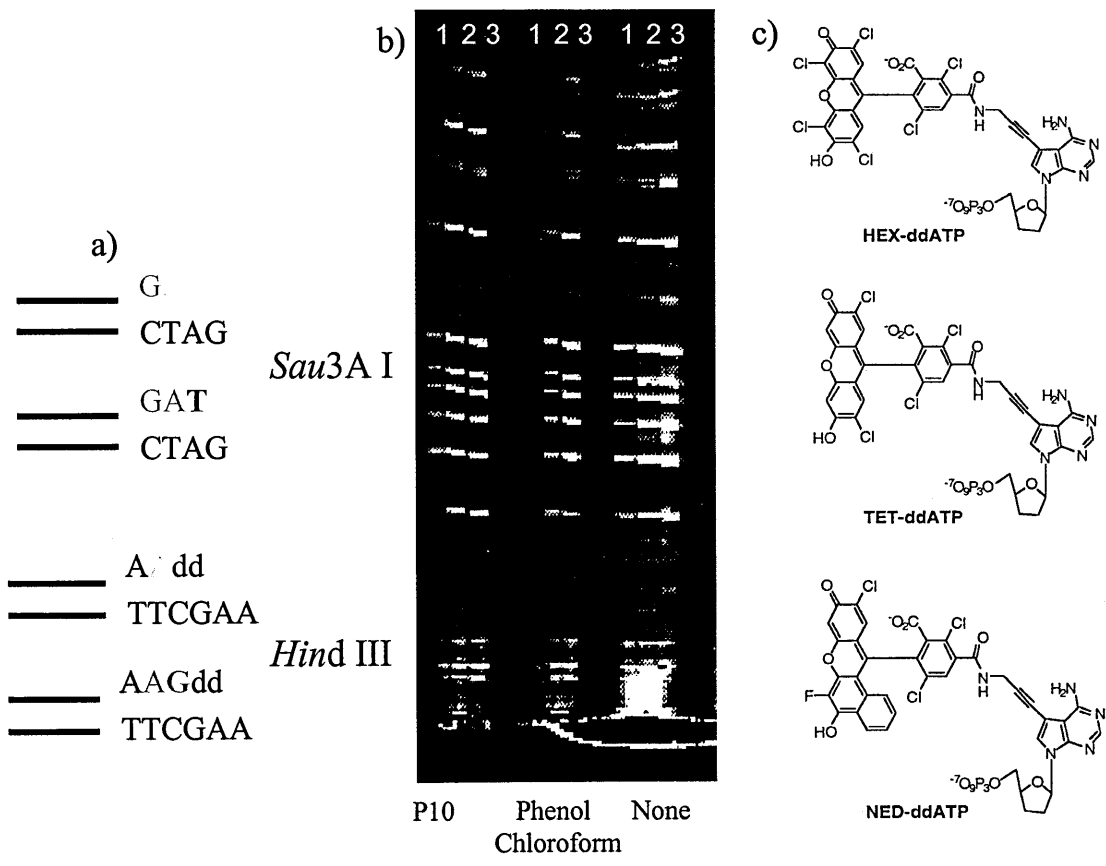


Figure 3.7: Labelling with spectrally distinct fluorophores. a) Labelled nucleotides of spectrally distinct fluorophores attached to the 5' over-hangs of *Sau3A* I and *Hind* III restriction fragments in positions 1, 2 and 3. Also shown are unlabelled nucleotides (grey) b) First position labelling of lambda DNA. 100ng (1), 200ng (2), and 500ng (3) of DNA are digested with *Hind* III, labelled using ddATP dye-terminators dye prior to subsequent digestion with *Sau3A* I. Signal strength of labelled fragments is compared between dye extraction techniques, P10 beads and phenol/chloroform. P10 dye extraction of 100 ng of lambda DNA give clear signal above background indicating that first position labelling provides a clear alternative to using dye-terminators and dNTPs for fill-in labelling. c) Spectrally distinct dye-terminators molecules which were custom conjugated onto ddATP and used for separate labelling and multiplexing of fingerprint samples. d) Titration of ddATP dye-terminators using chromosome 22 cosmid DNA.

3.3.4 One-step reaction

The next modification to be made to the fingerprinting protocol was to initiate a one step dual enzyme digest and labelling reaction based on the protocol published by Tang *et al.*, (1996). This adaptation would reduce the time required for a fingerprint reaction from 3^{1/2} hours to 1 hour prior to latent dye extraction. Initial results looked very promising with only a small decrease in the signal of the one-step reaction compared to that of the two-step (figure 3.8). The *Hind* III/*Sau*3A I combination used to generate fluorescent fingerprints were suitable for the one-step reaction as digest with *Hind* III results in a T in the first position available to incorporate a fluorescent ddATP whilst a *Sau*3A I digest would only incorporate a ddATP in the second position of in the presence of a dGTP. Fingerprints were generated in the presence and absence of unlabelled ddGTP in the reaction mix to determine whether *Sau*3A I fragments were being labelled in the one-step reaction in the presence of residual dGTP (figure 3.9a) or misincorporation of ddATP at first position. No discernable partial or background labelling was noted in either experiment.

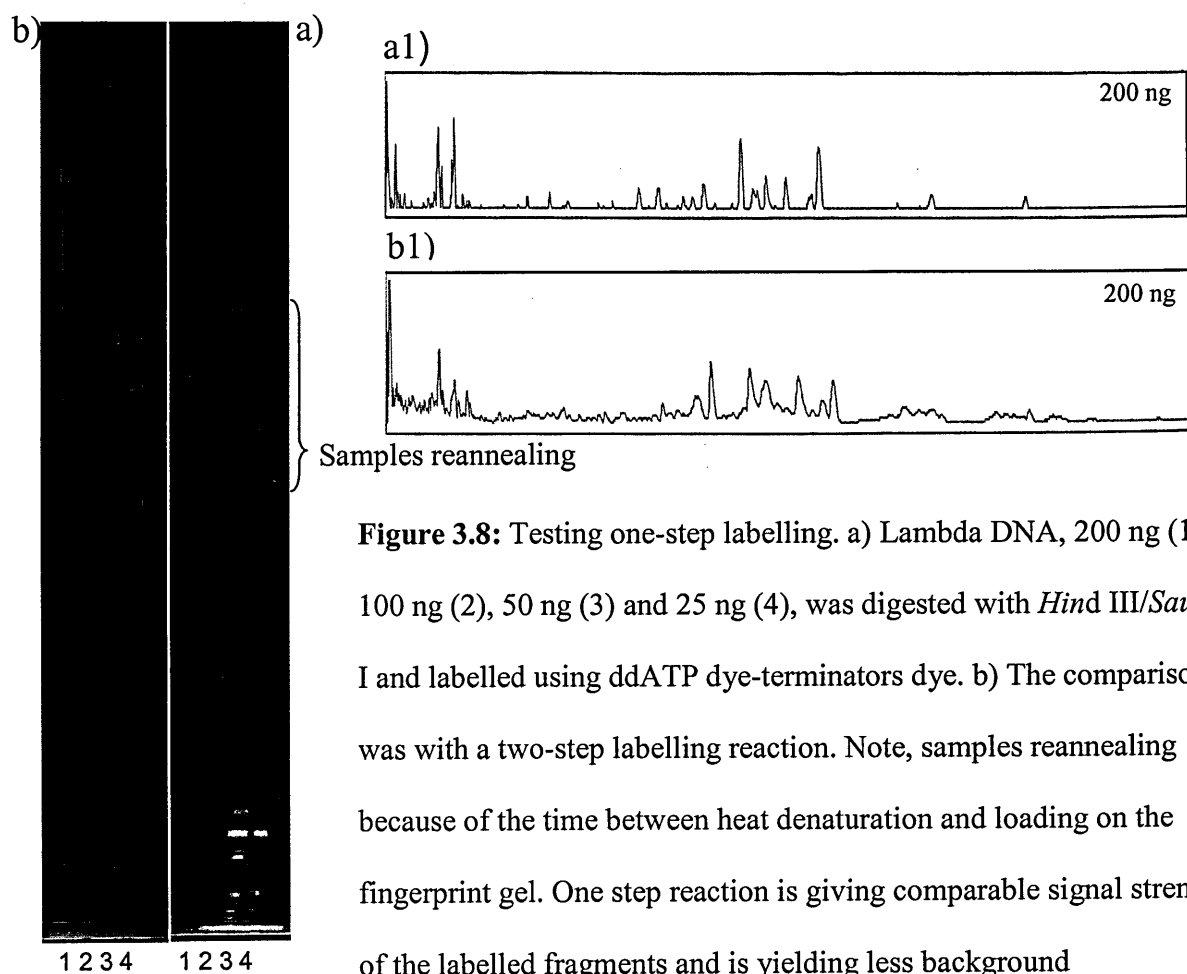


Figure 3.8: Testing one-step labelling. a) Lambda DNA, 200 ng (1), 100 ng (2), 50 ng (3) and 25 ng (4), was digested with *Hind* III/*Sau*3A I and labelled using ddATP dye-terminators dye. b) The comparison was with a two-step labelling reaction. Note, samples reannealing because of the time between heat denaturation and loading on the fingerprint gel. One step reaction is giving comparable signal strength of the labelled fragments and is yielding less background

3.3.5 DNA prep modifications

The protocol used for isolating cloned bacterial DNA for radioactive and initial fluorescent fingerprinting experiments was based upon the microprep procedure published by Gibson and Sulston (1987). Modifications to this procedure were made to improve DNA yield by utilizing Corning 2 μ m filter bottom plates to remove the supernatant from large molecular weight protein precipitated by alkaline-lysis. Adding RNase to T0.1E before final DNA resuspension replaced the need for RNA removal by lithium chloride precipitation and in doing so removed an additional DNA precipitation step (figure 3.9b). A moderate increase in signal was observed from the protocol using DNA extracted by the filter prep method. This is presumed to result from a higher DNA yield of the F prep compared to the M prep, attributable to the increased volume of supernatant transferred during alkaline lysis and to the reduction in the number of precipitation steps required before final DNA isolation.

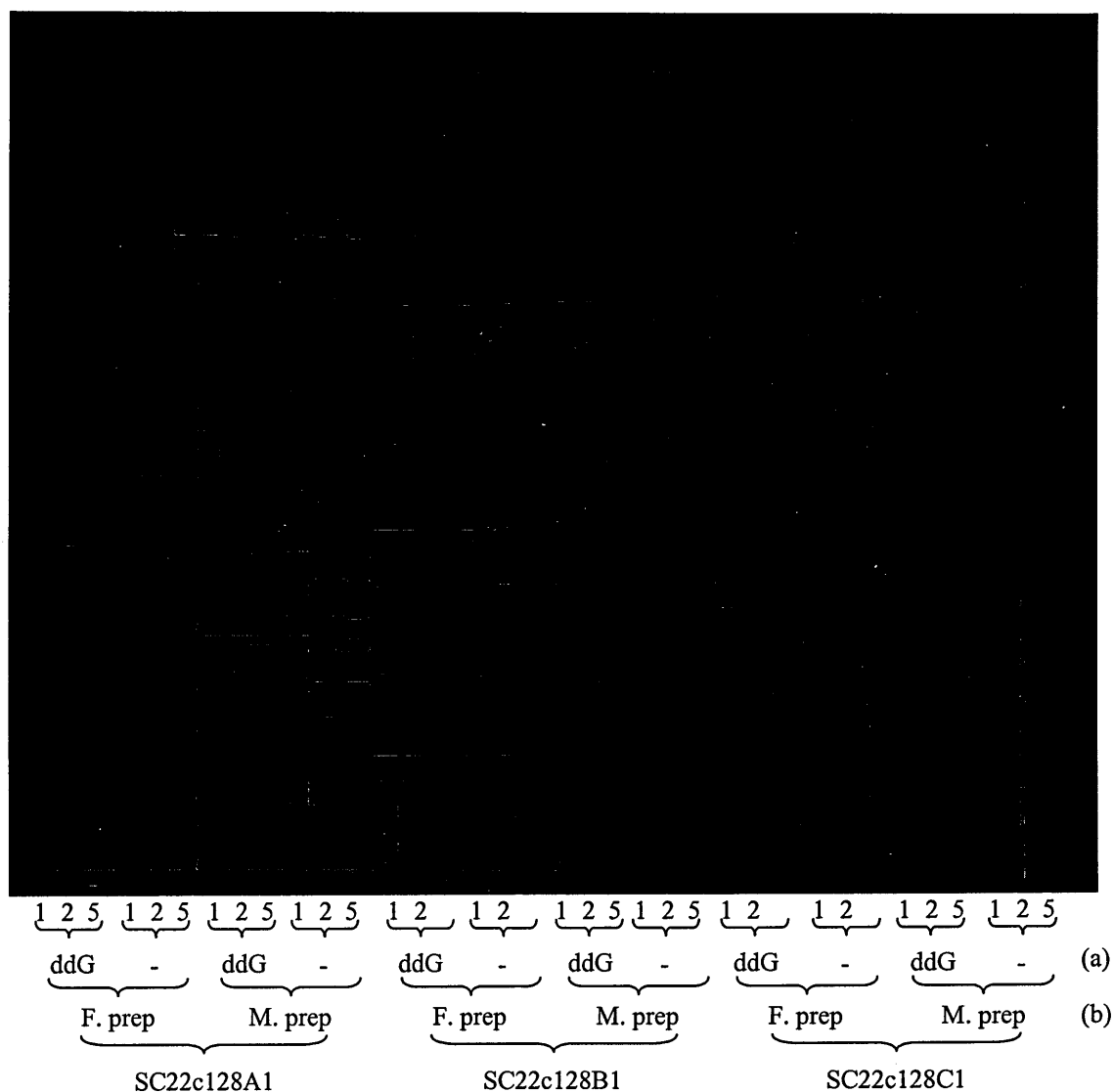


Figure 3.9: Testing one-step labelling and DNA prep protocols. a) Labelling of cosmid DNA (SC22c128A1, SC22c128B1, SC22c128C1) in a one step fingerprinting reaction in the presence and absence of unlabelled 1mM ddG. 1 μ l, 2 μ l and 5 μ l of fingerprint reaction were loaded per lane. No discernable difference was observed in the signal strength or level of background labelling (*Sau*3A I labelling) between one-step and two-step labelling reactions. b) A comparison of filterprep (F) and microprep (M) protocols for the isolation of cosmid DNA samples (see methods). A moderate increase in signal strength above background was observed in the filterprep samples.

3.3.6 New size standard

The separation of radioactive fingerprints is achieved by running samples and lambda *Sau3A* I marker on a 40cm denaturing polyacrylamide gel until the loading dye reaches the bottom of the gel. This form of fragment separation generates an exponential-like distribution of fragment sizes. Lambda *Sau3A* I marker in this context provides even distribution along the length of the gel. Fluorescent fingerprints are also separated on a denaturing polyacrylamide gel but, as fragment data is collected in real time, separation is more linear with increased separation of larger fragments.

Fluorescently labelled lambda *Sau3A* I marker was unsuitable for fingerprint fragment size determination because of uneven distribution of bands along the length of the gel. Uniform distribution of marker bands is necessary to accurately assign migration values to fingerprint bands for overlap analyses. An important additional feature of an appropriate restriction enzyme would be the generation of a G in the first position of the overhangs of the digested fragments, as this would permit incorporation of a red ddC fluorophore allowing a marker to be run in the same lane as green, yellow and blue fluorophore labelled ddA fingerprints. Another important factor in selecting a replacement enzyme is that its optimum temperature should be compatible with the conditions under which Taq FS polymerase end labels fingerprint fragments.

Two enzymes that fulfil the criteria of having a G in the first position for a labelled ddC nucleotide to anneal, *BsaI* I and *TaqI* I, were labelled and run with ddT labelled

lambda/*Sau*3A I to permit overlap comparison, figure 3.10. *Bsa*I gave a more uniform distribution of marker fragments along the length of the gel, particularly in the 100 bp to 2000 bp region of the gel in which the majority of fingerprint fragments would migrate. Overlapping the *Sau*3A I with *Bsa*I marker lanes clearly indicates the distribution differences between the two enzymes (figure 3.10).

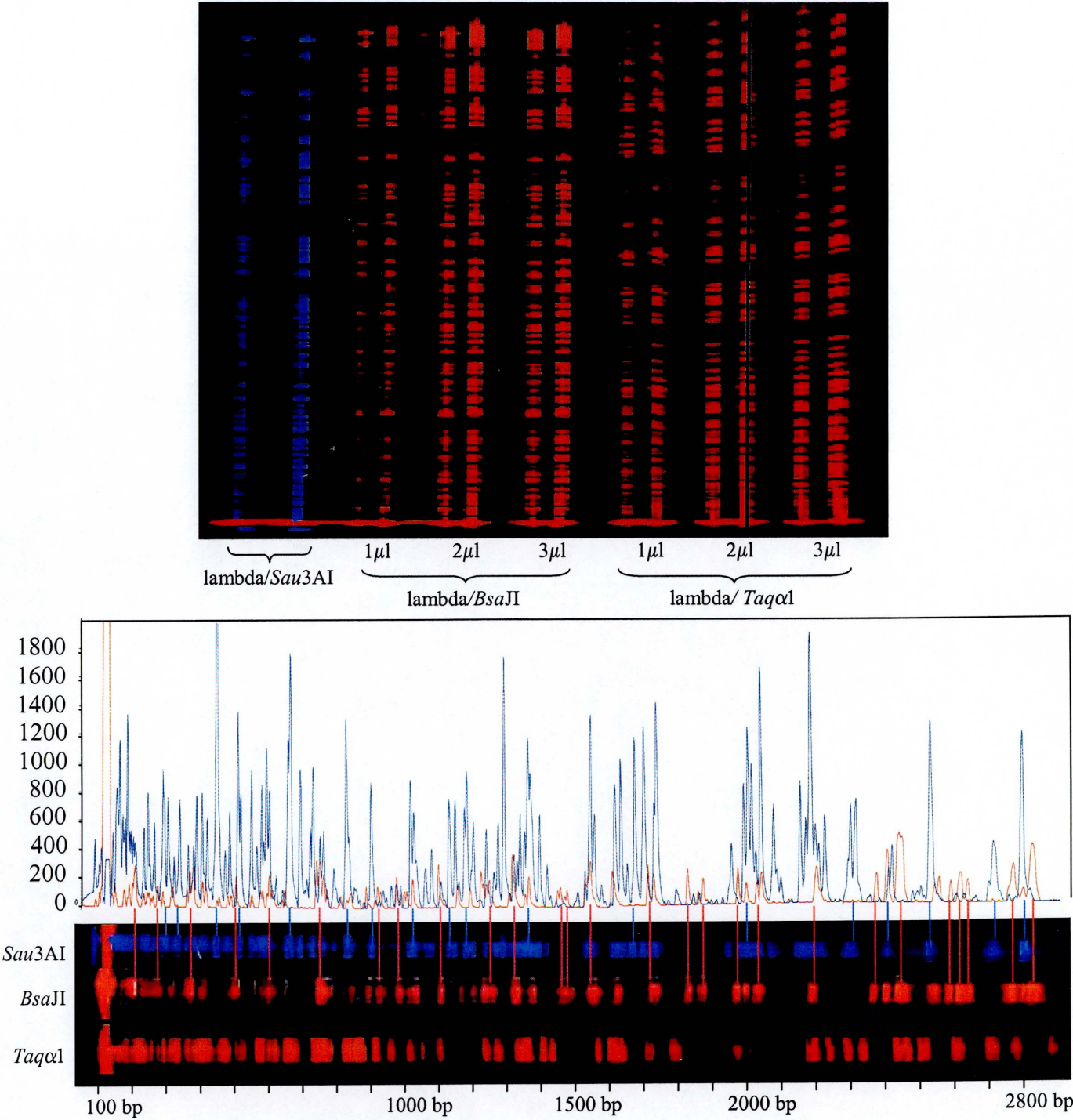


Figure 3.10: A comparison of labelled lambda digest fragments using *Sau3A* I, *BsaJ* I and *Taqα* 1 restriction enzymes. Lambda DNA labelled with fluorescent ddTTP (*Sau3A* I) and ddCTP (*BsaJ* I and *Taqα* 1) and loaded in different aliquots. b) *BsaJ* I generates a more uniform distribution of fragments in the 30 bp to 2.8 kb size range of in comparison to *Sau3A* I (which is used for generating the marker standard for radioactive fingerprints) and *Taqα* 1.

3.3.7 Data collection and processing

During protocol development data was collected on an ABI 373 and visualised using Genscan software version 2.0.2. Though the software was useful during the testing phase of the technique it was not designed to interpret the complexity of fingerprint or marker bands produced by the fluorescent fingerprinting. Instead, unprocessed gel images were collected using Prism Collection software (v1.1) running on an ABI 377 and downloaded onto a UNIX workstation. Data was edited using modified version of IMAGE before transfer into Fingerprinted Contigs (FPC) (Soderlund *et al.*, 1997) for analysis. This eliminated all of the gel processing, autoradiography and scanning that is associated with radioactive fingerprinting.

3.3.8 Reproducibility

Labelling the marker with a different fluorophore to the fingerprint fragments permits the incorporation of a marker in each fingerprint lane. This facilitates greater accuracy of mobility determination of fingerprint fragments within the 30 bp to 2.8 kb size range than was previously possible. To test the accuracy of fragment analyses and reproducibility of the labelling procedure, a PAC clone, dJ163I24, was fingerprinted 10 times with each of the three ddATP dyes and compared (figure 3.11). All fingerprints were highly reproducible. The migration values of seven fingerprint bands, representing an even distribution along the length of the gel, were compared between clones. In all cases examined, the variation of migration of bands in 30 independent fingerprints was $\pm 0.26\%$ (maximum observed: $\pm 11/4500$ intervals), which is less than the tolerance used in the analysis.

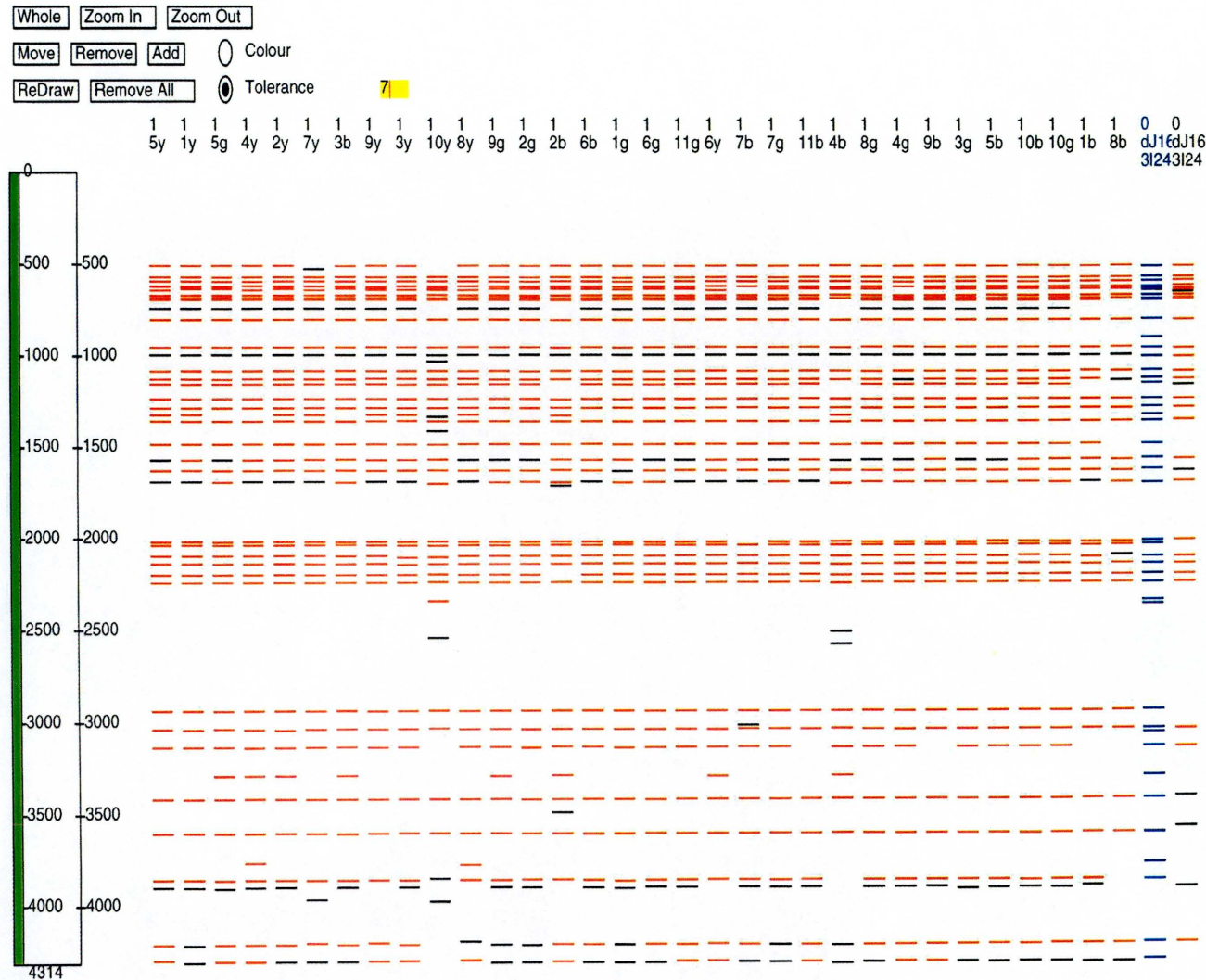


Figure 3.11: An FPC display of band labelling uniformity. 10 PAC, dJ163I24, duplicates were fingerprinted with one of each of the three ddATP fluorophores to test for labelling consistency, clone number followed by suffix b = ddATP-TET, y = ddATP-NED, g = ddATP-HEX. Horizontal red lines correspond to fingerprint bands that are within the matching tolerance, as discussed in chapter 2.22.2, of the original fingerprint (blue bands).

3.3.9 Validation of fluorescent fingerprinting

Once the labeling and reproducibility of the fluorescent technique was established a comparison of radioactive, fluorescent and non-isotopic fingerprinting was performed using 49 PAC clones from the 1.4 Mb contig constructed as described previously (see figure 3.1). The aim was independently to assemble clones from the contig using the different fingerprinting techniques and compare the results with overlaps defined by 14 clones representing a minimum set of clones for which complete sequence was now available (figure 3.12a). Vertical arrows in (figure 3.12b) represent the overlaps that were not found between clones in each of the four methods. Figure 3.12c represents the contigs as constructed by the fluorescent fingerprinting method. The vertical arrows coincide with those in figure 3.12b, denoting overlaps that were not detected by fingerprinting alone. There was excellent agreement between the contigs assembled using either the radioactive or fluorescent *Hind* III / *Sau*3A I data. Minor variations were observed where small overlaps between clones fell just outside the probability cut-off used. (These overlaps were originally detected by end-probe hybridisation, and later confirmed by the sequence).

There was also good agreement between the *Hind* III / *Sau*3A I results and those of the *Hind* III and *Eco*R I fingerprints resolved on agarose gels, but matches in the latter protocols required a higher statistical probability of overlap, i.e. smaller overlaps were not detected. This can be attributed in part to the fact that each agarose fingerprint pattern is divided into 2000 1 mm intervals along the length of a 20 cm lane as opposed to the 3400 and 4500 intervals of the radioactive and fluorescent fingerprints respectively. A smaller

number of intervals implies that there is a greater probability that bands will occur randomly in the same bin and contribute to background matches. However, it should be pointed out that the two approaches are both useful in different ways. The *Hind* III /*Sau*3A I method can detect smaller overlaps but samples 256 bp / 4096 bp (14%) of the insert DNA of a clone, and provides no information on the remainder of the sequence. By contrast the use of complete *Eco*R I, *Hind* III or similar digests resolved on agarose gels, although achieving lower resolution, does display bands representing all the DNA of the cloned insert. This data is therefore more appropriate for verifying the integrity of the sequence compared to all genomic clones covering the region. It also confers the ability to look for possible deletions or other rearrangements that result in detectable size alterations in individual restriction fragments.

Where all four methods failed to detect overlaps between adjacent clones (figure 3.12, 1a – c), the overlapping bands were only contained within two clones. This problem would be resolved with greater contig depth. Details of analysis of overlaps which were not detected by individual methods are given in the figure 3.12 legend.

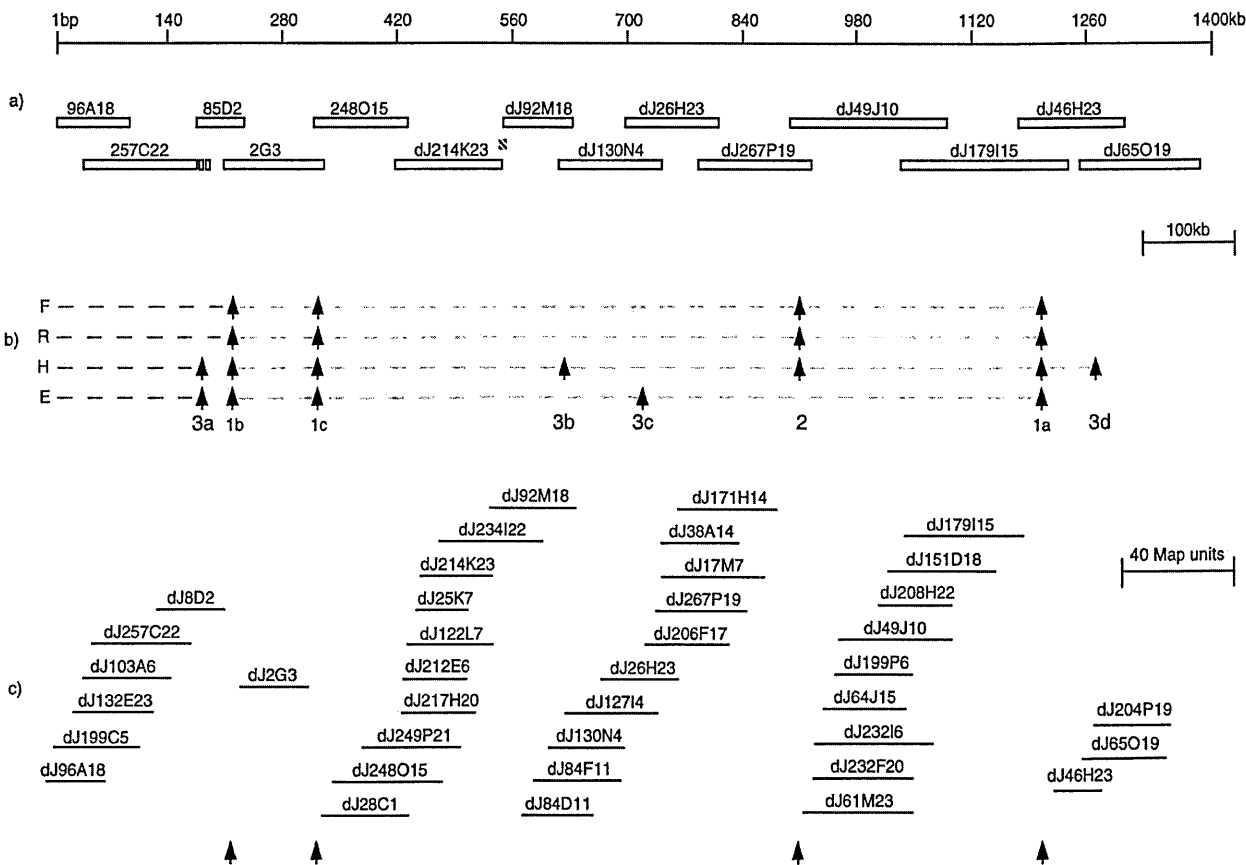


Figure 3.12: A comparison between fingerprinting methods of using 14 clones comprising a minimum tiling path. a) Finished sequence data were used to define the overlaps between clones and absolute length of each of the clones, represented as clear boxes and scale in kb (except dJ257C22, where data were incomplete). b) Vertical arrows denote overlaps that were not detected by each method: (F) fluorescence, (R) radioactive; (H) *Hind* III, and (E) *Eco*R I. As expected, there is variation based on recognition sites between the overlaps detected using *Hind* III (b and d) and those established with *Eco*R I, c). Details of the analysis of undetected overlaps are as follows: (Overlap 1a, 62 kb) Nine *Hind* III and

11 *EcoR* I fragments are present in this overlap on the basis of DNA sequence. Statistical probability on the basis of these bands shared between dJ179I15 and dJ46H23 is 1×10^{-4} (4) fluorescence, 1 radioactive, 4 *Hind* III, and 5 *EcoR* I (whose probability cutoffs for all matches are 4, 5, 7, and 7, respectively). (Overlap 1b, 25 kb) Clone dJ2G3 is unattached. Three *Hind* III or six *EcoR* I fragments shared with clone dJ85D2 are insufficient to score the overlap. (Overlap 1c, 11 kb) Clone dJ2G3 is unattached. Four *Hind* III or three *EcoR* I fragments shared with clone dJ248O15 are insufficient to detect the overlap. (Overlap 2, 24 kb) Overlap between dJ267P19 and dJ49J10 was not found by any of the *Hind* III methods. Six *Hind* III fragments are not sufficient to detect overlap. Arrows 3a-3d denote where only the agarose methods failed to find overlap. (Overlap 3a) Overlap between dJ257C22 and dJ85D2 could not be determined because of incomplete overlap data and therefore was not analyzed. (Overlap 3b, 18 kb) Four *Hind* III fragments shared between dJ130N4 and dJ92M18 are not sufficient to detect overlap. (Overlap 3c, 44 kb) Six *EcoR* I fragments shared between dJ130N4 and dJ267P19 are not sufficient to detect overlap. (Overlap 3d, 55 kb) 16 *Hind* III fragments between dJ46H23 and dJ65O19 should have been significant. The lack of overlap may be attributed to the migration of similar-sized fragments in the same location of the agarose gel and therefore not be representative of the cloned insert. (c) Although all but 1 of the 49 clones (dJ2G3) fell into contigs, only 4 of the contigs that lie within the sequence interval are represented. Arrows denote where the overlaps between clones were not found.

3.4 Discussion

The construction of a 1.4 Mb contig on human chromosome 13q provided the first opportunity to test the application of restriction digest fingerprinting of large insert clones (PACs) for the construction of a physical map and their utilisation as a sequencing resource. Results indicated that they are stable, provide coverage to this extent, and few/no discrepancies between clones suggested little rearrangement. The existing *Hind* III/*Sau*3A I fingerprinting proved suitable for the generation of PAC fingerprints therefore permitting integration of other types of smaller insert bacterial clones (Dunham *et al.*, 1999, Deloukas *et al.*, 2000).

The advent of large-insert bacterial clone libraries of PACs and BACs for the construction of high-resolution maps has facilitated sequencing and gene identification within chromosomal regions (Kudoh *et al.*, 1997, Hubert *et al.*, 1997, Guru *et al.*, 1997). Construction of a bacterial clone map in either a regional or a chromosome wide study relies on initial identification of the clones by using hybridisation- or PCR-based markers to screen available libraries. The existence of overlaps between clones may be identified on the basis of shared marker content, however, as a marker represents one point in the genomic DNA, no measurement of extent of overlap is obtained. In most regions of the human genome marker density is too low to achieve closure of all gaps by marker content alone. Alternative methods to define overlaps between bacterial clones include the hybridisation of end probes to clone arrays (Evans and Lewis, 1989), high resolution fluorescence *in situ* hybridisation (FISH) using DNA fibres (Wang *et al.*, 1996) and

matching of ends to complete insert sequences (Kupfer *et al.*, 1995, Roach *et al.*, 1995). End-probe hybridisations do not define the extent of overlap, also a limitation of whole cosmid-cosmid hybridisations (Xie *et al.*, 1993), and all hybridisation-based methods employing undefined sequences can yield false positive signals because of cross hybridisation of repeat motifs. The end-sequencing strategy provides precise information on extent of overlap but relies on extensive prior investment in sequencing all clones in the library and also does not permit assembly of contigs prior to sequencing of the inserts. Fibre-FISH, using bacterial clones as probes and yeast artificial chromosomes (YACs) as a target, provides good estimates of both the extent of overlaps and size of gaps between clones but require the existence of a well-defined YAC map across the region of interest and has yet to be scaled up. Fingerprinting, however, can detect overlaps where there is no marker available and gives an indication of the extent of each overlap.

Other approaches to fluorescent based fingerprinting have included ligation of fluorochrome-labeled oligonucleotide adaptors to *EcoR* I digests of cosmids (Lamerdin and Carrano 1993) and incorporation of fluorescent dideoxy terminators in 5' overhangs produced by endonuclease digestion (Ding *et al.*, 2001). The former technique uses agarose gels to resolve labeled fragments has been superseded by the VISTRA-green-stained agarose gel fingerprints (Marra *et al.*, 1997), in this chapter, and the latter technique results in a complex fragment pattern that is not necessarily amenable to the generation of large scale physical maps.

The fluorescent fingerprinting technique discussed in this chapter utilises three spectrally distinct dye-ddA terminators to label the restriction fragments of three different *Hind* III-*Sau*3AI endonuclease digests. The combination of three fingerprint samples plus a marker standard, labeled with a dye-terminator in a fourth colour, facilitates multiplexing and enhances the accuracy of data generation and overlap analyses. Improvements in data collection software, permitting the 64 multiplexed samples per gel, resulted in a two fold increase in data collection, increasing throughput to 192 clones per gel run. A requirement for the scale up in the construction of sequence-ready maps is the need to develop non-isotopic forms of contig construction. Fluorescent fingerprinting assists the progression towards large scale mapping by increasing throughput by multiplexing, enhancing the accuracy of the data generated and providing improved safety. Fluorescent fingerprinting has been successfully applied to the construction of a physical map of a region of mouse chromosome X (Mallon *et al.*, 2000) as well as large scale sequence-ready bacterial clone maps of human chromosomes 1, 6, 20 (Deloukas *et al.*, 2001) and X (Bentley *et al.*, 2000) as discussed in the next chapter.

Chapter 4

Construction of a sequence-ready bacterial clone contig of 1pcen – 1p13

- 4.1 Introduction**
- 4.2 Construction of sequence-ready map of 1pcen – 1p13**
 - 4.2.1 Small insert library construction
 - 4.2.2 Hybrid mapping of SIL markers
 - 4.2.3 Bacterial clone contig construction
- 4.3 Evaluation of SIL marker distribution in chromosome 1**
- 4.4 Comparisons of Published Maps**
 - 4.4.1 Physical maps
 - 4.4.2 Genetic map
 - 4.4.3 Radiation hybrid map
 - 4.4.4 A comparison of three maps
- 4.5 Discussion**

4.1 Introduction

Alterations of human chromosome 1 are among the most common form of chromosomal abnormality detected in human disease. Chromosomal aberrations localised to chromosome 1pcen-1p13 have been associated with human neoplasia such as acute megakaryoblastic leukaemia (Mercher *et al.*, 2001), radiation induced meningioma (Zattara-Cannoni *et al.*, 2001), colorectal Cancer (Nitta *et al.*, 1987), as well as other diseases such as non-goitrous hypothyroidism (Dracopoli *et al.*, 1986) and autosomal recessive ventricular tachycardia (Lahat *et al.*, 2001).

Previously, two attempts have been made to construct physical maps within 1pcen-1p13 (Carrier *et al.*, 1996, Brintnell *et al.*, 1997). These maps, primarily consisting of YACs, were constructed for the purposes of characterising the genic environment of the nerve growth factor gene (NGFB) (Carrier *et al.*, 1996) and for the elucidation of putative candidate genes within a smallest region of overlapping loss of heterozygosity (LOH) in breast cancer studies (Brintnell *et al.*, 1997). Though the YACs used in the construction of these maps provided a means of generating coverage of large genomic regions with relatively few clones, the comparative difficulty of constructing the libraries and of analysing the cloned DNA (including shotgun sequencing) means that YACs as the primary resource are not well-suited for the construction of sequence ready maps. Instead, YACs have provided a means of linking bacterial clone contigs where genomic sequence is not represented within the bacterial clone libraries.

In contrast to YACs, bacterial clone libraries are easier to make and the cloned DNA is more easily manipulated. The use of bacterial clones for construction of a high resolution sequence ready map within 1pcen-1p13 would not only facilitate the identification of disease genes but would also provide the basis for a detailed characterisation of the genomic landscape of the interval. This chapter describes the construction of a sequence ready bacterial clone map in 1pcen-1p13 and compares previously published genetic, radiation hybrid and physical maps within the interval.

4.2 Construction of sequence-ready map of 1pcen – 1p13

A hierarchical strategy was used to construct the map as follows (see figure 4.1). At the start of the project, 3642 markers were publicly available which had been localised to the region by genetic or RH mapping. To provide additional markers for map construction a small insert library (SIL) derived from flow sorted chromosomes was constructed (see section 4.2.1). SIL clones were picked at random and sequenced to generate novel STSs. A subset of these novel STSs were placed in the region by RH mapping. The combined set of markers was used to initiate contig coverage by screening large-insert bacterial clones. Bacterial clone coverage was supplemented with contigs generated by McPherson *et al.*, (2000) from a whole genome fingerprint database. Contigs from this database were selected for inclusion in the 1pcen-1p13 map if they overlapped with existing clone contigs on the basis of shared fingerprints and/or marker content. The map was completed by iterative rounds of walking, using sequences at or near the end of each contig to re-screen the available libraries for clones.

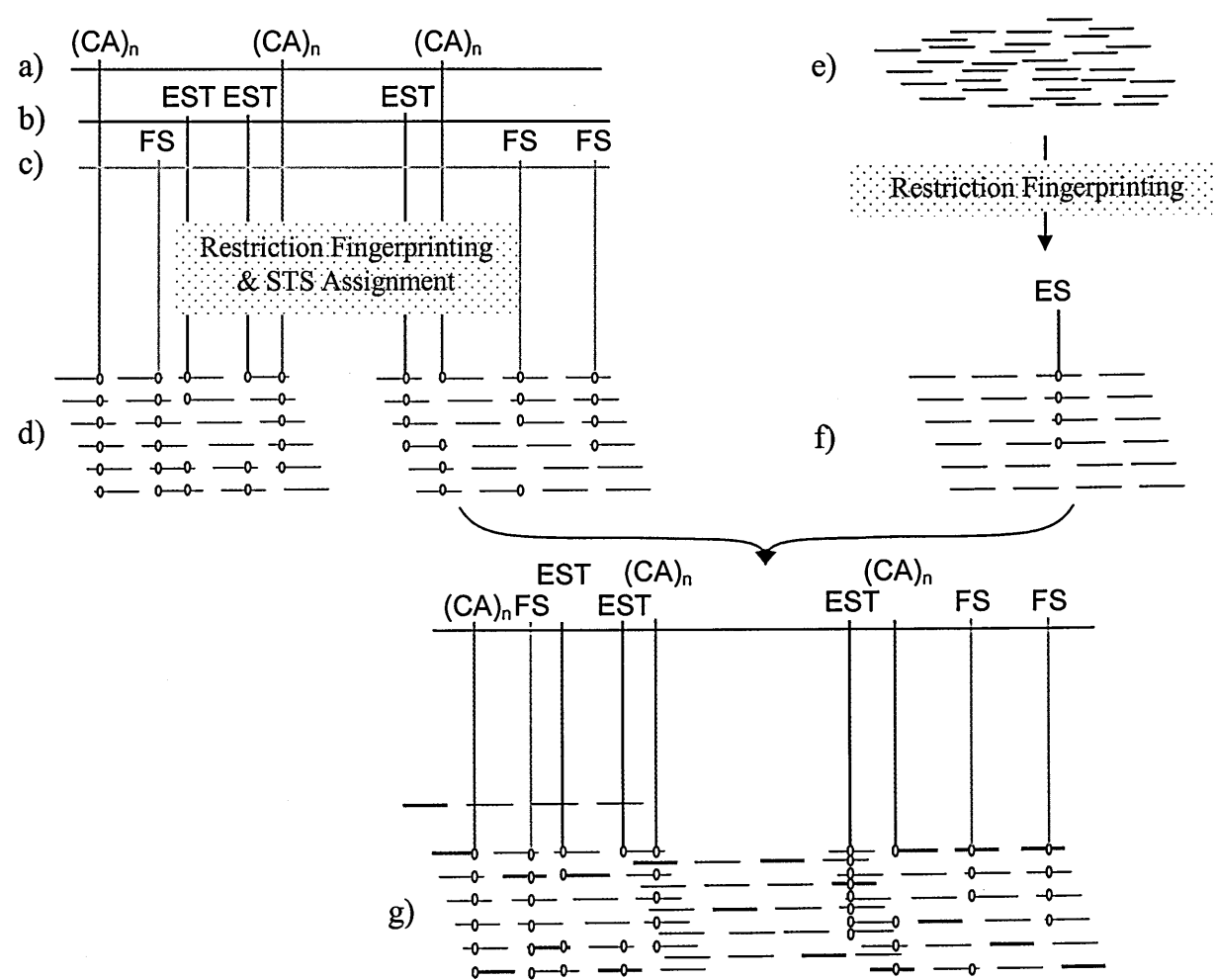


Figure 4.1: A representation of the two strategies used to construct a sequence-ready bacterial clone map of 1pc – 1p13. The hierarchical method utilises polymorphic genetic markers (CA)_n a), expressed sequence tags (EST) b) and markers generated by sequencing small insert libraries (FS) c) which are radiation hybrid mapped and screened across genomic libraries. Restriction fingerprinting and STS assignment is performed in parallel prior to data assimilation in FPC (orange lines, d). The whole genome fingerprinting approach utilises restriction digest fingerprinting of a 15-fold redundant genomic library e), including some marker data, to establish bacterial clone coverage f). Data from both these techniques is combined to generate contiguous map coverage g) proving a resource for the selection of a minimum tile path clones, bold green lines.

4.2.1 Small insert library construction

A bivariate flow karyotype of human DNA (figure 4.2a) was generated to facilitate purification of chromosome 1 DNA from other chromosomes (flow sorting was performed by Nigel Carter). Purified DNA was then completely digested with *Hind* III prior to cloning into pBluescriptII vector and electroporated into *E. coli* XL1 blue electrocompetent cells (figure 4.2b). Two hundred test recombinants were picked from Xgal indicator plates, miniprepmed (Birnboim *et al.*, 1979) and DNA separated by electrophoresis on a 1% agarose gel as undigested and digested to ascertain average insert sizes (figure 4.2c). Of the two hundred test recombinants, 96% contained inserts and the average size was estimated to be ~5.6 kb. Successful generation of sequence data from a high percentage of 400 test SIL clones (data not shown) prompted a further 7296 SIL clones to be picked and sequenced (by others). A 36% failure rate (2611) at the prepping stage reduced the number of sequence templates to 4685.

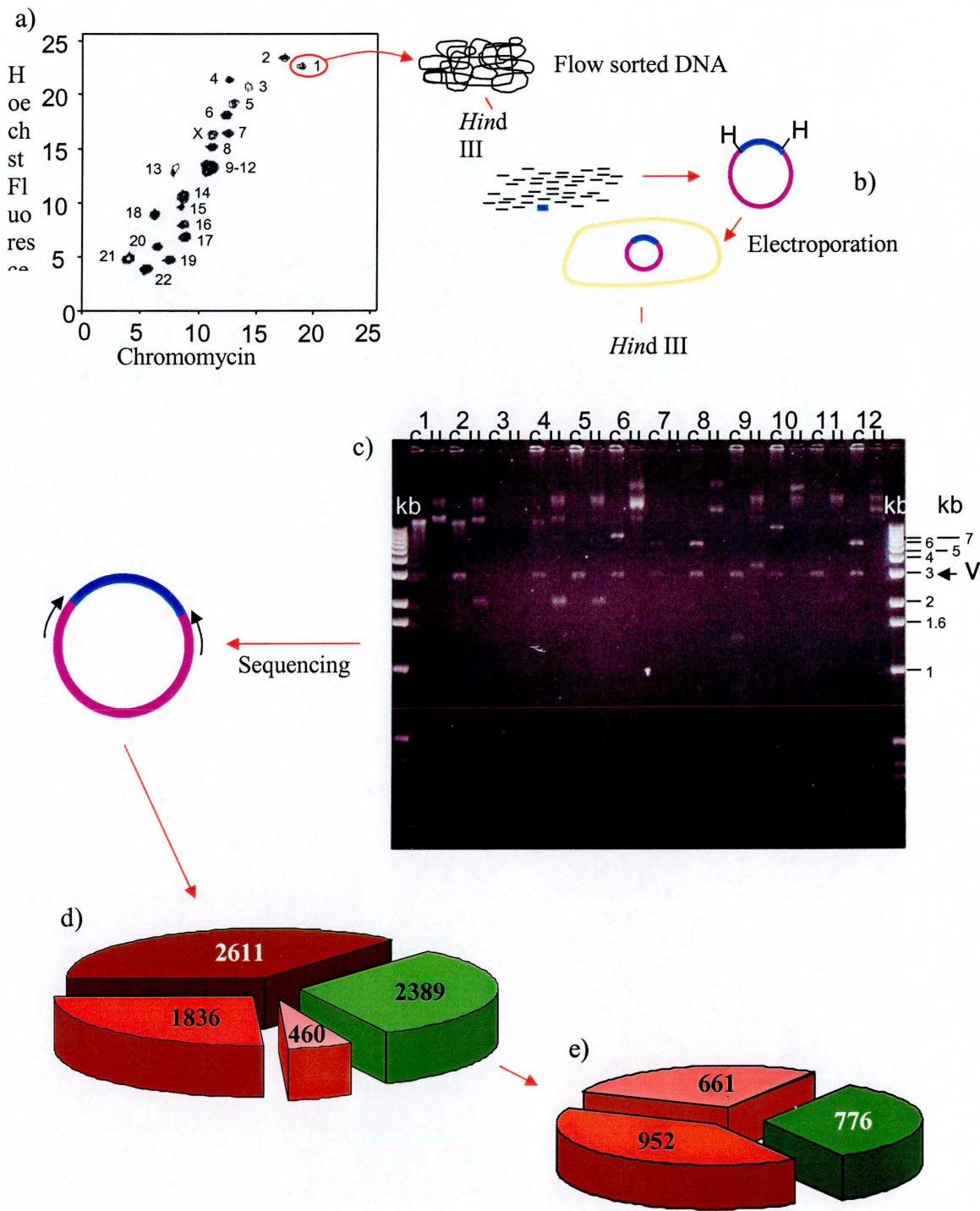


Figure 4.2: The construction of a chromosome 1 specific small insert library. a) A bivariate flow karyotype was generated to flow sort chromosome 1 DNA. b) DNA was completely digested with *HindIII*, cloned into pBluescriptII vector and electroporated into *E. coli* XL1 blue electrocompetent cells. c) Subclones were separated by electrophoresis cut (c) and uncut (u) on an agarose gel and insert sizes determined by use of 1 kb ladder (kb). The vector band (v) was used to correlate the insert size with the undigested band. d) Prior to primer design there were small insert library clone failures at prepping (dark red), sequencing (including sequence of < 80 bp (red)) and STS design stages (pink). Further failures e) were due to repeats contained within either primer (dark red) or during experimentation (pink). The total number of RH mapped flow sorted markers with unambiguous placement on the physical map is represented in figure 4.2e) (dark green).

Figure 4.3 illustrates the size distribution of the 4685 SIL clones that were sequenced. Of these clones, 49% had insert sequences that were inappropriate for primer design. This set comprised 8% that failed to produce sequence; 31% with sequences <80 bp; and 10% with sequence that did not satisfy primer design parameters (e.g. unequal or suboptimal GC content preventing primer design, PCR product size shorter than an acceptable minimum length). The remaining 2389 (51%) small insert library SIL clones sequences (31% of the original number of picked SIL clones) produced sequence from which primer pairs were could be designed (figure 4.2d).

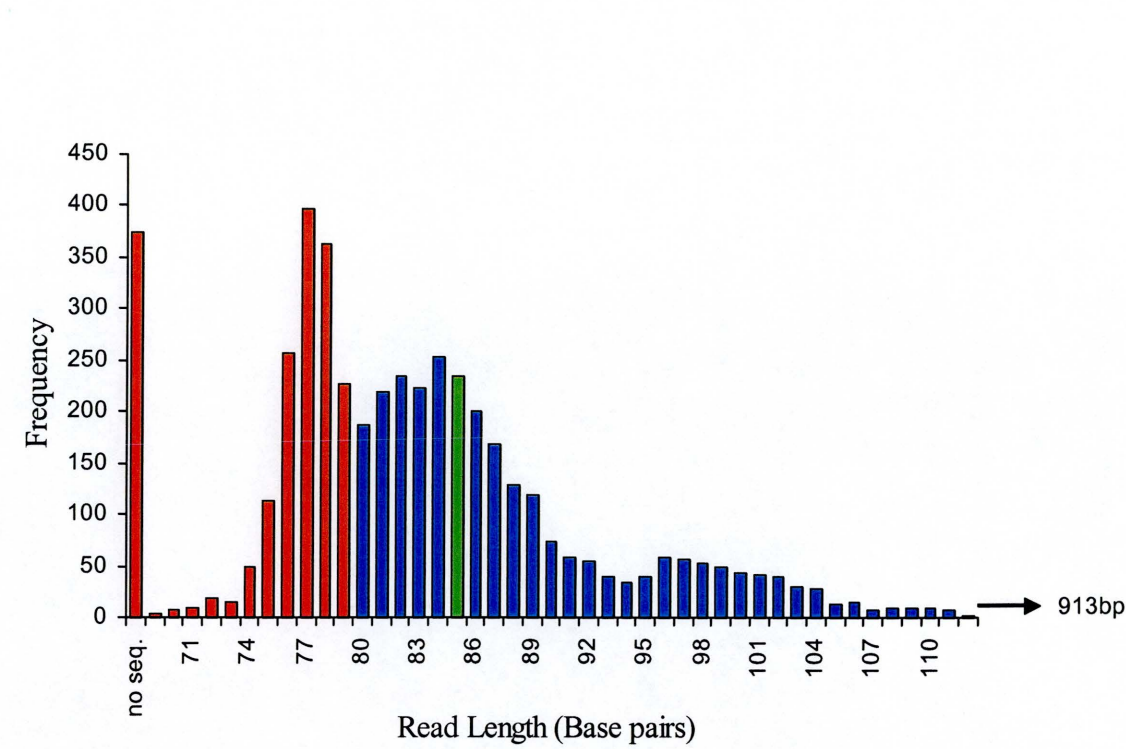


Figure 4.3: Sequence length and frequency of SILs passing STS design stage. Sequences too short for primer design (red), statistically significant proportion (91%) of STSs that generated sequence that were suitable for primer design (blue) and the mean read length, 85 base pairs (green).

4.2.2 Radiation Hybrid Mapping of SIL markers

All 2389 primer pairs were synthesised and tested by RH mapping (by others). Of these, 952 were rejected as at least one of a primer pair wholly or partly contained repeat sequence and a further 439 were experimental failures. These failures included mapping of a marker to multiple chromosomal locations, failure to map to a human chromosome and poor specificity (indicated by production of multiple PCR products generated when different annealing temperatures were used during PCR). The 776 flow sorted STS markers that were successfully

radiation hybrid mapped and placed uniquely on the physical map represent 11% of the flow sorted small insert library clones originally picked for sequencing. As a result of this work, the total number of unique markers in the chromosome 1 RH map was increased from 3642 to 4418.

4.2.3 Bacterial clone contig construction

The combined set of 204 markers localised to the 1pcen-1p13 interval by RH mapping were used to isolate large-insert bacterial clones for contig construction. Initially, each PCR assay was tested by amplification of genomic DNA and DNA from a chromosome 1p hybrid in order to establish optimal conditions for specificity (figure 4.4a). PCR products from the assays were then radiolabelled by PCR and hybridised in pools of 20 – 30 to genomic arrays of PAC clones (fig 4.4b). Positive PAC clones were picked into microtitre plates and re-arrayed on a bacterial clone polygrid filter. Probes were then hybridised individually to the polygrid filter. A total of 110 publicly available and flow-sorted markers were screened in pools across RPCI 1, 3 – 5 PAC libraries identifying 878 PAC clones (the remaining 86 available markers were PAC screened by others as part of the chromosome 1 mapping project). Hybridisation data was entered into a chromosome specific ACeDB database (Durbin and Thierry-Mieg 1994), 1ace. In parallel, positive bacterial clones identified by the pool hybridisation were subjected to restriction digest fingerprinting (Gregory *et al.*, 1996) (figure 4.4c) and marker hybridisation data from 1ace was assimilated within FPC (Soderlund *et al.*, 1997) following contig assembly. Minimum tile path clones representing bacterial clone coverage of island contigs generated by marker hybridisation, were selected for sequencing.

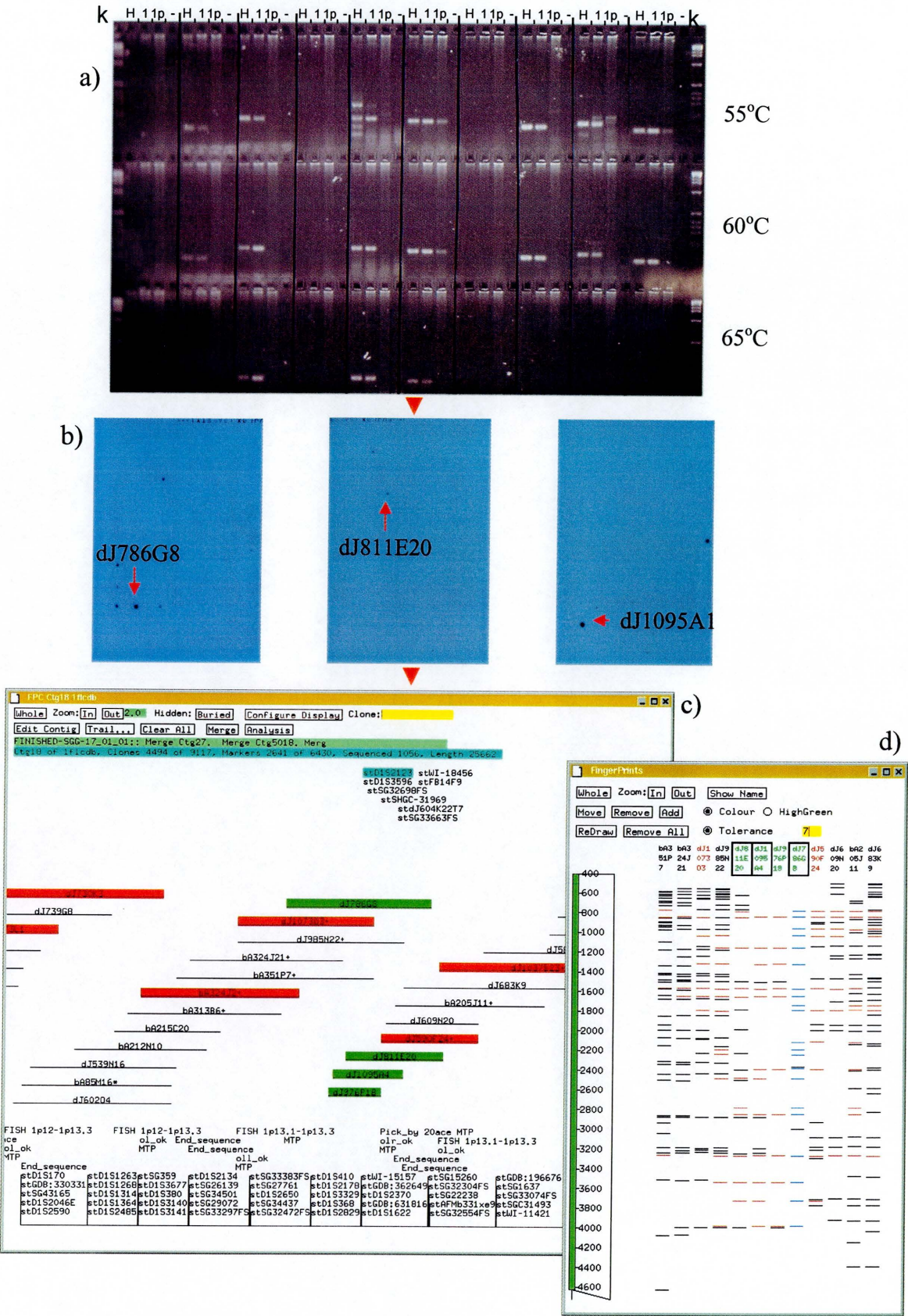
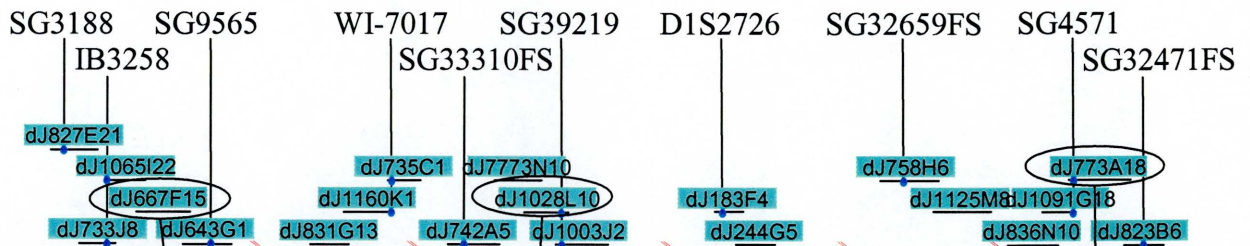


Figure 4.4: Generation of sequence ready bacterial coverage using the hierarchal strategy. a) An agarose gel showing PCR products generated at annealing temperatures of 55°C, 60°C and 65°C. The PCR reaction used total human DNA (H), chromosome 1 (1), chromosome 1p (1p) and a negative control (-) as template. b) Autoradiographs of an STS pool hybridisation to genomic PAC library filters, positives are indicated by red arrows. c) PACs identified by hybridisation were restriction digest fingerprinting, assembled into contigs and assimilated with STS data within FPC. d) The digitised fingerprints (black boxes) of 3 clones identified by pool screening and assembled within FPC.

Bacterial clone coverage of 1pcen-1p13 within the whole genome (WG) fingerprint database (McPherson *et al.*, 2001) was identified either by using the chromosome 1 markers associated with assembled contigs (where they were available), or by adding a representative set of experimental or virtual *Hind* III fingerprints of PAC clones isolated by the hierarchical strategy (Figure 4.5a). Placement of PACs with associated RH mapped STS data within the stringently assembled WG fingerprint database facilitated the localisation and joining of WG BAC contigs. A three-fold redundant tiling path of BAC clones was picked from the WG database (Figure 4.5b) and incorporated into the chromosome 1 specific fluorescent fingerprint database (as part of this thesis and the chromosome 1 project). Once WG BACs were assimilated into the 1pcen-1p13 PAC contigs a more optimal series of BAC and PAC clones were chosen (with more minimal overlaps) as the sequencing tile path (Figure 4.5c). The use of both hierarchical and WG fingerprint approaches resulted in the 1pcen-1p13 interval being covered by 2 bacterial clone contigs. The two bacterial clone contigs were fortuitously linked by 2.3 kb of unfinished sequence from BAC clone bA722J12, produced by

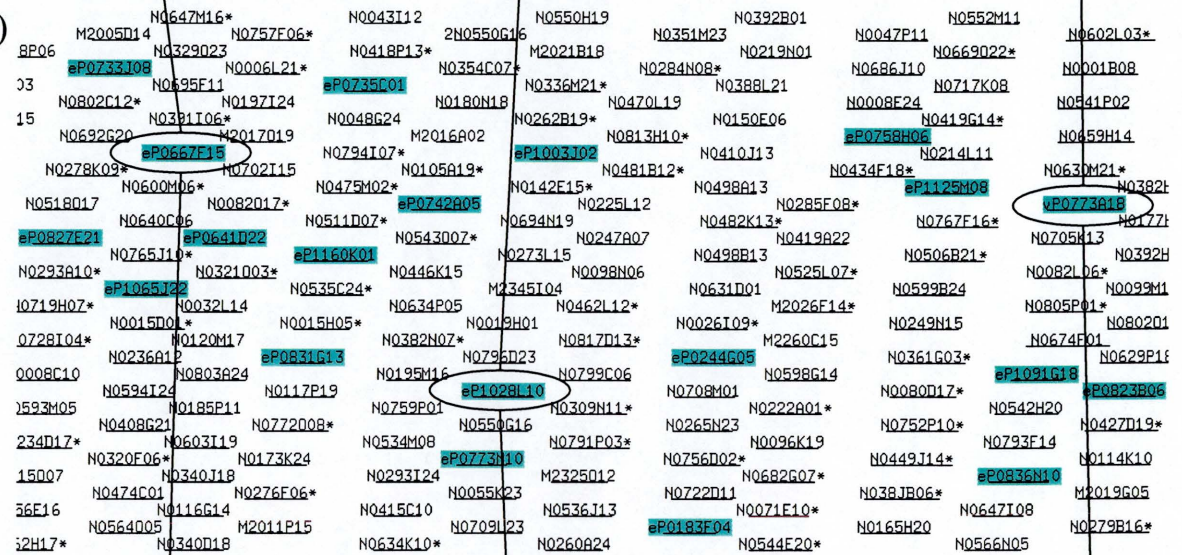
RIKEN Genomic Sciences Center as part of their chromosome 18 sequencing project. The clone appears to have been erroneously chosen by RIKEN as the unfinished sequence is placed uniquely on chromosome 1 by high BLAST score alignment.

a)



Hind III restriction fingerprinting

b)



fluorescent fingerprinting

c)

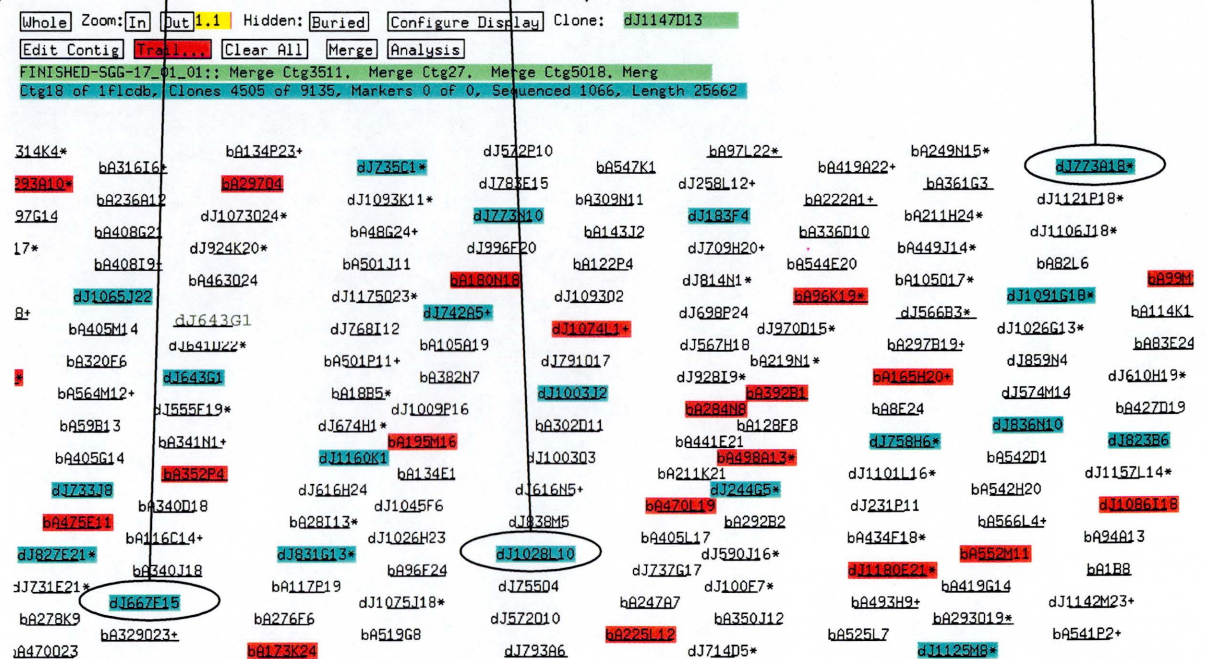


Figure 4.5: The assimilation of PAC contigs into whole genome and chromosome specific fingerprint databases. a) PAC clones representing bacterial clone coverage from the hierarchical mapping technique were added to the WG fingerprint database by either experimental or virtual restriction digest fingerprinting (light blue clones). b) A three fold redundant set of BACs were selected from the WG fingerprint database and incorporated into the chromosome 1 specific database by fluorescent fingerprinting. c) Minimum tile path clones are boxed in red, alignment between the 3 maps is shown by selected clones (circled).

The final 13 Mb bacterial clone contig covering human 1pcen-1p13.2 (figure 4.6a) includes 1130 bacterial clones (480 BACs, 648 PACs and 2 cosmids) and contains 250 markers by hybridisation. Two hundred and four of these markers (157 publicly available and 47 flow sorted) have associated RH mapping data. The final map contained an additional 46 markers without RH information; but these markers were added to the contig map by hybridisation. All markers have a unique chromosomal placement, i.e. either all or the majority of bacterial clones identified by hybridisation have fingerprints that assemble within the 1pcen-1p13.2 contig and to no other location the chromosome. A minimum tile path of 136 minimum clones (figure 4.6b), including 2 previously sequenced cosmids (AC000031 and AC000032), was selected for sequencing (by others) within the Sanger Institute. Figure 4.6c represents an FPC display of a 3 Mb region of the 13 Mb contig which illustrates the extensive coverage of independent map information which anchors clones across the 1pcen-1p13.2 contig. The 3 Mb interval is defined by two framework markers, D1S221 and D1S2746 (markers are denoted by yellow boxes, figure 4.6c). Also shown are markers with RH mapping data (light blue boxes) that were used to identify large insert bacterial clones by hybridisation to genomic library filters.

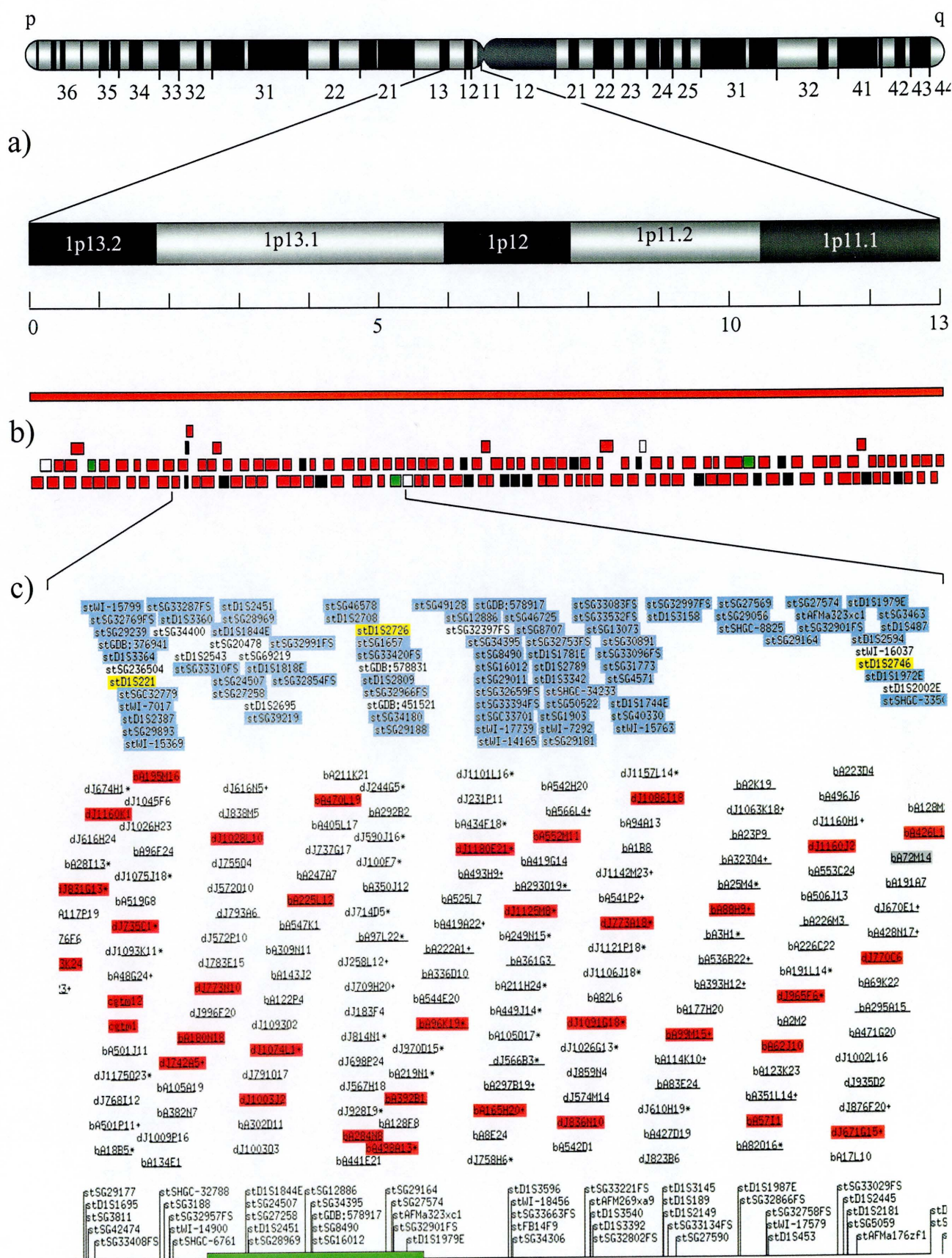


Figure 4.6: A representation of PAC and BAC contig coverage of 1pcen – 1p13. a) An ideogram of the region of bacterial clone contig coverage generated by this study as represented at 850 band resolution of human chromosome 1. b) An AceDB display of the minimum tile path of 136 clones from the 13 Mb contig. Represented are the sequencing statuses of minimum tile path clones (as of 14th October 2002), pre-shotgun (clear boxes), pre-finished (green boxes), finished sequence (red boxes) and submitted sequence (black boxes). c) a 3 Mb region of the final contig depicted in FPC reflecting the density of framework markers (yellow boxes), RH mapped markers (light blue boxes) and non-RH mapped markers (clear) positioned by hybridisation within the bacterial clone contig. Minimum tile path clones are highlighted in red.

4.3 Evaluation of SIL marker distribution in chromosome 1

The chromosomal distribution of 776 RH mapped STSs, originating from the flow sorted small insert library, was evaluated based on the fingerprint map (figure 4.4). The histogram in figure 4.7b depicts the number of STSs in 5 Mb intervals along the length of chromosome 1. The interval size was calculated directly from the fingerprint map using 4 bands / kb (see section 2.22.2). The average number of markers (14.7 / 5 Mb) varies appreciably next to the centromere and telomeres. This may be due to difficulties in cloning bias encountered when cloning chromosomal centromeric and telomeric repeat sequences (Doggett *et al.*, 1995). The overrepresentation of flow-sorted markers in some intervals may relate to sequence content. For example, a region of genomic sequence with a particular base composition (e.g. AT-rich)

may be particularly amenable to digestion with *Hind* III, and thus yield a high fraction of short (easily cloned) *Hind* III region compared to a GC-rich region. This bias would be reflected in the representation of inserts in the SIL, as the SIL was prepared from *Hind*III-digested DNA.

The distribution of the 776 flow sorted markers in the fingerprint-based map was compared to the radiation hybrid map of chromosome 1 (figure 4.7c). There is very good agreement between the two maps, with 12 STSs (1.5%) showing incongruent placement (blue dots). These discrepancies may result from low copy repeats (duplicates not being identified within radiation hybrid vectors) or by experimental error where the wrong STS has been hybridised to the gridded arrays of bacterial clones. The density of markers that have associated RH mapping data and unique chromosome hybridisation data within 1pcen-1p13, was increased from 12 / Mb to 17 / Mb upon addition of flow-sorted markers.

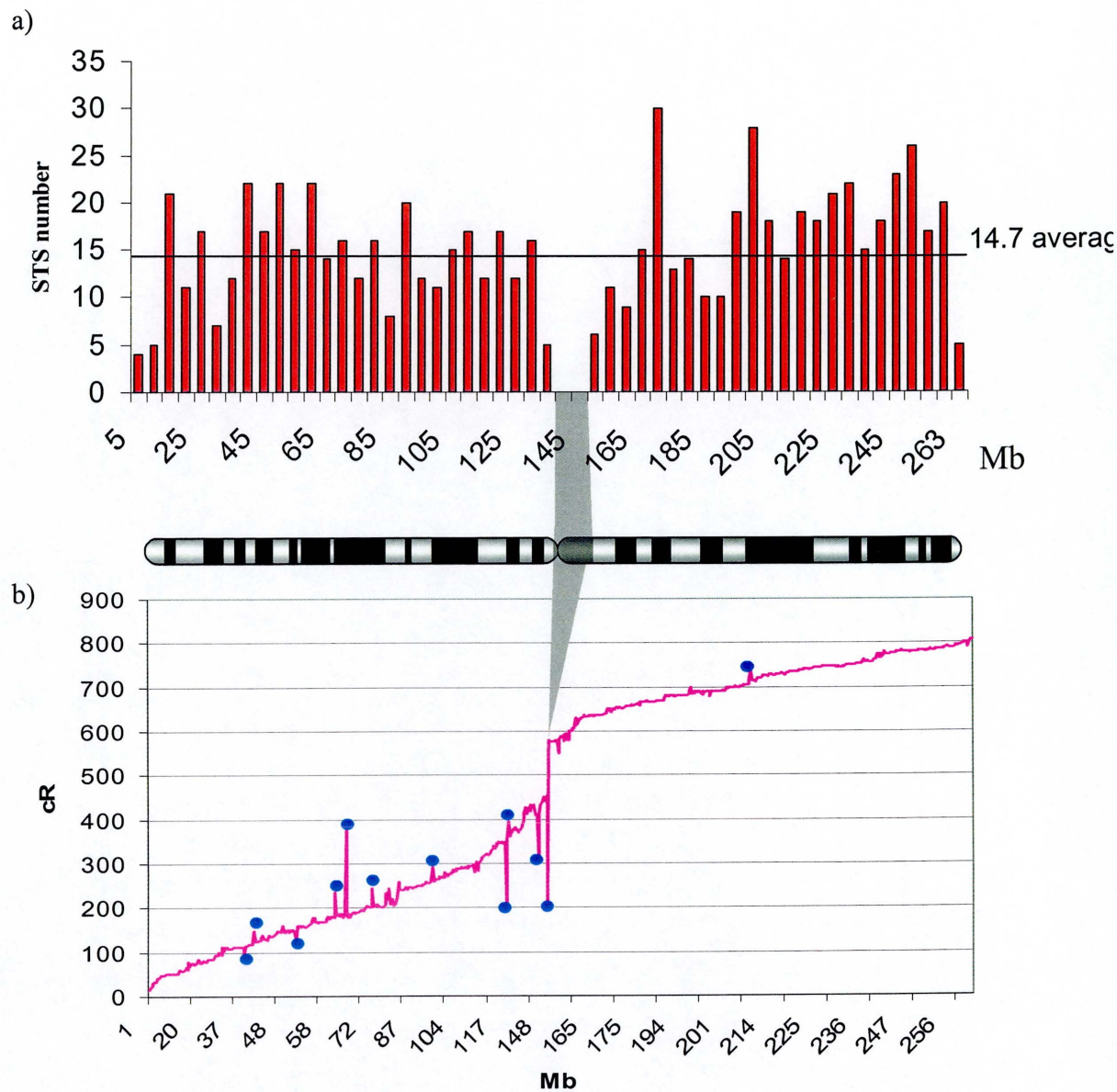


Figure 4.7: Chromosomal distribution of flow sorted markers and comparison to of radiation hybrid and physical maps. a) The chromosomal distribution of 776 RH mapped STSs originating from the flow sorted small insert library along the length of the chromosome in 5 Mb map intervals. b) A comparison of the radiation hybrid map of 778 flow sorted markers and their localisation to bacterial clone contigs by hybridisation, outliers are denoted by blue dots.

4.4 Comparison of Published Maps:

4.4.1 Physical maps

Two physical maps, consisting primarily of YACs, have previously been published within 1pcen-1p13 (Carrier *et al.*, 1996, Brintnell *et al.*, 1997). Carrier *et al.*, (1996) used genetic markers and STSs designed from genes localised to 1p13 to screen CEPH YAC libraries. Overlaps between the eight non-chimeric YACs used to build the 3 Mb contig around the NGFB locus were determined by long-range restriction mapping and by STS content data. Brintnell *et al.*, (1997) used a similar approach to generate YAC coverage (from CEPH and ICI YAC libraries) across an interval of 1p13.1 but also included CIT library BACs within the contig. Though the two contigs overlap, based on their shared content of marker D1S252, the Brintnell *et al.*, (1997) map extends distally by 1.7 Mb. Both maps, with the exception of one marker, were in broad agreement with the physical map described here (within the limits of localising a marker or gene by hybridisation to a YAC or YAC restriction fragments). One conflicting marker, D1S3347, was positioned within 1p13 by Brintnell *et al.*, (1997) but has subsequently been localised to 1p35.3 by RH mapping. BLAST analysis of D1S3347 places the marker in 1p35.1 and 1p12 via a high BLAST score and 95% sequence alignment (the parent sequence contains ambiguous bases, thus the <100% BLAST score). D1S3347 (synonymous with WI-8708) was derived from an EST. Subsequent alignment of the EST to genomic sequence (by Ensembl analysis) indicates the marker is derived from the 3' UTR of an mRNA isolated from small cell carcinoma lung tissue by the IMAGE consortium. The three exon gene is localised to 1p35.1 whilst a processed mRNA, inserted into the genomic

sequence in the reverse orientation, is contained within 1p12 and thus explains the discrepant placement of the marker in the Brintnell *et al.*, (1997) study.

4.4.2 Genetic map

The generation of a bacterial clone contig within 1pcen-1p13 permitted a comparison to be made with the genetic map of chromosome 1 (Dib *et al.*, 1996). The order and distance between 27 genetic markers placed uniquely in the bacterial clone contig by hybridisation was determined. There was very good agreement between the two maps in relation to marker order (figure 4.8), with the higher resolution bacterial clone map facilitating the separation of markers that had previously been placed within the same genetic interval. Two genetic markers showed discrepant placement; the first, D1S2852 (152.2 cM, 8.2 Mb) localises to its current position in the physical map by hybridisation and sequence alignment; the second, D1S418 (152.2 cM, 11.3 Mb), was positioned by weak hybridisation to two PAC clones within the contig. BLAST analysis of the sequence from which D1S418 was derived (which contains ambiguous bases) localises the marker within PAC clone dJ671G15 placing it in the correct physical map location. Incorrect placement of these markers within the Généthon genetic map may be attributed to the level of resolution provided by the number of meioses used to construct the map.

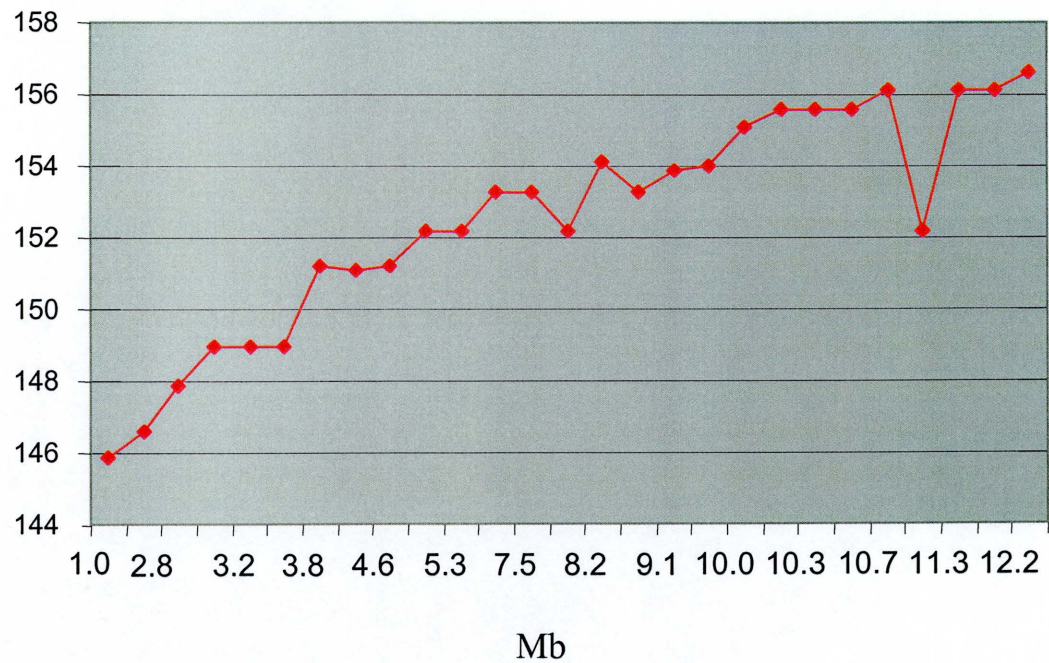


Figure 4.8: The distribution of genetic mapped markers positioned within the 1pc – 1p13 contig by hybridisation. The physical map is plotted on the X-axis in megabase (Mb) and the Y-axis in centimorgans (cM).

4.4.3 Radiation hybrid map

To investigate the order and resolution of radiation hybrid markers on the physical map, markers with unique hybridisation positions on the fingerprint map were plotted against their RH map locations. Figure 4.9 shows a good correlation for the most part between physical and RH maps but indicates a number of markers that appear to be poorly resolved on the RH map. Twenty seven markers show discrepant placement of >15 cR from their physical map position, the resolution of the chromosome 1 RH map (Panos Deloukas personal communication). One marker was subsequently placed correctly by BLAST analysis and a

second marker incorrectly placed because one of the primer pairs was designed within a repeat. The remaining 25 are placed on the physical map by unambiguous hybridisation and or electronic PCR (ePCR) (Schuler *et al.*, 1997).

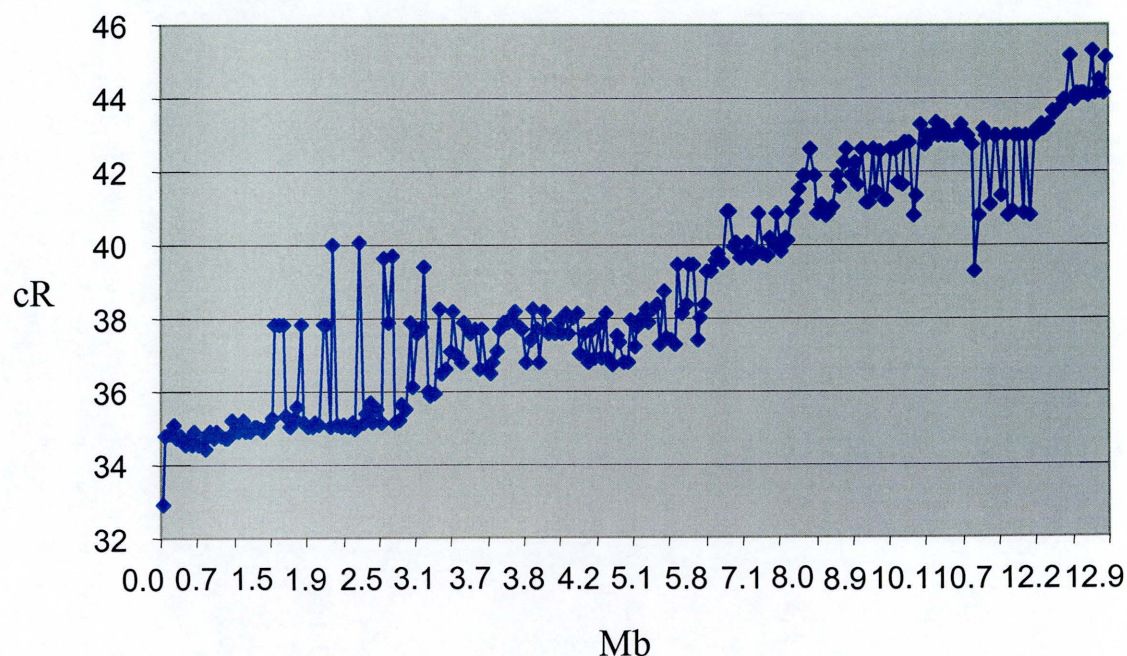


Figure 4.9: The distribution of radiation hybrid mapped markers positioned within the 1pc – 1p13 contig by hybridisation. The physical map is plotted on the X-axis in megabase (Mb) and the Y-axis in centi-ray (cR).

4.4.4 A comparison of three maps

The comparative accuracy of the genetic and radiation hybrid maps can be evaluated by plotting a set of markers contained within all three maps from the analyses above (figure 4.10). The genetic map shows good agreement with the physical map (discrepant markers being accounted for above) with markers placed within the same genetic interval being

resolved. The RH map provides higher resolution and is also mostly in good agreement with the other map and provides both more markers and a higher resolution than the genetic map. However it also shows more discrepancies in marker order (see chapter 7).

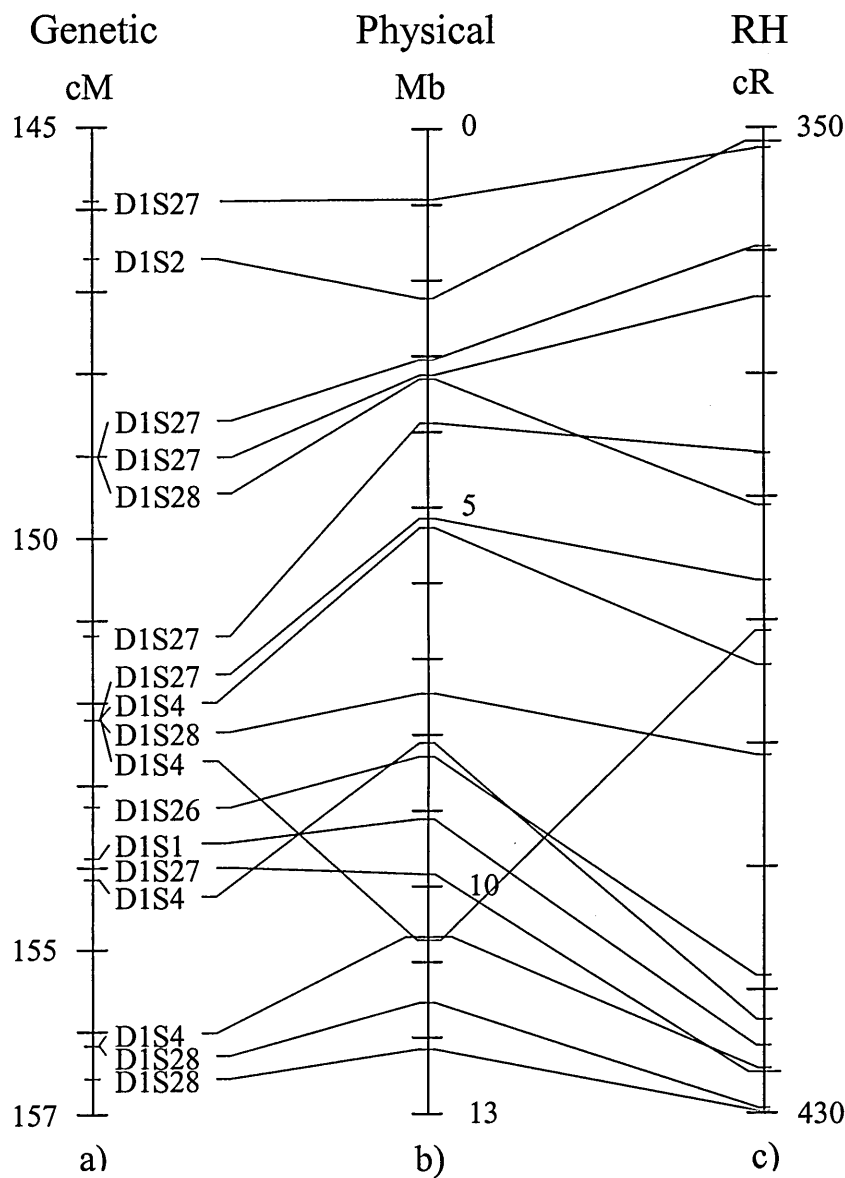


Figure 4.10: A comparison of marker distribution between genetic a), physical b) and radiation hybrid c) maps of 1pcen – 1p13. Only markers that were present on all three maps have been represented.

4.5 Discussion

Two different strategies were used to construct a 13 Mb bacterial clone contig of human chromosome 1pcen-1p13. Bacterial clone coverage was initiated by utilising publicly available markers, localised to 1pcen - 1p13 by RH mapping, to screen large insert PAC libraries. The non-random distribution of these markers (a large proportion of which had been derived for positional cloning projects or from ESTs, thus enriching marker density in disease regions or gene-rich regions, respectively) required the generation of flow sorted STSs. A total of 776 markers derived from a SIL, were successfully placed on the chromosome 1 specific radiation hybrid map and 47 of them mapped within the region 1pcen-1p13 markers. This supplemented the publicly available markers in the region (157) and increased the density of markers from 12 per Mb to 17 per Mb, above the target density of 15 per Mb (Olson *et al.*, 1993, Bentley *et al.*, 2000). PACs identified by genomic library screening of all markers within the interval were fingerprinted and assembled into contigs. Selected PACs from these island contigs were incorporated within the whole genome BAC fingerprint database by *Hind* III fingerprinting and overlap analysis. Clones from this database were retrieved and incorporated into the local study. At the end of the project, a three-fold redundant tile path of 480 BAC clones, from the whole genome fingerprint database, in addition to the 648 PACs, identified by library screening, constitute the 13 Mb contig.

The generation of contiguous physical map coverage has permitted a high resolution comparison to be made of genetic and radiation hybrid maps within the interval. The algorithms used to construct the RH map assume random distribution of breaks along the

length of the chromosome. Experimental data (Deloukas *et al.*, 1998) has shown that the high retention rate at the centromere, coupled with variation of DNA fragment sizes (in comparison to the rest of the chromosome), results in an overestimation of the cR distances between markers adjacent to the centromere. These anomalies explain why there are a relatively high percentage of markers that show discrepancies between the two maps and why the usual size estimate of 1 cR₃₀₀₀ to 250 kb (Deloukas *et al.*, 1998) does not hold within 1pcen-1p13. According to the RH map the 105 cR interval should be 26 Mb where as it has been shown to be ~13 Mb.

The relative uniformity of the physical map metric facilitated the resolution of markers that had previously been localised to the same interval on the genetic map. Apparent differences in recombination rate across the interval, as shown by the step-wise comparison of genetic and physical maps in figure 4.8, cannot be determined from the resolution of the bacterial clone contig and would have to be resolved by placement of the markers within contiguous genomic sequence. The physical map is not a uniform metric as it relies upon the existence of *Hind* III sites for the generation and overlapping of fingerprint bands; a clone with a large number of bands may contain the same amount of genomic sequence as a shorter clone with fewer bands.

It has been proven that there is a large variation in the rate of recombination along the length of a chromosome (IHGSC, 2001). Recombination rates at telomeres are greater than within chromosome arms which are in turn greater than regions adjacent to the centromere.

Therefore, it was not unexpected that a shorter genetic distance, 8.7cM defines a larger physical distance, 13 Mb, within 1pcen-1p13.

The bacterial clone map has provided a means by which a more accurate estimate of the physical size of the interval can be made, overcoming inherent levels of lower resolution within genetic and radiation hybrid mapping. High resolution sequence analysis of the 136 minimally overlapping bacterial clones selected for sequencing from the contig constructed here forms the basis of the next chapter.

Chapter 5

Sequence analysis of 1pcen – 1p13.2

5.1 Introduction

5.2 Sequence Composition Analysis

5.2.1 G-Banding

5.2.2 Isochores

5.2.3 Repeats

5.2.4 Low copy repeats

5.2.5 CpG Islands

5.2.6 Eponine

5.3 Gene Identification

5.3.1 Known genes

5.3.2 Novel genes

5.3.2.1 Splicing ESTs support the structure of a gene

5.3.2.2 mRNA support of novel coding features

5.3.3 Novel transcripts

5.3.4 Pseudogenes

5.4. Gene assessment

5.4.1 Alternative splicing

5.4.2 Genic features

5.4.2.1 Putative bidirectional promoters

5.4.2.2 Overlapping genes

5.5 Inferring function by protein homology

5.5.1. Identifying function through sequence homology

5.5.2. Identifying function by structural homology

5.6. Discussion

5.7. Appendix

5.1 Introduction

The production and analysis of human genomic sequence facilitates the systematic identification of genes and other functional units within the human genome. Accurate annotation of genes and characterisation of regulatory elements will not only help to identify disease genes but further our understanding of the biological systems in which all genes are involved.

Unfinished (draft) and finished genomic sequence has provided the foundation for these analyses. Analysis of draft sequence data can provide a powerful insight into a genomic landscape but because of its inherent limitations (incomplete genomic coverage, uncertain contig orientation and standard of trace data) it is preferable to use contiguous finished sequence. Finished sequence contains higher quality data: The criteria established in early genome sequencing projects (The *C. elegans* Sequencing Consortium 1998) and extended to the human genome required that all sequence be finished with an accuracy of >99.99%, leaving no gaps. This provides the best possible starting point to permit exact annotation of genes and characterisation of the genomic landscape. Furthermore, an accurate reference sequence allows for the identification of genetic variation, such as single nucleotide polymorphisms (SNPs) by comparison of additional high quality sequence traces to the finished sequence (see chapter 6). The availability of finished sequence also enables comparative analyses with other genomes to be performed. Such analyses can subsequently assist in the determination of gene structures at the sequence level and provide some insight into common evolutionary origins.

Finished sequence from 127 of the 136 PAC, BAC and cosmid minimum tile path clones, selected from the bacterial clone contig constructed in the previous chapter, enabled such a genomic analysis of 1pcen – 1p13 to be carried out. This chapter describes a detailed characterisation of repeat sequences (including high resolution GC and isochore analysis) and the localisation and annotation of known genes and identification of novel transcripts.

5.2 Sequence Composition Analysis

Eight sequence contigs, containing 127 minimum tile path clones, represented 95% coverage of 1pcen – 1p13 (11.8 Mb / 12.4 Mb) (figure 5.1a). This long range sequence continuity permitted a detailed investigation of the genomic landscape to be made, including GC profile, repeat content and CpG island identification (sequence analysis performed by James Gilbert).

5.2.1 G-Banding

Chromosome banding, produced by Giemsa staining of metaphase chromosomes, provides a means of partitioning regions of individual chromosomes for low-resolution cytogenetic mapping. Giemsa preferentially binds to AT rich regions of DNA therefore producing characteristic patterns of dark-staining or G(iemsa) bands (AT rich - GC poor) and light-staining or R(everse) bands (GC rich) (Francke *et al.*, 1994). The characterisation of GC content within an interval is important feature to determine, as variation of GC between

regions has been associated with differences in biological properties such as repeat composition, gene density and structure. *In situ* analysis of 54 clones from the mapped contig (see table 5.1) confirmed the localisation of the contig to 1pcen – p13, relative to the 850 cytogenetic G-banding pattern previously reported (reviewed in Bickmore *et al.*, 1989, Francke *et al.*, 1994) (see fig 5.1c). Examination of the genomic sequence within 1pcen – 1p13 indicates a correlation between variations in GC content across the interval (figure 5.1b) and the G and R bands (figure 5.1c). The relative position of the light bands, 1p13.1 and 1p11.2, show a good correlation with regions in the sequence of GC content higher than the genome average of 41% (blue dotted line). Conversely, the location of dark bands 1p13.2 and 1p12 correlate with regions of below-average GC content. The designation of 1p11.1 as a grey band (containing an intermediate GC content) seems to be born out by comparison with GC within the finished sequence.

Table 5.1: Fluorescence *in situ* hybridisation data of selected bacterial clones from 1pcen – p13. Data associated with clones listed in the first column can be placed on the map via accession clones in the third column.

Clone	FISH	Acc Clone	Acc number
RP11-401O13	1p13.2	RP11-356N1	AL390036
RP11-258P6	1p13.2-1p21.1	RP11-256E16	AL160171
RP4-667F15	1p12-1p13.3	RP4-667F15	AL138933
RP4-641D22	1p13.1-1p13.3	RP11-352P4	AL356389
RP5-831G13	1p13.3-1p21.1	RP5-831G13	AL355145
RP4-6768I12	1p13.3-1p21.1	RP5-1160K1	AL355310
RP11-195M16	1p13.3-1p21.3	RP11-195M16	AL450468
RP4-742A5	1p13.2-1p21.1	RP4-742A5	AL355817
RP4-773N10	1p13.1-1p13.3	RP4-773N10	AL160006
RP5-1003J2	1p12	RP5-1003J2	AL137790
RP5-1074L1	1p13.3-1p21.1	RP5-1074L1	AL355488
RP11-498A13	1p13.2-1p21.1	RP11-498A13	AL354713
RP11-96K19	1p13.2-1p21.1	RP11-96K19	AL360270

RP5-1019F20	1p13.1-1p13.3	RP11-96K19	AL360270
RP5-1180E21	1p13.1-1p13.3	RP5-1180E21	AL355816
RP4-758H6	1p13.3	RP5-1180E21	AL355816
RP5-836N10	1p13.1-1p13.3	RP5-836N10	AL391063
RP4-773A18	1p13.2-1p21.1	RP4-773A18	AL049557
RP11-534M8	1p13.2-1p21.1	RP11-88H9	AL512665
RP4-671G15	1p13.1-1p13.3	RP4-671G15	AL354760
RP4-580L15	1p13.1-1p13.3	RP4-580L15	AL158844
RP11-31F15	1p13.1-1p13.3	RP11-31F15	AL390242
RP4-658C17	1p11.1	RP4-658C17	AL139016
RP4-730K3	1p12-1p13.3	RP4-730K3	AL133517
RP5-1073O3	1p13.1-1p13.3	RP5-1073O3	AL137856
RP5-1037B23	1p13.1-1p13.3	RP5-1037B23	AL162594
RP4-543J13	1p13.1-1p13.3	RP4-543J13	AL121999
RP4-591B8	1p13.1	RP4-591B8	AL035410
RP5-1156J9	1p12-1p13.2	RP5-1156J9	AL133382
RP5-1000E10	1p12-1p13.3	RP5-1000E10	AL096773
RP5-1165D20	1p13.1-1p13.3	RP11-350E19	AL358372
RP4-666F24	1p13.1-1p13.3	RP4-666F24	AL109660
RP4-662B22	1p12-1p13.3	RP4-662B22	AL049825
RP5-940J24	1p13.1-1p13.3	RP5-940J24	AL157950
RP11-12L8	1p12-1p13.3	RP11-12L8	AL357137
RP5-1185H19	1p13.1-1p13.3	RP5-1185H19	AL121982
RP4-787H6	1p12-1p13.2	RP4-787H6	AL355538
RP5-1086K13	1p12-1p13.2	RP5-1086K13	AL390066
RP4-655N15	1p13.1-1p13.3	RP4-655N15	AL135798
RP4-753F5	1p13.1-1p13.3	RP4-753F5	AL157904
RP4-570D9	1p12-1p13.3	RP4-570D9	AL139248
RP11-188D8	1p12-1p13.2	RP11-188D8	AL358072
RP4-675C20	1p13.2	RP4-675C20	AL157902
RP11-172A5	1p11.1-1p13.1	RP4-675C20	AL157902
RP4-757N13	1p13.1-1p13.3	RP4-757N13	AL122007
RP4-776P7	1p13.1-1p13.3	RP4-776P7	AL121993
RP5-832K2	1pcen-1p12	RP5-832K2	AL139345
RP4-730H16	1p13.1-1p13.3	RP4-730H16	AL122006
RP5-876G11	1p11.1-1p13.1	RP11-94F13	AL606843
RP4-712E4	1p11.1	RP4-712E4	AL139420
RP5-920G3	1p12-1p13.3	RP5-920G3	AL121995
RP4-599G15	1p12-1p13.2	RP4-599G15	AL109966
RP4-656M7	1p11.1-1p13.1	RP4-656M7	AL139251
RP5-1042I8	1p11.1-1p13.2	RP5-1042I8	AL359752

5.2.2 Isochores

Another means of determining the different components of GC content from the interval is by isochore analysis. It has been demonstrated that human nuclear DNA can be resolved into a number of different components based on GC content when ultra-centrifuged in $\text{Cs}_2\text{SO}_4\text{-Ag}^+$ gradients. These studies led Bernardi *et al.*, (1985) to propose that the separated components, termed isochores, consist of long regions within which GC content is relatively homogeneous. The individual isochores were subsequently classified according to their relative GC content, i.e. light (GC poor) family members L1 and L2 contain <38% and 38-42%, GC respectively, whilst heavy (GC rich) family members, H1, H2 and H3 contain 42-47%, 47-52% and >52%, GC respectively. To determine the isochore content within 1pcen – 1p13, sequence contigs were analysed (by Jose Oliver) (Bernaola-Galvan *et al.*, 1996) and the results plotted against the GC and cytogenetic landscape of the interval (figure 5.1d). Plotting of the isochore family members shows that there is a very good correlation of variation in GC content and provides an additional level of resolution in comparison to the G-banding. Though the resolution of isochore analysis is less than that of a GC profile it allows for defined regional assessments of GC analysis across the interval. Chromosome bands 1p13.2, 1p13.1, 1p12, 1p11.2 and 1p11.1 gave average GC contents based on isochore analysis that was in accordance with their banding pattern as determined by Giemsa staining i.e. L2 (39.1%), H1 (43.9%), L1 (39.7%), H1 (42.4%) and L1 (39.7%) respectively. The majority of the 11.8 Mb of finished sequence of 1pcen – 1p13.2 is contained within GC poor L family isochores (57.3%) whilst H1 isochores (32.6%) make up the majority of the H family isochore coverage, with H2 and H3 isochores contributing 8.9% and 1.2% respectively. The average percentage GC for the entire interval is 41.5% (fluctuating between 30% to 58), which is marginally above the genome average of 41% (IHGSC, 2001).

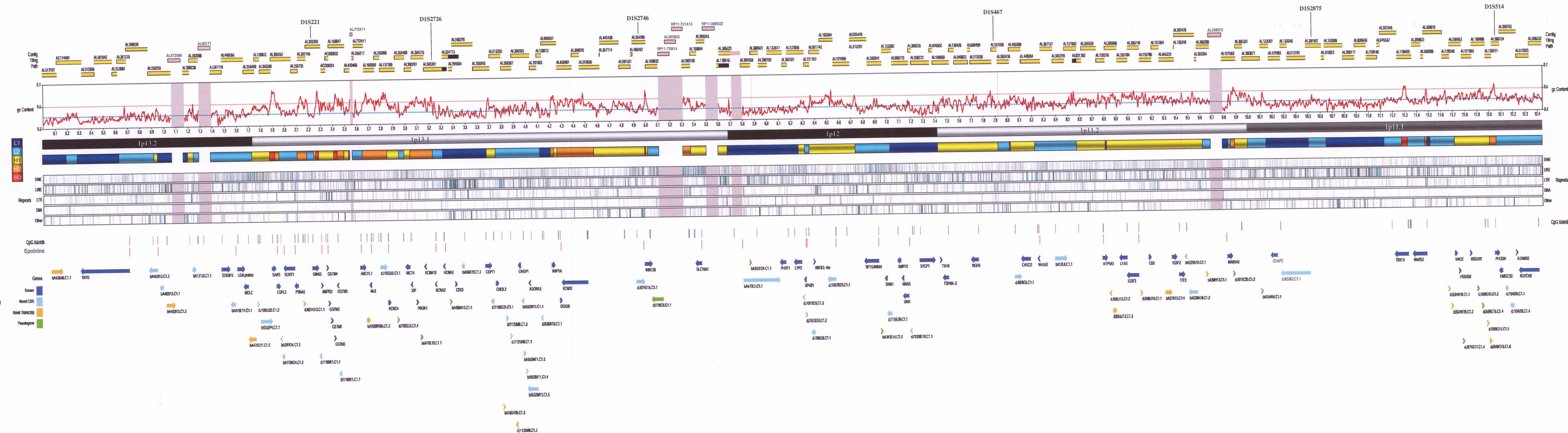


Figure 5.1: The genomic characterisation of human chromosome 1pc – 1p13. Figure 5.1a) represents the framework markers and 136 minimum tile path clones from the interval (finished clones with accession numbers are yellow, unfinished clones with accessions or clone names are light pink). Variations in GC profile, b), across the region are represented as a red line with the genomic average of 41% drawn as a dotted blue line. G (dark) and R (light) banding cytogenetic patterns of from Giemsa staining are illustrated in c). The results of isochore analysis are depicted in d), dark blue band = L1 isochore, light blue = L2, yellow = H1, orange = H2 and red = H3. Transposon derived repeats, short interspersed elements (SINEs), long interspersed elements (LINEs), long terminal repeat retrotransposons (LTRs), DNA transposons (DNA) and others are represented in e). Putative promoter and transcription start sites are represented by CpG islands and Eponine predictions, respectively, in f). Genes within the interval, and their classification, are represented in g). The direction of transcription and size of the gene within genomic sequence is indicated by the direction and length of the arrow drawn above the gene name.

5.2.3. Repeats

It is estimated that repeat sequences account for approximately 50% of the human genome (IHGC 2001). Therefore, assessment of repeat type and distribution is an important factor when characterising the genomic landscape within 1pcen – 1p13. Transposon-derived repeats, which account for approximately 90% of repeats in the human genome (IHGSC, 2001), were plotted by analyzing the sequence content within a 8000bp sliding window, sampled every 4000bp, with RepeatMasker (Smit and Green, unpublished,

<http://repeatmasker.genome.washington.edu>) (figure 5.1e). Repeat content was divided into short interspersed elements (SINEs, including Alu repeats), long interspersed elements (LINEs), long terminal repeat retrotransposons (LTRs), DNA transposons (DNA) and others. Whilst LTRs and DNA transposons exhibit a fairly uniform distribution across 1pcen – 1p13, LINE and SINE repeats share an inversely related distribution. LINE elements conform to their reported higher distribution within AT rich, dark band regions (Smit *et al.*, 1999) whilst SINE elements show a higher density in GC rich light bands. Interestingly, 1p13.1, a GC rich light band, contains a LINE ‘island’ which corresponds with an L1 isochore at approximately 3.5 Mb of the finished sequence link. The total repeat content within 1pcen – 1p13 of the various transposon-derived repeats is represented in table 5.2.

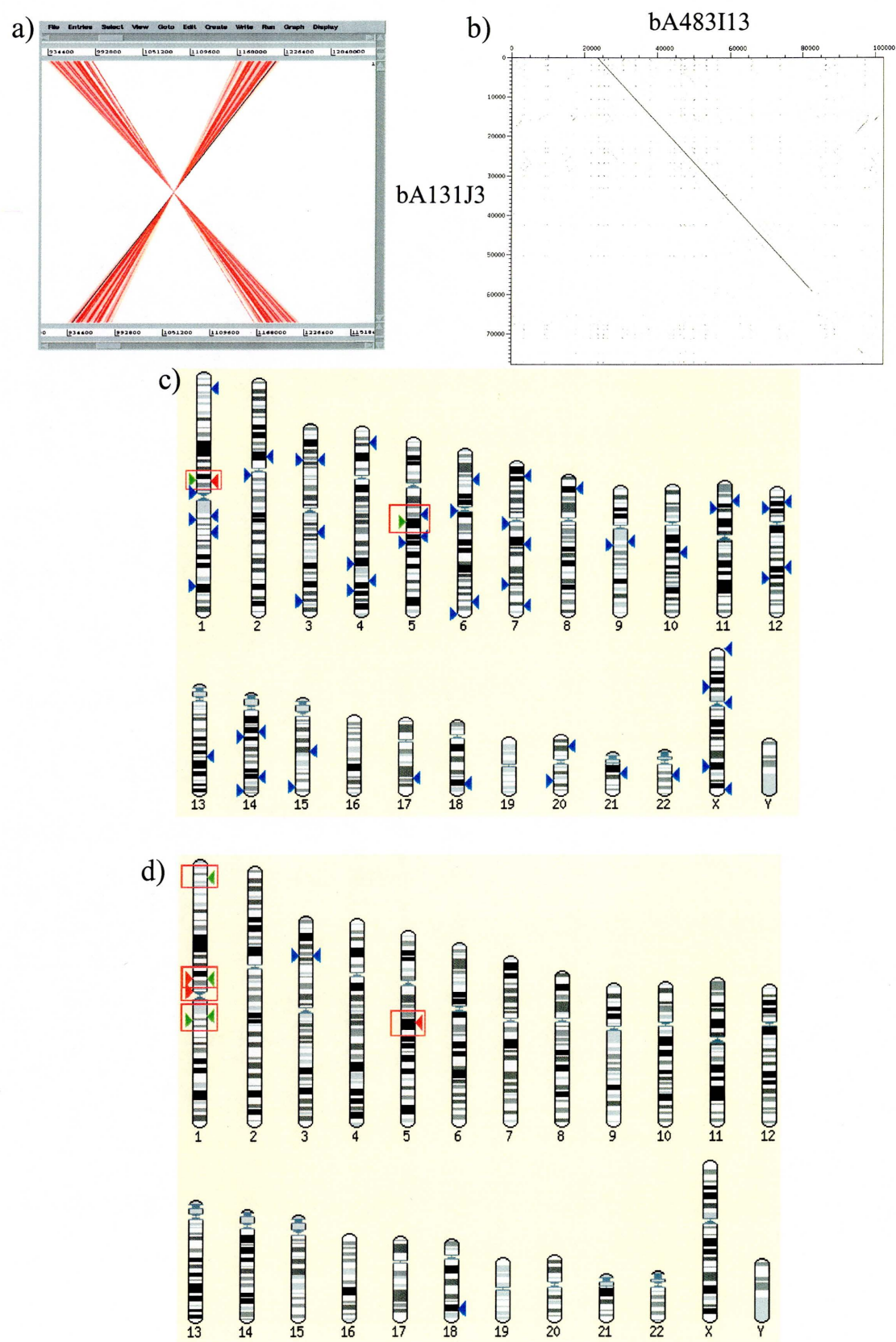
Table 5.2: The breakdown of repeat content within 1pcen – 1p13.2.

Repeat	Mb	Percentage
Alu	1.09	9.27
MIR	0.35	2.96
MIR3	0.05	0.45
Total SINE	1.49	12.68
L1	1.98	16.88
L2	0.55	4.71
L3	0.06	0.48
Total LINE	2.59	22.08
Total DNA	0.34	2.91
Total LTR	0.79	6.75
RNA	0.00	0.03
Unclassified	0.04	0.33
Total	5.26	44.77%

5.2.4. Low copy repeats

An estimated 3.3% of the human genome is duplicated in segments of greater than 1 kb with 90-99.5% sequence identity (IHGSC, 2001), with intrachromosomal duplications accounting for almost two thirds of these (i.e. 2% of the genome). To identify low copy repeats within 1pcen – 1p13 the 11.8Mb of finished sequence was initially analysed for repeats using RepeatMasker (Smit and Green, unpublished, <http://ftp.genome.washington.edu/RM/RepeatMasker.html>) to remove previously characterised common repeats and then compared to itself by BLAST analysis. ACT (<http://www.sanger.ac.uk/Software/ACT>), which was used to view intrachromosomal duplications after self-matches were removed (figure 5.2a), indicated two segmental duplications 59 kb in size and located 79 kb apart, with one copy of the repeat being inverted with respect to the second. Dotter (Sonnhammer *et al.*, 1995) analysis of the repeats (figure 5.2b) indicates the size and level of sequence homology (99%) of the low copy repeat shared between bA483I13 (AL359258) and (AL390038). BLAST analysis of the one duplicated region within Ensembl (<http://www.ensembl.org/>) indicated that the region was also involved in an interchromosomal duplication. Results indicated a match between the two closely linked regions in 1p12 (red boxes figure 5.2c) described above and an additional locus in 5q14.3 with a BLAST alignment of 99% and score of 15000. It was noted that a transcript was contained within each of the three segmentally duplicated regions. BLAST analysis of the mRNA (AK057395) within Ensembl identified an additional five high BLAST scoring loci, BLAST alignments of > 83% and scores of > 880, containing homologs to the duplicated mRNA (figure 5.2d).

The conservation in type and position of SINE repeats within the gene structures annotated from AK057395 suggests that the low copy repeat duplication arose since the divergence of *Homo sapiens* from mouse. The occurrence of Alu elements within the human genome coincides with the radiation of primates in the past 65 million years (Deininger *et al.*, 1986), therefore the duplication of this region must have occurred within this period of time (figure 5.2e).



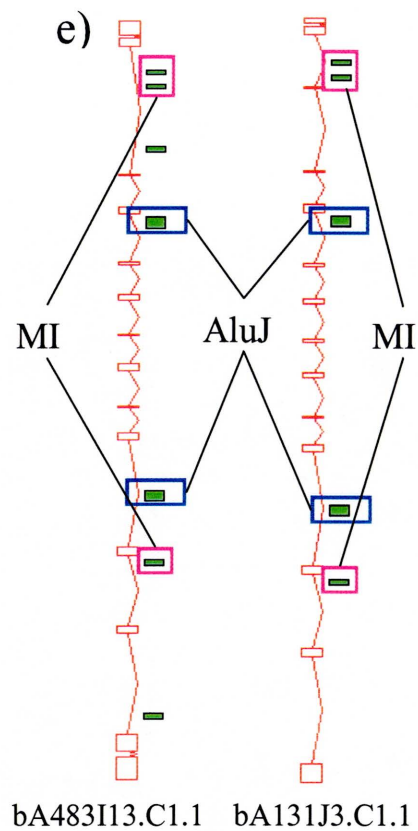


Figure 5.2: Low copy repeat detected within 1pc – 1p13. a) The relationship between two 59Kb inverted repeats, containing two novel genes, show an inverted relationship within ACT. b) Dotter displays the level of sequence homology between the low copy repeat regions. c) BLAST analysis of one of the low copy genomic repeat sequences within Ensembl identifies two regions of homology (red boxes). The adjacent region containing the repeat sequence is also identified (green arrow – chromosome 1) in addition to a homologous region on chromosome 5q14.3 (green arrow, red boxes, d). BLAST analysis of the mRNA from which the two chromosome 1 genes were derived shows high BLAST homology to two other regions of chromosome 1. e) Comparison of the repeat sequences contained within the original duplicated regions in 1pc – 1p13 reveals maintenance of SINE repeat family types

5.2.5. CpG islands

CpG islands are characteristic regions of GC-rich DNA that contain unmethylated CpG dinucleotides and are predicted to lay at the 5' ends of approximately 56% of human genes (Antequera and Bird, 1993). The occurrence of putative CpG islands (i.e. predicted by base composition, but without experimental testing of their methylation state) adjacent to the 5' ends of genes has been used as a means of identifying the sites of transcription initiation and therefore as an *in silico* assay to determine the completeness of gene annotation and, to a lesser extent, a method of estimating gene density. CpG islands within 1pcen – 1p13 were predicted (courtesy of Gos Micklem) by searching for DNA sequences of >400bp in length, >50% GC content and having an expected / observed CpG count of >0.6. A total of 94 CpG islands were predicted within 1pcen – 1p13. The distribution of CpG islands within isochores followed an expected association with GC content, with GC-poor L1 and L2 isochores containing 14 (0.57 CpG / Mb) and 20 (0.61 CpG / Mb) respectively, whilst GC-rich H1, H2 and H3 isochores contained 33 (1.01 CpG / Mb), 18 (2.02 CpG / Mb) and 9 (7.67 CpG / Mb) respectively. Detailed *in silico* annotation and experimental analysis of the region (see section 5.3) identified 102 full length gene structures, 58 of which (57%) were located adjacent to a putative CpG island. The percentage association of CpG islands to genes within the interval is very close to the predicted genome average of 56% (Antequerra and Bird, 1993). An interesting feature of the localisation of putative CpG islands within the interval is the apparent sharing of a CpG island by a pair of genes orientated on opposite strands of DNA suggesting the presence of a possible bi-directional promoter sequence (see section 5.4.2.1).

5.2.6 Eponine

Eponine (Down and Hubbard, 2002) was used to predict promoter regions associated with genes in the 1pcen – 1p13 region. The program is designed for detecting transcription start sites (TSSs) in human genomic sequence by identifying promoter core motifs within a 600 bp window located at the 5' ends of genes. Eponine is reported as having a >50% sensitivity of detecting annotated mRNA start sites based on human chromosome 22 data used in its design. A total of 70 TSS predictions were predicted within Ensembl (build 30) for clones making up the sequence link objects within 1pcen – 1p13. Of this number, 26 (37%) were associated with the 5' ends of complete genes (see section 5.4) and 17 (65%) corresponded with CpG islands, figure 5.1f.

5.3 Gene Identification

Having determined GC and CpG island content, *ab initio* gene prediction programs and sequence homology matching were used to identify coding features within the finished sequence. RepeatMasker was used to filter out transposon-derived repeats prior to alignment of all known protein and nucleotide sequences (EST and cDNA) via BLASTX and BLASTN, respectively (Altschul *et al.*, 1990). In parallel, gene prediction, using FGenesH (Solovyev *et al.*, 1995) and GENSCAN (Burge *et al.*, 1997), and exon prediction, using Hexon (Solovyev *et al.*, 1994) and GRAIL (Uberbacher *et al.*, 1996), was carried out to elucidate putative genes

or exons. The results of genomic sequence analysis were then assimilated and visualised within ACeDB (figure 5.3) (Durbin and Thierry-Mieg 1994).

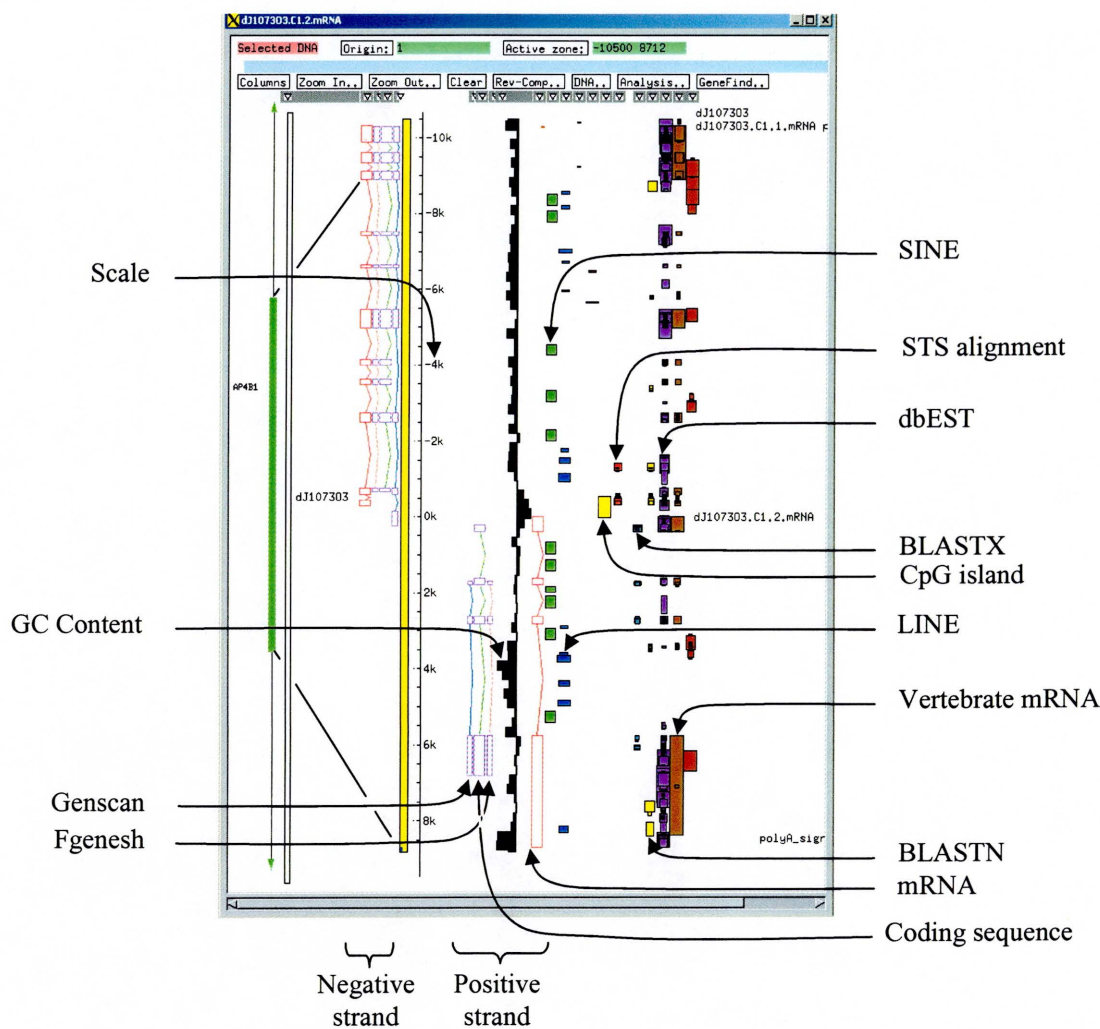


Figure 5.3: An ACeDB display of two annotated genes, including coding sequences, on opposite strands of DNA. Represented are LINE and SINE repeats as well as GC content and CpG island predictions. Vertebrate mRNAs, ESTs and STSs are positioned on genomic sequence by BLAST alignment.

Putative coding features (figure 5.1g), identified by *in silico* analysis and experimental support, were manually annotated and classified according to the level of coding support and completeness of gene structure. The features were divided into four categories: ‘known’ genes, for which an identical cDNA or protein sequence has been aligned to genomic sequence; ‘novel’ genes, those that contain an open reading frame (ORF), are identical to two or more splicing human ESTs, and/or have homology to genes or proteins from other species; ‘novel’ transcripts, similar to novel genes but an ORF cannot be determined; and ‘pseudogenes’, sequences that are homologous to known genes but with a disputed ORF. Manual annotation of these features involved overlaying correct gene structures onto the genomic sequence by accurately locating exon / intron boundaries of mRNAs and splicing ESTs, reviewing and resolving conflicts, and, where there was sufficient supporting data available, identifying 5’ and 3’ termini of genes.

5.3.1. Known genes

A total of sixty-seven known genes were localised to the interval by BLASTN matching of mRNAs at 100% alignment to genomic sequence. Table 5.3 includes the names of known genes, the accession number associated with the full length mRNA and the form of mRNA submission. The majority of the genes have official human genome nomenclature committee (HGNC) names (<http://www.gene.ucl.ac.uk/nomenclature/>), whilst italicised genes are those that have Locus Link entries associated submitted mRNAs (<http://www.ncbi.nlm.nih.gov/LocusLink/>) but for which an official gene name has not been assigned. Names in parentheses are original gene names as represented on figure 5.1g.

Table 5.3: Known genes localising to 1pcen – 1p13. *Italic symbols denote interim gene name.*

Gene Name	Gene	Acc. #	Reference
Vav 3 oncogene	VAV3	AF067817	Trenkle <i>et al.</i> , 2000
Syntaxin binding protein 3	STXBP3	D63506	Gengyo-Ando <i>et al.</i> , 1996
LGN protein	<i>LGN</i>	U54999	Mochizuki <i>et al.</i> , 1996
Mid-1-related chloride channel 1	<i>MCLC</i>	BC002939	Direct Submission
Seryl-tRNA synthetase	SARS	BC000716	Direct Submission
EGF LAG seven-pass G-type receptor 2	EGFL2	AF234887	Direct Submission
Sortilin 1	SORT1	X98248	Petersen <i>et al.</i> , 1997
Proteasome (prosome, macropain) subunit, alpha type, 5	PSMA5	X61970	DeMartino <i>et al.</i> , 1991
Guanine nucleotide binding protein (G protein), alpha inhibiting activity polypeptide 3	GNAI3	M27543	Sparkes <i>et al.</i> , 1987
Adenosine monophosphate deaminase 2 (isoform L)	AMPD2	U16272	Van den Bergh <i>et al.</i> , 1995
Glutathione S-transferase M4	GSTM4	BC015513	Direct Submission
Glutathione S-transferase M2	GSTM2	M63509	Vorachek <i>et al.</i> , 1991
Glutathione S-transferase M1	GSTM1	J03817	Seidegard <i>et al.</i> , 1988
Glutathione S-transferase M5	GSTM5	L02321	Takahashi <i>et al.</i> , 1993
Glutathione S-transferase M3	GSTM3	BC000088	Direct Submission
S-adenosylhomocysteine hydrolase-like 1	AHCYL1	AF315687	Dekker <i>et al.</i> , 2002
Aristaless-like homeobox 3	Alx3	AF008203	Direct Submission
Potassium voltage-gated channel, Shaw-related subfamily, member 4	KCNC4	M64676	Vega-Saenz de Miera <i>et al.</i> , 1992
Solute carrier family 16 (monocarboxylic acid transporters), member 4	SLC16A4 (MCT4)	U59185	Direct Submission
Hepatitis B virus x interacting protein	HBXIP (XIP)	XM_059235	Direct Submission
Prokineticin 1	PROK1	AF333024	Direct Submission
Potassium voltage-gated channel, shaker-related subfamily, member 10	KCNA10	U96110	Orias <i>et al.</i> , 1997
Potassium voltage-gated channel, shaker-related subfamily, member 2	KCNA2	L02752	Ramashwami <i>et al.</i> , 1990
Potassium voltage-gated channel, shaker-related subfamily, member 3	KCNA3	M85217	Attali <i>et al.</i> , 1992
CD53 antigen	CD53	M37033	Angelisova <i>et al.</i> , 1990
Choline/ethanolaminephosphotransferase	<i>CEPT1</i>	AF068302	Henneberry <i>et al.</i> , 1999
Chitinase 3-like 2	CHI3L2	U49835	Hu <i>et al.</i> , 1992
Oviductal glycoprotein 1	OVGP1	U09550	Direct Submission
Adenosine A3 receptor	ADORA3	L22607	Salvatore <i>et al.</i> , 1993
RAP1A, member of RAS oncogene family	RAP1A	M22995	Kitayama <i>et al.</i> , 1989
DEAD/H (Asp-Glu-Ala-Asp/His) box polypeptide 20	DDX20	AF171063	Charroux <i>et al.</i> , 1999
Potassium voltage-gated channel, Shal-related subfamily, member 3	KCND3	AF120491	Isbrandt <i>et al.</i> , 2000
Wingless-type MMTV integration site family, member 2B	WNT2B	AB045116	Direct Submission

Solute carrier family 16 (monocarboxylic acid transporters), member 1	SLC16A1	AL162079	Direct Submission
Putative homeodomain transcription factor 1	PHTF1	AJ011863	Raich <i>et al.</i> , 1999
Protein tyrosine phosphatase, non-receptor type 22 (lymphoid)	PTPN22 (LYP2)	AF077031	Direct Submission
Adaptor-related protein complex 4, beta 1 subunit	AP4B1	AF092094	Dell'Angelica <i>et al.</i> , 1999
HNOEL-iso protein	<i>HNOEL-iso</i>	AF201945	Direct Submission
Tripartite motif-containing 33	TRIM33 (TIF1GAMMA)	AF220137	Reymond <i>et al.</i> , 2001
Breast carcinoma amplified sequence 2	BCAS2 (DAM1)	AB020623	Nagasaki <i>et al.</i> , 1999
Adenosine monophosphate Deaminase 1 (isoform M)	AMPD1	M60092	Sabina <i>et al.</i> , 1992
Neuroblastoma RAS viral (v-ras) oncogene homolog	NRAS	X02751	Hall <i>et al.</i> , 1985
NRAS-related gene	<i>UNR</i>	AB020692	Nagase <i>et al.</i> , 1998
Synaptonemal complex protein 1	SYCP1	D67035	Kondoh <i>et al.</i> , 1997
Thyroid stimulating hormone, beta	TSHB	M23671	Direct Submission
Tetraspan 2	<i>TSPAN-2</i>	BC021675	Direct Submission
Nerve growth factor, beta polypeptide	NGFB	X52599	Direct Submission
Calsequestrin 2 (cardiac muscle)	CASQ2	D55655	Direct Submission
Nescient helix loop helix 2	NHLH2	M97508	Brown et al 1992
ATPase, Na+/K+ transporting, alpha 1 polypeptide	ATP1A1	BC003077	Direct Submission
CD58 antigen, (lymphocyte function-associated antigen 3)	CD58 (LFA3)	Y00636	Wallner <i>et al.</i> , 1987
Immunoglobulin superfamily, member 3	IGSF3	AF031174	Saupe <i>et al.</i> , 1998
CD2 antigen (p50), sheep red blood cell receptor	CD2	M16445	Seed <i>et al.</i> , 1987
Immunoglobulin superfamily, member 2	IGSF2	Z33642	Direct Submission
Transcription termination factor, RNA polymerase II	TTF2	AF080255	Direct Submission
Mannosidase, alpha, class 1A, member 2	MAN1A2	AF027156	Tremblay <i>et al.</i> , 1998
Ganglioside induced differentiation associated protein 2	GDAP2	AK000149	Direct Submission
WD repeat domain 3	WDR3	AF083217	Claudio <i>et al.</i> , 1999
T-box 15	TBX15	AK096396	Direct Submission
Tryptophanyl tRNA synthetase 2 (mitochondrial)	WARS2	AJ242739	Direct Submission
Hydroxyacid oxidase 2 (long chain)	HAO2	AF231917	Jones <i>et al.</i> , 2000
Hydroxy-delta-5-steroid dehydrogenase, 3 beta- and steroid delta-isomerase 2	HSD3B2	M77144	Lachance <i>et al.</i> , 1991
Hydroxy-delta-5-steroid dehydrogenase, 3 beta- and steroid delta-isomerase 1	HSD3B1	S45679	Dumont et al 1992
Phosphoglycerate dehydrogenase	PHGDH	BC011262	Direct Submission
3-hydroxy-3-methylglutaryl-Coenzyme A synthase 2 (mitochondrial)	HMGCS2	X83618	Direct Submission
A disintegrin and metalloproteinase domain 30	ADAM30	AF171933	Direct Submission
Notch homolog 2 (Drosophila)	NOTCH2	AF315356	Direct Submission

5.3.2. Novel genes

Novel genes (complete gene structures containing ORFs) were annotated from supporting evidence such as splicing EST and mRNA alignment or by the addition of *de novo* cDNA sequence. The cDNA clones, from which the *de novo* cDNA sequence was generated, were identified by pooled cDNA library screening with 41 primer pairs designed to exons contained within putative gene structures. The cDNA libraries, each of which represented 500,000 clones from nine different tissue types, were initially divided into twenty-five pools containing 20,000 cDNA clones and then recombined into superpools containing 100,000 clones (kindly provided by Jackie Bye). Superpools that were positive from initial exon specific cDNA library screening were then used to generate PCR products that linked between exons (link PCR) which were subsequently sequenced and aligned to the genomic structure of the gene. Validation of possible gene structures by the alignment of sequence from splicing ESTs, mRNAs or the *de novo* cDNA sequence resulted in the identification 35 novel genes.

Table 5.4 represents a summary of cDNA library screening and link PCR results from novel genes within 1pcen – 1p13. Where possible, primers were designed to satisfy previously established criteria (see section 2.6.1). Of the 96 cDNA primary pool screens, 71% (68) identified at least one cDNA library (see section 2.8.3). Libraries that yielded a PCR product (bold denoting a strong band on an agarose gel) are listed next to each primer, with the red lettered library being used as template for the link PCR experiment. Primer combinations used in the link PCR depended on the type of validation or extension required for each putative coding feature. A vectorette primer, 224, was used in combination with sense or anti-sense primers to extend the putative genes to 3' or 5' UTR respectively (figure 5.4).

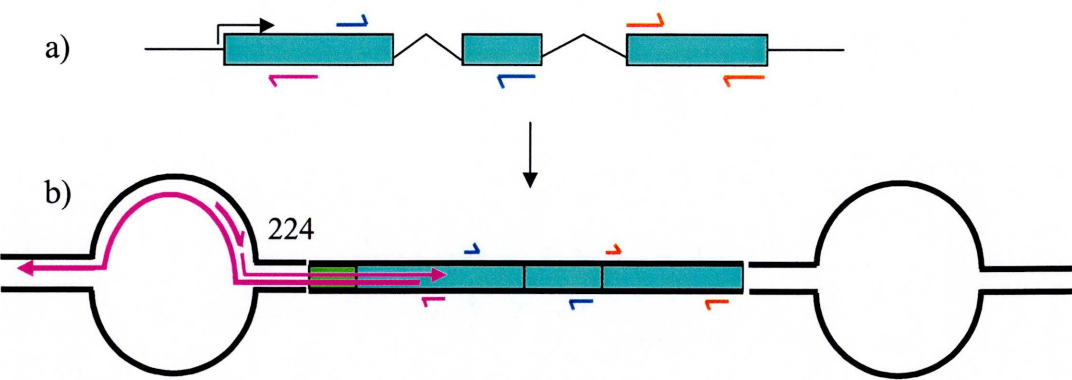


Figure 5.4: Primer combinations used to validate putative gene structures. a) Primers pairs, of the same colour, are designed to the annotated gene structure. Blue primers are designed between exons, red primers within an exon and the pink primer is designed to be used in conjunction with vectorette primer 224. Black arrow indicates the direction of transcription. b) cDNA clone with ligated vectorette arms. Exon specific primer (pink) anneals and elongates through the non-complementary vectorette arm before the 224 vector primer can anneal and elongate in the reverse direction. A normal PCR reaction from these initial templates then follows. Novel 5' cDNA sequence is represented in green.

Primer combinations within genes were also used to validate gene structures.

35% of the 93 vectorette and link PCR reactions resulted in the generation of single strong PCR product when run on a 2.5% agarose gel (Y in the Link' column of table 5.4) which was subsequently purified and sequenced (by others). A further 25% of PCR reactions generated a faint single band (R in the 'Link' column) which requires re-amplification prior to sequencing. Finally, 40% of the gene validation experiments (M within the Link column of table 5.4) resulted in the generation of multiple Link PCR products; these require refinement

of primer design (because of possible mispriming events) or an increase of the PCR *T_m* to increase the specificity of primer annealing. 81% (25) of the sequenced products yielded sequence which was subsequently aligned to the interval by BLAST analysis. Attempts were made to generate experimental data for 17 of the final total of 35 novel genes by cDNA screening. Sequence from link or extension PCR was generated from 12 (71%) of these possible gene structures, including the 6 genes with 5’ or 3’ extensions. Unsuccessful attempts were also made to extend five known genes (dark blue - table 5.4) in the 5’ direction so as to increase the size of 5’ UTR.

Table 5.4: cDNA primary pool and link PCR screening results. Gene structures are coloured according to their final category as drawn in figure 5.2. Columns correspond to gene name, the exon from which primer pairs were designed, the EMBL accession number associated with the primer pairs, whether a PCR product was generated from cDNA superpool screening (Y = yes, N = no), the cDNA library that yielded a PCR product, whether a vectorette (before /) or link PCR product (after /) was generated (Y = single strong band, R = faint single band, M = multiple bands) and whether the product was successfully sequenced. For key to cDNA library codes, see methods table 2.2

Gene	Exon	stSG	1 ^o	cDNA Library	Link	Seq
bA483113.C11.1.mRNA	e2	452926	Y	TD	Y/	N
	e2	452927	N			
	e5	452928	Y	HeLa B,C,E	R/	
	e7	452929	N			
aA483113.C11.2.mRNA	e1 5'UTR	452930	Y	FLU A, HP B-E, SK C		
	e4	452931	Y	FLU A, T A, HPB B,C,D,E, SK C	Y/	N
	e7	452932	Y	AH E		
	e10	452933	Y	AK B,E, AH A,D, He La E, T C, HP B-E, SK A-E		
	e12	452934	Y	AK B, AH A,D, He La A,E, T C, U E, HPB B-E, SK A-E		

	e14 3'UTR	452935	Y	AK B,E, AH A,B,C,D,E, He La A,E, T A,C,E, HPB B-E, SK A-E		
bA475E11.C1.1.mRNA	e1 5'UTR	452936	N			
	e5	452937	N			
	e6	452938	N			
	e10	452939	N			
	e13	452940	N			
bA297O4.C1.1.mRNA	e1 5'UTR	452941	N			
dJ831G13.C1.1.mRNA	e1	452942	Y	T D	R/M	
	e3	452943	Y	FLU D, T B,D		
	e4	452944	Y	T D	R/Y	N
bA180N18A.C1.2.mRNA	e1	452945	N			
dJ773N10.C1.1.mRNA	e2	452946	Y	SK C-E	R/	
dJ1003J2.C1.1.mRNA	e2	452947	Y	FLU D	R/N	
	e4	452948	Y	FLU D		
	e7	452949	N			
	e9	452950	Y	FLU C, T E, SK D	N/N	
	e12	452951	N			
bA470L19.C1.2.mRNA	e1	452952	N			
bA284N8.C1.1.1/2.mRNA	e2	452953	Y	SK B	Y/	N
bA163H20.C1.3.mRNA	e3	452954	Y	AH A,E	Y/Y	Y
	e5	452955	N			
	e7	452956	Y	FLU D, AH A-E	M/Y	Y
	e10	452957	N			
dJ1125M8.C1.1.mRNA	e2	452958	Y	FLU A-C,D,E, T E	M/N	
	e4	452959	Y	AK C,D, FLU A-E, AH E	/Y	Y
	e6 3'UTR	452960	Y	FLU A,B,D,E, AH C,E	M/Y	Y
dJ1125M8.C1.2.mRNA	e1	452961	Y	AK A,B,D, AH C, HP B	M/	
	e3	452962	N			
	e5	452963	N			
	e8	452964	N			
bA552M11.C1.4.1/2.mRNA	e2 .2	452965	N			
	e3/4 .1	452966	Y	AK A-D, FLU A, U C, SK B	M/Y	N
	e5	452967	Y	AK A,B, FLU A, U C	M/N	
bA552M11.C1.5.mRNA	e1/2	452968	Y	T A-E, SK A-C	Y/Y	Y
	e3/4	452969	Y	FLU A,C, T A-E	/Y	Y
	e5	452970	Y	FLU A-C, T A-E	R/Y	Y
dJ836N10.C1.1.mRNA	e2/3	452971	Y	T E	R/Y	Y
	e4	452972	Y	T E	R/Y	Y
dJ1073O3.C1.3.mRNA	e1	452973	Y	AK A,C, T E	Y/Y	Y
	e3	452974	Y	AK A,C, SK A	/Y	Y
dJ1037B23.C1.1.mRNA	e2	452975	N			
	e4	452976	Y	T A, SK C	R/Y	Y
	e6	452977	Y	SK C	/Y	Y

	e8 3'UTR	452978	Y	AH C-E, T E, U C, SK C,D	M/Y	Y
dJ1156J9.C1.1.mRNA	e1 5'UTR	452979	Y	AH D, T C, SK B	Y/	Y
dJ929G5.C1.1.mRNA	e2	452980	Y	He La C,D,E, T C	M/Y	Y
	e4	452981	Y	AK D,E, FLU D, AH A,B,C, He La A-E, T B,C, U A-E, HPB A-E, SK A	/Y	Y
	e6	452982	Y	AK D,E, FLU D, AH A,B,C,D, AB A,B,D,E, He La A,B,D,E, T B-D, U A-E, HPB A-E, SK A	/Y	Y
	e8	452983	Y	AK D,E, FLU D, AH A-C,D, AB A,B,D,E, He La A,B,D,E, T B-D,E, U A-E, HPB A-E, SK A	M/N	
bA12L8.C1.1.mRNA	e2	452984	Y	FLU C, AH C, T E, HPB E, SK E	R/	
dJ655H2.C1.2.mRNA	e1	452985	N			
	e2	452986	N			
dJ655H2.C1.3.mRNA	e2	452987	Y	AKA,C-E	M/	
dJ686H6.C1.1.mRNA	e1/2	452988	Y	T E	M/	
bA39H13.C1.1.mRNA	e1	452989	Y	T E	R/R	
	e2	452990	Y	T E	R/R	
bA40H21.C1.1.mRNA	e1	452991	Y	AK D,E, AH C	N/	
	e2	452992	Y	AH C, AB A, T E, HPB A		
dJ776P7.C1.1.mRNA	e1	452993	Y	AK A,B,E, T A,C,D,E	R/N	
	e1/2	452994	N			
	e4	452995	Y	T D,E,	Y/	Y
dJ832K2.C1.1.mRNA	e1	452996	Y	AH C, T C,E	M/Y	Y
	e6/7	452997	N			
dJ832K2.C1.2.mRNA	e2	452998	Y	AH C, T C,E, SK C,E	M/Y	Y
dJ832K2.C1.3.mRNA	e2	452999	Y	FLU C,E, AH E, T D	M/N	
	e5	453000	Y	AH E, T D,E, SK C	/N	
	e8	453001	Y	FLU B, T D	Y/R	Y
bA224F24.C1.1.mRNA	e1	453002	Y	AK E	Y/N	Y
	e4	453003	Y	AK E	/Y	N
	e6	453004	N			
	e8	453005	N			
	e11	453006	Y	AK E, T D,E	Y/Y	Y
	e15	453007	N			
dJ794L19.C1.1.mRNA	e1	453008	Y	AH E	M/R	
	e3	453009	Y	T E	/R	
	e5	453010	Y	AH B,E	/N	
	e8	453011	Y	AH E	M/N	
dJ934H19.C1.1.mRNA	e1	453012	N			
	e3	453013	Y	AK C,D, He La E, T A,E, HPB B,D,E	R/R	

dJ834N19.C1.2.mRNA	e2	453014	Y	AH C-E, T E	R/R	
dJ599G15.C1.5.mRNA	e1	453015	N			
dJ599G15.C1.6.mRNA	e1	453016	Y	FLU D, T E, HPB B	R/	
				AK C, FLU A,D, AH B,D,E, He La A-E, T C,E, U A,B,D, HPB A,B,D, SK A,C-E	M/N	
dJ104218.C1.4.mRNA	e2	453017	Y			
	e3	453018	Y	AK E, AH C,E, T E, SK E		
				AK C, FLU B,D,E, AH A,B,D,E, He La A,D,E, T C, HPB A,B,C,D	/N	
	e5	453019	Y			
	e7	453020	Y	T D,E		
	e9	453021	Y	AH C, T E, U D, HPB A	M/N	

5.3.2.1 Splicing ESTs support the structure of a gene

A proportion of the total number of novel genes identified within 1pcen – 1p13 were initially annotated as incomplete gene structures based upon *in silico* gene prediction and BLAST alignment of splicing ESTs to genomic sequence. Figure 5.5 outlines an example of how experimental support was generated for a putative gene feature, bA552M11.C1.5.mRNA, originally annotated from *in silico* prediction (figure 5.5a) and EST alignment (figure 5.5b). Primers were designed, where possible, to predicted exons (arrows – figure 5.5c) and screened across the 45 cDNA library superpools (figure 5.5d) to experimentally establish the full length gene structure. PCR results indicated (figure 5.5d - red arrows) that testis cDNA library superpools A-E were all positive when tested with each of the three primer pairs, whilst primer pair SG452969 provided an additional positive result for foetal liver A and C, and primer pair SG452970 provided a positive result for foetal liver A – C. PCR from primer SG452969 generated an additional faint band of an unexpected size at approximately 400bp (figure 5.5d - blue arrow). BLAST analysis indicated that the sense primer of SG452969 localised to 24 positions in the genome at a high BLAST score (maximally within 1pcen –

1p13) which may have resulted in the secondary product being generated from a mispriming event, unlike the other primers which were unique in the genome by BLAST analysis. The absence of a positive control band for primers SG452968 (1908bp) and SG452969 (848bp) could be attributed to the inability of the PCR reaction to produce a product from the genomic positive control by primer pairs which have been designed in separate exons.

Link PCR was performed using a combination of primer pairs (figure 5.5d) to both validate and extend the putative coding structure. Testis super pool A was used as the template for generating link PCR products for each of the three primer pairs. A primer designed to the vectorette bubble ligated to cDNA subclones, 224, was used to prime from the 5' end of the cDNA clone. Products from the PCR reaction were excised from agarose and sequenced (by others) and aligned to the genomic sequence. cDNA sequence supported the annotated gene structure, elongated the gene to incorporate a new 5' exon (spanning an existing known gene, ADORA3) and identified a novel splice variant. Subsequent BLAST analysis of the new gene identified an Image 5' cDNA clone, BI463020, (brown gene structure figure 5.5f) which, when aligned to genomic sequence, supported the annotation of the gene and the coding region (figure 5.5f green gene structure).

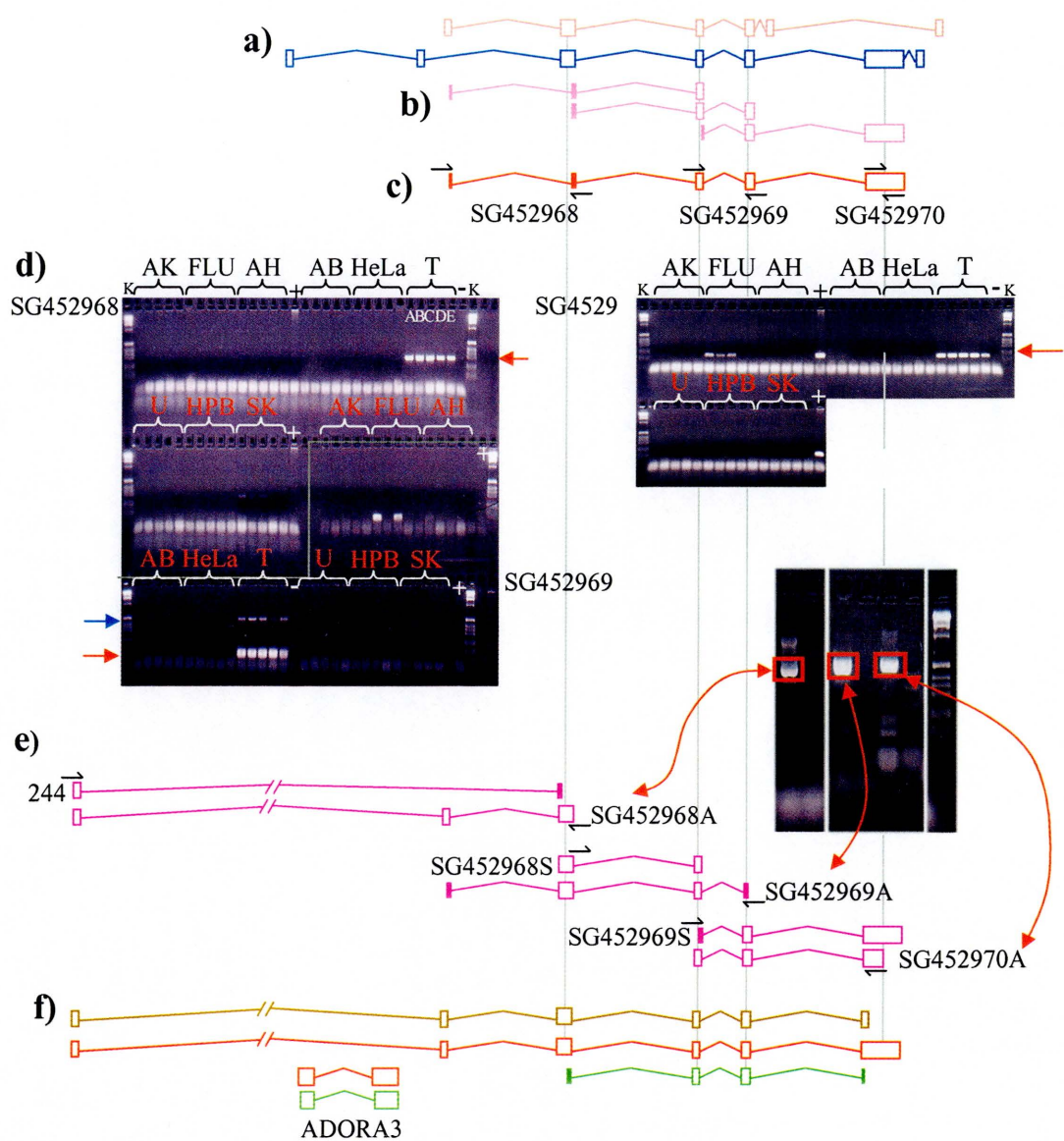


Figure 5.5: The annotation of a novel gene from *de novo* prediction and splicing EST alignment. a) *In silico* prediction of a novel gene is represented by Fgenesh (light pink) and GENSCAN (dark blue) structures. b) Alignment of splicing ESTs (pink) supports the presence of a gene. c) Annotation of a putative gene (red) enabled primer pairs to be designed (black arrows and accession numbers). d) PCR products from cDNA library screening, including negative (-) and positive controls (+), are run on a 2% agarose gel. e) Selected

cDNA libraries, from d), were then used as a template for the generation of vector and link PCR products using primer combinations (black arrows), which were then sequenced. f) The final gene structure is represented with the full length gene drawn in red, the coding in green and a newly submitted cDNA clone, BI463020, brown structure.

5.3.2.2. mRNA support of novel coding features

Genomic alignment of incomplete mRNAs derived either from human or other species can facilitate the identification of novel genes by providing experimental support for *in silico* predictions and splicing ESTs. Initial analysis of *in silico* prediction (figure 5.6a), EST (figure 5.6b) and mRNA alignment (figure 5.6c) to three overlapping sequence clones (RP11-224F24, RP5-832K2 and RP4-776P7) resulted in the annotation of four gene structures within 230 kb of each other on the same DNA strand (figure 5.6d). Three of the four putative coding features were based on overlapping splicing ESTs and the fourth by alignment of a novel incomplete mouse mRNA. Primers were designed, where possible, to predicted exons and, as previously described, screened across nine different cDNA libraries. Four of the twelve primer pairs (figure 5.6e) and table 5.4, 452996 – 453007) failed to generate products from cDNA library screening. Link PCR between putative coding structures was attempted because of the likelihood that they contributed to a single gene due to the orientation and proximity of these genes within a GC / gene poor band in which gene density is reportedly lower (IHGSC, 2001). Link PCR sequence derived from cDNA clones from within super pool testis C (figure 5.6f) – 452998 and 453001 (not shown)) facilitated the joining of gene features 3 and 4. BLAST analysis of GENSCAN and Fgenesh exon predictions that were not

supported by an mRNA or splicing EST identified a recently deposited partial human mRNA which, when aligned to genomic sequence, spanned features 2, 3 and 4 and overlapped the mouse mRNA used to annotate feature 1 by 90bp. The putative structure now had experimental support from a novel mouse mRNA (AK016477), which did not have a previously described translation stop site, and a novel human mRNA (AL833485) (figure 5.6g) which lacked a translation start site, splicing ESTs and novel cDNA sequence. A second iteration of BLAST searching identified a recently submitted human mRNA (AK091816) (figure 5.6g) which supported the structure annotated from mouse mRNA homology and which overlapped the downstream human mRNA. The full length gene, dJ832K2.C1.1.1, contains 49 exons spanning 230 kb, is adjacent to a predicted CpG island and contains a polyA signal and polyA site. BLAST analysis of the sequence contained within the 6.7 kb ORF, or the translated protein derived from it, failed to show homology to any known gene, (figure 5.6h).

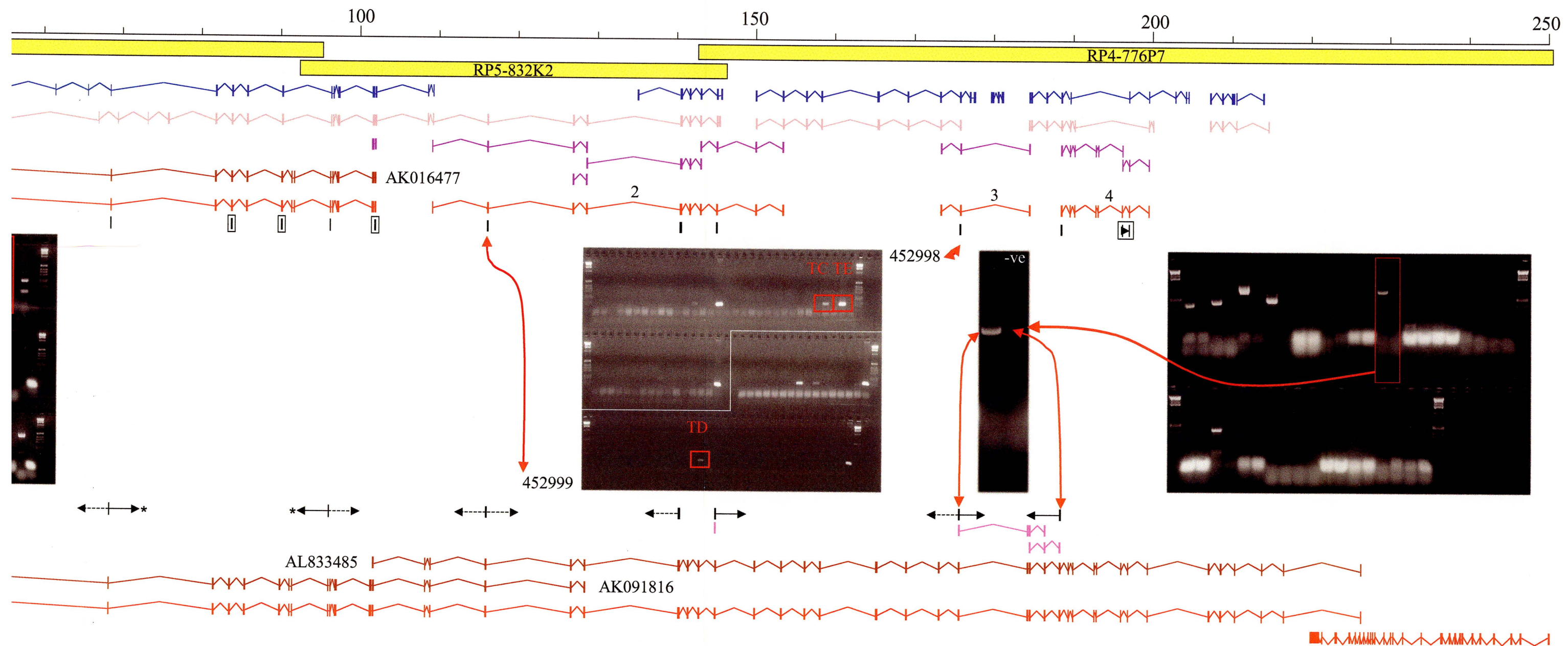


Figure 5.6: The annotation of a novel gene from *de novo* prediction, splicing EST and homologous mRNA alignment. a) *In silico* prediction of four distinct novel genes is represented by Fgenesh (light pink) and GENSCAN (dark blue) structures within three overlapping sequence clones (yellow boxes). b) Alignment of splicing ESTs and, c), a mouse mRNA to the genomic sequence supports *in silico* predictions and the presence of the four genes. d) Putative genes were annotated and, e) exon flanking primer pairs were designed and screened across cDNA libraries (the center gel is an example of cDNA library screening with two primer pairs). Primers that failed to produce a PCR product from a cDNA library are boxed. f) Selected cDNA libraries were then used as a template for the generation of vector and link PCR products. Arrows indicate where primer combinations successfully generated PCR products, dotted lines indicate link PCR failure and the arrow with an asterisk corresponds to the generation of a link PCR product but which subsequently failed to sequence. Vertical pink lines with no link to adjacent exons indicate where exon specific sequence was generated from 244 vector priming. g) Alignment of novel mRNA sequence supports the final gene structure, h), which was shown to overlap at its 3' end with an adjacent gene, WDR3.

5.3.3 Novel transcripts

cDNA library screening was also used to identify ORFs within gene structures which had been initially annotated as novel transcripts, i.e. genes which are similar to novel genes but for which an ORF cannot be identified. Following experimental analysis 16 gene structures remained in the novel transcript category. Three quarters of the final number of putative genes

(12 / 16) identified a cDNA clone within the library pools (table 5.4), but only 1 yielded any sequence from link PCR, but did not identify an ORF within the putative structure.

5.3.4 Pseudogenes

A total of 11 pseudogenes were identified within 1pcen – 1p13. These gene structures were the result of either insertion of a processed mRNA or an unspliced feature that has an interrupted open reading frame. Figure 5.7 is an example of a processed pseudogene in which the original coding structure is present in another region of the genome, in this case elsewhere on human chromosome 1. The example shown relates to the marker used by Brintnell *et al.*, (1997) (see chapter 4.4.1) to construct a YAC map within 1pcen – 1p13. As previously described, D1S3347 was derived from the 3' end of a gene, proline-rich nuclear receptor co-regulatory protein 2 (PNRC2) (pink box figure 5.7). The full length gene (figure 5.7a) is derived from 1p35.3, whilst the processed mRNA (figure 5.7b) has been incorporated in the genomic DNA in 1p12 (figure 5.7c). Evidence of mRNA processing can be found by the presence of a polyA tail incorporated into the genomic sequence (figure 5.7d). Whilst it may be possible that the insertion of a processed mRNA into the genomic sequence may result in continued expression of the gene, in this instance the open reading frame of the PNRC2 transcript is disrupted by the occurrence of multiple *de novo* stop codons.

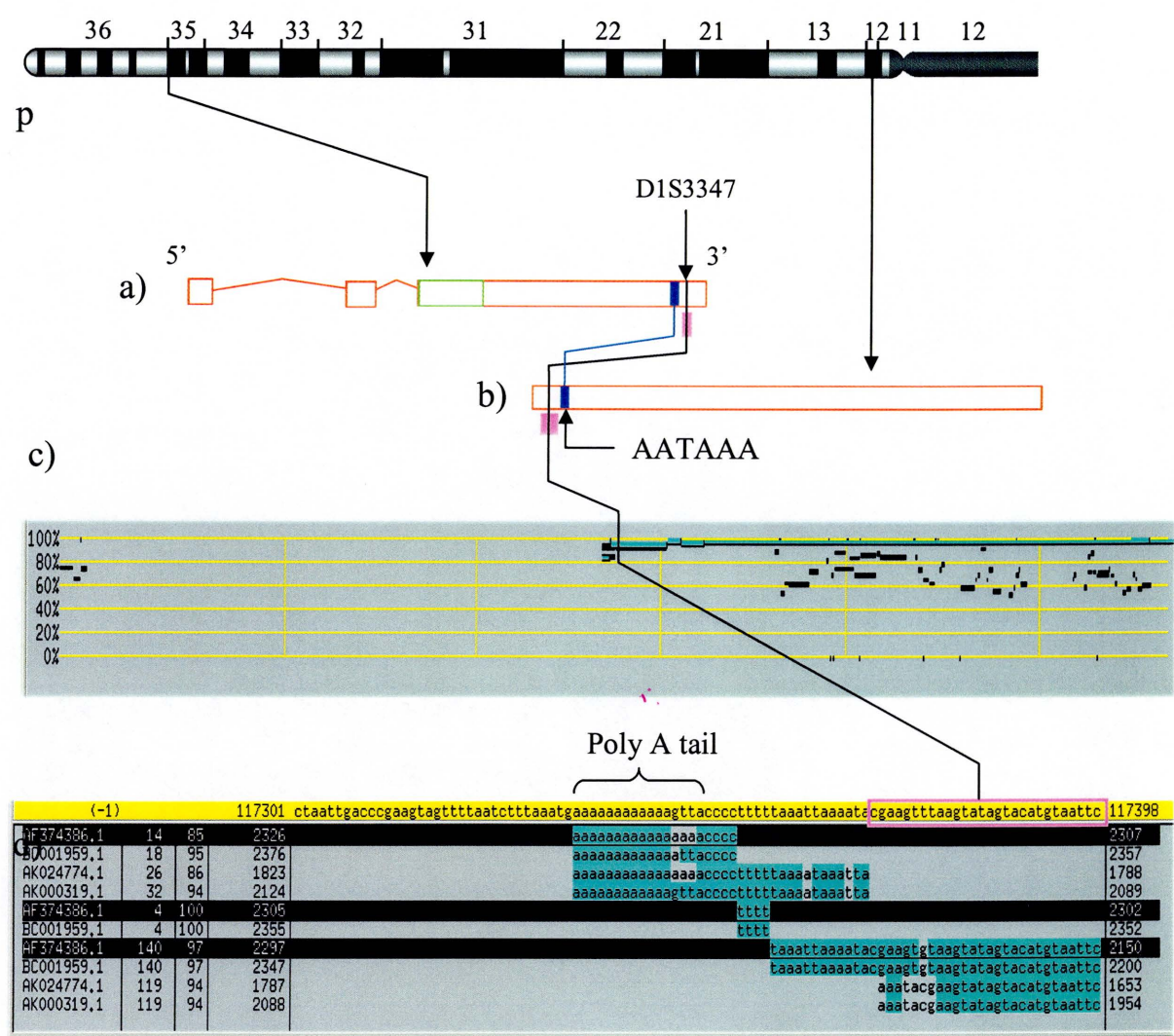


Figure 5.7: The characterisation of a processed pseudogene to 1p12, the original of which localised to 1p35. Arrows indicate where the functional gene, a), and pseudogene, b), are located on chromosome 1. D1S3347 was derived from the 3' UTR of the functional gene. Evidence that the pseudogene is processed originates from the identification of a polyA signal and the presence of a polyA tail, which is added during pre-mRNA processing. Figures 5.7c) and d) show the genomic alignment of cDNA AF374386 within BLIXEM which indicates the presence of a pseudogene.

5.4. Gene assessment

As previously mentioned, CpG islands can be used as a means of localising transcription start sites of genes. The 5' ends of 56% of genes within the interval are located next to a predicted CpG island, the same as the previously reported percentage (Antequera and Bird, 1993). The identification of a polyadenylation (polyA) signal at the 3' end of a gene can be used to assess the completeness of gene annotation as the consensus sequence, usually AATAAA, is found adjacent to the termination of transcription.

Analysis of the coding features annotated within 1pcen – 1p13 indicated that 76% of the 102 genes possessed a polyA signal within 50 bases of their 3' ends. Sixteen percent of the polyA signals contained an alternative ATTAAG motif (the second most common polyA signal) which was slightly higher than the previously reported number, 14.9%, contained within 12 genes (Beaudoing *et al.*, 2000). Another important feature to annotate is the site of polyadenylation. Genomic alignment of sequence from the mRNA which is adjacent to a 3' polyA tail permits the localisation of the site at which the pre-mRNA is cleaved prior to the addition of the poly A tail. The generation of mRNAs sequences from cDNA libraries by oligo dT priming can, however, lead to aberrant mRNAs sequences being produced. These aberrant sequences may be generated by contaminant genomic DNA acting as the template for oligo dT priming from polyA tracts in genomic sequence, or oligo dT primers may anneal to polyA tracts within the mRNA and result in a truncated coding structure.

Figure 5.8 shows the alignment of an mRNA, AF119043, submitted as a full length coding sequence of the transcriptional intermediary factor 1 gamma gene. The alignment of AF119043 (figure 5.8c and d) at the 3' UTR of the gene (figure 5.8a) indicates that the mRNA was more likely to have been generated by oligo dT priming from a tract of polyAs present in cDNA sequence which is also present in the genomic sequence. Evidence that the complete 3' UTR may not be present within the mRNA is yielded by the alignment of more ESTs 1.4kb further 3' to the position of AF119043 (figure 5.8b); these 3' ESTs contain a polyA signal. Figure 5.8e indicates the alignment of a cluster of 3' ESTs to genomic sequence which indicates where the 3' UTR of TIF1G terminates. The actual full length of the gene will, however, require further experimental support, by cDNA library screening for example, as there is not complete coverage of the 3' UTR in overlapping ESTs.

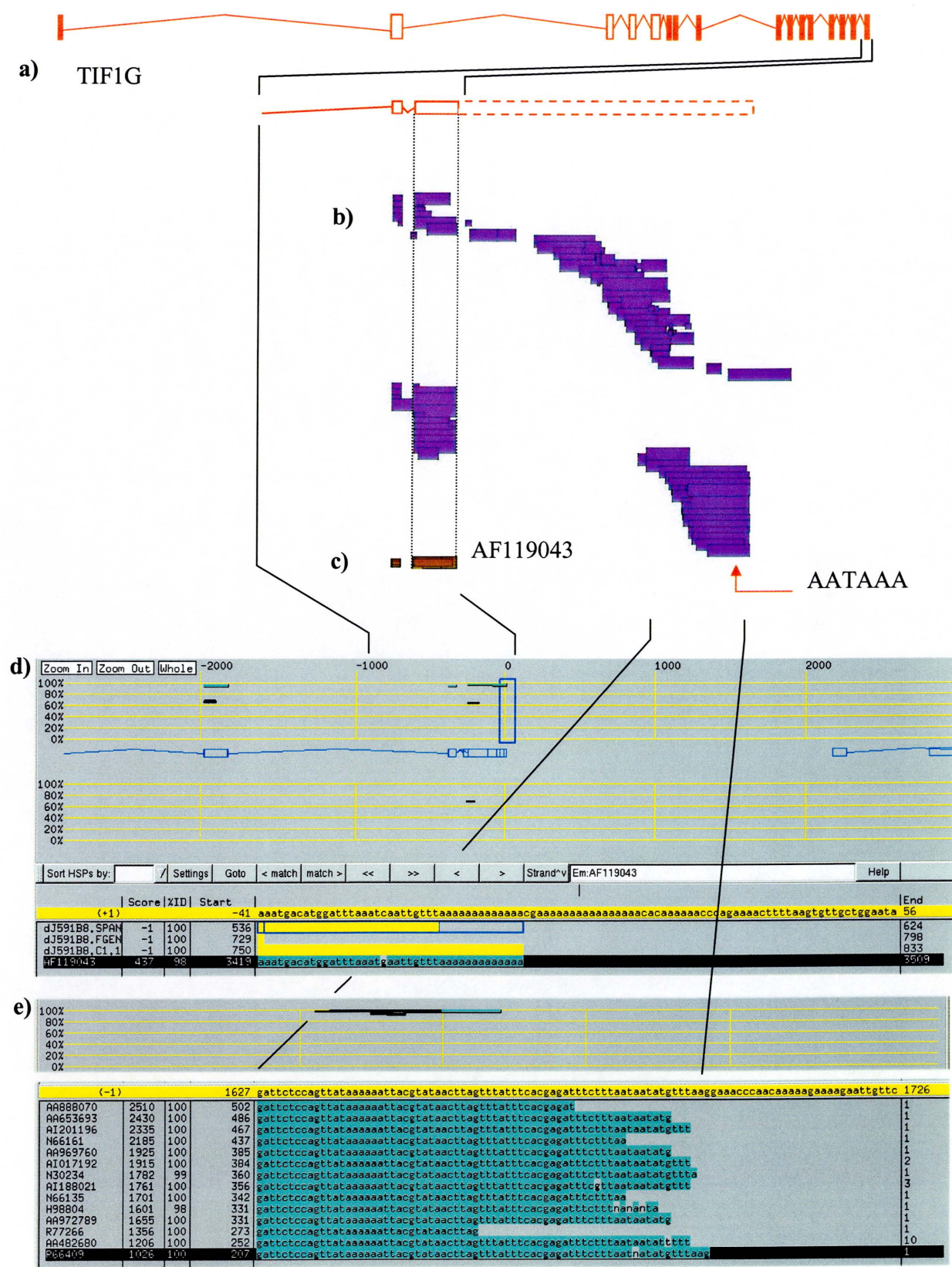


Figure 5.8: Incomplete polyA primed mRNA. a) The annotated structure of the transcriptional intermediary factor 1 gamma using the alignment of an mRNA, AF119043 (c and d) submitted as a full length transcript. Alignment of a cluster of 3' ESTs to the genomic sequence (b and e) indicates the full length gene (including a polyA signal) extends beyond the submitted end (red dotted box, a).

The site of polyadenylation was identified within 16% of full length genes. The majority of mRNA sequence used in this study to characterise the 3' end genes, were submitted to the public databases without polyA tails therefore precluding identification of the polyadenylation site.

5.4.1 Alternative splicing

The diversity of protein coding sequence within complex organisms may be attributed in part to the widespread occurrence of gene processing mechanisms. Examples include multiple transcription start sites, pre-mRNA editing and post-translational modifications, and alternative pre-mRNA splicing all of which may be important sources of protein diversity. Alternative splicing is a highly regulated process that is capable of producing many different proteins from a single gene. It is estimated that 35 – 59% of all human genes are subject to alternative splicing (Modrek and Lee 2002) but this is likely to be an underestimate because the identification of splice variation is dependent upon EST alignment. The average alternative isoform / gene ratio detected so far ranges from 2.6 on human chromosome 22 to 3.2 on human chromosome 19, with approximately 70% of splice variants affecting amino

acid sequence of the encoded protein (IHGSC, 2001). Only 16 genes (15%) within 1pcen – 1p13 show evidence of splice variants. This fraction may be expected to increase after further iteration of EST alignment to the genomic sequence. Figure 5.9 is an example of a gene, adenosine monophosphate deaminase 2 (AMPD2), which has 4 different transcripts. On the basis of translation of each transcript isoform to predict open reading frames which start at the first AUG codon, each isoform would be expected to encode a distinct polypeptide. AMPD2 regulates the intracellular production of adenosine by competing with cytosolic 5' nucleotidase in a mechanism which regulates contractile binding in mammalian skeletal muscle. Four different splice variants (figure 5.9a-d) were annotated using previously characterised mRNA sequence. Alignment of spliced ESTs not only supported the four known gene structures but also identified a previously uncharacterised putative splice variant. This new gene structure may be a novel AMPD2 functional variant as it provides evidence for an ORF that is different from the previous four (i.e. it lacks the amino acids encoded by the second exon).

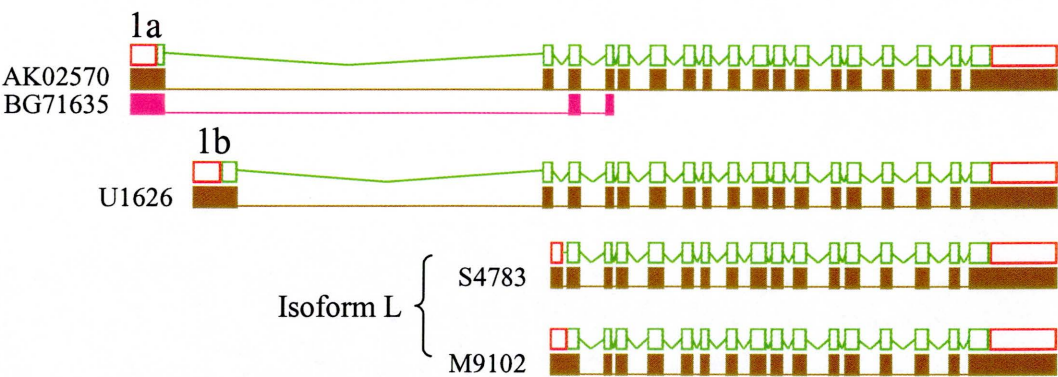


Figure 5.9: Splice variants of adenosine monophosphate deaminase 2 (AMPD2). Four splice variants were annotated (coding green boxes, UTR red boxes) by alignment of known mRNAs (brown boxes) to genomic sequence. Alignment of novel EST, BG716359 (pink box), identified a fifth potential splice variant. This variant would encode an altered protein which lacked the 43 amino acids encoded by exon 2.

5.4.2. Genic features

Detailed annotation of coding structures within a contiguous genomic sequence has provided the opportunity to investigate the context in which genes are positioned within the genome. An interesting feature to arise from the analysis of 1pcen – 1p13 is the head to head, and head to tail juxtaposition of genes which raises queries about the possible functional consequences about such gene localisation.

5.4.2.1. Putative bidirectional promoters

Within the annotated sequence of 1pcen-13, a pair of genes was observed to be orientated head to head on opposite strands of DNA. The genes, WDR3 – GDAP2 (figure 5.10a) were located in a bidirectional fashion and in each instance the 5' UTR of each gene was contained within the same CpG island. It has previously been reported that at least twenty loci have pairs of genes juxtaposed in a head to head orientation with many of these being implicated in DNA repair mechanisms (Shimada *et al.*, 1989, Platzer *et al.*, 1997, Xu *et al.*, 1997, Connelly *et al.*, 1998, Galgoczy *et al.*, 2001). Genes that encode proteins involved in systems such as DNA replication, cell cycle regulation and metabolic pathways, which are commonly associated with CpG islands (Gardiner-Gardner and Frommer 1987), have also been found in this particular bidirectional orientation (Adachi *et al.*, 2002). If there is a functional consequence for these genes to be related in this fashion, it may be that a common promoter element is utilised for co-ordinated expression.

The bidirectional gene pair includes two known genes, WDR3 and GDAP2. WDR3 is a member of a widely expressed family of proteins which are characterised by a gly-his and trp-aspartate (GH-WD) repeat and believed to facilitate the formation of heterotrimeric or multiprotein complexes. WD family members are involved in a variety of cellular processes including cell cycle progression, signal transduction, apoptosis and gene regulation. GDAP2 (ganglioside-induced differentiation-associated protein 2) was identified as one of 10 different mRNAs highly expressed in a neuroblastoma cell line which had been transfected with a GD3 synthase cDNA construct (Liu *et al.*, 1999). Again, the GDAP genes are expressed in most

tissues and, like WDR3, have an inferred involvement in signal transduction (Liu *et al.*, 1999). The commonality of promoter elements suggests that they may share common function and have some form of coordinated cellular expression. Experimental evidence for co-ordinate expression may be obtained by cloning the putative promoter region in a reporter construct, for example a luciferase promoter assay.

5.4.2.2. *Overlapping genes*

Only two genes were identified as possessing overlapping pre-mRNA structures. The 3' UTR of UNR (gene upstream of NRAS) and the 5' UTR of NRAS (neuroblastoma RAS viral oncogene homolog) were shown to overlap by 415bp (figure 5.10b). UNR contains four different 5' splice variants, and differential use of polyA signals would also allow for multiple 3' ends, whilst NRAS has a polyA signal and polyA site but no additional isoforms were identified. It is difficult to ascertain a possible functional or regulatory relationship between UNR and NRAS as UNR does not have a primary protein structure or sequence homology to any known gene. However, coordinated regulation is inferred on the basis of the same spatial relationship being maintained in species from which NRAS has been isolated and, to a lesser extent, that both genes were expressed in all tissues examined (Jeffers *et al.*, 1990). The role of NRAS, as an oncogene playing a role in cellular proliferation, differentiation and transformation, and conceivably may be differentially regulated by splice variants of UNR.

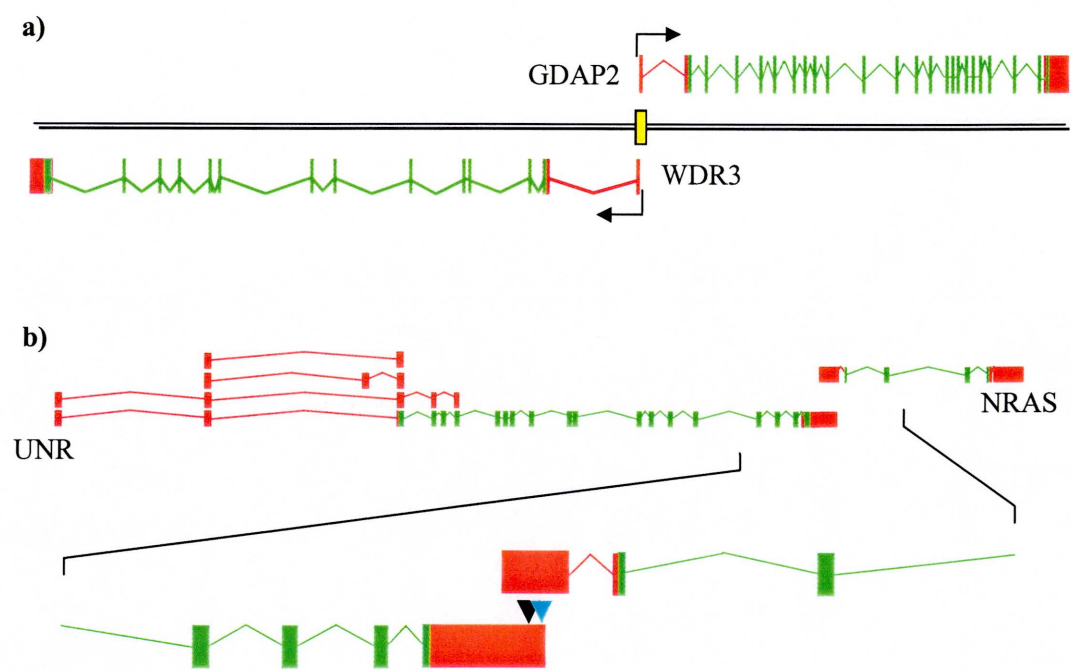


Figure 5.10: Genes in genomic context. Head to head orientation of a pair of genes (a) that share a CpG (yellow box) between the first non-coding exon (red box, coding green box) of each gene. Figure 5.10b depicts two genes, *UNR* and *NRAS*, whose 3' and 5' non-coding sequences partly overlap, respectively. PolyA signal (black arrow) and polyA site (blue arrow) are represented in the 3' UTR of *UNR*.

5.5 Inferring function by protein homology

Greater than one third of all full length coding features identified within 1pcen – 1p13 were novel genes. The possible function of these genes can be inferred by homology, at both nucleotide and amino acid sequence level, with previously characterised genes from either

human or other species. These types of analyses may facilitate the association of a novel coding feature to an existing gene family or may assist in predicting gene function by identifying the individual protein domains within the gene.

5.5.1. Identifying function through sequence homology

To investigate the means of identifying gene function through DNA and protein homology gene, bA12L8.C1.1 (figure 5.11a), was analysed within PIX (<http://www.hgmp.mrc.ac.uk/Registered/Webapp/pix/>) and PSI-BLAST (<http://www.ncbi.nlm.nih.gov/BLAST/>). bA12L8.C1.1 was annotated from a full length uncharacterised IMAGE mRNA and was supported by sequence from cDNA library screening. Analysis of the translated mRNA within PIX (which uses a suite of programs to characterise features within the protein) predicted four transmembrane domains (figure 5.11b). The four helical structures were each predicted by three different transmembrane programs, TMHMM (Sonnhammer *et al.*, 1998), TMPRED (Persson and Argos 1994) and TMAP (Milpetz *et al.*, 1995), which cumulatively supports the presence of the structure within the sequence. A depiction of the possible *in situ* protein structure is represented by figure 5.11c. PSI-BLAST (<http://www.ncbi.nlm.nih.gov/BLAST/>) was used to identify sequence homology to the putative transmembrane protein. Analysis of the novel protein identified a 74% homology to a sugar transporter domain within the conserved domain database (CDD) originating from PFAM (figure 5.11d, e). In parallel, BLAST alignment of the protein sequence showed a 99% homology to a hypothetical human protein, NP_060890 (not shown). The protein was derived from the direct submission of a previously described

mRNA (but not aligned by annotation here) which is purported to show homology to the *Drosophila* Orct gene and mammalian carnitine transporters, a family of genes which are involved in transmembrane organic ion transportation.

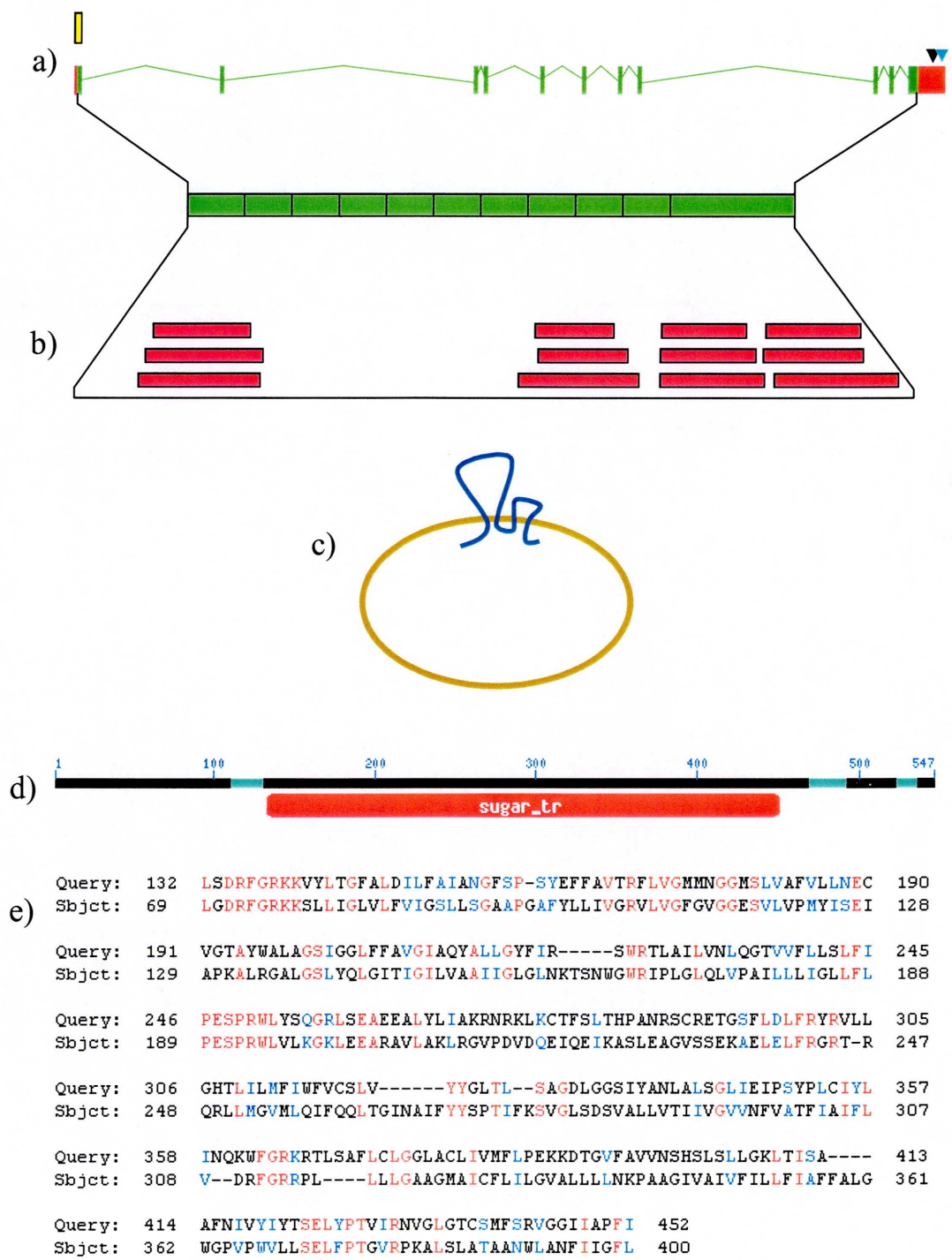


Figure 5.11: Putative assignment of structure and function of a novel gene. Figure 5.11a is the full length gene structure (including CpG island (yellow box), polyA signal (black arrow) and site (blue arrow)) of novel gene, bA12L8.C1.1. b) PIX analysis of the coding sequence identified four transmembrane domains (red boxes) giving rise to a putative cellular conformation, c). PSI-BLAST analysis of the novel gene identified putative functional domains (a sugar transporter within the conserved domain database, d) and sequence alignment of the highest percentage homolog by BLAST alignment, to a hypothetical protein, NP_060890, subject in e). Homologous residues between the two proteins are shown in red and conservative residues in blue.

5.5.2. Identifying function by structural homology

Another means of characterising the function of a novel protein is by utilising a sequence-to-structure-to-function analysis. Using this method, the function of a protein can be inferred from a homologous protein whose 3-D structure has already been elucidated. This analysis was used to predict the function of a novel gene bA483I13.C1.2. A structural homologue of the novel gene was identified by BLAST alignment of the translated protein with previously characterised motifs within Swiss-Model (Peitsch *et al.*, 1993). The novel protein showed the highest matching probability with the previously elucidated structure of 1VRK (Mirzoeva *et al.*, 1999) which is the peptide binding complex formed between calmodulin (CaM) and RS20, the CaM recognition site peptide from vertebrate smooth muscle cells. The X-ray crystallographic structure of 1VKR permitted the 3D structure of the novel protein to be predicted by amino acid sequence alignment. To determine the putative tertiary structure of

the novel protein it was first read into DeepView (Guex *et al.*, 1997) and then aligned to the template protein, 1VRK (figure 5.12a). The sequence alignment was edited to reduce the energy state of each group contained within the new structure by the introduction of gaps between amino acid residues (figure 5.12b). Adjustment of the amino acid sequence ensured that the side chains of the new structure were not in conflict, thus stabilising the new conformation. The two protein structures were then superimposed (figure 5.12c). Residues of the predicted novel protein structure are coloured according to their energy state, i.e. best fitting residues are blue and the least are red. Superimposition of the putative 3-dimensional structure (figure 5.12d) provided visual confirmation of the structural similarity between the proteins. Whilst this type of analyses provides some evidence for the function of the novel protein (by structural homology to a previously characterised protein) experimental support would be required to more accurately define novel protein function, particularly in light of structural differences between 1VRK and bA483I13.C1.1 as denoted by the red asterisk in figure 5.12d.

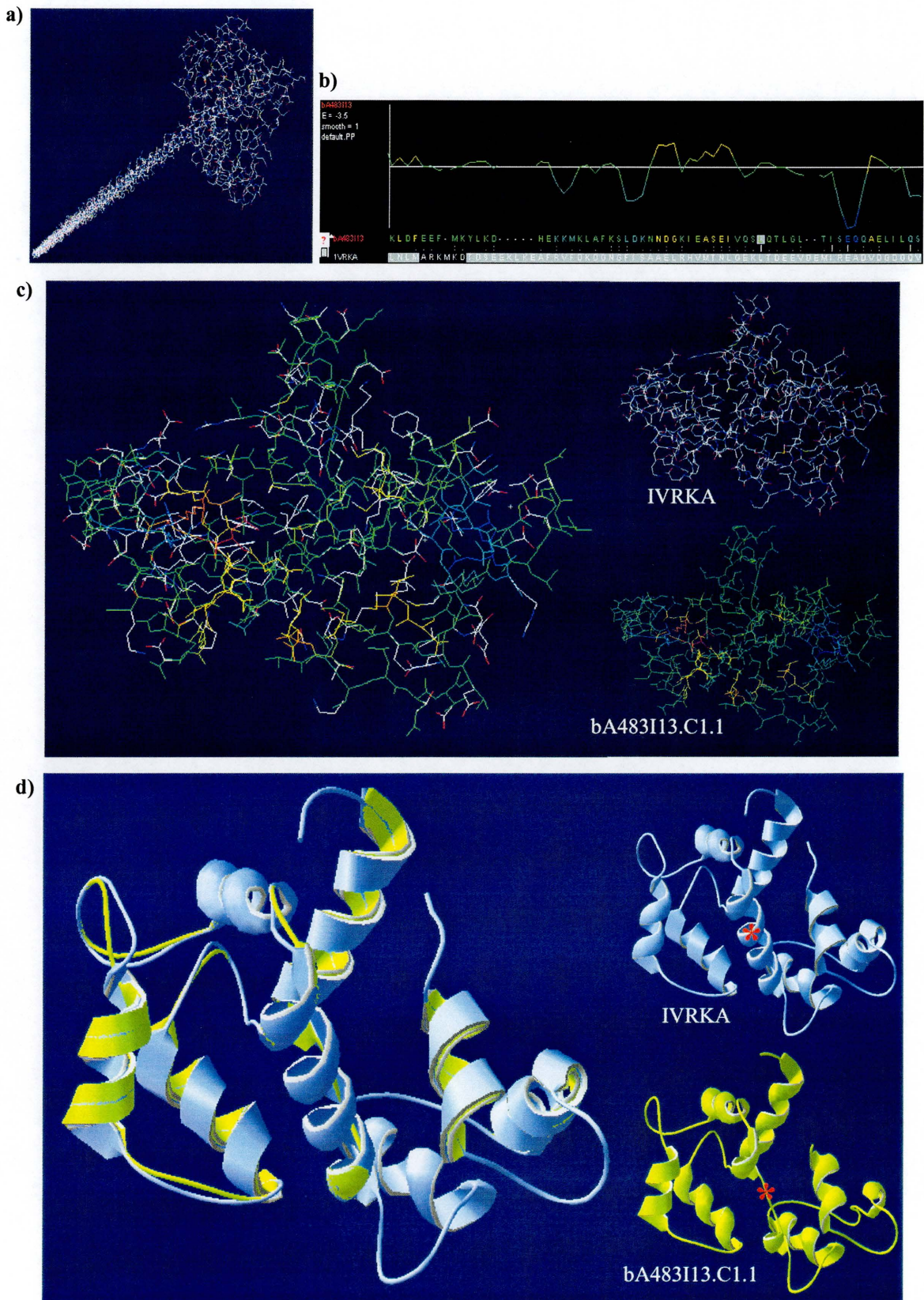


Figure 5.12: Identification of putative functional domain of a novel protein. Structural alignment was initiated by threading the novel protein (5.12a, rod structure) on characterised 3D protein. b) The novel protein is edited to reduce threading energy of new structure. c) The putative novel 3D structure is superimposed with the energy of amino acid sequences coloured red (high) to blue (low). d) Superimposition of ribbon conformations of novel and known protein structures. The asterisk denotes differences between two protein structures.

5.6. Discussion

A comprehensive characterisation of the genomic landscape contained within a 12.4Mb region of 1pcen – 1p13 is described. A correlation is made between the DNA profile of the interval with giemsa staining and isochore partitioning, repeat content and gene distribution. The detailed annotation of eight contiguous finished sequence links (see appendix, table 5.5) representing 95% coverage of the interval, has determined the genomic structure of 102 full length genes, including 67 known and 35 novel protein coding genes. In addition, 16 novel transcripts and 11 pseudogenes have also been identified.

Genes are typically associated with functional elements within genomic sequence whose presence can help determine whether the full length structure of a gene has been correctly elucidated. The detection of these elements aids the determination of full length gene annotation. Whilst some of these elements are relatively easy to identify, for example exon - intron boundaries by mRNA/EST alignment, translation start and stop sites and polyadenylation signals by motif recognition, others such as promoters, are more difficult to characterise. Promoters and other regulatory elements residing at the 5' ends of genes which

act as a template upon which transcription factors assemble prior to the initiation of RNA synthesis, are inherently difficult to identify using *in silico* methods because they do not contain consistently shared sequence motifs. There are, however, some characteristic features associated with, or contained within, the predicted structure of a promoter. These features can be used to aid the identification of promoters and, in doing so, help to localise the 5' end of a gene.

A degree of sequence motif conservation within the core of the promoter permits *in silico* prediction of transcription start sites (TSS) of human genes. Eponine (Down and Hubbard, 2002), the TSS prediction program used herein, uses TATA box motifs flanked by regions of C-G enrichment in conjunction with a predicted CpG island to identify the TSS of a gene. This program has a reported sensitivity (being able to detect a known mRNA start) of 54% and a selectivity (the proportion of predictions that are confirmed by a known mRNA start) of 74%. A representation of the constraint distributions and sequence motifs Eponine uses to identify the gene TSS is represented in figure 5.13. As previously mentioned, predicted CpG islands can also be used to help identify the full length transcript and promoter region as they are associated with approximately 56% of 5' ends of genes (Antequera and Bird, 1993). Two thirds of the 102 known or novel genes from 1pcen – 1p13 were associated with either a CpG island (57%) or an Eponine prediction (9%), while 17% of genes within the region were associated with both.

Figure 5.13 represents a 'generic' gene structure with a predicted TSS and CpG island at the 5' end of the gene and red (untranslated) and green boxes (translated) represent the

transcribed length of the gene. Splice donor, GT, and splice acceptor, AG, consensus sequences (contained within 99.9% of all introns (Levine *et al.*, 2001)) used by the spliceosome to excise introns during pre-mRNA processing are highlighted, as are consensus poladenylation signal (AATAAA) and polyadenylation sites. Processing of the pre-mRNA (figure 5.13) results in the removal of introns, the addition of a 5' guanine cap (dark blue box) and a polyA tail. The optimal consensus sequence at the site of translation initiation, GCC^A/_GCCAUGG (Kozak, 1987), which includes the two bases which exert the strongest effect, a G at the first base after the translation start, AUG, and a purine (preferably A) three nucleotides upstream, are also shown. Whilst the model of a single promoter effecting the transcription of a single gene product is relatively easy to discern, there are examples of tissue specific promoter regulation and coordinated expression of genes sharing a promoter that complicates our understanding of how promoters function.

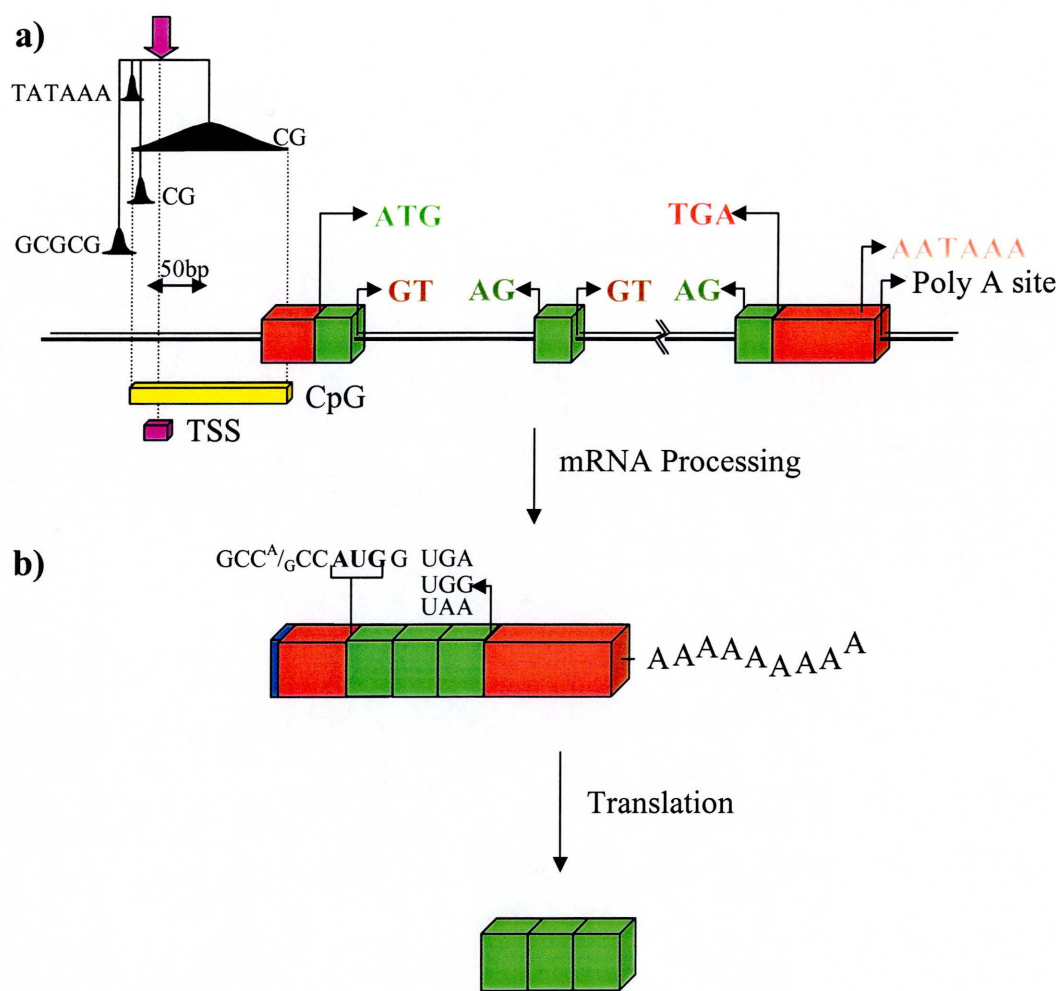


Figure 5.13: Generic structure of a gene. Figure 5.13a represents the regulatory elements (predicted CpG island and transcription start site consensus motifs (purple box)) at the 5' end of the gene, translation start (green lettering) and stop sites (red lettering), polyA signal (pink lettering) and sites and exon splice donor (dark red lettering) and acceptor sites (dark green lettering). b) Processing of pre-mRNA results in the addition of guanine 5' cap and addition of a polyA tail. Also represented is the Kozak consensus sequence and translation start and stop sites. Translation of the gene subsequently follows.

The annotation of a full length coding feature within the context of genomic sequence is only the starting point when trying to fully characterise a novel gene. Whilst the regulation and tissue distribution of gene expression poses a difficult question, the function of the encoded protein product is perhaps a more difficult problem to resolve. There are two different approaches that are used to assign a putative function to a novel protein. The sequence-to-function approach utilizes a two dimensional pair wise sequence alignment or motif alignment to suggest protein function in a novel gene on the basis that structural homology reflects functional similarity. This method was used when predicting the transmembrane sugar transporting role function to the novel gene bA12L8.C1.1. The second approach is to utilize a sequence-to-structure-to-function paradigm. This technique is believed to be more powerful because the development of the structure is more in accord with how the protein functions. However, the folds of a protein alone cannot determine its function as proteins with similar folds may have completely different utility. It is the combination of dimensional structure, active sites and protein – protein complexes which will provide a more precise aid in predicting novel gene function. The limitation of the *in silico* methods described above is that they require a degree of homology to be identified (whether at the level of primary or tertiary structure) with a protein of known structure or function. The library of these known models will need to be increased by experimental methods of structure determination and complex formation to broaden the applicability of this approach.

The structure and function of a gene and its cognate protein are inherently determined by the genomic sequence from which it is transcribed and elements which affect its regulation. Alterations within these coding elements by as little as a single base change may result in

conformational and functional consequences. The next chapter details the development of assays designed to identify these changes within a number of genes, including a gene family localised to 1pcen – 1p13, and discusses the potential affects these changes may have.

5.7. Appendix

Table 5.5: Minimum tile path clones and accessions from the 1pcen – 1p13.2 contig (October 2002). Boxes denote contiguous blocks of finished sequence.

1	Link_bA436H6	AL513187	bA436H6
2		AC114491	AC114491
3		AL513206	bA382F13
4		AL591042	bA480L11
5		AL353892	dJ547O1
6		AL391235	bA320L5
7		AL390036	bA356N1
8		AL359258	bA483I13
9	In Finishing	AL672086	dJ673H23
10	Link_bA131J3	AL390038	bA131J3
11		AL392088	dJ964H19
12	In Auto-analysis	AL160171	bA256E16
13	Link_bA293A10	AL591719	bA293A10
14		AL449266	bA475E11
15		AL356488	dJ1065J22
16		AL138933	dJ667F15
17		AL356389	bA352P4
18		AL390252	bA297O4
19		AL356735	bA173K24
20		AL355145	dJ831G13
21		AL355310	dJ1160K1
22		AC000031	cgtm1
23		AC000032	cgtm12
24		AL158847	dJ735C1
25		AL450468	bA195M16
26	Re-submission	AL772411	bA180N18B
27	Link_dJ742A5	AL355817	dJ742A5
28		AL772412	bA180N18A
29		AL160006	dJ773N10
30		AL355990	dJ1028L10
31		AL137790	dJ1003J2
32		AL355488	dJ1074L1
33		AL390797	bA225L12
34		AL358215	bA470L19
64	Link_bA512F24	AL391058	bA512F24
65		AL389921	bA228G5
66		AL390759	bA473L1
67		AL133517	dJ730K3
68		AL365321	bA324J2
69		AL137856	dJ1073O3
70		AL731797	dJ786G8
71		AL591742	dJ590F24
72		AL162594	dJ1037B23
73		AL121999	dJ543J13
74		AL512291	dJ802H15
75		AL035410	dJ591B8
76		AL390241	bA343L14
77		AL133382	dJ1156J9
78		AL096773	dJ1000E10
79		AL390235	dJ1146M22
80		AL358372	bA350E19
81		AL645502	bA109G4
82		AL109660	dJ666F24
83		AL139428	dJ977F20
84		AL049825	dJ662B22
85		AL606499	dJ1034E9
86		AL512638	dJ663N10
87		AL157950	dJ940J24
88		AP001393	bA722J12
89		AL592436	bA710N8
90		AL450389	dJ929G5
91		AL449264	bA485H8
92		AL357137	bA12L8
93		AL365318	bA159M11
94		AL121982	dJ1185H19
95		AL831782	dJ636P16
96		AL355538	dJ787H6
97		AL136376	dJ655J12

35		AL365361	bA284N8	98		AL390066	dJ1086K13
36		AL354713	bA498A13	99		AL355794	dJ781D12
37		AL391064	bA392B1	100		AL356748	dJ686J16
38		AL360270	bA96K19	101		AL135798	dJ655N15
39		AL355816	dJ1180E21	102		AL157904	dJ753F5
40		AL513202	bA165H20	103		AL445231	bA27K13
41		AL356387	dJ1125M8	104		AL139248	dJ570D9
42		AL390195	bA552M11	105		AL391476	bA229A19
43		AL391063	dJ836N10	106		AL365264	bA287H7
44		AL139012	dJ1091G18	107		AL360298	bA39H13
45		AL049557	dJ773A18	108	In Finishing	AL358072	bA188D8
46		AL450997	dJ1086I18	109	Link_dJ675C20	AL157902	dJ675C20
47		AL390070	bA99M15	110		AL365331	bA42I21
48		AL512665	bA88H9	111		AL390877	bA134N8
49		AL357114	bA57I1	112		AL122007	dJ757N13
50		AL445426	bA62J10	113		AL121993	dJ776P7
51		AL591521	dJ965F6	114		AL139345	dJ832K2
52		AL450407	dJ1160J2	115		AL513191	bA224F24
53		AL354760	dJ671G15	116		AL391557	bA506J19
54		AL109932	dJ770C6	117		AL512823	dJ881A21
55	In Finishing		bA72M14	118		AL122006	dJ730H16
56	In Auto-analysis	AL603832	bA426L16	119		AL390117	bA116P22
57	Pre-Sequencing		bA721A13	120		AL606843	bA94F13
58	Link_dJ522D1	AL390729	dJ522D1	121		AL139148	dJ630J13
59		AL158844	dJ580L15	122		AL845532	bA183H8
60		AL390242	bA31F15	123		AL357045	dJ794L19
61	In Finishing	AL357055	bA389O22	124		AL139420	dJ712E4
62	Link_dJ658C17	AL139016	dJ658C17	125		AL359823	dJ610L12
63	Re-submission	AL365225	bA179A5	126		AL590288	bA212F6
				127		AL359915	bA418J17
				128		AL139346	dJ834N19
				129		AL359553	dJ871G17
				130		AL121995	dJ920G3
				131		AL109966	dJ599G15
				132		AL139251	dJ656M7
				133		AL589734	dJ683H9
				134		AL359752	dJ1042I8
				135		AL512503	bA323K8
				136		AL596222	bA114O18

Table 5.6: Primer pairs designed for the validation of predicted gene structures by cDNA library screening. Red background denotes primer pairs for which no PCR product was generated from cDNA library screening.

Gene	Exon	stSG	Primer 1 (S)	Primer 2 (A)	Size	1pool
bA483I13.C1.1.mRNA	e2	452926	GGTATCTGCCGACCCTTGT	GAGTAGGCAGTAGCTTGAGT	147	Y
bA483I13.C1.3.mRNA	e2	452927	GCAGTCTGGAGATTGGTGA	TGCATCATGACTTTCAAGCG	102	N
	e5	452928	GGGATTATTGATTGTGCAA	CGGCATAAGGTACAATGCCT	100	Y
	e7	452929	GGTTTCACCTCAAACATCAT	ACATCTCTTTATAACACAGG	164	N
ba475E11.C1.2.mRNA	e1 5'UTR	452930	TGACGGCTGAAGAAACAGTG	CTCCAGGGCCAGCATACTAA	104	Y
	e4	452931	GCTTTTGACTTTGCCTCGTC	GCTTCCTATCAGCAGGGATG	128	Y
	e7	452932	CAGCACTCAACCAGCAATGT	TCCAGGATTACGAGGAGTGC	149	Y
	e10	452933	ATGAGACTCCTAAGCAGCCG	GGGCAGCACTTTGACGTATT	137	Y
	e12	452934	ATACCTGGAGTGGCTGGATG	GTGTGCCAACAAACACGAAC	100	Y
	e14 3'UTR	452935	CGAAGAGGCCCTTATTACC	GGAGTGCACACCAACAACCTG	166	Y
ba475E11.C1.1	e1 5'UTR	452936	AGGCTATGCATAGTGAGACT	GCTTGACTTAGAAGCGTCTC	155	N
	e5	452937	ACTGCAGGGACACCTTGAAC	CCAACGATTGTTGATTCTGTG	105	N
	e6	452938	TTGGAGATGCTGCTTGAAGA	AGAGAAGGTGGAGGCCAAGT	117	N
	e10	452939	GAAGCAAAACGTGGAGAAAA	TTGAATCTGAGTGTGGTGCC	92	N
	e13	452940	CTTCCAAATCCAGCCCTACA	ATGGGTTGCTACCAACTTGC	127	N
ba297O4.C1.1.mRNA	e1 5'UTR	452941	GCCACTATTGGGAGACCAAG	GTAGAGCCAGAGGTTTCGACG	124	N
dJ831G13.C1.1.mRNA	e1	452942	CTTTGCTATTTTCGCCTTCG	CTGAAGGGATAGCCAAATGC	123	Y
	e3	452943	CCTTCACCTTCTTCTGGCTG	CTTCCTCTCCATGGCACACT	120	Y
	e4	452944	GCTCAGTGCTTCTGTGCAG	TGGCTGCTAGGAACCACTCT	146	Y
ba180N18A.C1.2.mRNA	e1	452945	CCCACTGATCGTGAACAACA	CTCTGAGTCTTTGCGCTGGT	154	N
dJ773N10.C1.1.mRNA	e2	452946	CAGCCTGCATCTTCCTCTTT	AGACCTTCTCCAGTCTCTCC	125	Y
dJ1003J2.C1.1	e2	452947	CCCTGAATGAGAAGGAGCTG	CACGGACTCAGTGACATGCT	148	Y
	e4	452948	CTGTCTCTTTGTGGGGCTGT	ACAGGACATTCACTCCAGGG	102	Y
	e7	452949	ACCCAGGTCTTCTTTGCCTT	GCCAACACTGACGTGAAGAA	134	N
	e9	452950	CCTTCATCGCCTTCACTGAG	GTGAACATCTCCTTGGGCAC	169	Y
	e12	452951	CGCTACCTGTATTTCCCCAA	CCCTTCTGTAGGACACGGA	149	N
ba470L19.C1.2.mRNA	e1	452952	CACCAAGCATTCCATACGTG	GAACCCAATGGGGATTCTTT	150	N
ba284N8.C1.2/3	e2	452953	ATGCTCGGCTGTCTTCAAGT	AATGGTGAGTCATTCTGGGC	128	Y
ba165H20.C1.3.mRNA	e3	452954	TGTTACTTCACCAACTGGGC	TGGTGATCTCGTTGTTCTGC	127	Y
	e5	452955	TTCCACTCCTGAGAACCACC	CTGCACCAGGACAGTGAAGA	151	N
	e7	452956	CTATGACCTCCATGGCTCCT	ACATTGAGGTAGCGTTGCT	96	Y
	e10	452957	AACAACCTTGGAGGTGCCAT	TTGTACTCTGCAGGCCCAGA	124	N
dJ1125M8.C1.1mRNA	e2	452958	GCGGATAACTACCTTTTGG	AAATAACACCCAGGCCCTCT	128	Y
	e4	452959	ATGCAGGCAGGTACCAGAAA	TTCTTAAATCGAGGCACCAA	91	Y
	e6 3'UTR	452960	ACGTTACTGTGGCCCTCTTG	ACAGAAACCCACAGACCCAG	154	Y
dJ1125M8.C1.2	e1	452961	GAATGGAGGAGCAGGGTGTA	TCCAGGTAGTTGGTGAAGGG	121	Y
	e3	452962	ACAACAGGTTCAATCCAGC	TGTCATAGCCCAGGAACACA	105	N
	e5	452963	ACCCGCCAGTATTGTGGAGA	GGCAATCTGCCAGTACAGTT	107	N
	e8	452964	AACAATGGCTACTGCAGGCT	CTAGGCAGAGAAGGCAAAGC	153	N
ba552M11.C1.4.1/2	e2 .2	452965	ACCACGTGGGATTTGATGTT	GGATGCCAAATTAAGAGCCA	137	N
	e3/4 .1	452966	CCTTTTGTGCTGGGGTTCTA	GCTGGAGGATCTGAGTGAGG	121	Y

	e5	452967	TGAGGCTTGAATCCATTTC	CTCTGGCCAGGAAAAGACTG	175	Y
bA552M11.C1.5	e1/2	452968	TGCTTCCTTCCAGTCATGTG	TGGTCAGGCAGGACATAGTG	120	Y
	e3/4	452969	CAGGCAACAAAACCAGAAGC	CCCAAACCCGTGATCAGTAT	103	Y
	e5	452970	ATCATTTGCAGCCAGGTAGC	GTCCCCAATCCAGATTCTCC	154	Y
dJ836N10.C1.1	e2/3	452971	GGAAGAACAAGGAAAAGGGC	CTCAATGCTTCCCCTCACTG	176	Y
	e4	452972	AAAAGCCAGAGCTTCCTGAC	TGTGGTCCCTTTCTTCTTGT	120	Y
dJ1073O3.C1.3	e1	452973	CTGGGCTGAAAAGTGTGT	GTTGGGCTCAAGAAGTCCAT	134	Y
	e3	452974	GACCTGGTGTGCTCAGGATT	TTCCCATTTGATCATACCCGT	144	Y
dJ1037B23.C1.1.mRNA	e2	452975	TCCCTCTTCTGCTAATCCCC	ACCTCAGCTGGGATATCTGG	122	N
	e4	452976	AGCGTGGACTTGGGAGAGAT	GTGATGTCCATCGCCTTGAG	107	Y
	e6	452977	TAGGAGTCTGTCTGTGGGG	TTACCTCCACCAAGGAGTGC	114	Y
	e8 3'UTR	452978	AAACAGTGTGTGCAGTCGC	CATCACCTTGGGAGACACAA	144	Y
dJ1156J9.C1.1	e1 5'UTR	452979	ACCTTGGAGCGGGATCTTAT	TGCCAGGGAATTGTTGTATG	127	Y
dJ929G5.C1.1.mRNA	e2	452980	TCCTGTGTGAAGAGTGGCTCC	TCCAGAATAAGTGGATTCGG	157	Y
	e4	452981	GTTTGTGTTTCGTGCCCTTT	TATTGCACAATGCCCTGGTA	120	Y
	e6	452982	CAGTAACAATGCCACTGGCC	CTTCTTTACTCGCCGTTTCAT	118	Y
	e8	452983	GCAATATGACAAGGACCGCT	TACGAGGCTGAAGTCCAAGC	121	Y
bA12L8.C1.1.mRNA	e2	452984	CATCCTCATTGCACTGGTTG	TGCACGTGCTTATGGATCTC	159	Y
dJ655J12.C1.2.mRNA	e1	452985	AAGACAAGGAAGAGCACCTG	GAGTCCTTGAAGTGGTCGGA	120	N
	e2	452986	GCTCTGTTTCAGGAAAATGCC	TGATCATCAGTGAGCCAAGC	165	N
dJ655J12.C1.3.mRNA	e2	452987	AGTCCTCCCTGAACTGTTGC	TGGGCATGAGATAAAACACG	106	Y
dJ686J16.C1.1.mRNA	e1/2	452988	GGGCAGTGTCCAATTTATGG	GGAAGGAGGACTGATGGTGA	116	Y
bA39H13.C1.1.mRNA	e1	452989	AAAAACCCAGCTGGACAATG	TCAGCAAGATTCTCGGTCT	142	Y
	e2	452990	ATCTGGAAGCAGAGCCAGTA	CCATTTCAGAGCTTCTGTGC	90	Y
bA42I21.C1.1.mRNA	e1	452991	CACATGCGTCGGCTTAAATG	CCTCCACGATCGATGTTTCT	95	Y
	e2	452992	CCCTCGTGGGAAAGACATA	TGCTGGGGGAAAAGATTACT	139	Y
dJ776P7.C1.1	e1	452993	GGCACTCTATTGCGACGTCT	CTCCATCATCCCAGGACACT	99	Y
	e1/2	452994	GCTGAGAGGATTATGGAGGC	CTGAACTCTGCCCCCTTACCA	101	N
	e4	452995	CTGTCTCTCCACTGGAATGT	TTCCGAGGTGAAGGAGAAAAG	145	Y
dJ832K2.C1.1.mRNA	e1	452996	AAAAACTCCAGGACCTCCGT	ACCTGCAGCCTCAGTTTCAC	171	Y
	e6/7	452997	CCGCATAATACCACCTTTT	CAGCTGTTTCGTTTGCATCT	131	N
dJ832K2.C1.2.mRNA	e2	452998	CCTCCAAACACAGGCTCTCT	CATGATGTACCTGCCAGCTC	126	Y
dJ832K2.C1.3.mRNA	e2	452999	CCTTCAAGAAGCCATAAGC	CAACATTGGAGTGGAGAGCA	146	Y
	e5	453000	AGGCAAGGATAACGCAGAGA	CTTAGGTTCTGGTTGGTGGG	133	Y
	e8	453001	ATCCCTTCAGCACTCACTCC	TCTTTGGGTTTTTCTTTGCC	98	Y
bA224F24.C1.1.mRNA	e1	453002	TTAGAGGCCAATGCTTCTCC	AGCGAGGGTCCCATATCTT	95	Y
	e4	453003	ACGGCAGCAAAAGCAATTAT	TTCTTTTCATTTTCCCCTCG	125	Y
	e6	453004	GGGCTTTAACAATCCTCAGC	CTGGTTAACTGCTGCCAGGT	124	N
	e8	453005	TTGCCTGCTTGATGTATGAC	CTCTGAAGTTGGCATGGCTT	131	N
	e11	453006	AAGAAGATCTCGTCCACCC	GACAGAGTGAGGGCAGAAGG	105	Y
	e15	453007	AGCAACCGAGAACCTTCAGA	AGAGACTCATGTTGGGGCTG	149	N
dJ794L19.C1.1.mRNA	e1	453008	GGCGGCTAAAATGAGTGAAA	ATAGACAGGTCCAGCCCCTT	141	Y
	e3	453009	AGGATGTTTCTGCCATGAG	TTTTATTGTCCACAGGCACA	94	Y
	e5	453010	CTCGAGTTCATGTGATTTCG	AGGCCGTAAGTGTGGTGAAC	123	Y
-	e8	453011	TACCAACTCCTCCCTCGTTG	CATGTGTGGTGATGAGGAGC	137	Y
dJ834N19.C1.1.mRNA	e1	453012	TACCGGTCAGACTCCAGGTC	AGGTCTCTTCTTTGCCTCC	93	N
	e3	453013	CAGTAACTGAGGAGGGCCAC	GGCTGCGATAGAAAGCAAAG	143	Y
dJ834N19.C1.2.mRNA	e2	453014	AGACGAGGTCTTGCCACATT	GCATGGTGGCTTATGCTGTA	108	Y

dJ599G15.C1.5.mRNA	e1	453015	TCGCTAGCCATTATCCAACC	CCTGTCCTTGTAGTGGGCAT	129	N
dJ599G15.C1.6.mRNA	e1	453016	ACTCTTCAGGAGCCACATGC	TCTACTGGAAGAGCACCAGC	95	Y
dJ1042I8.C1.4.mRNA	e2	453017	ATGCTGGCCACAATCTACCT	GATCACTCCCCACAGCACTT	127	Y
	e3	453018	TGGTCCAGTGAGAAAGCAGA	CCGGCCATTTGAGTTACAAG	125	Y
	e5	453019	GGAACGAGAGCTGATCCAGT	AGCTGTTCTCGGAAGTCCTG	138	Y
	e7	453020	GGAGGAATGTGCCATCACTT	GAGCATCCTGCCATTTCATCT	152	Y
	e9	453021	AGGAAGCTGCAGGAGTCTGA	CCAAGAAAGTGCCTTCACAA	124	Y

Chapter 6

The identification and analysis of single nucleotide polymorphisms

- 6.1 Introduction**
- 6.2 Gene Annotation**
- 6.3 Identifying SNPs within Gene Families**
- 6.4 Primer Design**
- 6.5 DNA screening**
- 6.6 Sequence Generation and Assembly**
- 6.7 Exon coverage of sequence contigs**
 - 6.7.1 Validation and localisation of known SNPs
 - 6.7.2 Identification of novel SNPs
- 6.8 SNP Analysis**
 - 6.8.1 Validating SNPs within highly homologous genes
 - 6.8.2 Validating SNPs
 - 6.8.2.1 Known*
 - 6.8.2.2 Novel*
 - 6.8.2.3 Suspect candidate SNPs*
 - 6.8.2.4 Rejected candidate SNPs*
 - 6.8.3 Effect of Sequence variation upon gene structure
- 6.9 Discussion**

6.1 Introduction

Genetic variation, locus specific differences in sequence between individuals, has arisen within the human population primarily through unique mutational events some time in the past. The genetic variants (polymorphisms) in present-day chromosomes reflect these historical mutational events, and analysis of them can therefore be used as a means of determining evolutionary relationships between populations and individuals.

Single nucleotide polymorphisms (SNPs) are the most common form of genetic variation within the human genome. On this basis, comparison of any two human genomic sequences would identify approximately 2.5 million single base pair variations, at a frequency of 1 SNP every 1.25 kb (Li *et al.*, 1991, ISNPMG, 2001). A subset of these variants will cause an alteration in an encoded function, for example with respect to transcription, translation, or the structure or catalysis of a protein. More over, any of these functional changes which are deleterious to health represent a genetic contribution to a human disease state. These functional variants, and other polymorphisms which are linked to them, can be investigated to characterise genetic contributions to human disease. From a disease perspective, the sequence polymorphisms of an individual can contribute to the severity, age of onset and susceptibility to disease, or even the physiological response to the drug treatment.

The association between a polymorphism and a disease phenotype can be studied by direct or indirect approaches (reviewed by Collins, 1998). In the direct approach, a functional variant allele is tested directly for association with the phenotype under study, for example a case-control study. The frequency of a variant allele is compared in

the case population and in an equivalent group of matched controls. A skew in the frequency of an allele is indicative of an association, which can then be confirmed by additional population genetic studies and functional studies. This approach depends on prior identification of putative functional variants; given the range and possible low frequency of many of these, a systematic study is required to provide the candidate functional variants for such studies. The alternative, indirect approach is carried out by testing variants (usually SNPs) selected by genomic position, for association with the phenotype in the association study. This approach depends on adequate association (i.e. linkage disequilibrium) between the SNP(s) used in the test, and the unknown functional variant, which is likely to be nearby in the genome. An association detected by the indirect approach therefore results in identification of candidate regions within the genome to target the search for the functional variant(s) which then require confirmation in the same way described above.

While large-scale studies will lead to a well-characterised panel of SNPs for genome-wide indirect association studies to search for new genes and variants involved in human disease, a more targeted small scale approach can be carried out by selecting candidate genes for SNP discovery and association studies. The identification of SNPs within coding sequence (cSNPs) in genes of medical importance, and associating coding and structural changes with gene function, will be essential to our understanding and treatment of human disease. Additional studies of gene regulatory regions may also be required to find other functional variants which alter transcriptional processes, but search for cSNPs represents a valuable first step in targeted SNP searches in candidate genes. This chapter outlines an approach to the identification of cSNPs within a family of genes localised to 1pcen – 1p13 (GSTM1-5) which has inferred association with

increased cancer susceptibility. Seven other genes of medical interest, the majority of which are involved in drug metabolism, are also included in this investigation. Diseases associated with genetic variation within these additional loci include gastric (Tsukino *et al.*, 2002) and lung (Nakachi *et al.*, 1991) cancer as well as susceptibility to treatment by chemotherapy (Allan *et al.*, 2001).

6.2 Gene Annotation

Correct annotation of coding features in their genomic context is central to the accurate design of primers for the identification of single nucleotide polymorphisms that are located within genes. The genes, GSTM 1 - 5, localised to chromosome 1p13 by mRNA / EST BLAST alignment and were annotated during the course of the full genic characterisation of 1pc – 1p13, as described in the previous chapter. The remaining genes considered in this study were either previously annotated as part of a chromosome specific sequencing project, GSTT1 on chromosome 22 (by others), or by *de novo* annotation of clone based sequence within a project specific ACeDB database. These genes, GSTP1, CYP1A1, CYP1A2, CYP2A6, CYP3A4 and NFE2L2, were localised to chromosomes 11, 15, 15, 19, 7 and 2, respectively, by BLAST alignment and the full length structure was manually annotated within clone based sequence.

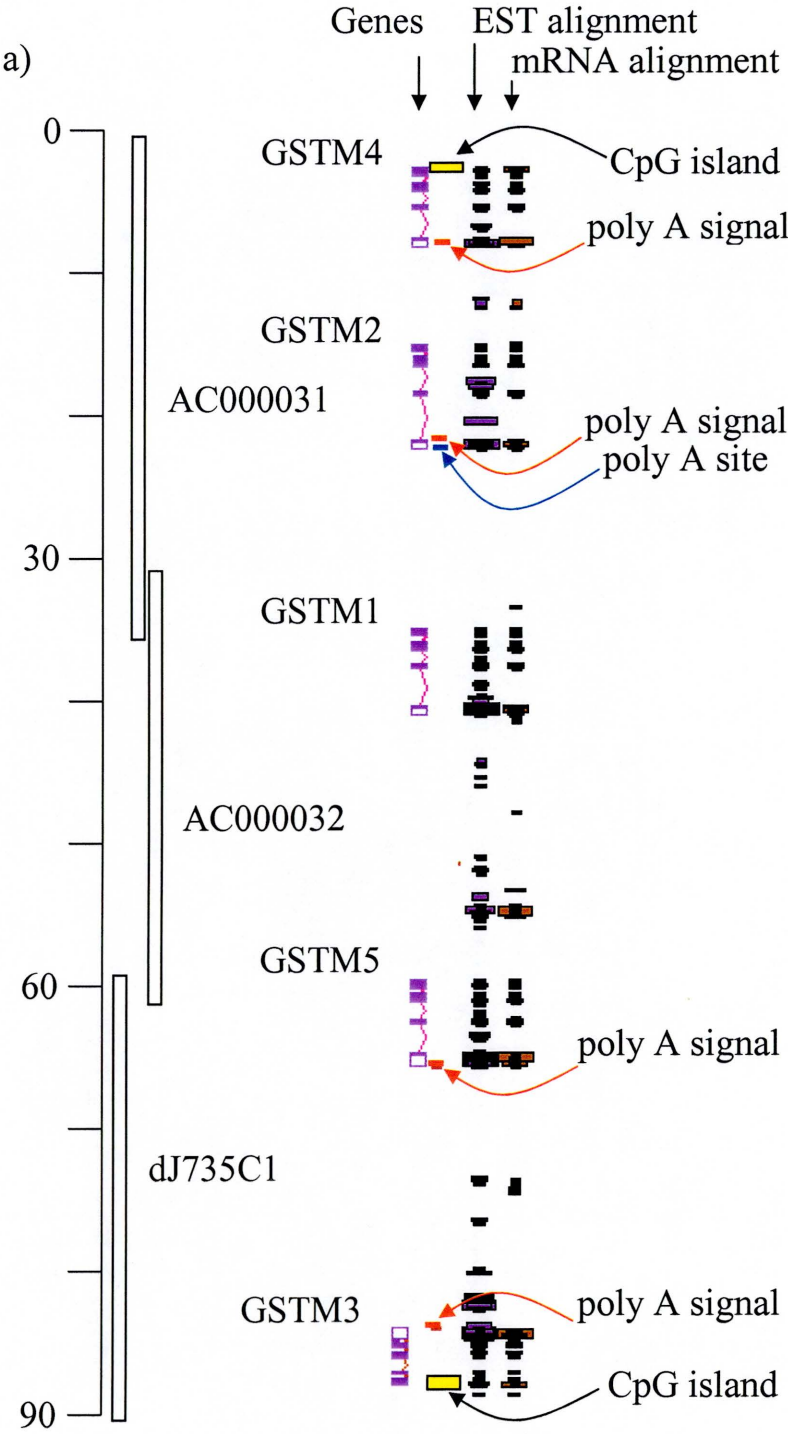
6.3 Identifying SNPs within Gene Families

To date, 69% (19626/28574) of known and predicted proteins show homology to existing proteins within Interpro (<http://www.ebi.ac.uk/protome/>), suggesting a large

proportion of genes in the human genome are members of a gene family. It is therefore an important consideration when designing primers to identify cSNPs that the assay will identify SNPs from the correct gene and not from a closely related family member.

GSTM 1 – 5 were used as a model to assess the difficulties of designing and generating sequence from exon specific primers from closely related genes.

Glutathione S-transferases are a functionally diverse multi-gene family of soluble enzymes which are involved in the detoxification of a wide variety of chemicals via conjugation and reduction of glutathione (Booth *et al.*, 1961, Mannervik and Danielson, 1988). Mammalian GSTs are divided into five main classes, alpha (A), mu (M), pi (P), theta (T) and zeta (Z) and exist as dimeric proteins, with only subunits within the same class forming homodimers. In general, members of the same class share more than 40 – 50% sequence identity but less than 25-30% sequence identity with GSTs in other classes (Hayes and Pulford, 1995). Within the GSTM family, four of the five members (GSTM1, 2, 4 and 5) share a > 70% genomic sequence homology whilst the fifth gene, GSTM3, which is transcribed in the opposite direction, shares a low genomic sequence homology but a high percentage identity with the other four genes at the coding nucleotide (>77%) and amino acid level (>78%). All five genes are evenly distributed within a 90kb interval spanned by one PAC clone (dJ735C1) and two previously sequenced cosmids ctgm1, (AC000031) and cgtm12 (AC000032) (Xu *et al.*, 1998), as displayed in figure 6.1a. The structure of all five genes is assumed to be complete as polyA signals were identified within all genes, whilst CpG islands have been localised to the 5' end of GSTM4 and GSTM3. The consensus GSTM gene structure contains 8 exons, the majority of which are identical in size between family members. The intron size is also conserved with introns 3, 5 and 7, showing most variation (figure 6.1b).



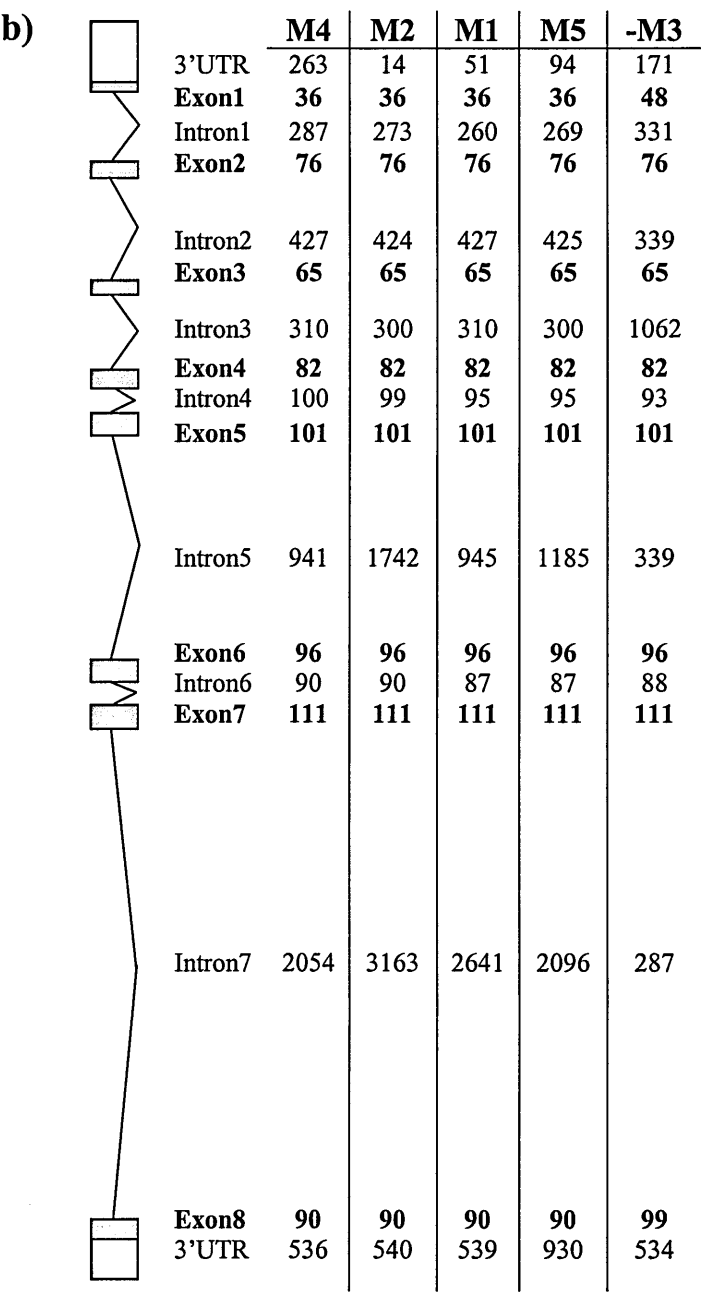


Figure 6.1: An ACeDB display of GSTM 1 – 5 and a generic GSTM gene structure.

- a) The annotated structures of GSTM 1 – 5 contained within two overlapping cosmids (AC000031 and AC000032) and one PAC (dJ735C1) clone. Supporting EST and mRNA sequence, in addition to poly A signals, sites and CpG islands are also shown.
- b) A generic GSTM gene structure with base pair sizes of exons and introns. Red boxes and green boxes represent untranslated and translated sequence, respectively.

To facilitate the identification of primer pairs that would uniquely flank GSTM exons the genomic sequence of each of the GSTM loci, including approximately 1000 bp preceding the 5' UTR and approximately 500 bp beyond the 3' UTR, was aligned. Sequence was exported from 1ace in Fasta format and analysed within ClustalW (Higgins *et al.*, 1994) prior to editing in GeneDoc (Nicholas *et al.*, 1997) (figure 6.2).

Figure 6.2 (inserted at end of chapter 6): A genomic sequence alignment of GSTM 1 – 5: Bases that were in common between all 5 nucleotide sequences were coloured red, 4 sequences green, 3 sequences blue and 2 or less black. 5' and 3' untranslated regions have been shaded yellow whilst coding sequence has been shaded grey and the corresponding exon denoted. PolyA signals at the 3' and sites, where detected, were boxed in black and red, respectively. Coloured shading (yellow, orange, dark green, pink, blue and light green) indicate the positions where primers could be designed within the genomic sequence relative to coding features.

6.4 Primer Design

Attempts were made to design exon flanking primers for each of the 91 exons contained within the 12 target genes. Primers were designed as outlined in materials and methods (section 2.16.1) but with an optimal PCR product size of 600bp. In some instances, because of sequence and product size constraints, primer pairs were designed across multiple exons (e.g. GSTM4 exons 3/4 and 6/7) or overlapped to ensure complete exon coverage (e.g. NFE2L2 exon 5a, b), as listed in table 6.1. All 5' and 3' UTR primer pairs were designed to incorporate as much of the untranslated region as possible. Three exons did not have working assays associated with them; primers from exon 8 of GSTM1 and GSTM2 failed primer design due to the high percentage of sequence conservation within the introns of the two genes, whilst the sense primer of exon 2 from GSTM2 failed during primer synthesis due to the enforced high GC content (80%) of the primer.

Table 6.1: A summary of the primers designed to the exons of 12 genes for the detection of coding polymorphisms. EMBL accession number associated with the primer pairs and estimated PCR product sizes are also listed.

Gene	Chr	Exon	stSG #	Size (bp)
GSTM4	1	e1	452701	528
		e2	452702	724
		e3/4	452703	566
		e5	452704	527
		e6/7	452705	701
		e8	452706	689
		e1	452707	408
		e2	452708	534
		e3/4	452709	719
		e5	452710	614
GSTM2	1	e6/7	452711	508
		e8		
		e1	452712	448
		e2	452713	535
		e3	452714	484
		e4/5	452715	468
		e6/7	452716	709
		e8		
GSTM1	1	e1	452717	448
		e2	452718	548
		e3/4	452719	878
		e5	452720	409
		e6/7	452721	663
		e8	452722	621
		e1	452723	520
		e2/3	452724	622
		e4/5	452725	463
		e6/7	452726	567
GSTM5	1	e8	452727	748
		e1	452723	520
		e2/3	452724	622
		e4/5	452725	463
		e6/7	452726	567
GSTM3	1	e8	452727	748
		e1	158595	465
		e2	158596	384
		e3	158597	385
		e3/4	158591	399
		e5	158592	399
		e6	158593	399
		e7	158594	498
		e1	140015	348
		e2	140017	351
GSTM1	22	e3	452728	276
		e4	452729	406
		e5	140020	659

Gene	Chr	Exon	stSG #	Size (bp)
CYP1A1	15	e1a	452730	556
		e1b	452731	533
		e2/3/4	452732	564
		e5/6	452733	637
		3' UTRa	452734	620
		3' UTRb	452735	697
		e1a	452736	700
		e1b	452737	536
		e2/3	452738	753
		e4	452739	511
CYP1A2	15	e5	452740	484
		e6	452741	464
		e1/2	452742	722
		e3/4	452743	626
		e5	452744	588
		e6	452745	404
		e7	452746	467
		e8	452747	443
		e9	452748	538
		e1	452755	613
CYP2A6	19	e2	452756	519
		e3	452757	510
		e4	452758	549
		e5/6	452759	589
		e7	452760	592
		e8	452761	476
		e9	452762	512
		e10	452763	523
		e11	452764	654
		e12	452765	419
CYP3A4	7	e13a	452766	669
		e13b	452767	791
		e1	452768	589
		e2	452769	419
		e3	452770	577
		e4	452771	527
		e5a	452772	649
		e5b	452773	695
		3' UTR	452774	756

6.5 DNA screening

DNA from the Coriell CEPH/Utah reference family collection (<http://locus.umdj.edu/ccr>) was used as template for the generation of exon specific PCR products. A summary of the 47 DNAs used, which represent the founders of the collection, are listed in table 6.2. The pedigree from which one of the DNA originated, CEPH/Utah pedigree 1333 (red underline), is shown in figure 6.3. All individuals used in this study are Caucasian and of Northern European extraction.

Table 6.2: A summary of the CEPH/Utah DNA used for the generation of exon sequence. The maternal grandmother DNA listed in red was not used in this study.

Family ID	Paternal Grandfather	Paternal Grandmother	Maternal Grandfather	Maternal Grandmother
1331	NA07007	NA07340	NA07016	NA07050
1333	NA07049	NA07002	NA07017	NA07341
1341	NA07034	NA07055	NA06993	NA06985
1346	NA12043	NA12044	NA12045	NA12046
1347	NA11879	NA11880	NA11881	NA11882
1362	NA11992	NA11993	NA11994	NA11995
1408	NA12154	NA12236	NA12155	NA12156
1416	NA12248	NA12249	NA12250	NA12251
1423	NA11917	NA11918	NA11919	NA11920
1334	NA12144	NA12145	NA12146	NA12239
1340	NA06994	NA07000	NA07022	NA07056
1420	NA12003	NA12004	NA12005	NA12006

CEPH/Utah Pedigree 1333

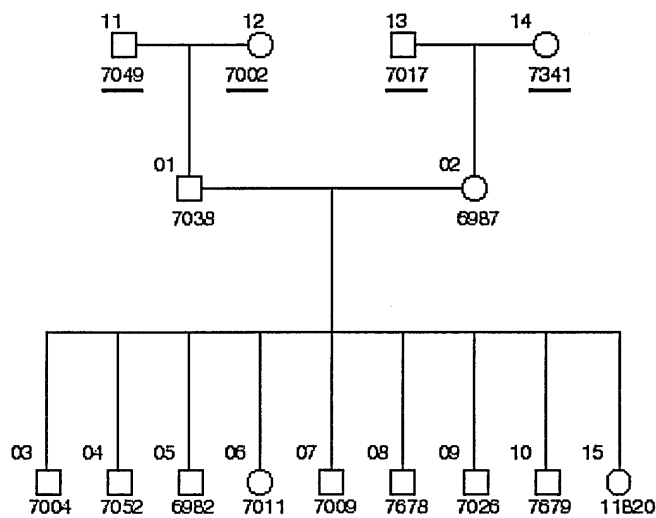


Figure 6.3: A CEPH pedigree. Pedigree represents four of the DNAs used (red underlines) in the *de novo* generation of cSNPs from the CEPH/Utah family collection.

The plate format of the exon specific – CEPH DNA PCR reactions was designed so that all primer pairs were screened across four CEPH DNAs within one 384 well microtitre plate. An aliquot of PCR products from each well of the first, DNAs 1-4, and second plates, DNAs 5-8, were separated by gel electrophoresis to determine the success rate of PCR reactions prior to sequencing (by others). Figure 6.4 shows an example of the resultant PCR products separated by gel electrophoresis, generated at a T_m of 60°C from CEPH DNAs 5-8, of primer pairs designed to exons 1, 2, 3 and 4 of GSTM4. Product sizes of the three exon specific primers were shown to correspond with their estimated size from genomic sequence, 528 bp, 744 bp and 526 bp respectively, but variation in intensity and multiplicity of bands was observed.

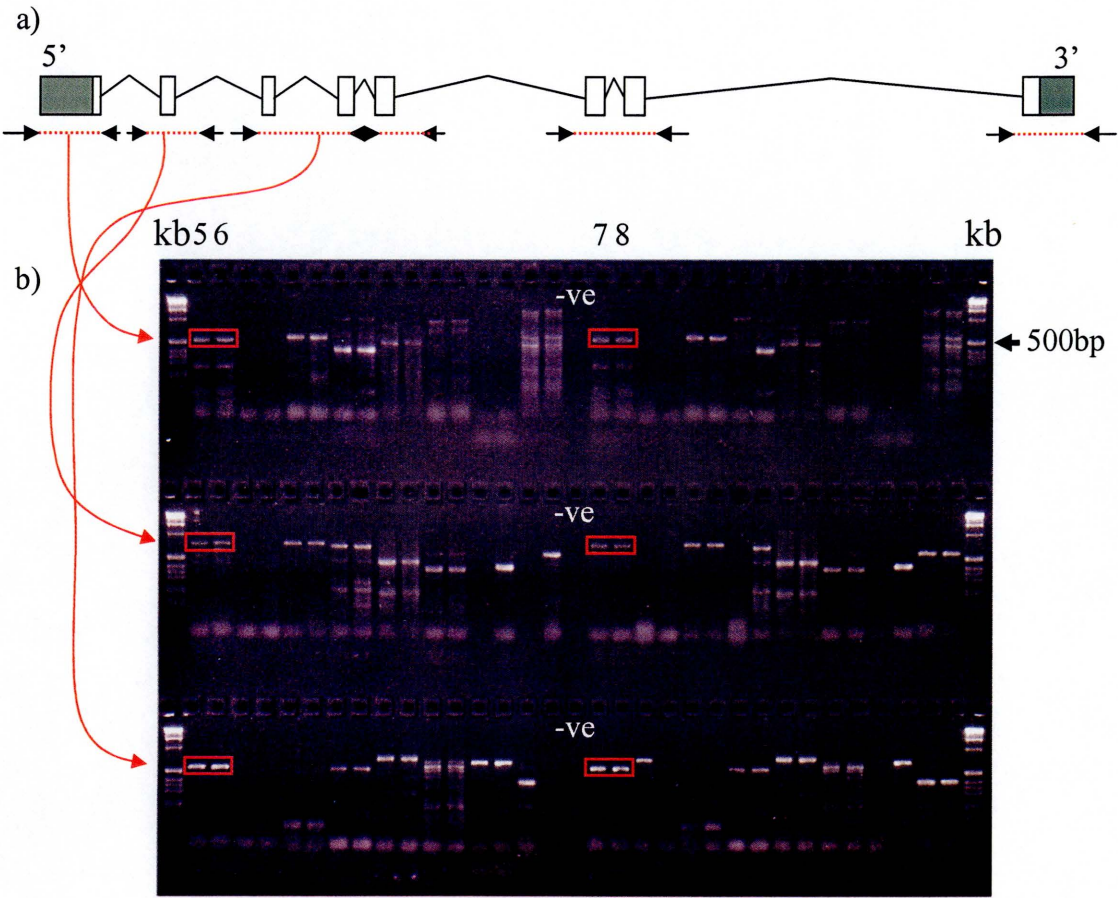


Figure 6.4: Screening of CEPH DNAs with exon specific primer pairs designed to GSTM4. a) Exon specific primer pairs were designed to an annotated gene structure of GSTM4. b) Red arrows indicate the amplification of a 500 bp product from CEPH DNAs 5 – 8 from exons1, 2, 3 and 4 at 60°C. A size marker was included to size PCR products (kb).

Initial collation of PCR results from electrophoresis of the first two plates (CEPH DNAs 1-8) indicated that well locations C7 – G7 from the primer microtitre plate (exon 5 – GSTP1, 3' UTRa – CYP1A1, exon 7 – CYP2A6, exon 4 – CYP3A4 and exon 3 – NFE2L2, respectively) consistently failed to generate a PCR product. This error was systematic (caused by blocked pins on a liquid handling robot and not through any primer design or DNA template problem) and the missing PCR reactions were repeated. In this instance, each of the 47 CEPH DNAs was tested with the missing primer pairs, in addition to two working GSTM1 primers. Repetition of 158592, 452734, 452746, 452758 and 452770 resulted in three of the five PCR reactions yielding strong single bands following electrophoresis, whilst 158592 generated multiple bands and 452734 failed to generate any product. Products from the repeated round of PCR reactions were sequenced (by others) with those generated from the initial experiment (figure 6.5a).

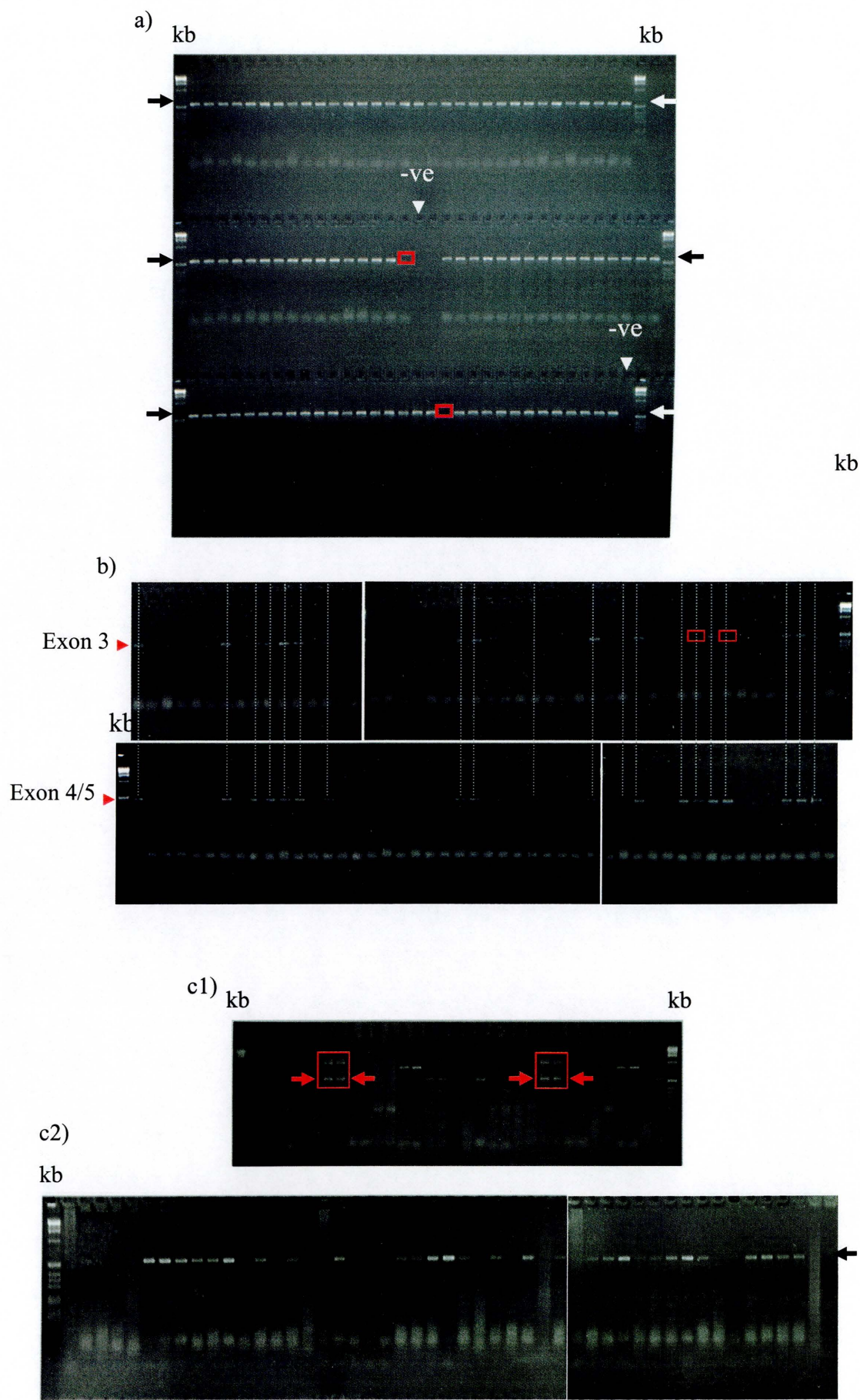
GSTM1 is known to be a null allele within 50% of the population (Board *et al.*, 1990); therefore parallel generation of PCR products from all DNAs would permit an estimation of the percentage of CEPH individuals that miss both copies of the gene. Whilst the intensity of the PCR products when assessed by agarose gel electrophoresis was faint (figure 6.5b), a reproducible relationship could be observed between the DNAs that produced a band from exon 3 and exon 4 / 5 specific primers, thereby confirming the presence of the gene in these individuals. Eighteen of the forty seven DNAs (38%) generated a PCR product for the aforementioned primers whilst a further two DNAs yielded products for one of the primer pairs. The lower observed occurrence of null alleles within the sample set (38% observed compared to 50% expected) may be due to a population bias for the occurrence of the null status of the gene within the

Northern European Caucasian population or may be due to the failure of the faint PCR products to be detected from the electrophoresis gels.

To investigate whether increasing the annealing temperature of primers during the PCR reaction would obviate the production of multiple products, six pairs of primers which generated multiple bands in the first experiment (158592, 452712, 452717, 452731, 452764 and 452767) were tested across each of the 47 CEPH DNAs at 65°C. Two of the six re-tested primer pairs yielded a strong single band following electrophoresis, whilst the remainder failed to generate any product. One of the two successful primer pairs that worked at the more stringent annealing temperature, 453731 covering the 3' end of CYP1A1 exon one, is shown in figure 6.5c. The use of a higher annealing temperatures in PCR reactions as a 'clean-up step' has subsequently been adopted by the Sanger Institute project involved with the large scale production of exon specific sequences.

Figure 6.5 (see over): PCR products from exon primers using CEPH DNA as template.

a) PCR primers from exon 4 of CYP3A4 (452758) and exon 3 of NFE2L2 (452770) screened across 47 CEPH DNAs at an annealing temperature of 60°C. Included are size markers (kb), expected PCR product sizes (black arrows) and negative controls (T_{0.1}E). DNAs for which no PCR product was generated at boxed in red. b) PCR products generated by primers designed to exons 3 and 4 / 5 and screened across 47 CEPH DNAs generated at an annealing temperature of 60°C. Dotted grey lines join CEPH DNAs that are thought to contain the GSTM1 gene. DNAs for which no PCR product was generated at boxed in red. c1) Initial screening of CEPH DNAs produces multiple bands at 60°C (red box). Increasing the stringency of primer annealing temperature to 65°C c2) results in the generation of a single PCR product (black arrows).



Analysis of the PCR reactions from the 77 primer pairs, covering 91 coding exons of the 12 target genes listed in table 6.3, revealed that 71 (92%) of primers generated bands from at least one of the eight CEPH DNAs when products were separated by gel electrophoresis. The number of working PCR assays was further reduced when primers that produced multiple bands, without the presence of a single band in one of the eight DNAs, were subtracted. These 62 assays (81% of the total) contained two primer pairs (CYP1A1 – exon 1b and GSTM5 – exon 1) for which the products were generated at a primer annealing temperature of 65°C.

Table 6.3: A summary of exon specific PCR reaction results using CEPH DNAs 1 – 8 as a template. GSTM1 – 5 coloured shading corresponding to primers in figure 6.2, the presence ‘Y’ (yellow shaded if there were multiple bands) or absence ‘N’ of PCR products upon gel electrophoresis is listed under the CEPH DNA columns. Pink shading indicates products generated at an annealing temperature of 65°C. Grey box, CEPH DNA 3, indicates possible degradation due to high failure rate.

CEPH DNAs										CEPH DNAs									
Target	Exon	1	2	3	4	5	6	7	8	Target	Exon	1	2	3	4	5	6	7	8
GSTM4	e1	Y	Y	N	N	Y	Y	Y	Y	CYP1A1	e1a	Y	Y	Y	Y	Y	Y	Y	Y
	e2	N	N	N	Y	Y	Y	Y	Y		e1b	Y	Y	Y	Y	Y	Y	Y	Y
	e3/4	N	N	Y	Y	Y	Y	Y	Y		e2/3/4	Y	Y	Y	Y	Y	Y	Y	Y
	e5	N	N	N	Y	Y	Y	N	Y		e5/6	N	N	N	N	N	N	N	N
	e6/7	N	N	N	Y	Y	Y	Y	Y		3' UTRa	N	N	N	N	N	N	N	N
	e8	N	N	N	Y	Y	Y	Y	Y		3' UTRb	Y	Y	Y	Y	Y	Y	Y	Y
GSTM2	e1	N	N	N	Y	Y	Y	Y	Y	CYP1A2	e1a	Y	Y	N	Y	Y	Y	Y	Y
	e2										e1b	Y	Y	N	Y	Y	Y	Y	Y
	e3/4	N	N	N	Y	Y	Y	Y	Y		e2/3	Y	Y	N	Y	Y	Y	Y	Y
	e5	N	N	N	Y	Y	Y	Y	N		e4	Y	N	Y	N	Y	N	Y	N
	e6/7	N	N	Y	Y	Y	Y	Y	Y		e5	Y	Y	N	Y	Y	Y	Y	Y
	e8										e6	Y	Y	Y	Y	Y	Y	Y	Y
GSTM1	e1	Y	N	N	N	N	N	Y	Y	CYP2A6	e1/2	Y	Y	Y	Y	Y	Y	Y	Y

	e2	Y	N	N	N	Y	N	Y	N		e3/4	Y	Y	N	Y	Y	Y	Y	Y
	e3	Y	N	N	N	N	N	Y	N		e5	Y	Y	N	Y	Y	Y	Y	Y
	e4/5	Y	N	N	N	N	N	Y	N		e6	Y	Y	Y	Y	Y	Y	Y	Y
	e6/7	Y	N	N	N	N	N	Y	N		e7	Y	Y	Y	Y	Y	Y	Y	Y
	e8										e8	Y	Y	N	Y	Y	Y	Y	Y
											e9	Y	Y	Y	Y	Y	Y	Y	Y
GSTM5	e1	N	N	Y	Y	N	N	Y	Y										
	e2	Y	Y	Y	Y	Y	Y	Y	Y	CYP3A4	e1	N	N	N	N	N	N	N	N
	e3/4	Y	Y	N	Y	Y	Y	Y	Y		e2	Y	Y	Y	Y	Y	Y	Y	Y
	e5	Y	Y	N	N	Y	Y	N	N		e3	Y	Y	Y	Y	Y	Y	Y	Y
	e6/7	Y	Y	N	Y	Y	Y	Y	Y		e4	Y	Y	Y	Y	Y	Y	Y	Y
	e8	Y	Y	N	Y	Y	Y	Y	Y		e5/6	Y	Y	N	Y	Y	Y	Y	Y
											e7	Y	Y	N	Y	Y	Y	Y	Y
GSTM3	e1	Y	Y	Y	Y	Y	Y	Y	Y		e8	Y	Y	Y	Y	Y	Y	Y	Y
	e2/3	Y	Y	N	Y	Y	Y	Y	Y		e9	Y	Y	Y	Y	Y	Y	Y	Y
	e4/5	Y	N	N	N	Y	N	N	N		e10	Y	N	Y	N	Y	N	Y	N
	e6/7	Y	Y	Y	Y	Y	Y	Y	Y		e11	N	N	N	N	N	N	N	N
	e8	Y	Y	N	Y	Y	Y	Y	Y		e12	N	Y	Y	Y	Y	Y	N	Y
											e13a	Y	Y	N	Y	Y	Y	Y	Y
GSTP1	e1	N	N	N	N	N	N	N	N		e13b	Y	Y	Y	Y	Y	Y	N	Y
	e2	N	N	N	N	N	N	Y	Y										
	e3	Y	Y	Y	Y	Y	Y	Y	Y	NFE2L2	e1	N	Y	N	N	N	Y	N	Y
	e3/4	N	N	N	N	N	N	N	N		e2	Y	Y	N	Y	Y	Y	Y	Y
	e5	Y	Y	N	N	Y	Y	N	N		e3	Y	Y	Y	Y	Y	Y	Y	Y
	e6	Y	Y	N	N	Y	Y	Y	Y		e4	Y	Y	N	Y	Y	Y	Y	Y
	e7	Y	Y	N	Y	Y	Y	Y	Y		e5a	Y	Y	Y	Y	Y	Y	Y	Y
											e5b	Y	Y	N	Y	Y	Y	Y	Y
GSTT1	e1	Y	Y	N	Y	Y	Y	N	Y		3' UTR	Y	Y	Y	Y	Y	Y	Y	Y
	e2	Y	Y	N	Y	Y	Y	N	Y										
	e3	Y	N	Y	N	Y	N	N	Y										
	e4	Y	Y	Y	Y	Y	Y	N	Y										
	e5	Y	Y	Y	Y	Y	Y	N	Y										

6.6 Sequence generation and assembly

Dye-terminator sequencing, using exon specific primers and PCR products is described in section 6.5, was carried out by Sarah Lindsay and the high throughput sequencing facility at the Sanger Institute. PCR products were sequenced and then run on ABI 3700 and 3730 sequencing machines. Bases within sequence reads were ‘called’ using Phred (Ewing *et al.*, 1998) and assembled within Phrap (Ewing *et al.*, 1998) utilising, amongst other criteria, Phred assigned base-quality values (Q-values). Sequence reads were assembled and imported into gene specific directories by Sarah Hunt. Vector masked and quality clipped sequences reads, together with the consensus sequence, were viewed within gene specific Gap4 (Bonfield *et al.*, 1995) databases.

Genomic coverage of the assembled exon specific sequence contigs was determined within the respective ACeDB databases by exact alignment of 10 – 15 good quality bases (light sequences within the assembled contig, figure 6.6) from either end of a sequence assembly. The number of reads contained within an assembly was determined to be the total number of reads contained within a sequence contig.

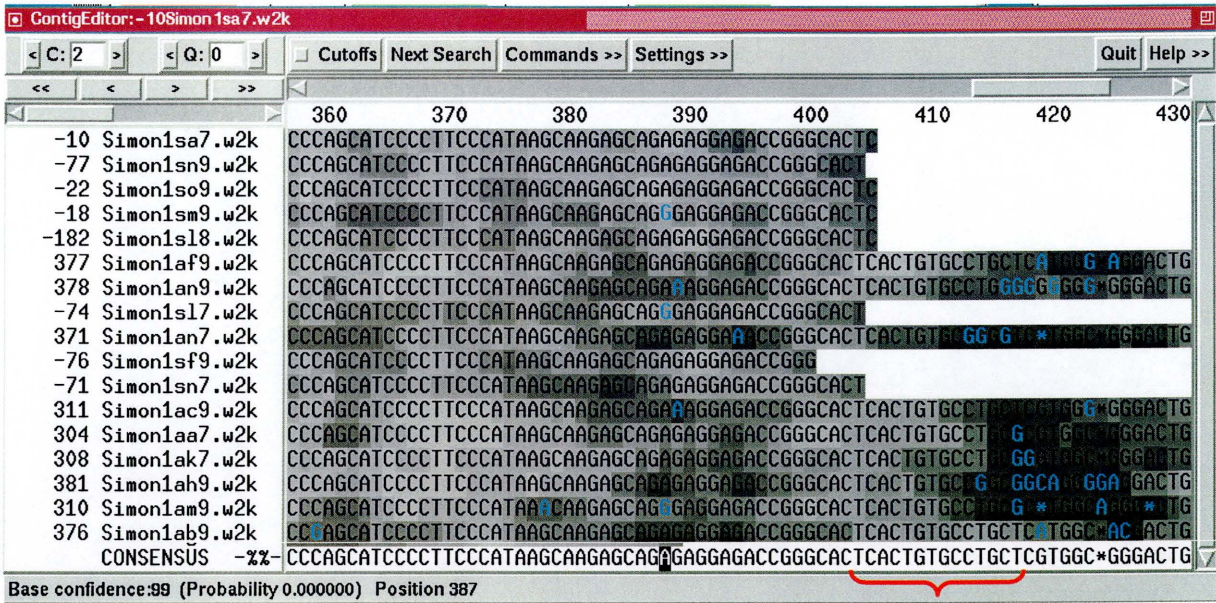
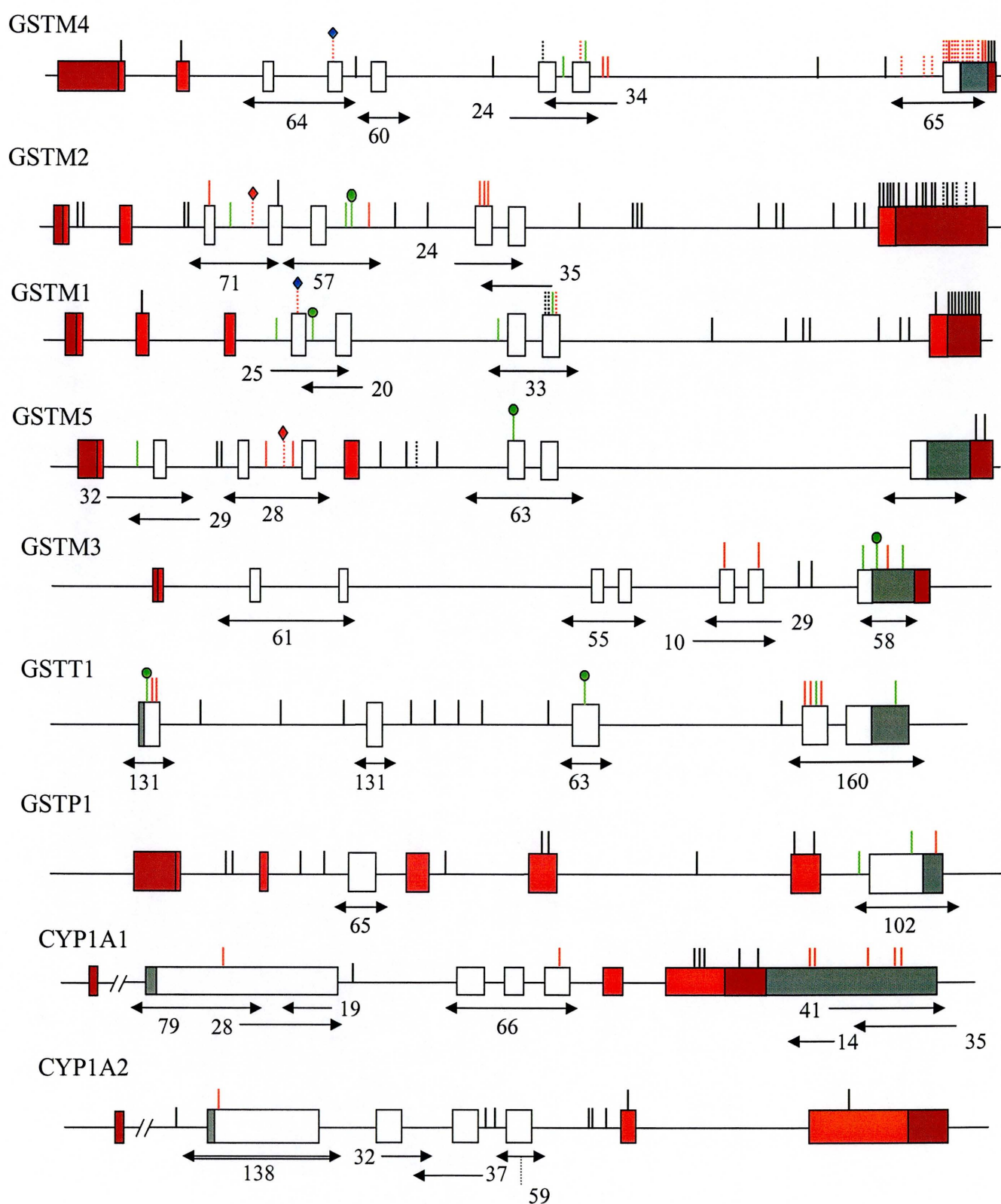


Figure 6.6: Assembly of *de novo* exon specific sequences shown in Gap4. Red brackets indicate the consensus sequence that was used to determine the extent of sequence coverage by alignment within 1ace.

6.7 Exon coverage of sequence contigs

A minimum of ten good quality sequence reads, including both sense and anti-sense reads, was used as the criteria for determining whether *de novo* sequence had successfully been generated to identify known and novel SNPs within an exon. Fifty six of the 77 initial primer pairs (73%) provided data which could be assembled into sequence contigs using the above criteria. This represents 79% of primer pairs excluding those for which PCR assays failed to produce a product. These 56 sequence contigs account for 67 of the 91 exons (74%) from the 12 target genes. Sequences derived from 17 (30%) of the PCRs were assembled separately as groups of sense or anti-sense reads. These were paired up and counted as a single contig when calculating coverage figures.



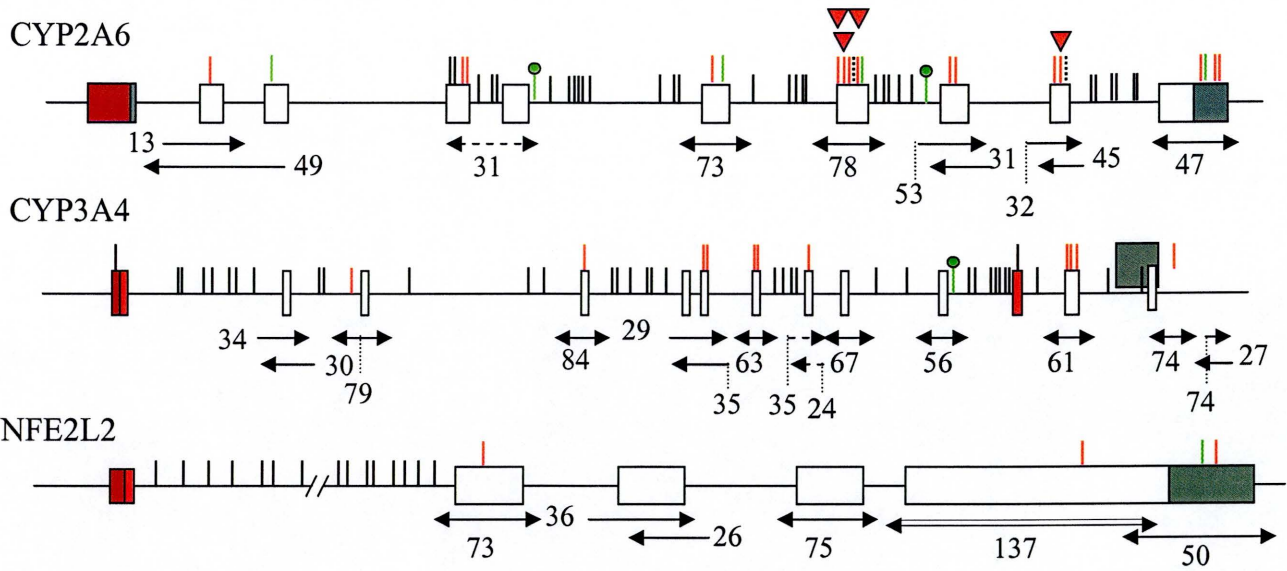


Figure 6.7: A summary representation of the *de novo* sequence coverage of exons from the target genes. Clear and grey boxes represent *de novo* sequence coverage of exons and untranslated region, respectively (not drawn to scale); exons and UTR without sequence coverage are red and dark red, respectively. Double headed arrows indicate sequence from both primer pairs assembled into one contig (number indicates the total number of reads assembled); single headed arrows specify assembly of sequence from one primer; double lined arrows are where four primers have been assembled. Black vertical lines represent known SNPs not covered by sequence coverage; black dotted vertical lines indicate where the flanking sequence from the known SNP did not align to genomic sequence; red vertical lines are known SNPs not identified by this study; vertical red dotted lines are known SNPs with multiple loci within genomic sequence (red and blue diamonds denote where extended genomic flanking sequence alignment was required to localise the SNP); green vertical lines are known SNPs found within *de novo* sequence; green vertical lines with round heads are novel SNPs identified here.

6.7.1 Validation and localisation of known SNPs

One hundred and three (35%) of the two hundred and ninety one known SNPs, which are derived from dbSNP (<http://www.ncbi.nlm.nih.gov/SNP/index.html> URL), and localised to the 12 genes of interest within Ensembl (<http://www.ensembl.org/>), are covered by the *de novo* sequence contigs (figure 6.8a). To assess whether these SNPs were present within annotated gene structures the known SNPs, and their flanking sequence, were aligned to the genomic sequence within respective ACeDB databases. This alignment identified 17 SNPs which are primarily found within GSTM4, but also localised to multiple genes and 8 SNPs for which the submitted sequence could not be found when carrying out the alignment using 15-20 bp either side of the SNP, including each allele in the search.

The remaining 76 known SNPs were localised along with their flanking sequence within the *de novo* sequence contigs by sequence matching within respective Gap4 databases. Each read of the assembled sequence contigs were then checked manually for the presence or absence of the relevant SNP allele, in either homozygous or heterozygous form (figure 6.8c). An important consideration when identifying known SNPs within the sequence assembly was the orientation of the sequence contig relative to the forward or reverse read data associated with the submitted SNP. The majority, 59 (78%), of the 76 uniquely localised known SNPs were not found within the CEPH DNAs tested here. Of the remaining 17 SNPs (22%), 8 were determined to be located within coding sequence, and 9 were located within non-coding sequence.

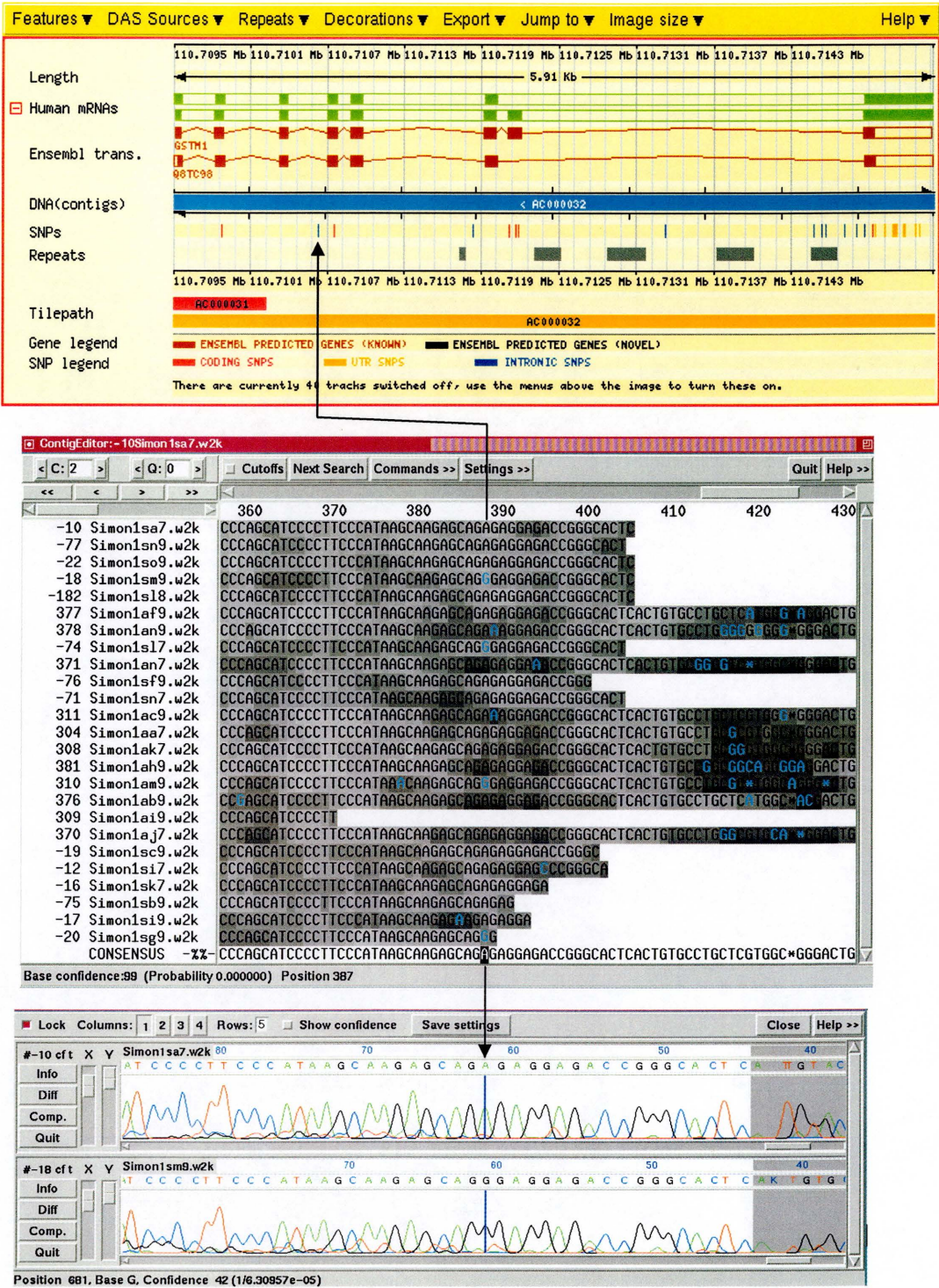


Figure 6.8: Identification of a known SNP which is within intron 3 of GSTM1.

Represented is the known SNP within Ensembl, a), the specific nucleotide position within a sequence assembly displayed in a Gap4 database, b), and the homozygous sequence reads for each allele.

6.7.2 Identification of novel SNPs

To more readily identify novel SNPs within assembled Gap4 sequence contigs the quality value of the reads was converted into grey-scale and the ambiguous base calls, and potential novel SNPs, were coloured blue (figure 6.8b). Ambiguous bases were then checked manually within all traces. A putative novel SNP was identified when the base containing the homozygous minor allele had a quality value of 30 (Q-30) or the heterozygote, containing both alleles, was surrounded by bases with > Q-30 quality values. Nine novel SNPs, three of which were located within coding sequence, were identified within the 12 target genes. Additional support for a novel SNP was obtained by checking the reverse read for each read pair. A breakdown of known and novel SNP numbers are listed in table 4 whilst a summary of the placement of all SNPs within annotated gene structures can be found in figure 6.7.

Table 6.4: A summary of the known and novel SNPs associated with 12 target genes.

Gene	Known SNPs	With Seq Coverage	Uniquely Assigned	Align to Genomic	Not Observed	Observed	Coding	Novel	Coding
GSTM4	32	23	8	7	5	2	1	0	-
GSTM2	43	8	7	7	5	2	-	1	-
GSTM1	26	7	5	3	-	3	1	1	-
GSTM5	12	4	4	3	2	1	-	1	1
GSTM3	7	5	4	4	3	1	1	1	-
GSTP1	13	3	3	3	1	2	1	0	
GSTT1	16	7	7	7	5	2	1	2	2
CYP1A1	13	7	7	7	7	0	-	0	-
CYP1A2	9	1	1	1	1	0	-	0	-
CYP2A6	54	23	23	19	16	3	3	2	-
CYP3A4	47	11	11	11	11	0	-	1	-
NFE2L2	19	4	4	4	3	1	-	0	-
TOTAL	291	103	84	76	59	17	8	9	3

6.8 SNP Analysis

Under conditions of random mutation it is expected that half as many nucleotide transitions occur (purine→ purine or pyrimidine→pyrimidine) as transversions (pyrimidine↔ purine), table 6.5 (Dawson *et al.*, 2001). In addition, as the strand on which the change has occurred is unknown, no distinction can be made between A↔G and C↔T and between C↔A and G↔T. Analysis of 28 SNPs contained within this data set revealed that 19 transitions (68%) occur approximately twice as often as 9 transversions (32%) (table 6.6). The observed contradiction to the expected frequency has previously been reported (Horton *et al.*, 1998; Dawson *et al.*, 2001; Halushka *et al.*, 1999, Deutsch *et al.*, 2001). A possible reason for the occurrence of an increased number of C↔T (G↔A) transversions may be due to the deamination of 5-methylcytosine that occurs frequently at CpG dinucleotides.

Table 6.5: Expected occurrence of transitions and transversions in genomic sequence.

	A	T	C	G
A	-			
T	Transversion	-		
C	Transversion	Transition	-	
G	Transition	Transversion	Transversion	-

Table 6.6: The observed number of transitions and transversions of known and novel SNPs within the 12 target genes.

Variation	Number	Percentage
C↔T (G↔A)	19	68.00%
Transitions	19	68.00%
C↔A (T↔G)	6	21.00%
C↔G	3	11.00%
A↔T	-	-
Transversions	9	32.00%

Of the 28 detected novel and known SNPs, 12 were localised to introns, 5 to 3' untranslated regions, whilst 11 occurred within exons (table 6.7). Seven of the 11 coding SNPs resulted in synonymous changes, i.e. maintaining amino acid type by codon usage, whilst the remaining four SNPs resulted in an amino acid change. Each of the four amino acid changes were caused by substitutions in the first base of the codon, two of which resulted in a conservative change (maintaining a similar amino acid type, for example valine to an isoleucine change maintains an aliphatic, hydrophobic amino acid) and the remaining two changes were non-conservative changes.

Table 6.7: Exonic SNP analysis.

Gene	Exon	Position	Allele change	Codon change	Encoded a. a.	Synon	Cons
GSTM4	7	78	C ↔ T	TTT ↔ TTC	phe ↔ phe	yes	-
GSTM1	7	72	C ↔ T	GAC ↔ GAT	asp ↔ asp	yes	-
GSTM5	6	22	T ↔ C	TTG ↔ CTG	leu ↔ leu	yes	-
GSTM3	8	91	G ↔ A	GTA ↔ ATA	val ↔ iso	no	yes
GSTT1	1	13	C ↔ T	CTG ↔ TTG	leu ↔ leu	yes	-
GSTT1	3	110	A ↔ C	ACG ↔ CCG	thr ↔ pro	no	no
GSTT1	4	155	G ↔ A	GTA ↔ ATA	val ↔ iso	no	yes
GSTP1	7	111	A ↔ C	AGT ↔ ACT	ser ↔ ser	yes	-
CYP2A6	2	37	T ↔ C	TTG ↔ CTG	leu ↔ leu	yes	-
CYP2A6	5	117	C ↔ T	CGC ↔ CGT	arg ↔ arg	yes	-
CYP2A6	6	100	C ↔ T	CGC ↔ TGC	arg ↔ cys	no	no

6.8.1 Validating SNPs within highly homologous genes

One of the difficulties encountered whilst identifying valid SNPs associated with GSTM 1- 5 paralogues was to determine whether a SNP was valid (i.e. two allelic variants at the same locus) or merely the alignment of two locus specific base pair variants, one from each of two closely related gene family members. A comparison between the

known SNPs localised to GSTM 1 – 5 and the number which were uniquely placed (columns 2 and 4 in table 6.4) indicates the scale of the problem that was encountered, i.e. 65% of GSTM1 SNPs that had *de novo* sequence coverage localised to other GSTM loci. Three criteria were used to assist with the elucidation of a valid candidate SNP from locus specific variants of paralogous genes; 1) the SNP must be found within *de novo* sequence traces, 2) it must be in Hardy-Weinberg (H-W) equilibrium (i.e. allele 1 = p and allele 2 = q, $p^2 + 2pq + q^2 = 1$) and 3) the alternative allele should not be present as a base variant in a paralogous gene. Valid SNPs were divided into ‘known’, i.e. those that have a dbSNP entry, and ‘novel’, i.e. those identified in this study. ‘Suspect candidate’ SNPs fulfilled criteria 1) and 2) but the alternate SNP allele was be present within a homologous gene. ‘Rejected candidates’ are not observed in sequence traces (due to BLAST alignment of the flanking sequence of a SNP from a closely related gene family member), the alternative allele was present within paralogues and it was not in H-W equilibrium. The observed occurrence and genic location of known, novel, suspect and rejected GSTM 1 – 5 SNPs is shown in table 6.8.

Table 6.8: Summary of categorised GSTM 1 – 5 SNPs.

Status	Exon	Intron	3' UTR	Total
Known	1	4	2	7
Novel	-	3	-	3
Suspect	3	1	-	4
Rejected	6	3	9	18

6.8.2 Validating SNPs

6.8.2.1 Known SNPs

The presence of a valid known SNP was easily detected once its location within the *de novo* sequence contig had been identified using flanking sequence matches within the respective Gap4 database. The alternative minor allele, even when present as a heterozygote, was clearly discernable within good quality sequence. An additional example of a known SNP, dbSNP: 737497, is shown in figure 6.9. The SNP was found within the *de novo* sequence as a homozygote in major and minor alleles and localises to intron 3 within GSTM1. The T233C SNP was submitted to dbSNP by The SNP Consortium (TSC). The orientation of the flanking sequence had been designated as a forward read within dbSNP. However, integration of the cosmids (from which the SNP was derived) within the minimum tile path (chapter 4) indicated the submission, and therefore the SNP alleles, was in the wrong orientation. The allele frequency of the major and minor alleles, with Q-values >30, was 0.75 and 0.25, respectively, from 24 chromosomes sampled. The SNP was also in H-W equilibrium.

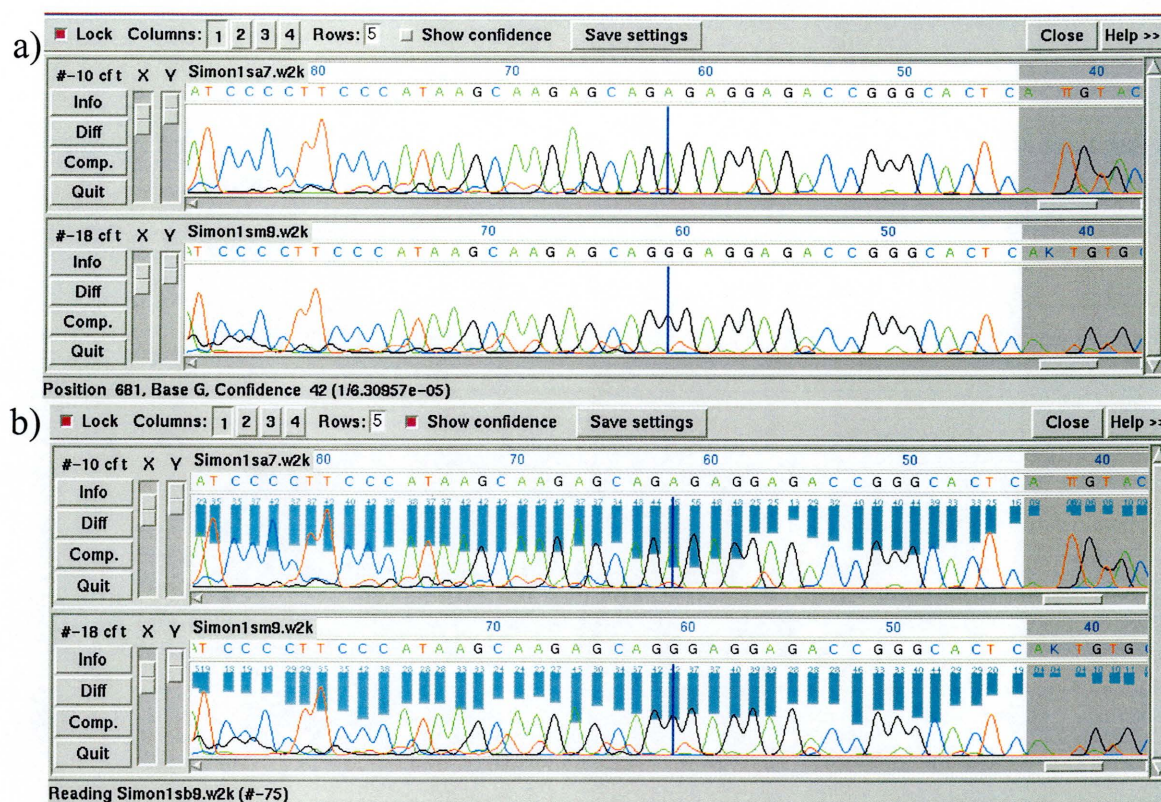


Figure 6.9: The identification of a known T/C SNP, dbSNP: 737497. a) Assembled GAP4 traces used to identify this SNP are displayed in the reverse orientation. The top trace is the homozygous major allele and the bottom trace is the homozygous minor allele. b) Q-values associated with the SNP nucleotides.

6.8.2.2 Novel SNPs

Novel SNPs were validated using support from the base quality values, either of the homozygote minor allele or of the surrounding bases for a heterozygote allele. Where possible, SNPs were verified within reverse reads. All novel SNPs that were identified as part of this study were in HW equilibrium. Figure 6.10 is an example of a novel A152C SNP localised to intron 5 of GSTM2 and identified in the opposite orientation. Allele frequencies of the major (0.96) and minor (0.4) alleles were determined from a sample of 48 chromosomes.



Figure 6.10: A novel A/C SNP identified within intron 3 of GSTM2. a) Assembled Gap4 traces for the homozygous major allele, top trace, and the heterozygous minor allele, bottom trace (in the reverse orientation). b) Assembled traces (from 6.10a) with associated Q values.

6.8.2.3 Suspect candidate SNPs

Within Ensembl, dbSNP entries 1056806 and 506008 were localised to exon 7 of GSTM1 and 4 in positions 72 and 78, respectively. These two SNPs were also localised within GSTM1 and GSTM4 in dbSNP. Alignment of the SNPs within the coding sequence, figure 6.11, revealed that the minor allele, T at position 72 and C at position 78, was present within other gene family members. Therefore, it was uncertain if these

suspect SNPs were valid, or were incorrectly aligned to the genomic sequence. Errors associated with SNPs that have been identified by sequence based detection may arise from; re-sequencing without careful selection of primers; lesser quality shotgun sequencing and subsequent alignment of the genomic read; the alignment of the SNP derived reference sequence to more than one genomic position. The positions of dbSNP:1056806 and dbSNP:506008 were localised within the assembled sequence contigs of exon 7 in GSTM1 and GSTM4. Analysis of the sequence traces at positions 72 and 78 revealed that major and minor alleles could be identified therefore satisfying criteria 1), however detailed analysis of the flanking sequence for each SNP uniquely assigned 1056806 to GSTM1 and 506008 to GSTM4. Having determined that, within the data set described here, the two SNPs belonged to different genes, the allele frequencies and H-W equilibrium were calculated (therefore satisfying criteria 2). The allele frequencies of dbSNP:1056806 were 0.58 and 0.42, whilst the frequencies of dbSNP:506008 were 0.85 and 0.15. Both loci were determined to be in H-W equilibrium.

Having proven, within this data set, the SNPs were locus specific, there remains the possibility the minor allele may have arisen from the production of sequence from a mispriming event of a gene family member. Whilst there is a high degree of sequence conservation within exon 7 there are single base variants between loci which should be present in the sequence traces if the primers had misprimed. The bases of the alternative alleles, located at positions 28, 68, 80 and 85 of figure 6.11, should be present as heterozygous alleles in all traces. Analysis of the sequence failed to show any bi-allelic reads at these positions therefore supporting the unique assignment of the two submitted SNPs

Figure 6.11: The alignment of coding sequence for the GSTM1 – 5 genes using ClustalW and representation within GeneDoc. Exons are alternatively coloured light blue and grey. Red boxes denote the position of SNPs dbSNP:1056806 and dbSNP:506008 at positions 72 GSTM1 and position 78 GSTM4, respectively. Dotted red boxes indicate nucleotide variants between genes which permitted that unique assignment of the two SNPs.

6.8.2.4 Rejected candidate SNPs

The identification of SNPs by mRNA BLAST alignment to genomic sequence can erroneously localise SNPs within highly homologous genes. Seventeen GSTM SNPs with *de novo* sequence coverage were rejected as candidate SNPs within this study because they could not be uniquely placed by genomic alignment within a chromosome specific ACeDB. Thirteen of these SNPs could not be uniquely assigned due to the failure of two of the five paralogous genes to generate 3'UTR sequence (to which the majority of ambiguous matches aligned). Detailed analysis of one of the remaining four rejected candidates, dbSNP: 3211191, which localised to exon 4 of GSTM1 and GSTM4 (blue diamond in figure 6.7), indicated that exact sequence alignment of 20 bp either side of the SNP failed to align uniquely assign it to either individual GSTM gene. There was 100% sequence homology extending for 58 bases 5' and 41 bases 3' of the SNP into intron 3 and intron 5, respectively. The observation of a single base difference between the two genes, in the present study, allowed assignment of the read and therefore the SNP to GSTM4. A second SNP that failed to localise to a unique position by sequence matching was dbSNP: 402505. The SNP was located within intron 3 of GSTM2 and 5. It had 100% homology both 5' and 3' of the SNP but nucleotide

differences at 155 bases 5' and 46 bases 3' of the SNP, from the present study, permitted assignment of the SNP to GSTM5. The remaining two of the seventeen unlocalised SNPs were rejected on based upon similar arguments to those examples described above.

6.8.3 Effect of sequence variation upon gene structure

A novel SNP, identified within the *de novo* sequence of GSTT1, provided the opportunity to examine the effects allelic variation may have upon the translated amino acid sequence and protein structure. The protein encoded by GSTT1, like the GSTM family members, is a phase 2 enzyme that detoxifies carcinogenic metabolites, for example halomethanes, by conjugation of glutathione which changes the polarity of the metabolite making them more readily excreted (Mannervik *et al.*, 1988).

It has previously been shown that the GSTT1 gene is absent from 38% of the population (Pemble *et al.*, 1994). Analysis of the set of DNAs examined in this study indicated that only 1 of 8 CEPH DNAs tested, NA07017, failed to generate a PCR product from any primer pair of the 5 exons from the gene. The lower observed null percentage (13%) compared to that previously reported may relate to the small sample set tested.

The novel A110C SNP, within exon 3 of GSTT1, results in a first base substitution of amino acid 104 causing a non-synonymous, non-conservative change of a threonine to a proline (Thr104-Pro). Threonine is an aliphatic amino acid that has a neutral side chain whereas proline is an amino acid with a secondary group. Alignment of the protein domain containing the single nucleotide polymorphism was performed within PFAM

(<http://www.sanger.ac.uk/Software/Pfam/>). Of the 751 proteins that have conserved homology to the domain encoding the Thr104 – Pro nucleotide variant none contain a proline at position 104. This suggests that the protein conformation resulting from the non-synonymous, non-conservative SNP is not usually assumed by GSTT1 or any closely related protein domain. A homologous protein with an elucidated 3-D structure was identified within PDB by sequence alignment to investigate what effect the SNP may have upon the conformation of GSTT1. 3LJR, whose 3-D structure as a dimer conjugated with glutathione substrate was elucidated by X-ray diffraction, is a glutathione S-transferase family member, GSTT2, that shows a 55% sequence homology with GSTT1 (figure 6.12). The substitution Thr104 to Pro in GSTT1 corresponds to Asp104 to Pro in 3LJR. Viewing the elucidated 3-D structure within ICMLite (<http://www.molsoft.com/products/icmlite.htm>, Abagyan *et al.*, 1994) (with assistance from Robert Steward) shows Asp104 is at the C-terminal of an α -helix and shares a hydrogen bond with Trp101. This hydrogen bond cannot exist with a Pro substitution, since the Pro residue is cyclic with no free NH group. The loss of this hydrogen bond by an introduction of a Pro may destabilise the 3D conformation of the protein (Karvonen *et al.*, 1998).

The substitution of a proline at amino acid position 104 may have a significant affect upon the function of the protein as Asp 104 (in 3LJR) conjugates with the glutathione substrate within the other subunit of the homodimer. The structural affect the proline substitution may also be important as an adjacent residue, Arg 107, interacts with the glutathione substrate on the same subunit (figure 6.13). Therefore a change in geometry caused by Thr104 – Pro may effect the conformation of active site binding residues (thereby effecting protein function). Further experimental studies would be required to

determine whether the introduction of a Pro at amino acid position 104 would affect GSTT1 enzyme function when conjugating glutathione as a homodimer.

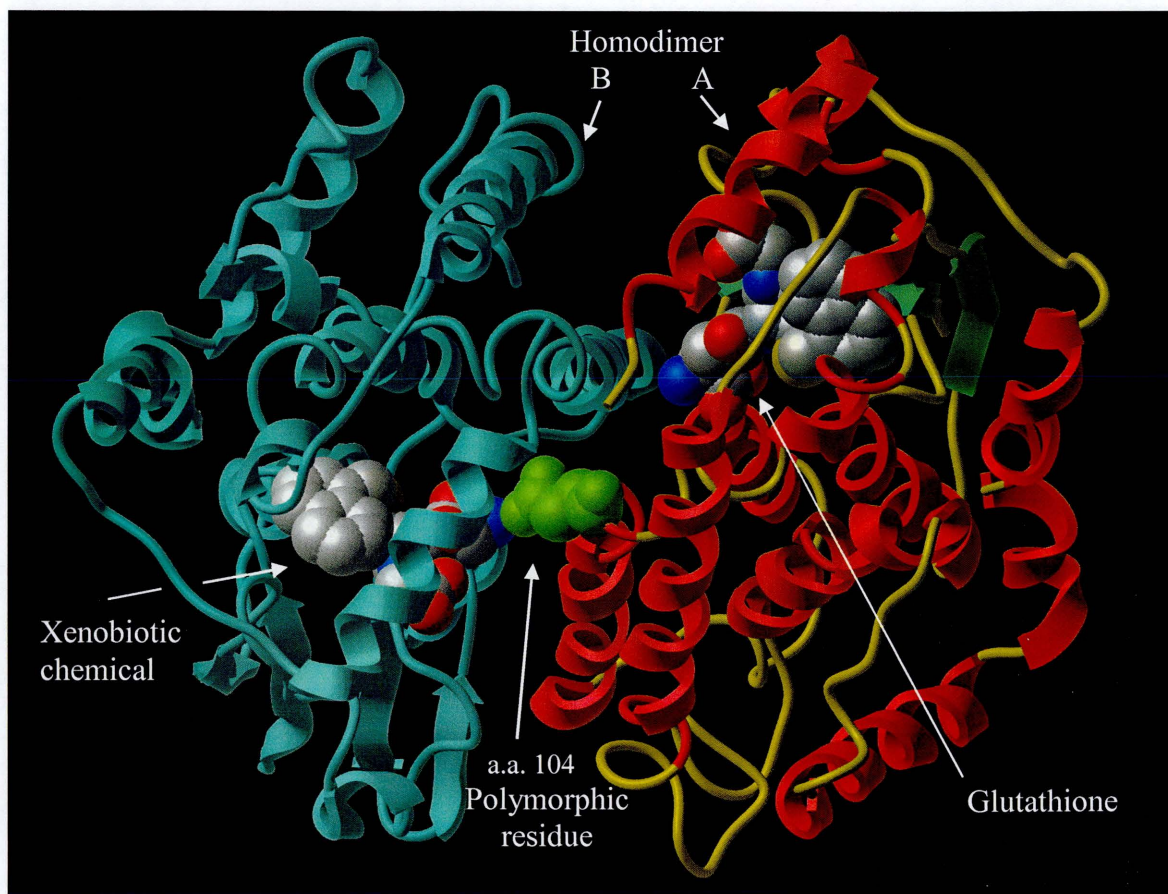


Figure 6.12: A 3-D representation within ICMLite of the homodimeric GST model, 3LJR. The model was used to interpret the effect that a novel cSNP within GSTT1 may have upon the structure of the protein. Shown are the two GST units that form the dimer (yellow/red and green) conjugated with glutathione and xenobiotic biochemicals. The polymorphic Asp104Pro residue is drawn in green at the C-terminal of an α -helix.

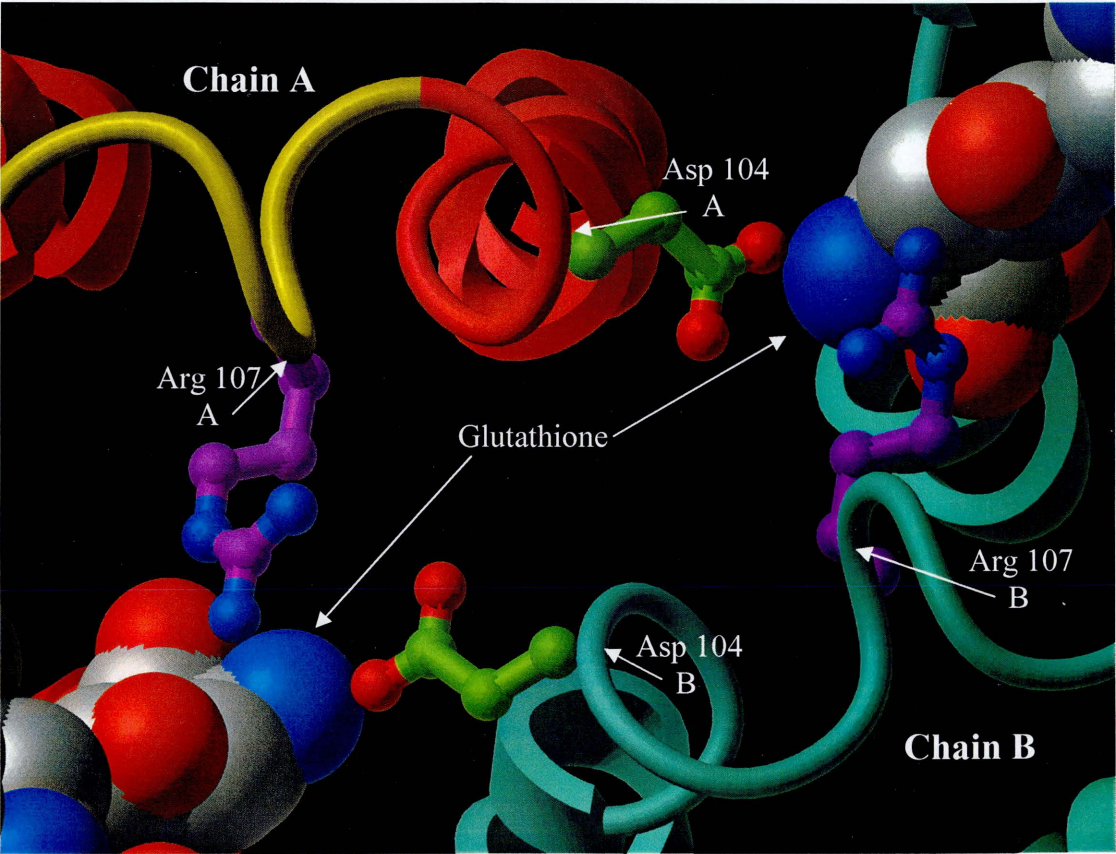


Figure 6.13: A vertical cross-sectional view of glutathione conjugating amino acid residues of 3LJR. Polymorphic amino acid residue, Asp 104, conjugates with the glutathione molecule on the opposite chain in the homodimer, chain B. Arg107 on chain A conjugates with glutathione residue within the same chain. The conformation of the dimer means that hydrogen bonding conjugation is reciprocated between dimers.

6.9 Discussion

Novel sequence coverage has been generated for 77 (85%) exons from 12 genes that has identified 17 known and 9 novel SNPs. Exon specific primers were designed within highly homologous glutathione-S-transferase Mu 1 – 5 paralogous genes and seven other genes of medical interest to facilitate the unique assignment of known and identify novel SNPs.

The unambiguous localisation of SNPs within genomic sequence is central to determining the biological effects of coding SNPs or to their use in the construction of haplotype maps. Two known SNPs, with multiple loci according to the Ensembl genome database, were uniquely localised with sequence contigs assembled from the GSTM exon specific PCR products. A further 2 known SNPs with multiple loci, whose placement was not resolved within *de novo* sequence contigs, were uniquely assigned by sequence alignment of extended flanking sequence within an ACeDB database.

Fifty five of the 291 known SNPs localising to the genes in this study were not detected within exon, and partial flanking intron, specific sequence contigs. The absence of these SNPs does not necessarily mean that they are false but may instead be attributed to the ethnicity of the population from which the SNP was derived being different to the population tested here. Alternatively, the number of chromosomes contained within the reads of the sequence assembly may not be sufficient to detect the SNP if it has a low minor allele frequency (in this study, it would be unlikely for a minor allele of around 1% or less to be detected).

Eight known SNPs covered by *de novo* sequence failed to align to genomic sequence within genes structures in respective ACeDB databases. This may be caused by nucleotide differences within draft sequence from which the SNPs were identified (for example, dbSNP: 2545753 within exon 6 of CYP2A6) which were not subsequently present in the finished sequence. The alignment of mRNA sequence to genomic sequence to aid SNP identification may also cause inaccuracies in SNP assignment if there are errors in original mRNA sequence (for example, dbSNP: 1061604 within exon 8 of CYP2A6). In addition, if the mRNA was derived from a closely related paralogous gene, it is possible the mRNA sequence may be misaligned to the genomic sequence of a highly homologous locus.

There are approximately 60,000 coding SNPs present within the human genome (ISMWG, 2001), corresponding to 1-2 per gene per individual. However, the effect of these SNPs upon the function of genes is largely unknown. Many of these cSNPs will result in synonymous amino acid changes due to codon redundancy or conservative non-synonymous changes by the substitution of an amino acid of similar properties. However, a proportion of cSNPs will result in non-synonymous non-conservative changes that, depending on the amino acid substitution, may cause changes in the structural integrity and/or biological function of the protein. As discussed in the previous chapter, the structure, function and interaction of the majority of human gene products is largely unknown. The determination and characterisation of protein structures and the networks in which they interact, together with the elucidation of genuine SNPs within coding features will contribute to our understanding of the metabolic differences between individuals.

This chapter describes the possible effect that a non-synonymous, non-conservative coding SNP, Thr104 – Pro, may have upon the structure and function of the GSTT1 protein. Since this work, discovery of the same SNP in a Swedish population has been published (Alexandrie *et al.*, 2002). Experimental investigation by Alexandrie *et al.*, (2002) has confirmed that the variant does indeed have a functional consequence. The so-called GSTT1*B allele was reported as having a frequency of 0.05 in Swedish Saamis, the same as observed within the CEPH DNAs used here. An ELISA assay showed that a stable protein product was not produced by individuals who had previously been genotyped as non-conjugators, lacking a GSTT1 protein that could functionally conjugate methyl chloride. Western blot analysis was also used to determine that the functional protein was absent within erythrocyte lysates from non-conjugating individuals. The association of the GSTT1*B, allele in conjunction with the functional GSTT1*A or the null GSTT1*0 allele, may explain why individuals that were previously thought to produce functional copies of the GSTT1 protein are associated with the non-conjugating phenotype.

68781	68782	68783	68784	68785	68786	68787	68788	68789	68790	68791	68792	68793	68794	68795	68796	68797	68798	68799	68800	68801	68802	68803	68804	68805	68806	68807	68808	68809	68810	68811	68812	68813	68814	68815	68816	68817	68818	68819	68820	68821	68822	68823	68824	68825	68826	68827	68828	68829	68830	68831	68832	68833	68834	68835	68836	68837	68838	68839	68840	68841	68842	68843	68844	68845	68846	68847	68848	68849	68850	68851	68852	68853	68854	68855	68856	68857	68858	68859	68860	68861	68862	68863	68864	68865	68866	68867	68868	68869	68870	68871	68872	68873	68874	68875	68876	68877	68878	68879	68880	68881	68882	68883	68884	68885	68886	68887	68888	68889	68890	68891	68892	68893	68894	68895	68896	68897	68898	68899	68900																																																																		
68991	68992	68993	68994	68995	68996	68997	68998	68999	69000	69001	69002	69003	69004	69005	69006	69007	69008	69009	69010	69011	69012	69013	69014	69015	69016	69017	69018	69019	69020	69021	69022	69023	69024	69025	69026	69027	69028	69029	69030	69031	69032	69033	69034	69035	69036	69037	69038	69039	69040	69041	69042	69043	69044	69045	69046	69047	69048	69049	69050	69051	69052	69053	69054	69055	69056	69057	69058	69059	69060	69061	69062	69063	69064	69065	69066	69067	69068	69069	69070	69071	69072	69073	69074	69075	69076	69077	69078	69079	69080	69081	69082	69083	69084	69085	69086	69087	69088	69089	69090	69091	69092	69093	69094	69095	69096	69097	69098	69099	69100	69101	69102	69103	69104	69105	69106	69107	69108	69109	69110	69111	69112	69113	69114	69115	69116	69117	69118	69119	69120	69121	69122	69123	69124	69125	69126	69127	69128	69129	69130	69131	69132	69133	69134	69135	69136	69137	69138	69139	69140	69141	69142	69143	69144	69145	69146	69147	69148	69149	69150	69151	69152	69153	69154	69155	69156	69157	69158	69159	69160	69161	69162	69163	69164	69165	69166	69167	69168	69169	69170	69171	69172	69173	69174	69175	69176

Chapter 7

Discussion

- 7.1 Genome Mapping and Sequencing**
- 7.2 The determination of coding features**
- 7.3 Assigning gene function**
- 7.4 Sequence variation**
- 7.5 Conclusion and future work**

7.1 Genome Mapping and Sequencing

The generation of genome-wide physical maps of biologically complex organisms with large (i.e. multi-gigabase) genomes has relied upon the application of strategies developed for the characterisation of smaller (~1-100 megabase) genomes. At the time of their construction, the cosmid and lambda clone physical maps of *Caenorhabditis elegans* (*C. elegans*) (Coulson *et al.*, 1986) and *Saccharomyces cerevisiae* (*S. cerevisiae*) (Olson *et al.*, 1986), respectively, were intended to facilitate the cloning of known genes and to serve as a genomic archive. It was during the construction of these physical maps that concomitant improvements in sequencing technologies enabled a whole genome sequencing strategy to be developed. Clones from the physical map that represented the genomic archive were used as the substrate for subcloning and shotgun sequencing. As size of the clones used to construct these maps was equivalent to large viral genomes, which had already been successfully sequenced using the random shotgun approach (e.g. 48 kb bacteriophage λ (Sanger *et al.*, 1982)), it was clear that the equivalent strategy could be applied to sequencing whole genomes. The limiting factor would be the availability of a complete clone map and sufficient resources to complete the sequencing. For example, results from the *C. elegans* pilot sequencing project were published (Sulston, *et al.*, 1992) some 6 years after the physical map was reported to be 60% complete (Coulson *et al.*, 1986). The publication reported the assembly of 120 kb of completed sequence by separate shotgun sequencing of 3 selected cosmid clones (two of which overlapped) from the physical map. This report, therefore, confirmed the feasibility of this approach and the value of the map in characterising large genomes.

At this point in time, clone coverage of the human genome was limited to small YAC or bacterial clone contigs which had been constructed during positional cloning projects. The use of YACs in attempts to rapidly construct chromosome specific (Chumakov *et al.*, 1992, Foote *et al.*, 1992) and genome wide clone maps (Chumakov *et al.*, 1995, Hudson *et al.*, 1995) demonstrated that larger insert clones could be used to generate a map of the whole genome. Indeed, the adoption of YACs, which have an average insert size of 1 Mb (Chumakov *et al.*, 1995) theoretically reduced the complexity of mapping the human genome (1x coverage of 3 GB requiring approximately 3,000 clones) This approximated the complexity of the earlier work where the nematode genome was mapped using 40 kb cosmids (1x coverage of 100 Mb requiring approximately 2,500 clones). However, the instability and chimerism of YACs, in addition to the difficulties of isolating the cloned insert compared to bacterial cloning systems, meant that YACs could not practically provide a sufficiently reliable or convenient resource for the generation of genomic sequence. The development of large insert PACs (Iaonnou *et al.*, 1994) and BACs (Shizuya *et al.*, 1992) provided clones with an insert large enough to permit the feasible generation of genomic coverage (1x coverage of the human genome requiring ~25,000 clones) (as described in chapter 4) and a cloning system that was amenable to large-scale sequencing (as described in chapter 5). The development of marker-based maps using genetic, RH or YAC mapping techniques (genetic: Weissenbach *et al.*, 1992, Dib *et al.*, 1996; RH: Schuler *et al.*, 1996; Deloukas *et al.*, 1998; YAC: Hudson *et al.*, 1995; genome; Foote *et al.*, 1992; Collins *et al.*, 1995) provided the necessary long-range and independent map information to act as a framework on which bacterial clone coverage could be generated (Olson *et al.*, 1993, Bentley *et al.*, 2001). In addition, the evolution of fingerprinting techniques (Coulson *et al.*, 1986, Olson *et al.*, 1986), as described in chapter 3 (Gregory *et al.*, 1997, Marra *et*

al., 1997), provided the tools by which sequence ready bacterial clone maps of large genomes could be constructed.

The chromosome specific, clone by clone approach that the Human Genome Project utilised to generate sequence of the human genome provided a means by which the work of many separate groups could be coordinated and a method by which highly accurate genomic sequence (>99.99%) could be produced. The principles demonstrated in the nematode project (Coulson *et al.*, 1986) proved effective, and essential for the successful production of the human genome sequence. Problem solving (in particular resolution of the sequence of repeats, or technically difficult regions) was facilitated by the modular clone-based nature of the project; while long-range map information added weight to the clone order.

Celera, a private company that published a draft version of the human genome (Venter *et al.*, 2001) in parallel to the publicly funded project (IHGSC 2001), purported to have assembled the human genome exclusively by a whole genome shotgun (WGS) strategy. However, they too ultimately relied upon a clone based map by incorporating a "perfect tiling path" of the HGP data into their sequence assembly. Specifically, 10 million 'faux' reads in a regular ordered pattern were generated by dividing up the public assembly into overlapping segments of 550 bp each, thus capturing the overall synthesis of all the information used to assemble the public domain sequence. The public sequence data used by Celera was thus derived from an accurately assembled clone based physical map and effectively representing complete genomic coverage (Waterston *et al.*, 2002). Projects to sequence large genomes using a WGS strategy have also proved impossible to finish with high accuracy. This was illustrated by the reliance

upon clone based finishing of the WGS assembly for the *Drosophila* genome (Celniker *et al.*, 2002). Similarly, both the human and the mouse genome sequences are being finished using a large-insert bacterial clone based approach.

The next phase in the evolution of physical map construction was driven by the availability of ordered genomic sequence. Conservation of sequence and long range order, between organisms that are sufficiently closely related, means that the genome of one species can act as the template upon which a physical map of another can be built and, in doing so, elucidate the homologous relationship between them (Thomas *et al.*, 2002). The success of the comparative physical mapping approach was demonstrated by construction of a clone map of the mouse genome using the assembled human genome sequence as a template. In this study, human genomic sequence was used to align stringently assembled BAC fingerprint contigs by matching mouse BAC end sequences (BESs) to their corresponding locations in the human genome. Ordered and orientated contigs (previously assembled by fingerprinting) were subsequently joined following further fingerprint analysis and addition of available genetic and radiation hybrid markers. The availability of BESs from a highly redundant fingerprint assembly of BAC clones, and using the strategy outlined above, greatly simplified the process of contig assembly, as the majority of the 7,500 contigs generated in the first fingerprinting phase were juxtaposed correctly relative to each other on the basis of homology between the two genomes. As a result, 7,500 x 7,500 possible joins (more than 56 million) was reduced to analysis of <10,000 putative joins. This permitted the construction of a physical map covering 98% of the 2500 Mb mouse genome, contained within 296 contigs, in approximately 12 months (see accompanying paper). The same approach could be adopted for any genome where there is sufficient sequence homology to allow

alignment of BESs (or equivalent sequence tags), plus sufficient homology between the template genome and the genome under study. The approach has important applications both for genomes where the full genome sequence is anticipated, and also (perhaps even more importantly) is a cost-effective way to provide access to regions of a genome for which there are no plans to generate genomic sequence on any scale.

Whilst a clone by clone approach proved successful for the generation of human sequence, the possible contribution of WGS data to large projects has continued to be evaluated. The main advantages of WGS are that the production of data is very rapid, can be highly automated, avoids cloning biases of BAC systems, and is very cost-effective. The assembly inherent from the sequence alignment also provides important mapping information which is unbiased by additional experimental mapping systems or procedures. While it remains true that WGS in isolation has disadvantages which prevent completion of either the map or finished sequence of a large genome, the possibility of combining the advantages of both approaches has been explored. A hybrid strategy emerged from the *Drosophila* project, and has since been adopted for the mouse genome. Seven fold WGS coverage was generated from sub-cloned plasmids of varying sizes which, when assembled with BESs, generated 96% coverage of the euchromatic portion of the mouse genome. This estimate was derived by assessing the amount of WGS coverage provided which matched 187 Mb of finished mouse sequence. For a second, independent estimate, a genomic alignment of a curated collection of cDNAs to the WGS assembly was also used. This alignment included 96.4% of cDNA bases. Paired-end reads from large insert plasmids and BACs provided the scaffold upon which the assembled whole genome shotgun sequence was ordered and orientated, and simultaneously integrated BAC clones into the sequence. A tiling

path of BAC clones from the physical map is currently being used for directed finishing of the draft genomic sequence. The physical map helped to assemble the sequence scaffold, whilst the WGS data increased the rate of clone based finishing (MGSC 2002).

If WGS sequence data can accurately place BACs via their BESs within the sequence assembly, is a restriction fingerprint database actually required? The answer is probably yes. Whilst BES localisation within a whole genome shotgun assembly facilitates a more optimal minimum tiling path selection, overlaps within fingerprinting contigs can link sequence assemblies (as reported by the assembly of the mouse WGS sequence (MGSC 2002)). Three hundred and seventy-seven anchored ‘supercontigs’ were generated by assembling plasmid and BAC end sequences in the WGS assembly. This number was reduced to 88 when two or more sequence supercontigs were localised within a single restriction fingerprint contig. The overlaps generated by fingerprint analysis may also be able to resolve errors in the genomic assembly where, for example, low copy repeats may have resulted in a compression of the sequence assembly. The proven success of assembling genome wide physical maps, the cost of constructing a >15 fold genomic BAC library and the ease with which genome-wide fingerprint databases can be assembled, has lead to the construction of several genomic fingerprint databases, table 7.1. Whilst genome-wide fingerprint maps will facilitate the large-scale characterisation of many varied species, the construction of small region specific sequence-ready maps will continue to be important for detailed inter-species sequence comparisons (Thomas *et al.*, 2002).

Table 7.1: Organisms for which genome-wide fingerprint databases have or are being constructed.

Organism	Reference
<i>A. thaliana</i>	Marra et al 1999
Rice	Tao et al. 2000
<i>H. sapiens</i>	McPherson et al 2001
<i>M. musculus</i>	Gregory et al 2002
<i>R. rattus</i>	http://www.bcgsc.ca/lab/mapping
<i>C. neoformans</i>	http://www.bcgsc.ca/lab/mapping
Bovine	http://www.bcgsc.ca/lab/mapping
Porcine	http://www.nps.ars.usda.gov/
<i>D. rerio</i>	http://www.sanger.ac.uk/Projects/D_rerio/
Soybean	http://hbz.tamu.edu/soybean.html

7.2 The identification of coding features

The availability of human genomic sequence provides the framework upon which the structure of genes and their regulatory elements can be placed. The existence of genes as protein-coding genes, pseudogenes (Harrison *et al.*, 2002), non-protein-coding RNA transcripts (Mattick *et al.*, 2001) and genes arising from genomic duplications (Bailey *et al.*, 2002) requires a multifaceted approach to gene discovery. The three main methods used for large-scale genome analysis, *in silico* prediction of gene structures, sequence alignment of expressed and genomic sequences and identification of conserved sequences between different species, are described in chapter 5. These approaches are preferentially used in combination to assist correction for the shortcomings of each method. For example, *in silico* gene identification can lead to over prediction and false negatives (Guigo *et al.*, 2000). EST and cDNA sequence alignment can be confounded by artefactual or unprocessed clones in cDNA libraries. Cross species sequence comparison, for example between human and mouse, can also identify

homologies outside genes and regulatory elements (Deloukas *et al.*, 2001, Kondrashov and Shabalina *et al.*, 2002).

An important facet of fully identifying all coding features within any organism is the availability of high quality finished genomic sequence. Annotation of genes using draft sequence, which may contain regions of low quality, incomplete or unordered data, may lead to inaccurate annotation of genes and possibly errors in inference of the protein products derived from them. Another important consideration is reanalysis of existing annotation. The continual emergence of new sequence data from independent studies, and reanalysis of genomic sequence on a regular basis (or on demand), is required to ensure incorporation of all available evidence for genes and other features. The genomic alignment of larger sets of non-redundant ESTs and cDNAs, derived from a wider range of tissues or of sequence from related organisms, may assist to fully define gene structures, identify novel coding features or regulatory regions. Recent publications detailing the re-annotation of human chromosome 22 (Collins *et al.*, 2003) and *Drosophila* genomes (Misra *et al.*, 2002), which list structural changes to genes previously identified, indicate that the characterisation of all coding features will require several iterations of automatic analysis, manual annotation and directed laboratory work. Other examples of comparative analysis have also revealed new regulatory elements or genes (Pennacchio *et al.*, 2001, Gottgens *et al.*, 2002). The identification of genic features such as the 5' and 3' ends of genes, splice variants and even the functional determination of non-coding genes such as anti-sense RNAs (Green *et al.*, 1986), will take many years of painstaking study.

7.3 Assigning gene function

Characterisation of the functional product of a gene is not achieved directly by the identification of translated amino acid sequence contained within the open reading frame of the coding sequence. Within a genomic context, the final sequence and structure of an mRNA and the encoded protein may be influenced by priming from multiple promoters, splice variation within the coding exons or the existence of alternative polyadenylation sites, as discussed in chapter 5. Post-translational processing can also result in modification of a protein product. Whilst *in vivo* and *in vitro* studies within model organisms, by chemical mutagenesis and gene targeting can identify gene function by generating an observable phenotype it may not always be clear how a disruption of the target gene has given rise to a particular effect within a complex network of gene interactions. Alternatively, protein function may be predicted by *in silico* structural analysis. The assignment of new function to a novel protein at a nucleotide sequence level comparison, however, may fail as BLAST analysis within the Protein Data Bank (PDB) was shown to only find 10% of the known relationships (Brenner *et al.*, 1998). Whilst iterative PSI-BLAST (Altschul *et al.*, 1997) is more sensitive, relationships are still missed.

An alternative approach is the sequence-to-function method which uses pair-wise sequence or motif alignment to derive significant homologies between proteins and hence suggest similarity of function. Whilst these methods are powerful, they are not ideally suited to identify loss or gain of function during protein evolution and encounter difficulties when assigning function as protein databases become more diverse (Skolnick and Fetrow 2000). Alternatively, the possible function of a protein may be

suggested by comparison of three-dimensional structure to proteins of known function. Since the tertiary structure of proteins of common function is likely to be more conserved than their primary structures (amino acid sequences), attempts have been made to classify groups of proteins based on structural and phylogenetic relationships, e.g. SCOP (Murzin *et al.*, 1995). A second approach describes proteins according to their structural characteristics, such as class of architecture and fold type. In practice both approaches are used, initially grouping proteins according to their sequence homology and then by their structural descriptors (Thornton *et al.*, 1999).

The application of the sequence to structure to function approach aims to determine the structure of a protein and then to identify the functionally important residues, as described in chapter 6. *Ab initio* folding can be used to predict a native structure based on domains contained within the protein. A process known as threading utilises a known structure as a template upon which proteins of up to 500 residues can be moulded. These three dimensional structures can then be used to infer function by analysis of internal or external residues, the shape and molecular composition of the protein or the juxtaposition of individual groups. The prediction of protein folds, their 3D structure and function is, however, primarily reliant upon experimental evidence, either as a basis for modelling or as support for a prediction. X-ray crystallography and nuclear magnetic resonance spectroscopy are methods by which these proteins structures have been experimentally determined.

The identification of well conserved, functionally important residues within primary and tertiary structures of some protein families can assist to predict the function of novel proteins. Based upon the conservation of an Asp-Thr(Ser)-Gly amino acid sequence at

their active sites Pearl and Taylor (1987a, 1987b) concluded that retroviral proteases could belong to aspartic protease family. Modelling and subsequent structural comparisons between aspartic proteases, which contain 300 residues and an active site in each of its two domains, and retroviral proteases, that do not exceed 130 residues and have only one active site, led Pearl and Taylor to hypothesise that the retroviral enzymes may be dimeric aspartic proteases. This prediction was subsequently proven by the expression of the retroviral proteases in *E. coli* (Meek *et al.*, 1989) and by the determination of its crystal structure (Navia *et al.*, 1989)

In many cases, however, even in these well characterised families, the catalytic component may be recognisable, but the specific substrate binding properties may be difficult to determine. Additional protein domains (encoded by separate exons) which are required for function, but localise to other regions of the protein, are less readily elucidated by homology alone. For this, direct experimental approaches are required to determine the substrate and products in the appropriate biochemical pathway. For example protein binding assays, using yeast two hybrid systems, can identify interacting binding proteins. Knockouts, or natural mutants, may be investigated to determine the biochemistry of the altered phenotype in some detail. For example, a defective enzyme may result in accumulation of abnormally high levels of substrate, and comparison of normal vs. mutant systems will reveal candidates as possible substrates.

Additional information can be gained by determining the cellular and tissue localisation of the protein. The co-localisation of proteins in a highly tissue-specific pattern may provide evidence for some level of protein interaction. The fusion of the sequence encoding a novel protein to the sequence of a reporter molecule in a shuttle vector can

be used to determine cellular localisation if the construct can be introduced into a physiologically relevant cell line. This work may be followed up, for example, by manipulation of the construct and introduction into embryonic stem cells in order to create a transgenic animal model where the gene is under control of the endogenous promoter. This would enable investigation of the expression of the gene presumably in response to physiologically natural intracellular and extracellular signals. The cellular distribution of the signal molecule should, therefore, reflect the distribution of the natural gene product. Data from co-localisation experiments may be correlated with protein-protein interaction studies, and possibly analysis (e.g. by mass spectrometry) of the components of co-purified complexes, to build a picture of the interactions between specific proteins

7.4 Sequence variation

The key to understanding the effects of sequence variation within protein-coding genes is the identification of genuine sequence variants from accurately annotated gene structures and determination of the functional effect that a variant has upon the encoded protein, or on expression of the gene. Chapter 6 describes the generation of exon specific sequences from a collection of twelve medically important genes, including five closely related members of a gene family. The design of primers which are uniquely localised within the genome, in conjunction with detailed analysis of the sequence flanking the SNP, permitted identification of novel locus specific polymorphisms within highly homologous genes and the unique placement of SNPs which previously had been given multiple localisations within Ensembl and dbSNP. The functional effect a minor

coding SNP may have upon protein structure was predicted using protein modelling, as outlined in chapter 5. Whilst *in silico* prediction would always require experimental support (see also discussion above), it can be used to suggest the effects a SNP may have upon a protein structure and function. A novel non-synonymous, non-conservative coding SNP was identified within GSTT1, as part of this study.

The majority of genetic variation which contributes to cancer are somatic mutations caused by exposure to environmental carcinogens rather than inherited variants in susceptibility genes. However, genes that encode enzymes involved in the metabolism of carcinogens can be polymorphic and these polymorphisms may be related to elevated risk of cancer susceptibility. This mechanism illustrates the importance of genetic background and the effect on interaction between the individual and the environment. GSTT1 is a phase II enzyme that mediates the detoxification of xenobiotic chemicals by conjugation of glutathione which changes the polarity of the chemical and makes them more readily excreted. GSTT1 is a five exon gene which localises to 22q11.2 and is known to be absent from 38% of the population (Pemble *et al.*, 1994). The null genotype of GSTT1 has been implicated with increased risk of myelodysplastic syndromes (MDS) (Chen *et al.*, 1996), aplastic anemia (Lee *et al.*, 2001) and, in conjunction with a CYP1A1 mutation, has effects on live birth weight (Wang *et al.*, 2002). These studies indicate that the gene, by its absence, may influence the aetiology of disease. The identification of a novel non-synonymous non-conservative SNP, which may induce a change to conformation and function of the protein, as described in chapter 6, may also influence an individual's susceptibility to cancer.

7.5 Conclusions and future work

This thesis describes the application of a novel restriction fingerprinting technique to the generation of a sequence ready map of 1pcen – 1p13, the elucidation of the genic features within the interval and the characterisation of sequence variation within a selected number of these genes. In the short term, all these areas of research could be extended. The annotation of genes within the transcript map of the interval will require further work, as shown by the gain in information by the iterative annotation of *Drosophila* (Misra *et al.*, 2002) and human chromosome 22 (Collins *et al.*, 2003). Alignment of novel cDNAs and ESTs to genomic sequence may assist to further define gene structures, specifically the 5' and 3' ends, as well as identifying new genes and splice variants. Comparative sequence analyses, using species from a variety of evolutionary distances, will also help to better characterise the genes in the interval and also to identify regions that control their regulation.

Comparative sequence analysis could also be used to characterise the structural evolution of chromosome 1. Regions either side of the chromosome 1 centromere are contained within a contiguous homologous region on mouse chromosome 3. The investigation of gene order, number and orientation may assist to elucidate the number of chromosomal rearrangements that have taken place during the evolution of human chromosome 1 from the organisation of the ancestral karyotype.

The functional consequence of the novel non-synonymous, non-conservative SNP within exon 3 requires further investigation. The frequency of the non-synonymous, non-conservative GSTT1*B allele within other ethnic groups (besides the Northern

European population used here) could be investigated. In addition, other phenotype to genotype correlations of the Thr104 – Pro SNP within large prospective DNA collections, such as the Avon Longitudinal Study of Parents and Children, could be determined.

In the longer term, it is anticipated that substantial efforts will result in all of the genes in the human genome being investigated in detail. These studies will result in a fuller understanding of the specificity and range of biochemical structures and functions that are encoded in the human genome sequence. In general there is likely to remain a distinction between the study of functions encoded at the DNA level, which affect gene expression via transcriptional control, and the study of functions reflected at the protein level following translation, taking into account post-translational modifications (processes which are largely genetically determined). Without a genic catalogue, functional studies are necessarily limited to the investigation of a specific target – a gene, a protein, or a disease. These approaches are an essential part of fully interpreting the genome as they provide a means by which hypotheses can be experimentally tested and which produce valid and supplementary results. However, the production of a complete gene catalogue (if completion can indeed be measured or achieved) will provide the raw material for modelling whole systems. The extensive use of computational biology to suggest how such complex systems are made up of their interacting components will, in itself, enable predictions to be made of the system model. These predictions can be tested, both to determine the validity of the modelled system, and also to test the success of the methods used to derive the system.

A more complete knowledge of biochemical processes will yield a better understanding of complex disease and how it should be treated. At present, our knowledge is primarily

based on monogenic diseases. As the problem is reduced to a single gene, hypotheses for function can be tested by biochemical assays, protein structural studies, experimental knock-outs, or the study of naturally occurring mutants. The approach to complex disease centres on a similar approach, i.e. trying to identify the one or few dominant genetic factors which contribute the most significant effect to the overall phenotype. However, there is a realisation that these genetic factors may not fully explain the observed phenotype and that a proportion of the remaining factors may not be identified. In these instances, a comprehensive knowledge of the systems involved will be more informative than the approach of complex disease genetics, both in how the phenotype arises, and how it might be possible to intervene more effectively. This is potentially a true long-term value of the genome sequence, and its interpretation in a biochemical, biological and genetic context, for the advancement of medicine in the future.

Chapter 8

References

- Abagyan, R. A., Totrov, M.M., and Kuznetsov, D.N. ICM - a new method for protein modeling and design. Applications to docking and structure prediction from the distorted native conformation. (1994) *J Comp Chem*, **15**, 488 - 506.
- Adachi, N. and Lieber, M. R. Bidirectional gene organization: a common architectural feature of the human genome. (2002) *Cell*, **109**, 807-9.
- Adams, M. D., Celniker, S. E., Holt, R. A., Evans, C. A., Gocayne, J. D., Amanatides, P. G., et al. The genome sequence of *Drosophila melanogaster*. (2000) *Science*, **287**, 2185-95.
- Adams, M. D., Kelley, J. M., Gocayne, J. D., Dubnick, M., Polymeropoulos, M. H., Xiao, H., et al. Complementary DNA sequencing: expressed sequence tags and human genome project. (1991) *Science*, **252**, 1651-6.
- Adams, M. D., Soares, M. B., Kerlavage, A. R., Fields, C. and Venter, J. C. Rapid cDNA sequencing (expressed sequence tags) from a directionally cloned human infant brain cDNA library. (1993) *Nat Genet*, **4**, 373-80.
- Alexandrie, A. K., Rannug, A., Juronen, E., Tasa, G. and Warholm, M. Detection and characterization of a novel functional polymorphism in the GSTT1 gene. (2002) *Pharmacogenetics*, **12**, 613-9.
- Allan, J. M., Wild, C. P., Rollinson, S., Willett, E. V., Moorman, A. V., Dovey, G. J., et al. Polymorphism in glutathione S-transferase P1 is associated with susceptibility to chemotherapy-induced leukemia. (2001) *Proc Natl Acad Sci U S A*, **98**, 11592-7.
- Altschul, S. F., Gish, W., Miller, W., Myers, E. W. and Lipman, D. J. Basic local alignment search tool. (1990) *J Mol Biol*, **215**, 403-10.
- Altschul, S. F., Madden, T. L., Schaffer, A. A., Zhang, J., Zhang, Z., Miller, W., et al. Gapped BLAST and PSI-BLAST: a new generation of protein database search programs. (1997) *Nucleic Acids Res*, **25**, 3389-402.

- Altshuler, D., Pollara, V. J., Cowles, C. R., Van Etten, W. J., Baldwin, J., Linton, L., et al. An SNP map of the human genome generated by reduced representation shotgun sequencing. (2000) *Nature*, **407**, 513-6.
- Anderson, S. Shotgun DNA sequencing using cloned DNase I-generated fragments. (1981) *Nucleic Acids Res*, **9**, 3015-27.
- Anderson, S., Bankier, A. T., Barrell, B. G., de Bruijn, M. H., Coulson, A. R., Drouin, J., et al. Sequence and organization of the human mitochondrial genome. (1981) *Nature*, **290**, 457-65.
- Angelisova, P., Vlcek, C., Stefanova, I., Lipoldova, M. and Horejsi, V. The human leucocyte surface antigen CD53 is a protein structurally similar to the CD37 and MRC OX-44 antigens. (1990) *Immunogenetics*, **32**, 281-5.
- Ansari-Lari, M. A., Oeltjen, J. C., Schwartz, S., Zhang, Z., Muzny, D. M., Lu, J., et al. Comparative sequence analysis of a gene-rich cluster at human chromosome 12p13 and its syntenic region in mouse chromosome 6. (1998) *Genome Res*, **8**, 29-40.
- Antequera, F. and Bird, A. Number of CpG islands and genes in human and mouse. (1993) *Proc Natl Acad Sci U S A*, **90**, 11995-9.
- Arabidopsis Genome Initiative, T. Analysis of the genome sequence of the flowering plant *Arabidopsis thaliana*. (2000) *Nature*, **408**, 796-815.
- Attali, B., Romey, G., Honore, E., Schmid-Alliana, A., Mattei, M. G., Lesage, F., et al. Cloning, functional expression, and regulation of two K⁺ channels in human T lymphocytes. (1992) *J Biol Chem*, **267**, 8650-7.
- Bailey, J. A., Yavor, A. M., Viggiano, L., Misceo, D., Horvath, J. E., Archidiacono, N., et al. Human-specific duplication and mosaic transcripts: the recent paralogous structure of chromosome 22. (2002) *Am J Hum Genet*, **70**, 83-100.
- Bankier, A. T., Weston, K. M. and Barrell, B. G. Random cloning and sequencing by the M13/dideoxynucleotide chain termination method. (1987) *Methods Enzymol*, **155**, 51-93.

- Bates, G. P., Valdes, J., Hummerich, H., Baxendale, S., Le Paslier, D. L., Monaco, A. P., et al. Characterization of a yeast artificial chromosome contig spanning the Huntington's disease gene candidate region. (1992) *Nat Genet*, **1**, 180-7.
- Beaudoing, E., Freier, S., Wyatt, J. R., Claverie, J. M. and Gautheret, D. Patterns of variant polyadenylation signal usage in human genes. (2000) *Genome Res*, **10**, 1001-10.
- Bentley, D. R. The Human Genome Project--an overview. (2000) *Med Res Rev*, **20**, 189-96.
- Bentley, D. R., Deloukas, P., Dunham, A., French, L., Gregory, S. G., Humphray, S. J., et al. The physical maps for sequencing human chromosomes 1, 6, 9, 10, 13, 20 and X. (2001) *Nature*, **409**, 942-3.
- Bernaola-Galvan, P., Roman-Roldan, R. and Oliver, J. L. Compositional segmentation and long-range fractal correlations in DNA sequences. (1996) *Physical Review. E. Statistical Physics, Plasmas, Fluids, and Related Interdisciplinary Topics*, **53**, 5181-5189.
- Bernardi, G., Olofsson, B., Filipinski, J., Zerial, M., Salinas, J., Cuny, G., et al. The mosaic genome of warm-blooded vertebrates. (1985) *Science*, **228**, 953-8.
- Bickmore, W. A. and Sumner, A. T. Mammalian chromosome banding--an expression of genome organization. (1989) *Trends Genet*, **5**, 144-8.
- Bird, A. P. CpG-rich islands and the function of DNA methylation. (1986) *Nature*, **321**, 209-13.
- Birnboim, H. C. and Doly, J. A rapid alkaline extraction procedure for screening recombinant plasmid DNA. (1979) *Nucleic Acids Res*, **7**, 1513-23.
- Blattner, F. R., Plunkett, G., 3rd, Bloch, C. A., Perna, N. T., Burland, V., Riley, M., et al. The complete genome sequence of Escherichia coli K-12. (1997) *Science*, **277**, 1453-74.
- Board, P., Coggan, M., Johnston, P., Ross, V., Suzuki, T. and Webb, G. Genetic heterogeneity of the human glutathione transferases: a complex of gene families. (1990) *Pharmacol Ther*, **48**, 357-69.
- Boguski, M. S. and Schuler, G. D. ESTablishing a human transcript map. (1995) *Nat Genet*, **10**, 369-71.

- Bonfield, J. K., Smith, K. and Staden, R. A new DNA sequence assembly program. (1995) *Nucleic Acids Res*, **23**, 4992-9.
- Booth, J., Boyland, E., and Sims, P. An enzyme from rat liver catalyzing conjugation with glutathione. (1961) *Biochem J*, **79**, 516 - 524.
- Botstein, D., White, R. L., Skolnick, M. and Davis, R. W. Construction of a genetic linkage map in man using restriction fragment length polymorphisms. (1980) *Am J Hum Genet*, **32**, 314-31.
- Bouffard, G. G., Idol, J. R., Braden, V. V., Iyer, L. M., Cunningham, A. F., Weintraub, L. A., et al. A physical map of human chromosome 7: an integrated YAC contig map with average STS spacing of 79 kb. (1997) *Genome Res*, **7**, 673-92.
- Brenner, M., Lampel, K., Nakatani, Y., Mill, J., Banner, C., Mearow, K., et al. Characterization of human cDNA and genomic clones for glial fibrillary acidic protein. (1990) *Brain Res Mol Brain Res*, **7**, 277-86.
- Brenner, S. E., Chothia, C. and Hubbard, T. J. Assessing sequence comparison methods with reliable structurally identified distant evolutionary relationships. (1998) *Proc Natl Acad Sci U S A*, **95**, 6073-8.
- Brintnell, B., Hey, Y., Jones, D., Hoggard, N., James, L. and Varley, J. M. Generation of a contig comprising YACs and BACs within chromosome region 1p13.1. (1997) *Somat Cell Mol Genet*, **23**, 153-7.
- Brown, L., Espinosa, R., 3rd, Le Beau, M. M., Siciliano, M. J. and Baer, R. HEN1 and HEN2: a subgroup of basic helix-loop-helix genes that are coexpressed in a human neuroblastoma. (1992) *Proc Natl Acad Sci U S A*, **89**, 8492-6.
- Burge, C. and Karlin, S. Prediction of complete gene structures in human genomic DNA. (1997) *J Mol Biol*, **268**, 78-94.
- Burke, D. T., Carle, G. F. and Olson, M. V. Cloning of large segments of exogenous DNA into yeast by means of artificial chromosome vectors. (1987) *Science*, **236**, 806-12.
- C. elegans Sequencing Consortium, T. Genome sequence of the nematode C. elegans: a platform for investigating biology. The C. elegans Sequencing Consortium. (1998) *Science*, **282**, 2012-8.

- Carpten, J., Nupponen, N., Isaacs, S., Sood, R., Robbins, C., Xu, J., et al. Germline mutations in the ribonuclease L gene in families showing linkage with HPC1. (2002) *Nat Genet*, **30**, 181-4.
- Carrano, A. V., Lamerdin, J., Ashworth, L. K., Watkins, B., Branscomb, E., Slezak, T., et al. A high-resolution, fluorescence-based, semiautomated method for DNA fingerprinting. (1989) *Genomics*, **4**, 129-36.
- Carrier, A., Rosier, M. F., Guillemot, F., Goguel, A. F., Pulcini, F., Bernheim, A., et al. Integrated physical, genetic, and genic map covering 3 Mb around the human NGF gene (NGFB) at 1p13. (1996) *Genomics*, **31**, 80-9.
- Charroux, B., Pellizzoni, L., Perkinson, R. A., Shevchenko, A., Mann, M. and Dreyfuss, G. Gemin3: A novel DEAD box protein that interacts with SMN, the spinal muscular atrophy gene product, and is a component of gems. (1999) *J Cell Biol*, **147**, 1181-94.
- Chasman, D. and Adams, R. M. Predicting the functional consequences of non-synonymous single nucleotide polymorphisms: structure-based assessment of amino acid variation. (2001) *J Mol Biol*, **307**, 683-706.
- Chelly, J., Tumer, Z., Tonnesen, T., Petterson, A., Ishikawa-Brush, Y., Tommerup, N., et al. Isolation of a candidate gene for Menkes disease that encodes a potential heavy metal binding protein. (1993) *Nat Genet*, **3**, 14-9.
- Chen, C. L., Liu, Q. and Relling, M. V. Simultaneous characterization of glutathione S-transferase M1 and T1 polymorphisms by polymerase chain reaction in American whites and blacks. (1996) *Pharmacogenetics*, **6**, 187-91.
- Choo, K. H., Gould, K. G., Rees, D. J. and Brownlee, G. G. Molecular cloning of the gene for human anti-haemophilic factor IX. (1982) *Nature*, **299**, 178-80.
- Chumakov, I. M., Le Gall, I., Billault, A., Ougen, P., Soularue, P., Guillou, S., et al. Isolation of chromosome 21-specific yeast artificial chromosomes from a total human genome library. (1992) *Nat Genet*, **1**, 222-5.
- Chumakov, I. M., Rigault, P., Le Gall, I., Bellanne-Chantelot, C., Billault, A., Guillou, S., et al. A YAC contig map of the human genome. (1995) *Nature*, **377**, 175-297.

- Claudio, J. O., Liew, C. C., Ma, J., Heng, H. H., Stewart, A. K. and Hawley, R. G. Cloning and expression analysis of a novel WD repeat gene, WDR3, mapping to 1p12-p13. (1999) *Genomics*, **59**, 85-9.
- Coffey, A. J., Roberts, R. G., Green, E. D., Cole, C. G., Butler, R., Anand, R., et al. Construction of a 2.6-Mb contig in yeast artificial chromosomes spanning the human dystrophin gene using an STS-based approach. (1992) *Genomics*, **12**, 474-84.
- Cohen, D., Chumakov, I. and Weissbach, J. A first-generation physical map of the human genome. (1993) *Nature*, **366**, 698-701.
- Collins, F. S., Brooks, L. D. and Chakravarti, A. A DNA polymorphism discovery resource for research on human genetic variation. (1998) *Genome Res*, **8**, 1229-31.
- Collins, J. E., Cole, C. G., Smink, L. J., Garrett, C. L., Levensha, M. A., Soderlund, C. A., et al. A high-density YAC contig map of human chromosome 22. (1995) *Nature*, **377**, 367-79.
- Collins, J. E., Goward, M. E., Cole, C. G., Smink, L. J., Huckle, E. J., Knowles, S., et al. Reevaluating human gene annotation: a second-generation analysis of chromosome 22. (2003) *Genome Res*, **13**, 27-36.
- Connelly, M. A., Zhang, H., Kieleczawa, J. and Anderson, C. W. The promoters for human DNA-PKcs (PRKDC) and MCM4: divergently transcribed genes located at chromosome 8 band q11. (1998) *Genomics*, **47**, 71-83.
- Coulondre, C., Miller, J. H., Farabaugh, P. J. and Gilbert, W. Molecular basis of base substitution hotspots in *Escherichia coli*. (1978) *Nature*, **274**, 775-80.
- Coulson, A., Huynh, C., Kozono, Y. and Shownkeen, R. The physical map of the *Caenorhabditis elegans* genome. (1995) *Methods Cell Biol*, **48**, 533-50.
- Coulson, A., Sulston, J., Brenner, S., Karn, J. Toward a physical map of the genome of the nematode *Caenorhabditis elegans*. (1986) *Proc Natl Acad Sci U S A*, **83**, 7821-7825.
- Couzin, J. Human genome. HapMap launched with pledges of \$100 million. (2002) *Science*, **298**, 941-2.

- Cox, D. R., Burmeister, M., Price, E. R., Kim, S. and Myers, R. M. Radiation hybrid mapping: a somatic cell genetic method for constructing high-resolution maps of mammalian chromosomes. (1990) *Science*, **250**, 245-50.
- Dauwerse, J. G., Kievits, T., Beverstock, G. C., van der Keur, D., Smit, E., Wessels, H. W., et al. Rapid detection of chromosome 16 inversion in acute nonlymphocytic leukemia, subtype M4: regional localization of the breakpoint in 16p. (1990) *Cytogenet Cell Genet*, **53**, 126-8.
- Dawson, E., Chen, Y., Hunt, S., Smink, L. J., Hunt, A., Rice, K., et al. A SNP resource for human chromosome 22: extracting dense clusters of SNPs from the genomic sequence. (2001) *Genome Res*, **11**, 170-8.
- Deininger, P. L. a. D., G.R. The recent evolution of DNA repetitive elements. (1986) *Trends Genet*, **2**, 76-80.
- Dekker, J. W., Budhia, S., Angel, N. Z., Cooper, B. J., Clark, G. J., Hart, D. N., et al. Identification of an S-adenosylhomocysteine hydrolase-like transcript induced during dendritic cell differentiation. (2002) *Immunogenetics*, **53**, 993-1001.
- Dell'Angelica, E. C., Mullins, C. and Bonifacino, J. S. AP-4, a novel protein complex related to clathrin adaptors. (1999) *J Biol Chem*, **274**, 7278-85.
- Deloukas, P., Matthews, L. H., Ashurst, J., Burton, J., Gilbert, J. G., Jones, M., et al. The DNA sequence and comparative analysis of human chromosome 20. (2001) *Nature*, **414**, 865-71.
- Deloukas, P., Schuler, G. D., Gyapay, G., Beasley, E. M., Soderlund, C., Rodriguez-Tome, P., et al. A physical map of 30,000 human genes. (1998) *Science*, **282**, 744-6.
- DeMartino, G. N., Orth, K., McCullough, M. L., Lee, L. W., Munn, T. Z., Moomaw, C. R., et al. The primary structures of four subunits of the human, high-molecular-weight proteinase, macropain (proteasome), are distinct but homologous. (1991) *Biochim Biophys Acta*, **1079**, 29-38.
- Deutsch, S., Iseli, C., Bucher, P., Antonarakis, S. E. and Scott, H. S. A cSNP map and database for human chromosome 21. (2001) *Genome Res*, **11**, 300-7.

- Dib, C., Faure, S., Fizames, C., Samson, D., Drouot, N., Vignal, A., et al. A comprehensive genetic map of the human genome based on 5,264 microsatellites. (1996) *Nature*, **380**, 152-4.
- Ding, Y., Johnson, M. D., Chen, W. Q., Wong, D., Chen, Y. J., Benson, S. C., et al. Five-color-based high-information-content fingerprinting of bacterial artificial chromosome clones using type IIS restriction endonucleases. (2001) *Genomics*, **74**, 142-54.
- Doggett, N. A., Goodwin, L. A., Tesmer, J. G., Meincke, L. J., Bruce, D. C., Clark, L. M., et al. An integrated physical map of human chromosome 16. (1995) *Nature*, **377**, 335-65.
- Donis-Keller, H., Green, P., Helms, C., Cartinhour, S., Weiffenbach, B., Stephens, K., et al. A genetic linkage map of the human genome. (1987) *Cell*, **51**, 319-37.
- Down, T. A. and Hubbard, T. J. Computational detection and location of transcription start sites in mammalian genomic DNA. (2002) *Genome Res*, **12**, 458-61.
- Dracopoli, N. C., Rettig, W. J., Whitfield, G. K., Darlington, G. J., Spengler, B. A., Biedler, J. L., et al. Assignment of the gene for the beta subunit of thyroid-stimulating hormone to the short arm of human chromosome 1. (1986) *Proc Natl Acad Sci U S A*, **83**, 1822-6.
- Dumont, M., Luu-The, V., Dupont, E., Pelletier, G. and Labrie, F. Characterization, expression, and immunohistochemical localization of 3 beta-hydroxysteroid dehydrogenase/delta 5-delta 4 isomerase in human skin. (1992) *J Invest Dermatol*, **99**, 415-21.
- Dunham, I., Shimizu, N., Roe, B. A., Chisoe, S., Hunt, A. R., Collins, J. E., et al. The DNA sequence of human chromosome 22. (1999) *Nature*, **402**, 489-95.
- El-Rifai, W., Sarlomo-Rikala, M., Andersson, L. C., Knuutila, S. and Miettinen, M. DNA sequence copy number changes in gastrointestinal stromal tumors: tumor progression and prognostic significance. (2000) *Cancer Res*, **60**, 3899-903.
- Evans, G. A. and Lewis, K. A. Physical mapping of complex genomes by cosmid multiplex analysis. (1989) *Proc Natl Acad Sci U S A*, **86**, 5030-4.
- Ewing, B. and Green, P. Analysis of expressed sequence tags indicates 35,000 human genes. (2000) *Nat Genet*, **25**, 232-4.

- Ewing, B., Hillier, L., Wendl, M. C. and Green, P. Base-calling of automated sequencer traces using phred. I. Accuracy assessment. (1998) *Genome Res*, **8**, 175-85.
- Fields, C., Adams, M. D., White, O. and Venter, J. C. How many genes in the human genome? (1994) *Nat Genet*, **7**, 345-6.
- Fleischmann, R. D., Adams, M. D., White, O., Clayton, R. A., Kirkness, E. F., Kerlavage, A. R., et al. Whole-genome random sequencing and assembly of *Haemophilus influenzae* Rd. (1995) *Science*, **269**, 496-512.
- Foot, S., Vollrath, D., Hilton, A. and Page, D. C. The human Y chromosome: overlapping DNA clones spanning the euchromatic region. (1992) *Science*, **258**, 60-6.
- Forus, A., Weghuis, D. O., Smeets, D., Fodstad, O., Myklebost, O. and van Kessel, A. G. Comparative genomic hybridization analysis of human sarcomas: I. Occurrence of genomic imbalances and identification of a novel major amplicon at 1q21-q22 in soft tissue sarcomas. (1995) *Genes Chromosomes Cancer*, **14**, 8-14.
- Francke, U. Digitized and differentially shaded human chromosome ideograms for genomic applications. (1994) *Cytogenet Cell Genet*, **65**, 206-18.
- Galgoczy, P., Rosenthal, A. and Platzer, M. Human-mouse comparative sequence analysis of the NEMO gene reveals an alternative promoter within the neighboring G6PD gene. (2001) *Gene*, **271**, 93-8.
- Gardiner, K. Base composition and gene distribution: critical patterns in mammalian genome organization. (1996) *Trends Genet*, **12**, 519-24.
- Gardiner-Garden, M. and Frommer, M. CpG islands in vertebrate genomes. (1987) *J Mol Biol*, **196**, 261-82.
- Gengyo-Ando, K. and Mitani, S. Characterization of mutations induced by ethyl methanesulfonate, UV, and trimethylpsoralen in the nematode *Caenorhabditis elegans*. (2000) *Biochem Biophys Res Commun*, **269**, 64-9.
- Gibson, T. J. and Sulston, J. E. Preparation of large numbers of plasmid DNA samples in microtiter plates by the alkaline lysis method. (1987) *Gene Anal Tech*, **4**, 41-4.

- Gilbert, W. Why genes in pieces? (1978) *Nature*, **271**, 501.
- Gilbert, W. (1992) (Ed, Kelves, D. J. a. H., L.) Harvard University Press.
- Goffeau, A., Barrell, B. G., Bussey, H., Davis, R. W., Dujon, B., Feldmann, H., et al. Life with 6000 genes. (1996) *Science*, **274**, 546, 563-7.
- Goss, S. J. and Harris, H. New method for mapping genes in human chromosomes. (1975) *Nature*, **255**, 680-4.
- Gottgens, B., Barton, L. M., Gilbert, J. G., Bench, A. J., Sanchez, M. J., Bahn, S., et al. Analysis of vertebrate SCL loci identifies conserved enhancers. (2000) *Nat Biotechnol*, **18**, 181-6.
- Green, E. D. and Chakravarti, A. The human genome sequence expedition: views from the "base camp". (2001) *Genome Res*, **11**, 645-51.
- Green, E. D. and Olson, M. V. Chromosomal region of the cystic fibrosis gene in yeast artificial chromosomes: a model for human genome mapping. (1990) *Science*, **250**, 94-8.
- Green, E. D., Riethman, H. C., Dutchik, J. E. and Olson, M. V. Detection and characterization of chimeric yeast artificial-chromosome clones. (1991) *Genomics*, **11**, 658-69.
- Green, P. Whole-genome disassembly. (2002) *Proc Natl Acad Sci U S A*, **99**, 4143-4.
- Green, P. J., Pines O, Inouye M. The role of antisense RNA in gene regulation. (1986) *Annu Rev Biochem*, **55**, 569-97.
- Gregory, S. G., Howell, G. R. and Bentley, D. R. Genome mapping by fluorescent fingerprinting. (1997) *Genome Res*, **7**, 1162-8.
- Gregory, S. G., Sekhon, M., Schein, J., Zhao, S., Osoegawa, K., Scott, C. E., et al. A physical map of the mouse genome. (2002) *Nature*, **418**, 743-50.
- Gregory, S. G., Vaudin, M., Wooster, R., Coleman, M., Mischke, D., Porter, C., et al. Report of the fourth international workshop on human chromosome 1 mapping 1998. (1998) *Cytogenet Cell Genet*, **83**, 147-75.
- Guex, N. and Peitsch, M. C. SWISS-MODEL and the Swiss-PdbViewer: an environment for comparative protein modeling. (1997) *Electrophoresis*, **18**, 2714-23.

- Guigo, R., Agarwal, P., Abril, J. F., Burset, M. and Fickett, J. W. An assessment of gene prediction accuracy in large DNA sequences. (2000) *Genome Res*, **10**, 1631-42.
- Guru, S. C., Olufemi, S. E., Manickam, P., Cummings, C., Gieser, L. M., Pike, B. L., et al. A 2.8-Mb clone contig of the multiple endocrine neoplasia type 1 (MEN1) region at 11q13. (1997) *Genomics*, **42**, 436-45.
- Gyapay, G., Morissette, J., Vignal, A., Dib, C., Fizames, C., Millasseau, P., et al. The 1993-94 Genethon human genetic linkage map. (1994) *Nat Genet*, **7**, 246-339.
- Hall, A. and Brown, R. Human N-ras: cDNA cloning and gene structure. (1985) *Nucleic Acids Res*, **13**, 5255-68.
- Halushka, M. K., Fan, J. B., Bentley, K., Hsie, L., Shen, N., Weder, A., et al. Patterns of single-nucleotide polymorphisms in candidate genes for blood-pressure homeostasis. (1999) *Nat Genet*, **22**, 239-47.
- Hardison, R., Slightom, J. L., Gumucio, D. L., Goodman, M., Stojanovic, N. and Miller, W. Locus control regions of mammalian beta-globin gene clusters: combining phylogenetic analyses and experimental results to gain functional insights. (1997) *Gene*, **205**, 73-94.
- Hardison, R., Xu, J., Jackson, J., Mansberger, J., Selifonova, O., Grotch, B., et al. Comparative analysis of the locus control region of the rabbit beta-like gene cluster: HS3 increases transient expression of an embryonic epsilon-globin gene. (1993) *Nucleic Acids Res*, **21**, 1265-72.
- Harris, R. F. Hapmap flap. (2002) *Curr Biol*, **12**, R827.
- Harrison, P. M., Hegyi, H., Balasubramanian, S., Luscombe, N. M., Bertone, P., Echols, N., et al. Molecular fossils in the human genome: identification and analysis of the pseudogenes in chromosomes 21 and 22. (2002) *Genome Res*, **12**, 272-80.
- Hattori, M., Fujiyama, A., Taylor, T. D., Watanabe, H., Yada, T., Park, H. S., et al. The DNA sequence of human chromosome 21. (2000) *Nature*, **405**, 311-9.
- Hayes, J. D. and Pulford, D. J. The glutathione S-transferase supergene family: regulation of GST and the contribution of the isoenzymes to cancer chemoprotection and drug resistance. (1995) *Crit Rev Biochem Mol Biol*, **30**, 445-600.

- Heding, I. J., Ivens, A. C., Wilson, J., Strivens, M., Gregory, S., Hoovers, J. M., et al. The generation of ordered sets of cosmid DNA clones from human chromosome region 11p. (1992) *Genomics*, **13**, 89-94.
- Heiskanen, M., Karhu, R., Hellsten, E., Peltonen, L., Kallioniemi, O. P. and Palotie, A. High resolution mapping using fluorescence in situ hybridization to extended DNA fibers prepared from agarose-embedded cells. (1994) *Biotechniques*, **17**, 928-9, 932-3.
- Henneberry, A. L. and McMaster, C. R. Cloning and expression of a human choline/ethanolaminephosphotransferase: synthesis of phosphatidylcholine and phosphatidylethanolamine. (1999) *Biochem J*, **339** (Pt 2), 291-8.
- Higgins, D. G. CLUSTAL V: multiple alignment of DNA and protein sequences. (1994) *Methods Mol Biol*, **25**, 307-18.
- Hijikata, M., Ohta, Y. and Mishiro, S. Identification of a single nucleotide polymorphism in the Mx_A gene promoter (G/T at nt -88) correlated with the response of hepatitis C patients to interferon. (2000) *Intervirology*, **43**, 124-7.
- Hillier, L. D., Lennon, G., Becker, M., Bonaldo, M. F., Chiapelli, B., Chissoe, S., et al. Generation and analysis of 280,000 human expressed sequence tags. (1996) *Genome Res*, **6**, 807-28.
- Hoffman, H. M., Mueller, J. L., Broide, D. H., Wanderer, A. A. and Kolodner, R. D. Mutation of a new gene encoding a putative pyrin-like protein causes familial cold autoinflammatory syndrome and Muckle-Wells syndrome. (2001) *Nat Genet*, **29**, 301-5.
- Horton, R., Niblett, D., Milne, S., Palmer, S., Tubby, B., Trowsdale, J., et al. Large-scale sequence comparisons reveal unusually high levels of variation in the HLA-DQB1 locus in the class II region of the human MHC. (1998) *Journal Of Molecular Biology*, **282**, 71-97.
- Hoskins, R. A., Nelson, C. R., Berman, B. P., Laverty, T. R., George, R. A., Ciesiolka, L., et al. A BAC-based physical map of the major autosomes of *Drosophila melanogaster*. (2000) *Science*, **287**, 2271-4.
- Hsia, D. Y.-Y., Naylor, J., Bigler, J. A. Gaucher's disease: report of two cases in father and son and review of the literature. (1959) *New Eng. J. Med.*, **261**, 164-169.

- Hu, B., Trinh, K., Figueira, W. F. and Price, P. A. Isolation and sequence of a novel human chondrocyte protein related to mammalian members of the chitinase protein family. (1996) *J Biol Chem*, **271**, 19415-20.
- Hubert, R. S., Mitchell, S., Chen, X. N., Ekmekji, K., Gadowski, C., Sun, Z., et al. BAC and PAC contigs covering 3.5 Mb of the Down syndrome congenital heart disease region between D21S55 and MX1 on chromosome 21. (1997) *Genomics*, **41**, 218-26.
- Hudson, T. J., Engelstein, M., Lee, M. K., Ho, E. C., Rubenfield, M. J., Adams, C. P., et al. Isolation and chromosomal assignment of 100 highly informative human simple sequence repeat polymorphisms. (1992) *Genomics*, **13**, 622-9.
- Hudson, T. J., Stein, L. D., Gerety, S. S., Ma, J., Castle, A. B., Silva, J., et al. An STS-based map of the human genome. (1995) *Science*, **270**, 1945-54.
- Huntington's Disease Collaborative Research Group, T. A novel gene containing a trinucleotide repeat that is expanded and unstable on Huntington's disease chromosomes. (1993) *Cell*, **72**, 971-83.
- Hurst, L. D. and Eyre-Walker, A. Evolutionary genomics: reading the bands. (2000) *Bioessays*, **22**, 105-7.
- International Human Genome Sequencing Consortium, T. Initial sequencing and analysis of the human genome. (2001) *Nature*, **409**, 860-921.
- International SNP Map Working Group, T. A map of human genome sequence variation containing 1.42 million single nucleotide polymorphisms. (2001) *Nature*, **409**, 928-33.
- Ioannou, P. A., Amemiya, C. T., Garnes, J., Kroisel, P. M., Shizuya, H., Chen, C., et al. A new bacteriophage P1-derived vector for the propagation of large human DNA fragments. (1994) *Nat Genet*, **6**, 84-9.
- Irizarry, K., Kustanovich, V., Li, C., Brown, N., Nelson, S., Wong, W., et al. Genome-wide analysis of single-nucleotide polymorphisms in human expressed sequences. (2000) *Nat Genet*, **26**, 233-6.
- Isbrandt, D., Leicher, T., Waldschutz, R., Zhu, X., Luhmann, U., Michel, U., et al. Gene structures and expression profiles of three human KCND (Kv4) potassium channels mediating A-type currents I(TO) and I(SA). (2000) *Genomics*, **64**, 144-54.

- Jang, W., Hua, A., Spilson, S. V., Miller, W., Roe, B. A. and Meisler, M. H. Comparative sequence of human and mouse BAC clones from the mnd2 region of chromosome 2p13. (1999) *Genome Res*, **9**, 53-61.
- Jeffers, M., Paciucci, R. and Pellicer, A. Characterization of unr; a gene closely linked to N-ras. (1990) *Nucleic Acids Res*, **18**, 4891-9.
- Jeffreys, A. J., Wilson, V. and Thein, S. L. Hypervariable 'minisatellite' regions in human DNA. (1985) *Nature*, **314**, 67-73.
- Jones, J. M., Morrell, J. C. and Gould, S. J. Identification and characterization of HAOX1, HAOX2, and HAOX3, three human peroxisomal 2-hydroxy acid oxidases. (2000) *J Biol Chem*, **275**, 12590-7.
- Jurka, J. Sequence patterns indicate an enzymatic involvement in integration of mammalian retroposons. (1997) *Proc Natl Acad Sci U S A*, **94**, 1872-7.
- Kan, Y. W. and Dozy, A. M. Polymorphism of DNA sequence adjacent to human beta-globin structural gene: relationship to sickle mutation. (1978) *Proc Natl Acad Sci U S A*, **75**, 5631-5.
- Karvonen, M. K., Pesonen, U., Heinonen, P., Laakso, M., Rissanen, A., Naukkarinen, H., et al. Identification of new sequence variants in the leptin gene. (1998) *J Clin Endocrinol Metab*, **83**, 3239-42.
- Kent, W. J. BLAT--the BLAST-like alignment tool. (2002) *Genome Res*, **12**, 656-64.
- Kessler, M. M., Beckendorf, R. C., Westhafer, M. A. and Nordstrom, J. L. Requirement of A-A-U-A-A and adjacent downstream sequences for SV40 early polyadenylation. (1986) *Nucleic Acids Res*, **14**, 4939-52.
- Khan, A. S., Wilcox, A. S., Hopkins, J. A. and Sikela, J. M. Efficient double stranded sequencing of cDNA clones containing long poly(A) tails using anchored poly(dT) primers. (1991) *Nucleic Acids Res*, **19**, 1715.
- Khan, S. G., Muniz-Medina, V., Shahlavi, T., Baker, C. C., Inui, H., Ueda, T., et al. The human XPC DNA repair gene: arrangement, splice site information content and influence of a single

- nucleotide polymorphism in a splice acceptor site on alternative splicing and function. (2002) *Nucleic Acids Res*, **30**, 3624-31.
- Kiechle, M., Hinrichs, M., Jacobsen, A., Luttges, J., Pfisterer, J., Kommoss, F., et al. Genetic imbalances in precursor lesions of endometrial cancer detected by comparative genomic hybridization. (2000) *Am J Pathol*, **156**, 1827-33.
- Kim, U. J., Shizuya, H., de Jong, P. J., Birren, B. and Simon, M. I. Stable propagation of cosmid sized human DNA inserts in an F factor based vector. (1992) *Nucleic Acids Res*, **20**, 1083-5.
- Kimberling, W. J., Weston, M. D., Moller, C., Davenport, S. L., Shugart, Y. Y., Priluck, I. A., et al. Localization of Usher syndrome type II to chromosome 1q. (1990) *Genomics*, **7**, 245-9.
- Kitayama, H., Sugimoto, Y., Matsuzaki, T., Ikawa, Y. and Noda, M. A ras-related gene with transformation suppressor activity. (1989) *Cell*, **56**, 77-84.
- Knight, J. C., Udalova, I., Hill, A. V., Greenwood, B. M., Peshu, N., Marsh, K., et al. A polymorphism that affects OCT-1 binding to the TNF promoter region is associated with severe malaria. (1999) *Nat Genet*, **22**, 145-50.
- Kohara, Y., Akiyama, K. and Isono, K. The physical map of the whole E. coli chromosome: application of a new strategy for rapid analysis and sorting of a large genomic library. (1987) *Cell*, **50**, 495-508.
- Kohl, S., Baumann, B., Rosenberg, T., Kellner, U., Lorenz, B., Vadala, M., et al. Mutations in the cone photoreceptor G-protein alpha-subunit gene GNAT2 in patients with achromatopsia. (2002) *Am J Hum Genet*, **71**, 422-5.
- Kondo, S., Schutte, B. C., Richardson, R. J., Bjork, B. C., Knight, A. S., Watanabe, Y., et al. Mutations in IRF6 cause Van der Woude and popliteal pterygium syndromes. (2002) *Nat Genet*, **32**, 285-9.
- Kondoh, N., Nishina, Y., Tsuchida, J., Koga, M., Tanaka, H., Uchida, K., et al. Assignment of synaptonemal complex protein 1 (SCP1) to human chromosome 1p13 by fluorescence in situ hybridization and its expression in the testis. (1997) *Cytogenet Cell Genet*, **78**, 103-4.

- Kondrashov, A. S. and Shabalina, S. A. Classification of common conserved sequences in mammalian intergenic regions. (2002) *Hum Mol Genet*, **11**, 669-74.
- Kong, A., Gudbjartsson, D. F., Sainz, J., Jonsdottir, G. M., Gudjonsson, S. A., Richardsson, B., et al. A high-resolution recombination map of the human genome. (2002) *Nat Genet*, **31**, 241-7.
- Koop, B. F. and Hood, L. Striking sequence similarity over almost 100 kilobases of human and mouse T-cell receptor DNA. (1994) *Nat Genet*, **7**, 48-53.
- Kozak, M. An analysis of 5'-noncoding sequences from 699 vertebrate messenger RNAs. (1987) *Nucleic Acids Res*, **15**, 8125-48.
- Kritzler, R. A., Turner, J. Y., Lindenbaum, J., Magidson, J., Williams, R., Preisig, R., Phillips, G. B. Chediak-Higashi syndrome: cytologic and serum lipid observations in a case and family. (1964) *Am. J. Med*, **36**, 583-594.
- Kruglyak, L. and Nickerson, D. A. Variation is the spice of life. (2001) *Nat Genet*, **27**, 234-6.
- Kudoh, J., Nagamine, K., Asakawa, S., Abe, I., Kawasaki, K., Maeda, H., et al. Localization of 16 exons to a 450-kb region involved in the autoimmune polyglandular disease type I (APECED) on human chromosome 21q22.3. (1997) *DNA Res*, **4**, 45-52.
- Kupfer, K., Smith, M. W., Quackenbush, J. and Evans, G. A. Physical mapping of complex genomes by sampled sequencing: a theoretical analysis. (1995) *Genomics*, **27**, 90-100.
- Labay, V., Raz, T., Baron, D., Mandel, H., Williams, H., Barrett, T., et al. Mutations in SLC19A2 cause thiamine-responsive megaloblastic anaemia associated with diabetes mellitus and deafness. (1999) *Nat Genet*, **22**, 300-4.
- Lachance, Y., Luu-The, V., Verreault, H., Dumont, M., Rheaume, E., Leblanc, G., et al. Structure of the human type II 3 beta-hydroxysteroid dehydrogenase/delta 5-delta 4 isomerase (3 beta-HSD) gene: adrenal and gonadal specificity. (1991) *DNA Cell Biol*, **10**, 701-11.
- Lahat, H., Pras, E., Olender, T., Avidan, N., Ben-Asher, E., Man, O., et al. A missense mutation in a highly conserved region of CASQ2 is associated with autosomal recessive catecholamine-induced polymorphic ventricular tachycardia in Bedouin families from Israel. (2001) *Am J Hum Genet*, **69**, 1378-84.

- Lamerdin, J. E. and Carrano, A. V. Automated fluorescence-based restriction fragment analysis. (1993) *Biotechniques*, **15**, 294-303.
- Larsen, F., Gundersen, G., Lopez, R. and Prydz, H. CpG islands as gene markers in the human genome. (1992) *Genomics*, **13**, 1095-107.
- Lee, K. A., Kim, S. H., Woo, H. Y., Hong, Y. J. and Cho, H. C. Increased frequencies of glutathione S-transferase (GSTM1 and GSTT1) gene deletions in Korean patients with acquired aplastic anemia. (2001) *Blood*, **98**, 3483-5.
- Levine, A. and Durbin, R. A computational scan for U12-dependent introns in the human genome sequence. (2001) *Nucleic Acids Res*, **29**, 4006-13.
- Levy-Lahad, E., Wijsman, E. M., Nemens, E., Anderson, L., Goddard, K. A., Weber, J. L., et al. A familial Alzheimer's disease locus on chromosome 1. (1995) *Science*, **269**, 970-3.
- Li, W. H. and Sadler, L. A. Low nucleotide diversity in man. (1991) *Genetics*, **129**, 513-23.
- Liang, F., Holt, I., Pertea, G., Karamycheva, S., Salzberg, S. L. and Quackenbush, J. Gene index analysis of the human genome estimates approximately 120,000 genes. (2000) *Nat Genet*, **25**, 239-40.
- Litt, M. and Luty, J. A. A hypervariable microsatellite revealed by in vitro amplification of a dinucleotide repeat within the cardiac muscle actin gene. (1989) *Am J Hum Genet*, **44**, 397-401.
- Little, P., Curtis, P., Coutelle, C., Van den Berg, J., Dagleish, R., Malcolm, S., et al. Isolation and partial sequence of recombinant plasmids containing human alpha-, beta- and gamma-globin cDNA fragments. (1978) *Nature*, **273**, 640-3.
- Liu, H., Nakagawa, T., Kanematsu, T., Uchida, T. and Tsuji, S. Isolation of 10 differentially expressed cDNAs in differentiated Neuro2a cells induced through controlled expression of the GD3 synthase gene. (1999) *J Neurochem*, **72**, 1781-90.
- Loetscher, P., Alvarez-Gonzalez, R. and Althaus, F. R. Poly(ADP-ribose) may signal changing metabolic conditions to the chromatin of mammalian cells. (1987) *Proc Natl Acad Sci U S A*, **84**, 1286-9.

- Makalowski, W., Zhang, J. and Boguski, M. S. Comparative analysis of 1196 orthologous mouse and human full-length mRNA and protein sequences. (1996) *Genome Res*, **6**, 846-57.
- Mallon, A. M., Platzter, M., Bate, R., Gloeckner, G., Botcherby, M. R., Nordsiek, G., et al. Comparative genome sequence analysis of the Bpa/Str region in mouse and Man. (2000) *Genome Res*, **10**, 758-75.
- Mannervik, B. and Danielson, U. H. Glutathione transferases--structure and catalytic activity. (1988) *CRC Crit Rev Biochem*, **23**, 283-337.
- Marcelino, J., Carpten, J. D., Suwairi, W. M., Gutierrez, O. M., Schwartz, S., Robbins, C., et al. CACP, encoding a secreted proteoglycan, is mutated in camptodactyly-arthropathy-coxa vara-pericarditis syndrome. (1999) *Nat Genet*, **23**, 319-22.
- Marra, M., Kucaba, T., Sekhon, M., Hillier, L., Martienssen, R., Chinwalla, A., et al. A map for sequence analysis of the Arabidopsis thaliana genome. (1999) *Nat Genet*, **22**, 265-70.
- Marra, M. A., Kucaba, T. A., Dietrich, N. L., Green, E. D., Brownstein, B., Wilson, R. K., et al. High throughput fingerprint analysis of large-insert clones. (1997) *Genome Res*, **7**, 1072-84.
- Marshall, E. Drug firms to create public database of genetic mutations. (1999) *Science*, **284**, 406-7.
- Marth, G., Yeh, R., Minton, M., Donaldson, R., Li, Q., Duan, S., et al. Single-nucleotide polymorphisms in the public domain: how useful are they? (2001) *Nat Genet*, **27**, 371-2.
- Mattick, J. S. Non-coding RNAs: the architects of eukaryotic complexity. (2001) *EMBO Rep*, **2**, 986-91.
- Maxam, A. M. and Gilbert, W. A new method for sequencing DNA. (1977) *Proc Natl Acad Sci U S A*, **74**, 560-4.
- McPherson, J. D., Marra, M., Hillier, L., Waterston, R. H., Chinwalla, A., Wallis, J., et al. A physical map of the human genome. (2001) *Nature*, **409**, 934-41.
- Meek, T. D., Dayton, B. D., Metcalf, B. W., Dreyer, G. B., Strickler, J. E., Gorniak, J. G., et al. Human immunodeficiency virus 1 protease expressed in Escherichia coli behaves as a dimeric aspartic protease. (1989) *Proc Natl Acad Sci U S A*, **86**, 1841-5.

- Mercher, T., Coniat, M. B., Monni, R., Mauchauffe, M., Khac, F. N., Gressin, L., et al. Involvement of a human gene related to the *Drosophila* spen gene in the recurrent t(1;22) translocation of acute megakaryocytic leukemia. (2001) *Proc Natl Acad Sci U S A*, **98**, 5776-9.
- Milpetz, F., Argos, P. and Persson, B. TMAP: a new email and WWW service for membrane-protein structural predictions. (1995) *Trends Biochem Sci*, **20**, 204-5.
- Mirzoeva, S., Weigand, S., Lukas, T. J., Shuvalova, L., Anderson, W. F. and Watterson, D. M. Analysis of the functional coupling between calmodulin's calcium binding and peptide recognition properties. (1999) *Biochemistry*, **38**, 3936-47.
- Misra, S., 1, 2, Madeline A Crosby³, Christopher J Mungall^{2, 4}, Beverley B Matthews³, Kathryn S Campbell³, Pavel Hradecky³, Yanmei Huang³, Joshua S Kaminker^{1, 2}, Gillian H Millburn⁵, Simon E Prochnik^{1, 2}, Christopher D Smith^{1, 2}, Jonathan L Tupy^{1, 2}, Eleanor J Whitfield⁶, Leyla Bayraktaroglu³, Benjamin P Berman¹, Brian R Bettencourt³, Susan E Celniker⁷, Aubrey DNJ de Grey⁵, Rachel A Drysdale⁵, Nomi L Harris^{2, 7}, John Richter⁴, Susan Russo³, Andrew J Schroeder³, Sheng Qiang Shu^{1, 2}, Mark Stapleton⁷, Chihiro Yamada⁵, Michael Ashburner⁵, William M Gelbart³, Gerald M Rubin^{1, 2, 4, 7} and Suzanna E Lewis^{1, 2}
Annotation of the *Drosophila melanogaster* euchromatic genome: a systematic review. (2002) *Genome Biology*, **3**.
- Mochizuki, N., Cho, G., Wen, B. and Insel, P. A. Identification and cDNA cloning of a novel human mosaic protein, LGN, based on interaction with G alpha i2. (1996) *Gene*, **181**, 39-43.
- Modrek, B. and Lee, C. A genomic view of alternative splicing. (2002) *Nat Genet*, **30**, 13-9.
- Moore, M. J. and Sharp, P. A. Evidence for two active sites in the spliceosome provided by stereochemistry of pre-mRNA splicing. (1993) *Nature*, **365**, 364-8.
- Morton, N. E. Parameters of the human genome. (1991) *Proc Natl Acad Sci U S A*, **88**, 7474-6.
- Mouse Genome Sequencing Consortium, T. Initial sequencing and comparative analysis of the mouse genome. (2002) *Nature*, **420**, 520-62.

- Mulligan, L. M., Kwok, J. B., Healey, C. S., Elsdon, M. J., Eng, C., Gardner, E., et al. Germ-line mutations of the RET proto-oncogene in multiple endocrine neoplasia type 2A. (1993) *Nature*, **363**, 458-60.
- Mullikin, J. C., Hunt, S. E., Cole, C. G., Mortimore, B. J., Rice, C. M., Burton, J., et al. An SNP map of human chromosome 22. (2000) *Nature*, **407**, 516-20.
- Mungall, A. J., Edwards, C. A., Ranby, S. A., Humphray, S. J., Heathcott, R. W., Clee, C. M., et al. Physical mapping of chromosome 6: a strategy for the rapid generation of sequence-ready contigs. (1996) *DNA Seq*, **7**, 47-9.
- Murray, J. C., Buetow, K. H., Weber, J. L., Ludwigsen, S., Scherpbier-Heddema, T., Manion, F., et al. A comprehensive human linkage map with centimorgan density. Cooperative Human Linkage Center (CHLC). (1994) *Science*, **265**, 2049-54.
- Murzin, A. G., Brenner, S. E., Hubbard, T. and Chothia, C. SCOP: a structural classification of proteins database for the investigation of sequences and structures. (1995) *J Mol Biol*, **247**, 536-40.
- Myers, E. W., Sutton, G. G., Smith, H. O., Adams, M. D. and Venter, J. C. On the sequencing and assembly of the human genome. (2002) *Proc Natl Acad Sci U S A*, **99**, 4145-6.
- Nagasaki, K., Maass, N., Manabe, T., Hanzawa, H., Tsukada, T., Kikuchi, K., et al. Identification of a novel gene, DAM1, amplified at chromosome 1p13.3-21 region in human breast cancer cell lines. (1999) *Cancer Lett*, **140**, 219-26.
- Nagase, T., Ishikawa, K., Suyama, M., Kikuno, R., Hirose, M., and Miyajima, N., Tanaka, A., Kotani, H., Nomura, N. and Ohara, O. Prediction of the coding sequences of unidentified human genes.
- XII. The complete sequences of 100 new cDNA clones from brain which code for large proteins in vitro. (1998) *Dna Research*, **5**, 355-364.
- Nagata, T., Mugishima, H., Shichino, H., Suzuki, T., Chin, M., Koshinaga, S., et al. Karyotypic analyses of hepatoblastoma. Report of two cases and review of the literature suggesting

- chromosomal loci responsible for the pathogenesis of this disease. (1999) *Cancer Genet Cytogenet*, **114**, 42-50.
- Nakachi, K., Imai, K., Hayashi, S., Watanabe, J. and Kawajiri, K. Genetic susceptibility to squamous cell carcinoma of the lung in relation to cigarette smoking dose. (1991) *Cancer Res*, **51**, 5177-80.
- Nakamura, Y., Leppert, M., O'Connell, P., Wolff, R., Holm, T., Culver, M., et al. Variable number of tandem repeat (VNTR) markers for human gene mapping. (1987) *Science*, **235**, 1616-22.
- Navia, M. A., Fitzgerald, P. M., McKeever, B. M., Leu, C. T., Heimbach, J. C., Herber, W. K., et al. Three-dimensional structure of aspartyl protease from human immunodeficiency virus HIV-1. (1989) *Nature*, **337**, 615-20.
- Nicholas, K. B., Nicholas H.B. , and Deerfield, D.W. GeneDoc: Analysis and Visualization of Genetic Variation. (1997) *EMBNEW.NEWS*, **4**.
- Ning, Z., Cox, A. J. and Mullikin, J. C. SSAHA: a fast search method for large DNA databases. (2001) *Genome Res*, **11**, 1725-9.
- Nitta, N., Ochiai, M., Nagao, M. and Sugimura, T. Amino-acid substitution at codon 13 of the N-ras oncogene in rectal cancer in a Japanese patient. (1987) *Jpn J Cancer Res*, **78**, 21-6.
- Okubo, K., Hori, N., Matoba, R., Niiyama, T., Fukushima, A., Kojima, Y., et al. Large scale cDNA sequencing for analysis of quantitative and qualitative aspects of gene expression. (1992) *Nat Genet*, **2**, 173-9.
- Oliver, J. L. and Marín, A. A relationship between GC content and coding-sequence length. (1996) *Journal Of Molecular Evolution*, **43**, 216-23.
- Olson, M., Hood, L., Cantor, C. and Botstein, D. A common language for physical mapping of the human genome. (1989) *Science*, **245**, 1434-5.
- Olson, M. V., Dutchik, J. E., Graham, M. Y., Brodeur, G. M., Helms, C., Frank, M., et al. Random-clone strategy for genomic restriction mapping in yeast. (1986) *Proc Natl Acad Sci U S A*, **83**, 7826-30.

- Olson, M. V. and Green, P. Criterion for the completeness of large-scale physical maps of DNA. (1993) *Cold Spring Harb Symp Quant Biol*, **58**, 349-55.
- Orias, M., Bray-Ward, P., Curran, M. E., Keating, M. T. and Desir, G. V. Genomic localization of the human gene for KCNA10, a cGMP-activated K channel. (1997) *Genomics*, **42**, 33-7.
- Pan, S. S., Han, Y., Farabaugh, P. and Xia, H. Implication of alternative splicing for expression of a variant NAD(P)H:quinone oxidoreductase-1 with a single nucleotide polymorphism at 465C>T. (2002) *Pharmacogenetics*, **12**, 479-88.
- Parvari, R., HersHKovitz, E., Grossman, N., Gorodischer, R., Loeys, B., Zecic, A., et al. Mutation of TBCE causes hypoparathyroidism-retardation-dysmorphism and autosomal recessive Kenny-Caffey syndrome. (2002) *Nat Genet*, **32**, 448-52.
- Pearl, L. H. and Taylor, W. R. Sequence specificity of retroviral proteases. (1987a) *Nature*, **328**, 482.
- Pearl, L. H. and Taylor, W. R. A structural model for the retroviral proteases. (1987b) *Nature*, **329**, 351-4.
- Peitsch, M. C. and Jongeneel, C. V. A 3-D model for the CD40 ligand predicts that it is a compact trimer similar to the tumor necrosis factors. (1993) *Int Immunol*, **5**, 233-8.
- Pemble, S., Schroeder, K. R., Spencer, S. R., Meyer, D. J., Hallier, E., Bolt, H. M., et al. Human glutathione S-transferase theta (GSTT1): cDNA cloning and the characterization of a genetic polymorphism. (1994) *Biochem J*, **300** (Pt 1), 271-6.
- Pennacchio, L. A., Olivier, M., Hubacek, J. A., Cohen, J. C., Cox, D. R., Fruchart, J. C., et al. An apolipoprotein influencing triglycerides in humans and mice revealed by comparative sequencing. (2001) *Science*, **294**, 169-73.
- Pennacchio, L. A. and Rubin, E. M. Genomic strategies to identify mammalian regulatory sequences. (2001) *Nat Rev Genet*, **2**, 100-9.
- Pericak-Vance, M. A., Bebout, J. L., Gaskell, P. C., Jr., Yamaoka, L. H., Hung, W. Y., Alberts, M. J., et al. Linkage studies in familial Alzheimer disease: evidence for chromosome 19 linkage. (1991) *Am J Hum Genet*, **48**, 1034-50.

- Persson, B. and Argos, P. Prediction of transmembrane segments in proteins utilising multiple sequence alignments. (1994) *J Mol Biol*, **237**, 182-92.
- Petersen, C. M., Nielsen, M. S., Nykjaer, A., Jacobsen, L., Tommerup, N., Rasmussen, H. H., et al. Molecular identification of a novel candidate sorting receptor purified from human brain by receptor-associated protein affinity chromatography. (1997) *J Biol Chem*, **272**, 3599-605.
- Pfost, D. R., Boyce-Jacino, M. T. and Grant, D. M. A SNPshot: pharmacogenetics and the future of drug therapy. (2000) *Trends Biotechnol*, **18**, 334-8.
- Picoult-Newberg, L., Ideker, T. E., Pohl, M. G., Taylor, S. L., Donaldson, M. A., Nickerson, D. A., et al. Mining SNPs from EST databases. (1999) *Genome Res*, **9**, 167-74.
- Pinkel, D., Landegent, J., Collins, C., Fuscoe, J., Segraves, R., Lucas, J., et al. Fluorescence in situ hybridization with human chromosome-specific libraries: detection of trisomy 21 and translocations of chromosome 4. (1988) *Proc Natl Acad Sci U S A*, **85**, 9138-42.
- Pinkel, D., Straume, T. and Gray, J. W. Cytogenetic analysis using quantitative, high-sensitivity, fluorescence hybridization. (1986) *Proc Natl Acad Sci U S A*, **83**, 2934-8.
- Platzer, M., Rotman, G., Bauer, D., Uziel, T., Savitsky, K., Bar-Shira, A., et al. Ataxia-telangiectasia locus: sequence analysis of 184 kb of human genomic DNA containing the entire ATM gene. (1997) *Genome Res*, **7**, 592-605.
- Rabbitts, T. H. Bacterial cloning of plasmids carrying copies of rabbit globin messenger RNA. (1976) *Nature*, **260**, 221-5.
- Ragoussis, J., and Olavesen, M.G. (1997) *Chromosome walking*, O.U.P.
- Raich, N., Mattei, M. G., Romeo, P. H. and Beaupain, D. PHTF, a novel atypical homeobox gene on chromosome 1p13, is evolutionarily conserved. (1999) *Genomics*, **59**, 108-9.
- Ramashwami, M., Gautam, M., Kamb, A.A., Rudy, B., Tanouye, M.A. and Mathew, M.K. Human potassium channel genes: molecular cloning and functional expression. (1990) *Mol Cell Biol Neurosci*, **1**, 214 - 223.

- Rao, P. H., Houldsworth, J., Dyomina, K., Parsa, N. Z., Cigudosa, J. C., Louie, D. C., et al. Chromosomal and gene amplification in diffuse large B-cell lymphoma. (1998) *Blood*, **92**, 234-40.
- Reymond, A., Meroni, G., Fantozzi, A., Merla, G., Cairo, S., Luzi, L., et al. The tripartite motif family identifies cell compartments. (2001) *Embo J*, **20**, 2140-51.
- Riles, L., Dutchik, J. E., Baktha, A., McCauley, B. K., Thayer, E. C., Leckie, M. P., et al. Physical maps of the six smallest chromosomes of *Saccharomyces cerevisiae* at a resolution of 2.6 kilobase pairs. (1993) *Genetics*, **134**, 81-150.
- Roach, J. C., Boysen, C., Wang, K. and Hood, L. Pairwise end sequencing: a unified approach to genomic mapping and sequencing. (1995) *Genomics*, **26**, 345-53.
- Roest Crollius, H., Jaillon, O., Bernot, A., Dasilva, C., Bouneau, L., Fischer, C., et al. Estimate of human gene number provided by genome-wide analysis using *Tetraodon nigroviridis* DNA sequence. (2000) *Nat Genet*, **25**, 235-8.
- Roses, A. D. Pharmacogenetics and the practice of medicine. (2000) *Nature*, **405**, 857-65.
- Roses, A. D. Genome-based pharmacogenetics and the pharmaceutical industry. (2002) *Nat Rev Drug Discov*, **1**, 541-9.
- Royle, N. J., Clarkson, R. E., Wong, Z. and Jeffreys, A. J. Clustering of hypervariable minisatellites in the proterminal regions of human autosomes. (1988) *Genomics*, **3**, 352-60.
- Sabina, R. L., Fishbein, W. N., Pezeshkpour, G., Clarke, P. R. and Holmes, E. W. Molecular analysis of the myoadenylate deaminase deficiencies. (1992) *Neurology*, **42**, 170-9.
- Saiki, R. K., Gelfand, D. H., Stoffel, S., Scharf, S. J., Higuchi, R., Horn, G. T., et al. Primer-directed enzymatic amplification of DNA with a thermostable DNA polymerase. (1988) *Science*, **239**, 487-91.
- Salvatore, C. A., Jacobson, M. A., Taylor, H. E., Linden, J. and Johnson, R. G. Molecular cloning and characterization of the human A3 adenosine receptor. (1993) *Proc Natl Acad Sci U S A*, **90**, 10365-9.

- Sanger, F., Air, G. M., Barrell, B. G., Brown, N. L., Coulson, A. R., Fiddes, C. A., et al. Nucleotide sequence of bacteriophage phi X174 DNA. (1977) *Nature*, **265**, 687-95.
- Sanger, F., Coulson, A. R., Friedmann, T., Air, G. M., Barrell, B. G., Brown, N. L., et al. The nucleotide sequence of bacteriophage phiX174. (1978) *J Mol Biol*, **125**, 225-46.
- Sanger, F., Coulson, A. R., Hong, G. F., Hill, D. F. and Petersen, G. B. Nucleotide sequence of bacteriophage lambda DNA. (1982) *J Mol Biol*, **162**, 729-73.
- Saupe, S., Roizes, G., Peter, M., Boyle, S., Gardiner, K. and De Sario, A. Molecular cloning of a human cDNA IGSF3 encoding an immunoglobulin-like membrane protein: expression and mapping to chromosome band 1p13. (1998) *Genomics*, **52**, 305-11.
- Scherf, M., Klingenhoff, A. and Werner, T. Highly specific localization of promoter regions in large genomic sequences by PromoterInspector: a novel context analysis approach. (2000) *J Mol Biol*, **297**, 599-606.
- Schuler, G. D. Sequence mapping by electronic PCR. (1997) *Genome Res*, **7**, 541-50.
- Schuler, G. D., Boguski, M. S., Stewart, E. A., Stein, L. D., Gyapay, G., Rice, K., et al. A gene map of the human genome. (1996) *Science*, **274**, 540-6.
- Schutte, B. C., Carpten, J. D., Forus, A., Gregory, S. G., Horii, A. and White, P. S. Report and abstracts of the sixth international workshop on human chromosome 1 mapping 2000. Iowa City, Iowa, USA. 30 September-3 October 2000. (2001) *Cytogenet Cell Genet*, **92**, 23-41.
- Sedlacek, Z., Korn, B., Konecki, D. S., Siebenhaar, R., Coy, J. F., Kioschis, P., et al. Construction of a transcription map of a 300 kb region around the human G6PD locus by direct cDNA selection. (1993) *Hum Mol Genet*, **2**, 1865-9.
- Seed, B., Aruffo A. Molecular cloning of the CD2 antigen, the T-cell erythrocyte receptor, by a rapid immunoselection procedure. (1987) *Proc Natl Acad Sci U S A*, **84**.
- Seidegard, J., Vorachek, W. R., Pero, R. W. and Pearson, W. R. Hereditary differences in the expression of the human glutathione transferase active on trans-stilbene oxide are due to a gene deletion. (1988) *Proc Natl Acad Sci U S A*, **85**, 7293-7.

- Shackleton, S., Lloyd, D. J., Jackson, S. N., Evans, R., Niermeijer, M. F., Singh, B. M., et al. LMNA, encoding lamin A/C, is mutated in partial lipodystrophy. (2000) *Nat Genet*, **24**, 153-6.
- Shen, L. X., Basiilion, J. P. and Stanton, V. P., Jr. Single-nucleotide polymorphisms can cause different structural folds of mRNA. (1999) *Proc Natl Acad Sci U S A*, **96**, 7871-6.
- Sherry, S. T., Ward, M. H., Kholodov, M., Baker, J., Phan, L., Smigielski, E. M., et al. dbSNP: the NCBI database of genetic variation. (2001) *Nucleic Acids Res*, **29**, 308-11.
- Shimada, T., Fujii, H. and Lin, H. A 165-base pair sequence between the dihydrofolate reductase gene and the divergently transcribed upstream gene is sufficient for bidirectional transcriptional activity. (1989) *J Biol Chem*, **264**, 20171-4.
- Shizuya, H., Birren, B., Kim, U. J., Mancino, V., Slepak, T., Tachiiri, Y., et al. Cloning and stable maintenance of 300-kilobase-pair fragments of human DNA in *Escherichia coli* using an F-factor-based vector. (1992) *Proc Natl Acad Sci U S A*, **89**, 8794-7.
- Skolnick, J. and Fetrow, J. S. From genes to protein structure and function: novel applications of computational approaches in the genomic era. (2000) *Trends Biotechnol*, **18**, 34-9.
- Slim, R., Le Paslier, D., Compain, S., Levilliers, J., Ougen, P., Billault, A., et al. Construction of a yeast artificial chromosome contig spanning the pseudoautosomal region and isolation of 25 new sequence-tagged sites. (1993) *Genomics*, **16**, 691-7.
- Smit, A. F. Interspersed repeats and other mementos of transposable elements in mammalian genomes. (1999) *Curr Opin Genet Dev*, **9**, 657-63.
- Soderlund, C., Longden, I. and Mott, R. FPC: a system for building contigs from restriction fingerprinted clones. (1997) *Comput Appl Biosci*, **13**, 523-35.
- Solovyev, V. V., Salamov, A. A. and Lawrence, C. B. Predicting internal exons by oligonucleotide composition and discriminant analysis of spliceable open reading frames. (1994) *Nucleic Acids Res*, **22**, 5156-63.
- Solovyev, V. V., Salamov, A. A. and Lawrence, C. B. Identification of human gene structure using linear discriminant functions and dynamic programming. (1995) *Proc Int Conf Intell Syst Mol Biol*, **3**, 367-75.

- Sonnhammer, E. L. and Durbin, R. A dot-matrix program with dynamic threshold control suited for genomic DNA and protein sequence analysis. (1995) *Gene*, **167**, GC1-10.
- Sonnhammer, E. L., von Heijne, G. and Krogh, A. A hidden Markov model for predicting transmembrane helices in protein sequences. (1998) *Proc Int Conf Intell Syst Mol Biol*, **6**, 175-82.
- Soriano, P., Meunier-Rotival, M. and Bernardi, G. The distribution of interspersed repeats is nonuniform and conserved in the mouse and human genomes. (1983) *Proc Natl Acad Sci U S A*, **80**, 1816-20.
- Sparkes, R. S. C., V. H.; Mohandas, T.; Zollman, S.; Cire-Eversole, P.; Amatruda, T. T.; Reed, R. R.; Lochrie, M. A.; Simon, M. I Mapping of genes encoding the subunits of guanine nucleotide-binding protein (G-proteins) in humans. (1987) *Cytogenet Cell Genet*, **46**, 696.
- Staden, R. A new computer method for the storage and manipulation of DNA gel reading data. (1980) *Nucleic Acids Res*, **8**, 3673-94.
- Strittmatter, W. J., Saunders, A. M., Schmechel, D., Pericak-Vance, M., Enghild, J., Salvesen, G. S., et al. Apolipoprotein E: high-avidity binding to beta-amyloid and increased frequency of type 4 allele in late-onset familial Alzheimer disease. (1993) *Proc Natl Acad Sci U S A*, **90**, 1977-81.
- Sudo, K., Chinen, K. and Nakamura, Y. 2058 expressed sequence tags (ESTs) from a human fetal lung cDNA library. (1994) *Genomics*, **24**, 276-9.
- Sunyaev, S., Ramensky, V., Koch, I., Lathe, W., 3rd, Kondrashov, A. S. and Bork, P. Prediction of deleterious human alleles. (2001) *Hum Mol Genet*, **10**, 591-7.
- Taillon-Miller, P., Gu, Z., Li, Q., Hillier, L. and Kwok, P. Y. Overlapping genomic sequences: a treasure trove of single-nucleotide polymorphisms. (1998) *Genome Res*, **8**, 748-54.
- Takahashi, Y., Campbell, E. A., Hirata, Y., Takayama, T. and Listowsky, I. A basis for differentiating among the multiple human Mu-glutathione S-transferases and molecular cloning of brain GSTM5. (1993) *J Biol Chem*, **268**, 8893-8.

- Tang, X., Wang, Y., Li, H. O., Sakatsume, O., Sarai, A. and Yokoyama, K. DNA fingerprinting involving fluorescence-labeled termini of any enzymatically generated fragments of DNA. (1994) *Jpn J Hum Genet*, **39**, 379-91.
- Taniguchi, T., Fujii-Kuriyama, Y. and Muramatsu, M. Molecular cloning of human interferon cDNA. (1980) *Proc Natl Acad Sci U S A*, **77**, 4003-6.
- Tao, Q., Chang, Y-L., Wang, J., Huaming, C., Islam-Faridi, M.N., Scheuring, C. Wang, B., Stelly, D.M. Zhang, H-B. Bacterial Artificial Chromosome-Based Physical Map of the Rice Genome Constructed by Restriction Fingerprint Analysis. (2001) *Genetics*, **158**, 1711-1724.
- Taylor, K., Hornigold, N., Conway, D., Williams, D., Ulinowski, Z., Agochiya, M., et al. Mapping the human Y chromosome by fingerprinting cosmid clones. (1996) *Genome Res*, **6**, 235-48.
- Thierry-Mieg, D. a. A C. elegans DataBase. (1994) *unpublished*.
- Thiery, J. P., Macaya, G. and Bernardi, G. An analysis of eukaryotic genomes by density gradient centrifugation. (1976) *J Mol Biol*, **108**, 219-35.
- Thomas, J. W., Prasad, A. B., Summers, T. J., Lee-Lin, S. Q., Maduro, V. V., Idol, J. R., et al. Parallel construction of orthologous sequence-ready clone contig maps in multiple species. (2002) *Genome Res*, **12**, 1277-85.
- Thompson, J. D., Higgins, D. G. and Gibson, T. J. CLUSTAL W: improving the sensitivity of progressive multiple sequence alignment through sequence weighting, position-specific gap penalties and weight matrix choice. (1994) *Nucleic Acids Res*, **22**, 4673-80.
- Thornton, J. M., Orengo, C. A., Todd, A. E. and Pearl, F. M. Protein folds, functions and evolution. (1999) *J Mol Biol*, **293**, 333-42.
- Tilghman, S. M., Tiemeier, D. C., Seidman, J. G., Peterlin, B. M., Sullivan, M., Maizel, J. V., et al. Intervening sequence of DNA identified in the structural portion of a mouse beta-globin gene. (1978) *Proc Natl Acad Sci U S A*, **75**, 725-9.
- Tkachuk, D. C., Westbrook, C. A., Andreeff, M., Donlon, T. A., Cleary, M. L., Suryanarayan, K., et al. Detection of bcr-abl fusion in chronic myelogenous leukemia by in situ hybridization. (1990) *Science*, **250**, 559-62.

- Tremblay, L. O., Campbell Dyke, N. and Herscovics, A. Molecular cloning, chromosomal mapping and tissue-specific expression of a novel human alpha1,2-mannosidase gene involved in N-glycan maturation. (1998) *Glycobiology*, **8**, 585-95.
- Trenkle, T., McClelland, M., Adlkofer, K. and Welsh, J. Major transcript variants of VAV3, a new member of the VAV family of guanine nucleotide exchange factors. (2000) *Gene*, **245**, 139-49.
- Trofatter, J. A., MacCollin, M. M., Rutter, J. L., Murrell, J. R., Duyao, M. P., Parry, D. M., et al. A novel moesin-, ezrin-, radixin-like gene is a candidate for the neurofibromatosis 2 tumor suppressor. (1993) *Cell*, **75**, 826.
- Tsukino, H., Kuroda, Y., Qiu, D., Nakao, H., Imai, H. and Katoh, T. Effects of cytochrome P450 (CYP) 2A6 gene deletion and CYP2E1 genotypes on gastric adenocarcinoma. (2002) *Int J Cancer*, **100**, 425-8.
- Uberbacher, E. C., Xu, Y. and Mural, R. J. Discovering and understanding genes in human DNA sequence using GRAIL. (1996) *Methods Enzymol*, **266**, 259-81.
- Van den Bergh, F., Sabina RL. Characterization of human AMP deaminase 2 (AMPD2) gene expression reveals alternative transcripts encoding variable N-terminal extensions of isoform L. (1995) *Biochem J*, **312**, 401-410.
- Vega-Saenz de Miera, E., Moreno H, Fruhling D, Kentros C, Rudy B. Cloning of ShIII (Shaw-like) cDNAs encoding a novel high-voltage-activating, TEA-sensitive, type-A K⁺ channel. (1992) *Proc R Soc Lond B Biol Sci*, **248**, 9-18.
- Venter, J. C., Adams, M. D., Myers, E. W., Li, P. W., Mural, R. J., Sutton, G. G., et al. The sequence of the human genome. (2001) *Science*, **291**, 1304-51.
- Verma, I. M., Temple, G. F., Fan, H. and Baltimore, D. In vitro synthesis of DNA complementary to rabbit reticulocyte 10S RNA. (1972) *Nat New Biol*, **235**, 163-7.
- Vetrie, D. Isolation of the defective gene in X linked agammaglobulinaemia. (1993) *J Med Genet*, **30**, 452-3.

- Vorachek, W. R., Pearson, W. R. and Rule, G. S. Cloning, expression, and characterization of a class-mu glutathione transferase from human muscle, the product of the GST4 locus. (1991) *Proc Natl Acad Sci U S A*, **88**, 4443-7.
- Walker, A. P., Muscatelli, F. and Monaco, A. P. Isolation of the human Xp21 glycerol kinase gene by positional cloning. (1993) *Hum Mol Genet*, **2**, 107-14.
- Wallace, M. R., Marchuk, D. A., Andersen, L. B., Letcher, R., Odeh, H. M., Saulino, A. M., et al. Type 1 neurofibromatosis gene: identification of a large transcript disrupted in three NF1 patients. (1990) *Science*, **249**, 181-6.
- Wallner, B. P., Frey, A. Z., Tizard, R., Mattaliano, R. J., Hession, C., Sanders, M. E., et al. Primary structure of lymphocyte function-associated antigen 3 (LFA-3). The ligand of the T lymphocyte CD2 glycoprotein. (1987) *J Exp Med*, **166**, 923-32.
- Wang, D. G., Fan, J. B., Siao, C. J., Berno, A., Young, P., Sapolsky, R., et al. Large-scale identification, mapping, and genotyping of single-nucleotide polymorphisms in the human genome. (1998) *Science*, **280**, 1077-82.
- Wang, M., Duell, T., Gray, J. W. and Weier, H.-U. G. High sensitivity, high resolution physical mapping by fluorescence *in situ* hybridisation on to individually straightened DNA molecules. (1996) *Bioimaging*, **4**, 73-83.
- Wang, X., Zuckerman, B., Pearson, C., Kaufman, G., Chen, C., Wang, G., et al. Maternal cigarette smoking, metabolic gene polymorphism, and infant birth weight. (2002) *Jama*, **287**, 195-202.
- Wang, Z. and Moulton, J. SNPs, protein structure, and disease. (2001) *Hum Mutat*, **17**, 263-70.
- Waterston, R. H., Lander, E. S. and Sulston, J. E. On the sequencing of the human genome. (2002) *Proc Natl Acad Sci U S A*, **99**, 3712-6.
- Watson, J. D. a. C., F. A Structure for Deoxyribose Nucleic Acid. (1953) *Nature*, **171**, 171.
- Weber, J. L. and May, P. E. Abundant class of human DNA polymorphisms which can be typed using the polymerase chain reaction. (1989) *Am J Hum Genet*, **44**, 388-96.
- Weissenbach, J., Gyapay, G., Dib, C., Vignal, A., Morissette, J., Millasseau, P., et al. A second-generation linkage map of the human genome. (1992) *Nature*, **359**, 794-801.

- White, P. S., Forus, A., Matise, T. C., Schutte, B. C., Spieker, N., Stanier, P., et al. Report of the fifth international workshop on human chromosome 1 mapping 1999. (1999) *Cytogenet Cell Genet*, **87**, 143-71.
- Wickens, M. P., Buell, G. N. and Schimke, R. T. Synthesis of double-stranded DNA complementary to lysozyme, ovomucoid, and ovalbumin mRNAs. Optimization for full length second strand synthesis by *Escherichia coli* DNA polymerase I. (1978) *J Biol Chem*, **253**, 2483-95.
- Wilke, C. M., Guo, S. W., Hall, B. K., Boldog, F., Gemmill, R. M., Chandrasekharappa, S. C., et al. Multicolor FISH mapping of YAC clones in 3p14 and identification of a YAC spanning both FRA3B and the t(3;8) associated with hereditary renal cell carcinoma. (1994) *Genomics*, **22**, 319-26.
- Wyman, A. R. and White, R. A highly polymorphic locus in human DNA. (1980) *Proc Natl Acad Sci USA*, **77**, 6754-8.
- Xiang, Z., Morse, E., Hu, X. L., Flint, J., Chi, H. C., Grady, D. L., et al. A sequence-ready map of the human chromosome 1q telomere. (2001) *Genomics*, **72**, 105-7.
- Xie, Y. G., Han, F. Y., Peyrard, M., Ruttledge, M. H., Fransson, I., DeJong, P., et al. Cloning of a novel, anonymous gene from a megabase-range YAC and cosmid contig in the neurofibromatosis type 2/meningioma region on human chromosome 22q12. (1993) *Hum Mol Genet*, **2**, 1361-8.
- Xu, C. F., Chambers, J. A. and Solomon, E. Complex regulation of the BRCA1 gene. (1997) *J Biol Chem*, **272**, 20994-7.
- Xu, S., Wang, Y., Roe, B. and Pearson, W. R. Characterization of the human class Mu glutathione S-transferase gene cluster and the GSTM1 deletion. (1998) *J Biol Chem*, **273**, 3517-27.
- Zachmann, M. and Prader, A. Unusual heterozygotes of congenital adrenal hyperplasia due to 21-hydroxylase deficiency confirmed by HLA tissue typing. (1979) *Acta Endocrinol (Copenh)*, **92**, 542-6.

Zattara-Cannoni, H., Roll, P., Figarella-Branger, D., Lena, G., Dufour, H., Grisoli, F., et al.

Cytogenetic study of six cases of radiation-induced meningiomas. (2001) *Cancer Genet Cytogenet*, **126**, 81-4.

Zoubak, S., Clay, O. and Bernardi, G. The gene distribution of the human genome. (1996) *Gene*, **174**, 95-102.

Genome Mapping by Fluorescent Fingerprinting

Simon G. Gregory,¹ Gareth R. Howell, and David R. Bentley

The Sanger Centre, Wellcome Trust Genome Campus, Hinxton, Cambridgeshire CB10 1SA, UK

The construction of sequence-ready maps of overlapping genomic clones is central to large-scale genome sequencing. We have implemented a method for fluorescent fingerprinting of bacterial clones to assemble contig maps. The method utilizes three spectrally distinct fluorescently tagged dideoxy ATPs to specifically label the *Hind*III termini in *Hind*III and *Sau*3AI restriction digests of clones that are multiplexed prior to electrophoresis and data collection. There is excellent reproducibility of raw data, improved resolution of large fragments, and concordance between the results obtained using this and the equivalent radioactive protocol. This method also allows detection of smaller overlaps between clones when compared to the analysis of restriction digests on nondenaturing agarose gels.

Central to large-scale genomic sequencing is the construction of sequence-ready maps containing ordered sets of overlapping clones. To make the best choice of clones for the minimally overlapping set (or tiling path), the optimal strategy is to assemble a deep contig using a method that provides accurate information on the extent of each clone and its neighbors. Restriction digest fingerprinting can be used to process large numbers of bacterial clones rapidly and economically. Restriction patterns are visualized by polyacrylamide or agarose gel electrophoresis and can be scanned and analyzed to identify statistically significant overlaps. This information is then used to assemble contigs either automatically or following visual inspection of the raw data.

The approach was first developed to assemble contigs of cosmids or bacteriophage λ clones of the *Caenorhabditis elegans* (Coulson et al. 1986) and *Saccharomyces cerevisiae* (Olson et al. 1986; Riles et al. 1993) genomes, respectively. In the *C. elegans* project, purified cosmid DNA was digested with *Hind*III, end labeled, and recut with *Sau*3AI. The sizes of the products were then determined following electrophoresis on sequencing gels to obtain maximum resolution. The technique of generating overlapping fragment sets has also been used as the basis for other mapping projects with the aim of producing sequence-ready maps (Carrano et al. 1989; Heding et al. 1992; Taylor et al. 1996). As larger projects are undertaken, there is a need to streamline robust

methods by incorporating increased levels of automation, safety, and convenience so that they may be scaled up. With this aim in mind we have implemented a fluorescent fingerprinting technique based on the methods used in the *C. elegans* project by Coulson et al. (1986), with the modifications of Taylor et al. (1996) and Tang et al. (1994).

We have developed a one-reaction technique where purified bacterial clone DNA is digested with *Hind*III and *Sau*3AI, with the *Hind*III ends being specifically labeled with one of three fluorescent dye-labeled dideoxynucleotides in preparation for multiplexing and electrophoresis on a polyacrylamide gel. Fingerprint data are collected using a model 377 automated DNA sequencer (Perkin Elmer Applied Biosystems), analyzed, and visually checked before entry into the database.

RESULTS

The following developments were required to implement nonisotopic fingerprinting on a large scale. First, the "microprep" procedure to prepare clone DNAs in a 96-well format was modified as follows: The supernatants from the alkaline lysis step were passed through a filter-bottomed microtiter plate before isopropanol precipitation, and the samples were resuspended in T0.1E containing RNase and stored overnight at 4°C. This protocol resulted in an increased yield and, hence, signal intensity of the fingerprints, and also increased the pass rate from ~80%–90% to >95% using cosmids, fosmids, P1 or bacterial artificial chromosome [PAC (Iaonnou et al. 1994) or BAC (Shizuya et al. 1992), respectively] clones. We defined pass rate as the pro-

¹Corresponding author.
E-MAIL sgg@sanger.ac.uk; FAX (01223) 494919.

portion of clones producing fingerprints of sufficient quality to warrant data entry and analysis, expressed as a percentage of the total number of clones selected for DNA preparation and fingerprinting. The most common cause of fingerprint failure was poor quality or low-yield DNA preparations (data not shown).

Second, we substituted the previous marker set (a *Sau3AI* digest of λ DNA) with a *Bsa*II digest of λ DNA, which produced a more even distribution of fragments across the complete size range required. The optimum temperature for this enzyme was also compatible with the conditions used for end labeling by *Taq* FS polymerase, so that both steps could be carried out in a single reaction.

Third, the new fluorescently labeled dideoxy adenosine triphosphate (ddATP) derivatives were synthesized with the fluorophore dyes TET or NED attached (kindly provided by P.E. Applied Biosystems). As these and the previously available HEX ddATP are all fluoresceine derivatives (see Fig. 1), the mobility difference of identical fragments labeled with different fluorophores was identical (data not shown), thus eliminating the need for correction during analysis. The availability of the three different fluorescently tagged ddATP molecules allowed us to multiplex three clone fingerprints plus the marker digest in each lane of the gel (Fig. 2a).

All data were collected using ABI 377 Prism Collection software (v. 1.1), and the unprocessed gel images were downloaded onto a UNIX workstation from which the data file could be imported into *Image 3* (for more details concerning the installation and documentation of the Image software, see <http://www.sanger.ac.uk/Software/Image>) for further editing (Fig. 2b) before transfer to fingerprinted contigs (FPC) (Soderlund et al. 1997) for analysis (Sulston et al. 1988; Fig. 2c). This eliminated all of the gel processing, autoradiography, and scanning required for radioactive fingerprinting. Collection of the data in real time also improved the resolution of the larger fragments. This, when coupled with incorporation of the standard marker set in each lane, allowed us to determine the relative mobility of each fragment in the 30-bp to 2.8-kb size range detected by the marker digest with greater accuracy than was previously possible. This improvement is especially valuable for analysis of the more complex fingerprint patterns of clones with larger inserts (data not shown).

Some variation in the intensity of labeling across the size range of fingerprint bands was noted. The intensity of these bands proved to be consistent between the fingerprints of overlapping clones. We

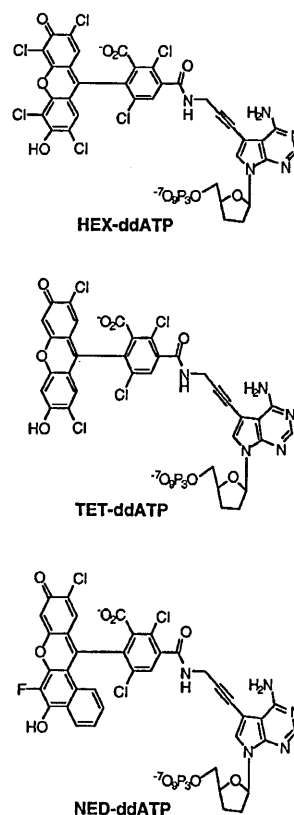


Figure 1 A representation of the chemical structures of HEX, TET, and NED, the three identically sized fluorophores used to produce fluorescent fingerprints.

believe that the observed band-specific variation is caused by the local context (sequence and/or conformation) at the ends of the DNA fragments being labeled by the Thermosequencase.

Unlike the single enzyme agarose-based fingerprinting methods (M. Marra, pers. comm.), we were not able to detect band multiplicity. The identification of bands of identical size and migration rate corresponding to a relative increase in signal strength of fingerprint bands is of less significance as the *Hind*III-*Sau*3AI fingerprints do not represent all of the cloned insert (see later).

The same PAC clone was fingerprinted 10 times with each of the three dyes and compared. All fingerprints were highly reproducible. The migration of specific fragments in independent fingerprints of the same or different clones was found to be the same within the tolerances set. In all cases examined, the variation of migration of bands in 30 independent fingerprints was $\pm 0.25\%$ (maximum observed; i.e., $\pm 11/4500$ intervals), which is less than the tolerance used in the analysis.

Next we fingerprinted the 49 PAC clones of a

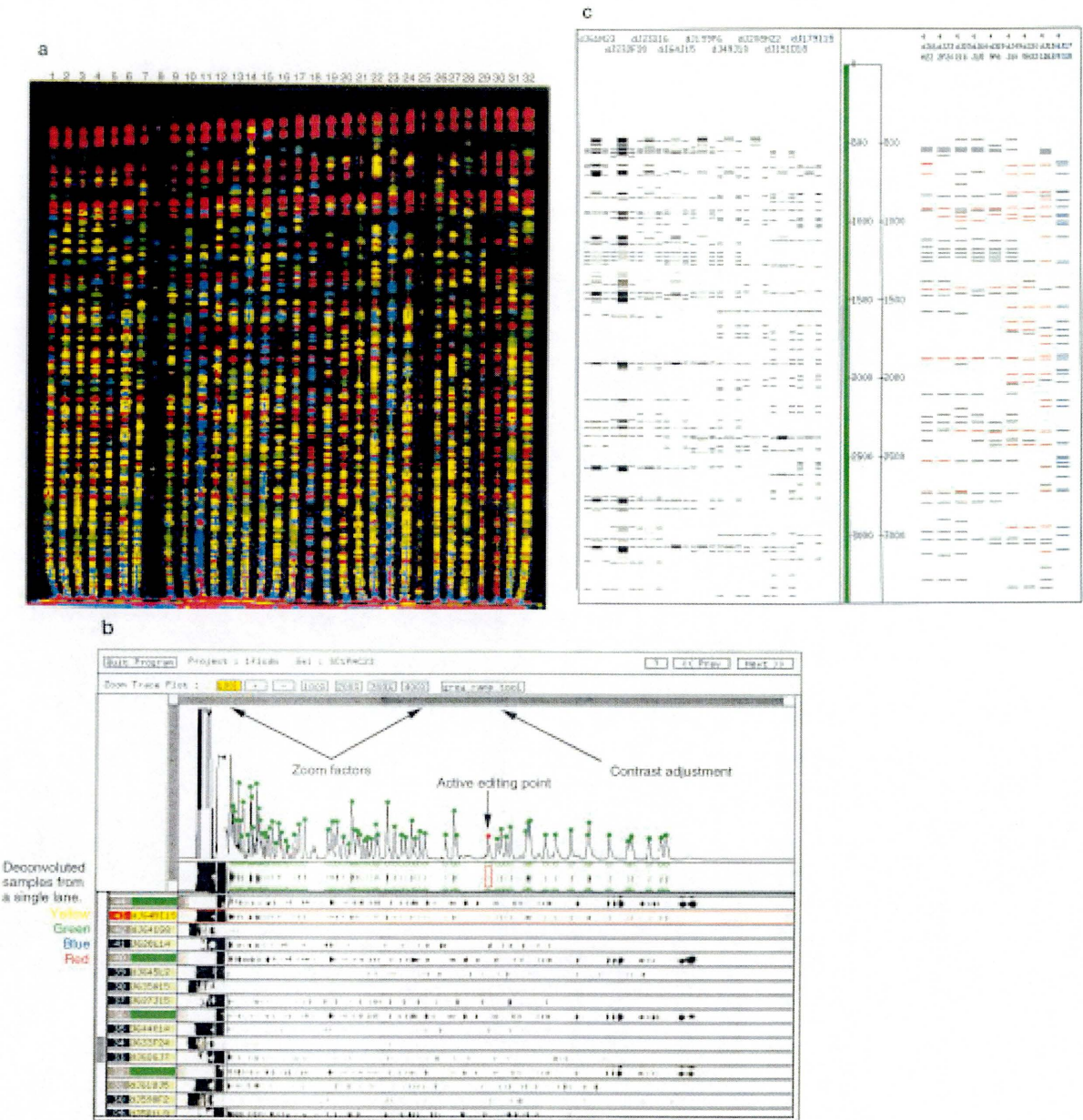


Figure 2 Fluorescent fingerprint electrophoresis data, entry, and analysis. (a) The gel image of a fluorescent fingerprint gel (ABI Prism GeneScan Analysis 2.0.2). The 32-lane gel contains three clones in each well, giving a present capacity of 96 clones per run. We are updating our collection of software to double the number of lanes per gel. (b) Editing of fingerprint bands using *Image3*. (c) Digitized images of gel traces and corresponding fingerprints in FPC.

1400-kb contig by both radioactive and fluorescent methods and compared another nonisotopic method in which digests of purified clone DNA are separated on SYBR green-stained agarose gels and the data are collected using a Fluorimager (Molecular Dynamics). Analysis of the data and contig as-

sembly was performed independently. The assembly results of each of the four different methods were compared to the overlaps defined by sequencing of the 14 clones of a minimum set (Fig. 3a). Vertical arrows in Figure 3b represent the overlaps that were not found between clones in each of the

four methods. Figure 3c represents the contigs as constructed by the fluorescent fingerprinting method. The vertical arrows coincide with those in Figure 3b, denoting overlaps that were not detected by fingerprinting alone. There was excellent agreement between the contigs assembled using either the radioactive or fluorescent *Hind*III-*Sau*3AI data. Minor variations were observed where small overlaps between clones fell just outside the probability cutoff used. (These overlaps were originally detected by end-probe hybridization and later confirmed by the sequence.)

There was also good agreement between the *Hind*III-*Sau*3AI results and those of the *Hind*III and *Eco*RI fingerprints resolved on agarose gels, but matches in the latter protocols required a higher statistical probability of overlap, that is, smaller overlaps were not detected. This can be attributed in part to the fact that each agarose fingerprint pattern is divided into 2000 intervals along a lane as opposed to the 3400 and 4500 intervals of the radioactive and fluorescent fingerprints, respectively. A smaller number of intervals implies that there is a greater probability that bands will occur randomly in the same bin and contribute to background matches. However, it should be pointed out that the two approaches are both useful in different ways. The *Hind*III-*Sau*3AI method can detect smaller overlaps, but samples 256/4096 bp (14%) of the insert DNA of a clone and provides no information on the remainder of the sequence. In contrast, the use of complete *Eco*RI, *Hind*III, or similar digests resolved on agarose gels, although achieving lower resolution, does display bands representing all of the DNA of the cloned insert. The latter method is therefore more appropriate for verifying the integrity of the sequence compared to all genomic clones covering the re-

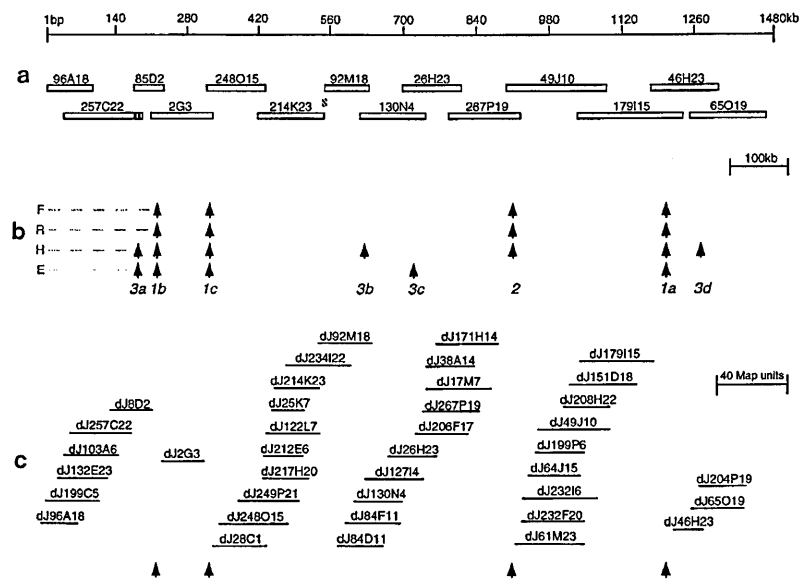


Figure 3 Comparative fingerprinting data of 49 clones covering a 1400-kb interval sequence that was determined from 14 clones comprising a minimum tiling path and a PCR product between 214K23 and 92M18 (hatched). (a) Finished sequence data were used to define the overlaps between clones and absolute length of each of the clones (except 257C22, where data were incomplete). (b) Vertical arrows denote overlaps that were not detected by each method. (F) Fluorescence, (R) radioactive; (H) *Hind*III, and (E) *Eco*RI. As expected, there is variation based on recognition sites between the overlaps detected using *Hind*III (3b and 3d) and those established with *Eco*RI (3c). Details of the analysis of undetected overlaps are as follows: (Overlap 1a, 62 kb) Nine *Hind*III and 11 *Eco*RI fragments are present in this overlap on the basis of DNA sequence. Statistical probability on the basis of these bands shared between 179I15 and 46H23 is 1×10^{-4} (–4) fluorescence, –1 radioactive, –4 *Hind*III, and –5 *Eco*RI (whose probability cutoffs for all matches are –4, –5, –7, and –7, respectively). (Overlap 1b, 25 kb) Clone 2G3 is unattached. Three *Hind*III or six *Eco*RI fragments shared with clone 85D2 are insufficient to score the overlap. (Overlap 1c, 11 kb) Clone 2G3 is unattached. Four *Hind*III or three *Eco*RI fragments shared with clone 248O15 are insufficient to detect the overlap. (Overlap 2, 24 kb) Overlap between 267P19 and 49J10 was not found by any of the *Hind*III methods. Six *Hind*III fragments are not sufficient to detect overlap. Arrows 3a–3d denote where only the agarose methods failed to find overlap. (Overlap 3a) Overlap between 257C22 and 85D2 could not be determined because of incomplete overlap data and therefore was not analyzed. (Overlap 3b, 18 kb) Four *Hind*III fragments shared between 130N4 and 92M18 are not sufficient to detect overlap. (Overlap 3c, 44 kb) Six *Eco*RI fragments shared between 130N4 and 267P19 are not sufficient to detect overlap. (Overlap 3d, 55 kb) 16 *Hind*III fragments between 46H23 and 65O19 should have been significant. The lack of overlap may be attributed to the migration of similar-sized fragments in the same location of the agarose gel and therefore not be representative of the cloned insert. (c) Although all but 1 of the 49 clones (2G3) fell into contigs, only 4 of the contigs that lie within the sequence interval are represented. Arrows denote where the overlaps between clones were not found.

gion. It also confers the ability to identify possible deletions or other rearrangements that result in de-

tectable size alterations in individual restriction fragments.

Where all four methods failed to detect overlaps between adjacent clones (Fig. 3b, overlaps 1a–1c), the overlapping bands were only contained within two clones. This problem would be resolved with greater contig depth. Details of analysis of overlaps that were not detected by individual methods are given in the legend to Figure 3.

In a more extensive comparison of fluorescent and radioactive methods, 96 and 785 clones were analyzed independently on chromosomes X and 1, respectively, using both fingerprinting methods. The initial pass rate of the fluorescent fingerprinting was markedly higher for the chromosome 1 analysis (87%), as compared to the radioactive method (65%). When repeat fingerprints were included in the data sets for both projects fluorescent fingerprinting yielded a marginally higher overall pass rate of 96% as opposed to 90% radioactively. Closer inspection of the analyzed fingerprint data revealed the same number of contigs had been generated that contained the same clones in identical order (data not shown). We are currently using the fluorescent fingerprinting technique in our chromosome mapping projects on chromosomes 1, 6, 20, and X. To date, we have fluorescently fingerprinted a total of 12,500 clones (generating 1216 contigs), which provide an estimated 156 Mb in contigs of sequence-ready map.

DISCUSSION

The advent of large-insert bacterial clone libraries of PACs and BACs for construction of high-resolution maps has facilitated sequencing and gene identification in chromosomal regions. Initial identification of the clones is achieved by using hybridization- or PCR-based markers to screen the available libraries. The degree of coverage of the region obtained following screening depends on the initial marker density and distribution. In regions of high marker density (when multiple markers are found in each bacterial clone) the existence of overlaps between clones may be identified on the basis of shared marker content. However, as a marker represents one point in the genomic DNA, no measure of the extent of overlap is obtained, and in most regions of the human genome at present the marker density is too low to achieve closure of all gaps by marker content alone. Fingerprinting can detect overlaps where there is no marker available and gives an indication of the extent of each overlap.

Alternative methods to define overlaps between

bacterial clones include the hybridization of end probes to clone arrays (Evans and Lewis 1989), high-resolution fluorescence in situ hybridization (FISH) using DNA fibers (Wang et al. 1996), and matching of end sequences to complete insert sequences (Kupfer et al. 1995; Roach et al. 1995). End-probe hybridizations do not define the extent of overlap, and the approach is not easily scaled up. The same limitation is true of whole cosmid-to-cosmid hybridizations (Xie et al. 1993), and all hybridization-based methods employing undefined sequences can yield false-positive signals because of cross-hybridization of repeat motifs. The end-sequencing strategy provides precise information on extent of overlap but relies on extensive prior investment in sequencing all the clones in the library and also does not permit assembly of contigs prior to sequencing of the inserts. Fiber-FISH, using bacterial clones as probes and yeast artificial chromosomes (YACs) as a target, provides good estimates of both the extent of overlaps and sizes of gaps between clones but requires the existence of a well-defined YAC map across the region of interest and has yet to be scaled up.

Previous approaches to fluorescent-based fingerprinting include ligation of fluorochrome-labeled oligonucleotide adaptors to *EcoRI* digests of cosmids that were resolved on agarose gels (Lamerdin and Carrano 1993); this is now superseded by the VISTRA-green-stained agarose gel fingerprints (M. Marra, pers. comm.) as used here. Our approach has extended this to multiplex *HindIII*–*Sau3AI* fingerprints of three clones (plus markers) using three novel dye-ddA terminators, thus enabling automatic data collection of 96 clones, increasing to 192 clones with 64 lane upgrades, for a 4.5-hr run and a steady-state throughput of 400 clones per person per week including analysis.

METHODS

Bacterial Clone DNA Preparation

Our microprep method is based on the alkaline lysis procedure of Birnboim and Doly (1979) and produces ~200 ng of PAC, BAC, fosmid, and cosmid DNA. Bacterial cultures (500 μ l) in 2 \times TY containing the appropriate antibiotic, were grown in 1-ml deep-well microtiter plates (Beckman), with shaking at 300 rpm at 37°C for 18 hr. A portion of the culture (250 μ l) was then transferred using a 50- to 250-multichannel pipette (Finnpipette) to a "U"-bottom microtiter plate (Greiner), and the cells were pelleted by centrifugation at 1000g for 4 min (PAC and BAC clones) or 2 min (cosmids, fosmids). The supernatant was discarded and the pellet resuspended by gently vortexing the pellet. Twenty-five microliters of solution I (50 mM glucose, 25 mM Tris, 1 mM EDTA, stored

at 4°C) was added to the wells using a 5- to 50-multichannel pipette (Finnpipette) and mixed by carefully tapping the side of the plate. Twenty-five microliters of solution II (0.2 M NaOH, 1% SDS, made fresh) was added and mixed as before, and left at room temperature for 5 min until the solution cleared. Twenty-five microliters of cold solution III (3.5 M K acetate, stored at 4°C) was added and mixed as described previously, and left at room temperature for 5 min. The total well volume was transferred to a 2 µm filter-bottomed plate (Millipore), which had been taped in place on a U-bottom microtiter plate (Greiner) containing 100 µl of isopropanol, and spun at 2500 rpm for 2 min at 20°C. After the filter plate was removed, the microtiter plate was left at room temperature for 30 min before spinning at 3200 rpm for 20 min at 20°C. The supernatant was removed, and the precipitated DNA was dried briefly before washing with 100 µl of 70% ethanol. After spinning at 3200 rpm the supernatant was removed, and the pellet was dried to ensure no ethanol remained and resuspended in 5 µl of T0.1E (pH 7.4) with RNase (10 mg/ml). Samples were stored at -20°C.

Fluorescent Marker

Three microliters of λ DNA (500 ng/µl NEB) was digested with 3.0 µl of *Bsa*II (2.5 U/µl) and labeled with 2.0 µl of ROX ddC (5.08 µM) (PE-ABI, cat. no. 402117) using 2.0 µl *Taq* FS (8 U/µl) in the presence of 5.0 µl of NEB2 buffer and 35.0 µl of T0.1E (pH 7.4) in a 500-µl microcentrifuge tube for 1 hr at 60°C. The DNA was recovered by the addition of 50.0 µl of 0.3 M Na acetate and 200 µl of 96% ethanol. The contents of the tube were mixed briefly by vortexing, left at room temperature (in the dark) for 15 min and then at -20°C for 20 min before spinning at 14,000 rpm for 20 min. After the supernatant was discarded the pellet was resuspended in 60.0 µl of T0.1E (pH 7.4) and 60.0 µl of blue dextran formamide dye (9.8 ml deionized formamide, 200 µl of 0.5 M EDTA, 0.01 grams of blue dextran), and mixed before use.

Fluorescent Fingerprinting

Reactions were carried out individually in wells of a U-bottom microtiter plate (Greiner) as follows. The fingerprinting mix for each fluorescent labeling reaction constituted 2.8 units of *Hind*III (20 U/µl), 3.7 units of Thermo Sequenase (32 U/µl) [or *Taq* FS (8 U/µl)], 0.14 µl of fluorescent ddA (10 µM) (HEX 403036c, NED 402997c, TET 402998c), and 3 units of *Sau*3AI (30 U/µl). Twenty microliters from the reaction mix was added to the clone DNA sample using a Hamilton repeat dispenser and incubated at 37°C for 1 hr. Seven microliters of 0.3 M Na acetate and 40.0 µl of 96% ethanol were added to each well, and appropriate samples (three differently labeled fragments) were pooled and the microtiter plate spun at 3200 rpm at 20°C for 20 min. The pellet was washed, by the addition of 100 µl of 70% ethanol, spun for 20 min at 20°C, and dried and resuspended in 5 µl of T0.1E. Two microliters of the marker solution was added to each well. The samples were denatured on a heated block for 10 min at 80°C prior to loading on a 377 Automated DNA Sequencer using a 0.2-mm, 12-cm, well-to-read 4.5% denaturing polyacrylamide gel and 64 lane combination. Reaction products were stored overnight at -20°C, when necessary, prior to the addition of the marker.

ACKNOWLEDGMENTS

We thank Louise McDonald, Deborah Scott, and the other

members of the fingerprinting group for testing the method; Marco Marra for advice concerning the development of the prepping method; Jillian Durham for help with sequence determination; and Richard Henfrey and Martin Johnson (PE Applied Biosystems) for technical advice and for arranging a supply of the new fluorescently labeled terminators. We also thank Darren Platt and Friedemann Wobus for developing and supporting the Image software.

The publication costs of this article were defrayed in part by payment of page charges. This article must therefore be hereby marked "advertisement" in accordance with 18 USC section 1734 solely to indicate this fact.

REFERENCES

- Birnboim H.C. and J. Doly. 1979. A rapid alkaline extraction procedure for screening recombinant plasmid DNA. *Nucleic Acids Res.* **7**: 1513-1523.
- Carrano, A.V., J. Lamerdin, L.K. Ashworth, B. Watkins, E. Branscomb, T. Slezak, M. Raff, P.J. de Jong, D. Keith, and L. McBride. 1989. A high-resolution, fluorescence-based, semiautomated method for DNA fingerprinting. *Genomics* **4**: 129-136.
- Coulson, A., J. Sulston, S. Brenner, and J. Karn. 1986. Toward a physical map of the genome of the nematode *Caenorhabditis elegans*. *Proc. Natl. Acad. Sci.* **83**: 7821-7825.
- Evans, G.A. and K.A. Lewis. 1989. Physical mapping of complex genomes by cosmid multiplex analysis. *Proc. Natl. Acad. Sci.* **86**: 5030-5034.
- Heding, I.J.J.P., A. Ivens, J. Wilson, M. Strivens, S. Gregory, J.M. Hoovers, M. Mannens, B. Redeker, D. Porteous, V. van Heyningen, and P.F.R. Little. 1992. The generation of ordered sets of cosmid DNA clones from human chromosome region 11p. *Genomics* **13**: 89-94.
- Iaonnou, I., C.T. Amemiya, J. Garnes, P.M. Kroisel, H. Shizuya, C. Chen, M.A. Batzer, and P.J. de Jong. 1994. A new bacteriophage P1-derived vector for the propagation of large human DNA fragments. *Nature Genet.* **6**: 84-89.
- Kupfer, K., M.W. Smith, J. Quackenbush, and G.A. Evans. 1995. Physical mapping of complex genomes by sampled sequencing: A theoretical analysis. *Genomics* **27**: 90-100.
- Lamerdin, J.E. and A.V. Carrano. 1993. Automated fluorescence-based restriction fragment analysis. *BioTechniques* **5**: 294-303.
- Olson, M.V., J.E. Dutchik, M.Y. Graham, G.M. Brodeur, C. Helms, M. Frank, M. MacCollin, R. Scheinman, and T. Frank. 1986. Random-clone strategy for genomic restriction mapping in yeast. *Proc. Natl. Acad. Sci.* **83**: 7826-7830.
- Riles L., J.E. Dutchik, A. Baktha, B.K. McCauley, E.C. Thayer, M.P. Leckie, V.V. Braden, J.E. Depke, and M.V. Olson. 1993. Physical maps of the six smallest chromosomes of *Saccharomyces cerevisiae* at the resolution of 2.6 kilobase pairs. *Genetics* **134**: 81-150.

GREGORY ET AL.

- Roach, J.C., C. Boysen, K. Wang, and L. Hood. 1995. Pairwise end sequencing: A unified approach to genomic mapping and sequencing. *Genomics* **26**: 345-353.
- Shizuya, H., B. Birren, U.J. Kim, V. Mancino, T. Slepak, Y. Tachiiri, and M. Simon. 1992. Cloning and stable maintenance of 330-kilobase-pair fragments of human DNA in *Escherichia coli* using an F-factor based vector. *Proc. Natl. Acad. Sci.* **89**: 8794-8797.
- Soderlund, C., I. Longden, and R. Mott. 1997. FPC: A system for building contigs from restriction fingerprinted clones. *Comput. Appl. Biosci.* **13**: 523-535.
- Sulston, J.E., F. Mallett, R. Durbin, and T. Horsnell. 1988. Software for genome mapping by fingerprinting techniques. *Comput. Appl. Biosci.* **4**: 125-132.
- Tang, X., Y. Wang, O. Li-Ho, O. Sakatsume, A. Sarai, and K. Yokoyama. 1994. DNA fingerprinting involving fluorescence-labeled termini of any enzymatically generated fragments of DNA. *BioTechniques Jpn. J. Hum. Genet.* **39**: 379-391.
- Taylor, K., N. Hornigold, D. Conway, D. Williams, Z. Ulinowski, M. Agochiya, P. Fattorini, P. de Jong, P.F.R. Little, and J. Wolfe. 1996. Mapping the human Y chromosome by fingerprinting cosmid clones. *Genome Res.* **6**: 235-248.
- Wang, M., T. Duell, J.W. Gray, and H.-U.G. Weier. 1996. High sensitivity, high resolution physical mapping by fluorescence *in situ* hybridisation on to individually straightened DNA molecules. *Bioimaging* **4**: 73-83.
- Xie, Y.G., F.Y. Han, M. Peyrard, M.H. Rutledge, I. Fransson, P. de Jong, J. Collins, I. Dunham, M. Nordenskjold, and J.P. Dumanski. 1993. Cloning of a novel, anonymous gene from a megabase-range YAC and cosmid contig in the neurofibromatosis type 2/meningioma region on human chromosome 22q12. *Hum. Mol. Genet.* **29**: 1361-1368.

Received May 22, 1997; accepted in revised form October 21, 1997.

The physical maps for sequencing human chromosomes 1, 6, 9, 10, 13, 20 and X

D. R. Bentley*, P. Deloukas*, A. Dunham*, L. French*, S. G. Gregory*, S. J. Humphray*, A. J. Mungall*, M. T. Ross*, N. P. Carter*, I. Dunham*, C. E. Scott*, K. J. Ashcroft*, A. L. Atkinson*, K. Aubin*, D. M. Beare*, G. Bethel*, N. Brady*, J. C. Brook*, D. C. Burford*, W. D. Burrill*, C. Burrows*, A. P. Butler*, C. Carder*, J. J. Catanese†, C. M. Clee*, S. M. Clegg*, V. Copley*, A. J. Coffey*, C. G. Cole*, J. E. Collins*, J. S. Conquer*, R. A. Cooper*, K. M. Culley*, E. Dawson*, F. L. Dearden*, R. M. Durbin*, P. J. de Jong†, P. D. Dhami*, M. E. Earthrowl*, C. A. Edwards*, R. S. Evans*, C. J. Gillson*, J. Ghorl*, L. Green*, R. Gwilliam*, K. S. Halls*, S. Hammond*, G. L. Harper*, R. W. Heathcott*, J. L. Holden*, E. Holloway*, B. L. Hopkins*, P. J. Howard*, G. R. Howell*, E. J. Huckle*, J. Hughes*, P. J. Hunt*, S. E. Hunt*, M. Izmajlowicz*, C. A. Jones*, S. S. Joseph*, G. Laird*, C. F. Langford*, M. H. Levasalho*, M. A. Leversha*, O. T. McCann*, L. M. McDonald*, J. McDowall*, G. L. Maslen*, D. Milstry*, N. K. Moschonas‡, V. Neocleous\$, D. M. Pearson*, K. J. Phillips*, K. M. Porter*, S. R. Prathalingam*, Y. H. Ramsey*, S. A. Ranby*, C. M. Rice*, J. Rogers*, L. J. Rogers*, T. Sarafidou‡, D. J. Scott*, G. J. Sharp*, C. J. Shaw-Smith*, L. J. Smink*, C. Soderlund*, E. C. Sotheran*, H. E. Steingruber*, J. E. Sulston*, A. Taylor*, R. G. Taylor*, A. A. Thorpe*, E. Tinsley*, G. L. Warry*, A. Whittaker*, P. Whittaker*, S. H. Williams*, T. E. Wilmer*, R. Wooster* & C. L. Wright*

* The Sanger Centre, Wellcome Trust Genome Campus, Hinxton, Cambridge CB10 1SA, UK
‡ Department of Biology, University of Crete and Institute of Molecular Biology and Biotechnology, PO Box 2208, 71409 Iraklion, Crete, Greece
\$ Neurogenetic Laboratory, The Cyprus Institute of Neurology and Genetics, 6, International Airport Avenue, PO Box 23462, 1683 Nicosia, Cyprus
† Children's Hospital-BACPAC Resources, 747 52nd Street, Oakland, California 94609, USA

We constructed maps for eight chromosomes (1, 6, 9, 10, 13, 20, X and (previously) 22), representing one-third of the genome, by building landmark maps, isolating bacterial clones and assembling contigs. By this approach, we could establish the long-range organization of the maps early in the project, and all contig extension, gap closure and problem-solving was simplified by containment within local regions. The maps currently represent more than 94% of the euchromatic (gene-containing) regions of these chromosomes in 176 contigs, and contain 96% of the chromosome-specific markers in the human gene map. By measuring the remaining gaps, we can assess chromosome length and coverage in sequenced clones.

The task of sequencing the 3,200 megabase (Mb) human genome

can be subdivided into individual chromosome projects ranging in size from 263 Mb (chromosome 1)¹ to about 35 Mb (chromosomes 21q and 22q)^{2,3}. Our strategy, in common with other groups⁴⁻⁶, was to map selected chromosomes individually, and then to combine the results with those of whole-genome mapping studies into a single map of the human genome⁷. Chromosome maps were constructed as follows (see Supplementary Information). First, we constructed a landmark map for each chromosome. Second, we identified bacterial clones (bacterial- or P1-derived artificial chromosomes (BACs or PACs)) from genomic libraries using the chromosome-specific landmarks, and assembled them into contigs on the basis of shared restriction enzyme fingerprints and landmark content. Third, contigs were extended and joined by chromosome walking. Walking was carried out using BAC end sequences generated in house from clones selected at the ends of contigs, or from the publicly available resources; joins were also made by identification of overlaps using genomic sequence data.

Clones that were representative of each contig were selected regularly for inclusion in the 'tiling path' (a set of minimally overlapping clones) for genomic sequencing⁸. Clones from the tiling path of each chromosome were deposited in the 'HumanMap' database at the Genome Sequencing Centre⁷ (<http://genome.wustl.edu/gsc/human/mapping/>), for integration with the data obtained by whole-genome fingerprinting. New clones were identified from this integrated dataset to assist the extension and closure of the chromosome maps (Table 1). A detailed description of tiling paths and the underlying clone contigs is available as Supplementary Information and will continue to be updated at www.sanger.ac.uk; all clones are publicly available.

A key question is the extent of coverage of each chromosome in the map. We analysed the coverage of the euchromatic regions on the basis of the assumptions given below and the approximate estimates that were available for chromosome length. Heterochromatic regions, which are estimated to comprise 3-15% of each chromosome (Table 1), are absent from the contigs analysed here. On the basis of the fingerprint bands in the maps (converted to Mb as described in Supplementary Information), 176 contigs represent 927 Mb, or 94% of the estimated total of 981 Mb euchromatin. Half of this (485 Mb) is in fifteen contigs of 22-62 Mb, that illustrates the extent of continuity obtained. We also analysed the representation of human gene markers in the map. The clone map contained 96% of the unique markers that were previously mapped to these chromosomes in GeneMap99 (ref. 9), and 90% were present in the genome sequence. As expected, this figure is higher for individual chromosomes 20 (99%) and 22q (98%), which are nearly or completely finished (Table 1).

Independent corroboration of the coverage of each chromosome required identification of the boundaries between euchromatic sequence and the centromeric, telomeric, and other heterochromatic repeat sequences, as well as measurement of the remaining gaps in the map. We have measured 52 of the 57 remaining gaps in

Table 1 Status of chromosome maps

Chromosome	Estimated length		Physical map			Gene map		
	Total	Euchromatin	Contigs	Euchromatin covered		Markers analysed	Markers in contigs	Markers in sequence
	(Mb)	(Mb)	(n)	(Mb)	(%)	(n)	(%)	(%)
1	263	238	78	226	95	4,769	94	87
6	183	178	13	170	96	2,942	96	92
9	145	123	21	113	92	1,771	98	90
10	144	139	14	124	89	2,022	99	91
13	114	98	7	102	105	1,028	98	90
20	72	67	6	61	91	1,159	99	99
22(q12-tel)	25.5	25.5	8	24.8	97	777	98	98
X(p21-q27)	115	112	29	106	94	925	93	88
Total	1,062	981	176	927	94	15,393	96	90

See methods in Supplementary Information for details.

the maps of chromosomes 6, 9, 10, 13 and 20 by fluorescent *in situ* hybridization (FISH), in addition to the gaps previously measured on chromosome 22. Clones immediately flanking each gap were hybridized to extended DNA fibres, interphase nuclei or metaphase chromosome spreads.

An example of this analysis is given for chromosome 10 (Fig. 1). Fourteen contigs account for 124.4 Mb of DNA. They contain pericentromeric satellite sequences, and also a subtelomeric sequence on the short arm which is <0.1 Mb from the telomere; the most distal clone on the long arm is <0.15 Mb from the telomere¹⁰. From FISH analysis, the total extent of euchromatic gaps is ≤ 4.2 Mb. From these measurements, the estimated coverage of euchromatin in the map can be revised from 89% (based on Morton's previous estimate; Table 1) to 96.7% (124.4 of 128.6 Mb). A 9.75-Mb restriction map that spans the centromere has been constructed for chromosome 10 (ref. 11). By anchoring this to the clone maps on both chromosome arms, we estimate that the size of the gap across the centromeric region is around 4.5 Mb. This analysis provides a new estimate of 133 Mb for the total length of the chromosome (Fig. 1), compared with the previous value of 144 Mb. In a similar analysis of chromosome 13, seven contigs span 102 Mb and the remaining gaps in the euchromatic region total a maximum of 5 Mb. This leads to a new, increased estimate of the size of the euchromatic region of 107 Mb, and the current coverage in the map is 95%.

Our strategy may form the basis for finishing the map and sequence of every human chromosome. Accurate measurement of all gap sizes assists our continued efforts to bridge the remaining gaps in clones, using other cloning systems (for example yeast artificial chromosomes (YACs), plasmids and bacteriophage

lambda), and characterization of the centromeric satellites and the remaining heterochromatic regions, including the short arms of the acrocentric chromosomes (13, 14, 15, 21 and 22), will enable us to determine the true physical extent of DNA in the human genome. □

Received 28 November; accepted 21 December 2000.

1. Morton, N. E. Parameters of the human genome. *Proc. Natl Acad. Sci. USA* **88**, 7474–7476 (1991).
2. The chromosome 21 mapping and sequencing consortium. The DNA sequence of human chromosome 21. *Nature* **405**, 311–319 (2000).
3. Dunham, I. *et al.* The DNA sequence of human chromosome 22. *Nature* **402**, 489–495 (1999).
4. Tilford, C. A. *et al.* A physical map of the human Y chromosome. *Nature* **409**, 943–945 (2001).
5. Montgomery, K. T. A high-resolution map of human chromosome 12. *Nature* **409**, 945–946 (2001).
6. Bruls, T. *et al.* A physical map of human chromosome 14. *Nature* **409**, 947–948 (2001).
7. The International Human Genome Mapping Consortium. A physical map of the human genome. *Nature* **409**, 934–941 (2001).
8. International Human Genome Sequencing Consortium. Initial sequencing and analysis of the human genome. *Nature* **409**, 860–921 (2001).
9. Deloukas, P. *et al.* A physical map of 30,000 human genes. *Science* **282**, 744–746 (1998).
10. Riethman, H. C. *et al.* Integration of telomere sequences with the draft human genome sequence. *Nature* **409**, 948–951 (2001).
11. Jackson, M. S., See, C. G., Mulligan, L. M. & Lauffart, B. F. A 9.75-Mb map across the centromere of human chromosome 10. *Genomics* **33**, 258–270 (1996).

Supplementary information is available on Nature's World-Wide Web site (<http://www.nature.com>) or as paper copy from the London editorial office of Nature.

Acknowledgements

We thank M. Sekhon, A. Chinwalla, J. McPherson and staff of the Genome Sequencing Centre, St. Louis for their assistance; the many collaborators who have contributed reagents and information to assist map construction on individual chromosomes; M. Jackson for helpful discussion; T. Cox, R. Pettett and the web team; and the Wellcome Trust for support.

Correspondence and requests for material should be addressed to D.R.B. (e-mail: drb@sanger.ac.uk).

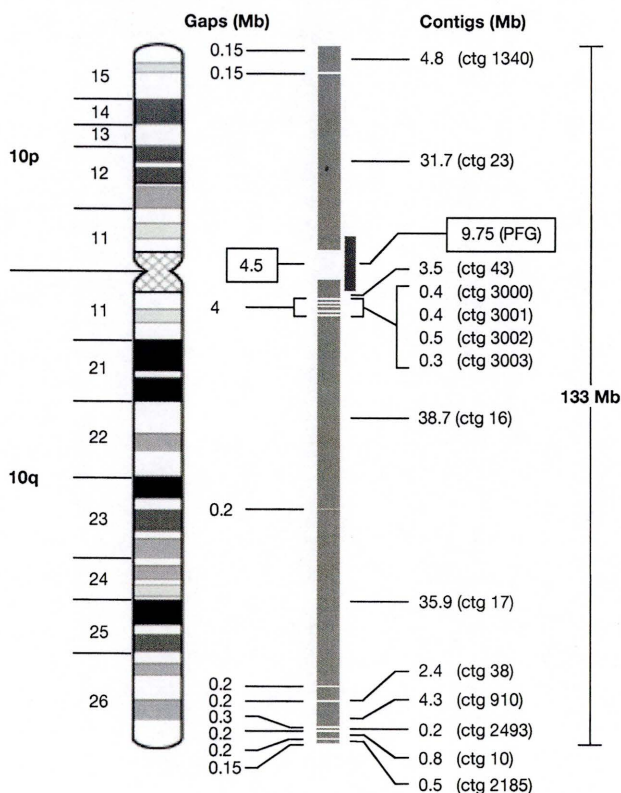


Figure 1 Physical map of chromosome 10. Clone contigs cover 124.4 Mb, euchromatic gaps cover 4.2 Mb, and the gap across centromeric satellites is 4.5 Mb¹¹. The separation between contigs 43 and 16 was determined as ~4 Mb on the basis of FISH of metaphase chromosome spreads, from which the sum of contigs 3000–3003 (1.6 Mb) was subtracted for a net gap coverage of 2.4 Mb in this region of 10q11.

A physical map of the human Y chromosome

Charles A. Tilford*, Tomoko Kuroda-Kawaguchi*, Helen Skaletsky*, Steve Rozen*, Laura G. Brown*, Michael Rosenberg*, John D. McPherson†, Kristine Wylie†, Mandeep Sekhon†, Tamara A. Kucaba†, Robert H. Waterston† & David C. Page*

* Howard Hughes Medical Institute, Whitehead Institute, and Department of Biology, Massachusetts Institute of Technology, 9 Cambridge Center, Cambridge, Massachusetts 02142, USA

† Genome Sequencing Center, Department of Genetics, Washington University School of Medicine, 4444 Forest Park Boulevard, St. Louis, Missouri 63108, USA

The non-recombining region of the human Y chromosome (NRY), which comprises 95% of the chromosome, does not undergo sexual recombination and is present only in males. An understanding of its biological functions has begun to emerge from DNA studies of individuals with partial Y chromosomes, coupled with molecular characterization of genes implicated in gonadal sex reversal, Turner syndrome, graft rejection and spermatogenic failure^{1,2}. But mapping strategies applied successfully elsewhere in the genome have faltered in the NRY, where there is no meiotic recombination map and intrachromosomal repetitive sequences are abundant³. Here we report a high-resolution physical map of the euchromatic, centromeric and heterochromatic regions of the NRY and its construction by unusual methods, including genomic clone subtraction⁴ and dissection of sequence family variants⁵. Of the map's 758 DNA markers, 136 have multiple locations in the NRY, reflecting its unusually repetitive sequence composition. The markers anchor 1,038 bacterial artificial chromosome clones, 199 of which form a tiling path for sequencing.

A physical map of the mouse genome

Simon G. Gregory*, Mandeep Sekhon†, Jacqueline Schein‡, Shaying Zhao§, Kazutoyo Osoegawa||, Carol E. Scott*, Richard S. Evans*, Paul W. Burridge*, Tony V. Cox*, Christopher A. Fox*, Richard D. Hutton*, Ian R. Mullenger*, Kimbly J. Phillips*, James Smith*, Jim Stalker*, Glen J. Threadgold*, Ewan Birney¶, Kristine Wylie†, Asif Chinwalla†, John Wallis†, LaDeana Hillier†, Jason Carter†, Tony Galge†, Sara Jaeger†, Colin Kremitzki†, Dan Layman†, Jason Maas†, Rebecca McGrane†, Kelly Mead†, Rebecca Walker†, Steven Jones‡, Michael Smith‡, Jennifer Asano‡, Ian Bosdet‡, Susanna Chan‡, Suganthi Chittaranjan‡, Readman Chiu‡, Chris Fjell‡, Dan Fuhrmann‡, Noreen Girn‡, Catharine Gray‡, Ran Guin‡, Letticia Hsiao‡, Martin Krzywinski‡, Reta Kutsche‡, Soo Sen Lee‡, Carrie Mathewson‡, Candice McLeavy‡, Steve Messervier‡, Steven Ness‡, Pawan Pandoh‡, Anna-Lisa Prabhu‡, Parvaneh Saeedi‡, Duane Smallus‡, Lorraine Spence‡, Jeff Stott‡, Sheryl Taylor‡, Wesley Terpstra‡, Miranda Tsai‡, Jill Vardy‡, Natasja Wye‡, George Yang‡, Sofiya Shatsman§, Bola Ayodeji§, Kelta Geer§, Getahun Tsegaye§, Alla Shvartsbeyn§, Elizabeth Gebregeorgis§, Margaret Krol§, Daniel Russell§, Larry Overton§, Joel A. Malek§, Mike Holmes§, Michael Heaney§, Jyoti Shetty§, Tamara Feldblyum§, William C. Nierman§, Joseph J. Catanese||, Tim Hubbard*, Robert H. Waterston†, Jane Rogers*, Pieter J. de Jong||, Claire M. Fraser§, Marco Marra‡, John D. McPherson† & David R. Bentley*

* The Wellcome Trust Sanger Institute, Hinxton, Cambridge CB10 1SA, UK

† Genome Sequencing Center, Washington University School of Medicine, St Louis, Missouri 63108, USA

‡ Genome Sciences Centre, British Columbia Cancer Agency, Vancouver, British Columbia V5Z 4E6, Canada

§ The Institute for Genomic Research, Rockville, Maryland 20850, USA

|| Children's Hospital Oakland Research Institute, Oakland, California 94609, USA

¶ EMBL—European Bioinformatics Institute, Hinxton, Cambridge CB10 1SD, UK

Department of Electrical Engineering, Washington University, St Louis, Missouri 63130, USA

A physical map of a genome is an essential guide for navigation, allowing the location of any gene or other landmark in the chromosomal DNA. We have constructed a physical map of the mouse genome that contains 296 contigs of overlapping bacterial clones and 16,992 unique markers. The mouse contigs were aligned to the human genome sequence on the basis of 51,486 homology matches, thus enabling use of the conserved synteny (correspondence between chromosome blocks) of the two genomes to accelerate construction of the mouse map. The map provides a framework for assembly of whole-genome shotgun sequence data, and a tile path of clones for generation of the reference sequence. Definition of the human–mouse alignment at this level of resolution enables identification of a mouse clone that corresponds to almost any position in the human genome. The human sequence may be used to facilitate construction of other mammalian genome maps using the same strategy.

The recent revolution in large-scale analysis of genomes has already yielded near-complete DNA sequences of a diverse range of organisms including bacteria, a yeast, a worm, a fly and humans^{1–7}. The sequence of the mouse genome will have a huge impact on biological research and human health. It will provide critical information and reagents for use in mouse experimental models. It will become possible to unravel the mechanisms of complex mammalian biological processes and human disease. The mouse genome sequence will provide the first opportunity to compare the complete sequence and organization of the human genome with that of another mammal. It will aid discovery and annotation of gene structures and other functionally important sequences in both genomes.

Assembly of each large genome sequence to date has been underpinned by production of a comprehensive map of overlapping large-insert bacterial clones (for example, cosmids⁸ or bacterial artificial chromosome (BAC) clones⁹)^{10–13} for sequencing, and, in some cases, for integration with whole-genome shotgun sequence data (refs 5, 7; see also review in ref. 14). The clones provide substrates for finishing each section of the genome sequence separately, making it easier to eliminate errors and to achieve a final accuracy of more than 99.99% (refs 14–16). The study of other large genomes requires physical maps of a similar standard for sequencing and biological studies.

Comparisons between genomes reveal homologous sequences, for example within individual genes, that reflect their common evolutionary origin and subsequent conservation. Similarity between genomes is also evident at the level of long-range sequence organization. A 'conserved segment' (also called a 'conserved linkage') refers to a region where the order of multiple genes on a

single chromosome segment (and hence the linkage between them) is the same in both species. A 'conserved synteny' refers to a region where the chromosomal location of multiple genes is conserved, but not necessarily their precise order^{17–19}. In general, the degree of similarity at all levels is higher between species that diverged more recently from a common ancestor. The long-range organization of the mouse and human genomes is very similar, and may comprise about 180 conserved syntenic regions^{6,17}. Detailed studies in some smaller regions suggest that precise gene order has been conserved, confirming the existence of conserved segments^{20,21}. The similarity in sequence organization between these two genomes suggests that the human genome can be used as a framework to map the mouse genome^{20,21}, and possibly other mammalian genomes as well. Alignment of the different genome maps over their entire length would simultaneously define the syntenic relationship between them at a new level of resolution, and accelerate the process of constructing the mouse clone map.

Using the human sequence as a framework

We constructed a physical clone map of the mouse genome in two phases. In the first phase, we compared restriction digest patterns ('fingerprints') of 305,716 BAC clones²². We identified overlaps between clones on the basis of similarity between fingerprints and used this information to construct 7,587 contigs of overlapping clones. In parallel, we determined sequences at the ends of the mouse DNA fragments cloned in the BACs (that is, BAC end sequences, or BESs). We aligned the mouse BAC contigs to the human genome sequence by identifying matches between human sequence and mouse BESs. We extended and joined contigs where possible after re-examining the fingerprint data. Overlapping fin-

gerprints were required to support each join, while juxtaposition of the mouse clone contigs along the human genome greatly accelerated the manual editing process. This phase resulted in generation of a human–mouse homology clone map. In the second phase, we used a set of independently mapped mouse markers (available in existing genetic and radiation hybrid maps of the mouse) to position the BAC contigs in the mouse genome. After further manual contig editing was carried out, we generated a mouse clone map comprising 296 contigs.

An illustration of the human–mouse homology clone map produced in the first phase is shown in Fig. 1. Within a 1.6-megabase (Mb) region of human chromosome 6 (6q16.1), 11 of the 15 segments of human sequence match to 29 of the BESs within a mouse BAC contig. This contig is located on mouse chromosome 4 (Mmu4). The syntenic relationship between the two genomes in this area was previously indicated by the proximity of the two loci *CNR1* and *GABRR1* (human) and their corresponding homologues *Cnr1* and *Gabrr1* (mouse) (also shown in Fig. 1). In our analysis here, a further 29 homologous crosslinks between these two loci are added.

We found 51,486 homologous crosslinks between the two genomes during this analysis, which corresponds to one match per 54 kb on average (assuming a 2.8-Gb mouse genome; see Methods). These matches were derived from a complete set of 453,962 BESs. Some 73% of the BESs contained more than 100 base pairs (bp) of contiguous unique sequence; we excluded the rest from the analysis.

In all, 1,326 of the BESs matched human chromosome 20 sequence. We found that 19% of them matched putative coding regions (163 matches to known genes, 80 to new genes, 8 to putative genes and 1 to a pseudogene). The rest were matches to other conserved sequences in introns (32%) and intergenic regions (49%). Human–mouse sequence homologies in non-coding regions have also been observed in other studies^{20,23,24}. From this analysis it is clear that non-coding homologies contributed significantly to the alignment.

Of the clones in the human genome tile path, 88% are collinear with the mouse BAC map (Table 1). For individual human chromosomes, coverage by aligned mouse contigs exceeds 80% on all except chromosome 19 (61%) and the Y chromosome (0%). Lower coverage of these human chromosomes can be accounted for by several factors. First, we used only BES matches with unique locations in the human tile path for the alignment. BESs matching regions of human sequence containing dispersed low-copy repeats were filtered out of the analysis. Such regions are known on human chromosome 19 (notably including zinc-finger-containing genes among others^{21,25}). Second, a significant fraction of chromosome 19 clones (49 in all) are included in the total in Table 1 but contain pericentromeric repetitive sequence, and any BES matches to them were excluded. A further 118 clones on chromosome 19 were covered by contigs aligned in our study, but we did not score them in Table 1 because they contained no high-scoring matches to BESs. This is reflected in the low overall density of BES matches on

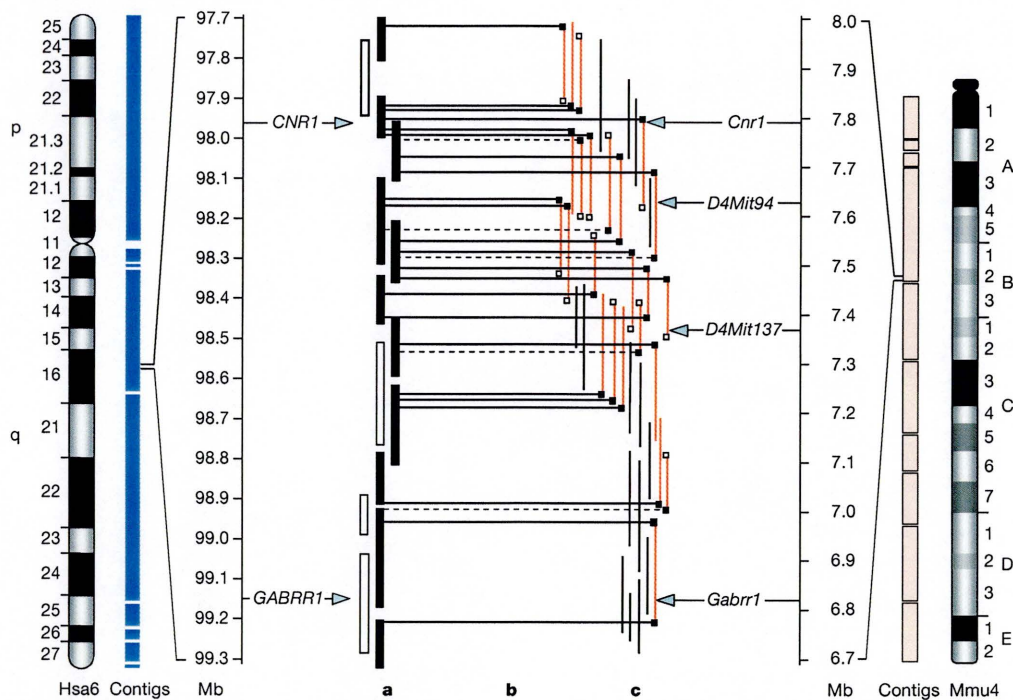


Figure 1 Construction of human–mouse homology clone map. Alignment between part of human chromosome 6 (Hsa6) and mouse chromosome 4 (Mmu4). Clone contigs are shown as blue and pale pink boxes, respectively. A 1.6-Mb interval is enlarged, showing part of Hsa6q16.1 aligned to a 1.3-Mb mouse BAC contig. The accompanying megabase scale for Hsa6 starts from one end of the chromosome (ptel, 0 Mb; qtel, 172 Mb), whereas the megabase scale shown for the mouse contig starts at one end of that contig. **a**, Human accessions. Filled and clear boxes denote accessions with and without matches to BESs, respectively. **b**, Matches between human sequence and BESs. Black lines denote high-homology BLAST matches and dashed lines indicate medium-homology BLAST matches (see Methods for details). **c**, Mouse BAC clone contig. All clones having at least one BES

that matches a human accession are shown in red (black and white squares at the ends of clones denote BESs with and without matches to human accessions, respectively). Black lines represent a subset of the other clones in the contig (the rest have been omitted for clarity, but can be viewed in Supplementary Information). Previous alignment of the two human loci *CNR1* and *GABRR1* with their mouse homologues can be viewed in the NCBI versus MGD alignment (<http://www.ncbi.nlm.nih.gov/Homology>). Another human locus (*RNGTT*) lies between *CNR1* and *GABRR1* in the human sequence, and its murine homologue (*Rngtt*) is present in the NCBI versus MGD alignment; however, *Rngtt* has not been placed in the mouse clone map yet. *D4Mit94* and *D4Mit137* are additional mouse markers that have been placed in the clone map by this study.

Table 1 Summary statistics of human-mouse homology clone map

Human chromosome number	Human sequence available (Mb)	Human-mouse sequence matches		Number of clones in human tile path	Clones in human tile path that are covered in mouse	
		Total	Per Mb		Number	Per cent
1	239	4,888	20.5	2,179	2,080	95
2	242	4,783	19.8	1,951	1,675	86
3	204	3,667	18.0	1,700	1,493	88
4	189	2,747	14.5	1,612	1,510	94
5	182	2,892	15.9	1,973	1,682	85
6	176	3,264	18.5	1,800	1,666	93
7	161	2,957	18.4	1,518	1,342	88
8	143	2,310	16.2	1,210	1,040	86
9	114	2,505	22.0	963	883	92
10	140	2,531	18.1	1,132	1,014	90
11	139	2,606	18.7	1,134	1,013	89
12	137	2,206	16.1	1,022	943	92
13	99	1,318	13.3	851	798	94
14	90	2,103	23.4	655	642	98
15	82	1,721	21.0	671	573	85
16	81	1,470	18.1	726	666	92
17	81	1,585	19.6	656	612	93
18	79	1,226	15.5	616	564	92
19	46	507	11.0	841	512	61
20	61	1,326	21.8	632	608	96
21	34	507	14.9	475	432	91
22	34	439	12.7	345*	279	81
X	149	1,925	12.9	1,555	1,276	82
Y	26	0	0.0	208	0	0
All	2,928	51,483	17.5	26,425	23,283	88

*For chromosome 22, the finished sequence was divided into abutting 100-kb segments for this analysis.

this chromosome (Table 1) and may be the result of chromosome-specific low-copy repeats, as observed previously^{21,25}. We were not able to align any mouse contigs to the human Y chromosome. Two reasons may account for this. First, much of the human Y sequence is repetitive (with Y-specific, X-Y and autosome-Y homologies), and mouse BES matches to these regions would have been excluded. Second, only 39% of the BESs were derived from a male mouse library, and we estimate that only about 0.4% of the BESs were therefore derived from the mouse Y chromosome.

Of the total coverage of the mouse BAC map (in 211 contigs), 97% (2,658 Mb) is aligned to the human genome sequence. The

other 3% (84 Mb, in 85 contigs) may not have been aligned at this stage for several reasons. First, the BESs may not find matches in the human sequence because the human sequence is incomplete. In a recent analysis, 3% of a curated set of 10,212 full-length human complementary DNAs (taken from the set in the 'reference sequence project', <http://www.ncbi.nlm.nih.gov>) were found to have no match in the human sequence (using BLAT²⁶ to identify matches with more than 95% identity between cDNA and the human genome sequence (NCBI Build 28); J.Kent and D. Haussler, personal communication). This fraction is sufficient to account for all of the unplaced mouse contigs. Second, most of the unplaced contigs are

Table 2 Summary statistics of mouse physical clone map by chromosome

Mouse chromosome number	Size estimate (Mb)		Total contigs			
	Old*	New	Number	Coverage (Mb)	Percentage of old size estimate	Percentage of new size estimate
1	216	196	10	211	98	108
2	209	190	13	186	89	98
3	180	163	8	173	96	106
4	177	160	10	145	82	90
5	170	154	24	156	92	101
6	166	151	16	157	95	104
7	156	141	14	143	92	101
8	149	135	12	140	94	104
9	144	131	15	127	88	97
10	145	131	9	135	93	103
11	142	129	6	107	75	83
12	146	132	8	126	86	95
13	131	119	11	132	101	111
14	134	121	8	130	97	107
15	122	111	7	108	89	98
16	114	103	7	101	88	97
17	116	105	6	95	82	91
18	116	105	6	96	83	91
19	82	74	4	65	80	88
X	187	170	30	132	71	78
Y	86	78	4	14	17	18
Subtotal			228	2,679	87	96
Unlocalized			68	60		
Total	3,088	2,800	296	2,739	89	98

*Taken from ref. 47.

short and contain few BESs. The production of additional mouse sequence in these contigs may allow identification of homology crosslinks, and hence alignment of the contigs to the corresponding region in the human genome. Third, there may be insufficient homology between the two genomes in some regions.

The mouse clone map

The mouse genome comprises 19 autosomes plus the two sex chromosomes, X and Y. In contrast to the human genome, all the mouse chromosomes are acrocentric (that is, the centromere is at or near one end). To construct the clone map for each mouse chromosome, we made use of the available genetic map (<http://www-genome.wi.mit.edu/cgi-bin/mouse/index>) of 6,559 gene-specific or simple sequence length polymorphism (SSLP) markers^{27–29}, and also a radiation hybrid (RH) map³⁰ of 13,558 markers, which included a subset of 2,446 of the markers previously ordered in the genetic map. This provided a total unique set of 18,379 markers. We placed 48% (8,789) of these markers within the mouse BAC contigs using the BESs or matches to available mouse genomic sequence, or by hybridization of markers to arrayed BAC clones^{31–33}. We then added another 8,203 markers to the map by hybridization to the BACs. As a result, we were able to assign a unique position and orientation on a mouse chromosome to 203 contigs (containing 2,631 Mb, or 96% of the map coverage), and a chromosome assignment (but not a position) to 25 more contigs (containing a total of 47 Mb). A further 68 contigs (containing 60 Mb) have no chromosomal assignment. A summary of the mouse map by chromosome is shown in Table 2.

Most mouse BAC contigs contained multiple mouse markers (average 57 markers per contig). We compared the order of markers within the contigs to the order suggested previously by the genetic and RH data. Overall, there was excellent agreement between the order of markers in each map, as illustrated for example on mouse chromosome Mmu2 (see Fig. 2; and Supplementary Information for all chromosomes). There was also concordance of the marker order in the clone map with that of the European Union RH map

(http://www.genoscope.cns.fr/externe/English/Projets/Projet_ZZZZ/rhmap.html). The availability of integrated map information permitted assessment of the remaining 27 minor conflicts. We found two conflicts between the clone map and both the genetic and RH maps. The other 25 were conflicts solely with the RH map, and occur in regions where the genetic map offers limited or no resolution. For example, we inspected the RH data in the 80–90-Mb region of Mmu2 (Fig. 2) and found that the number of obligate breaks between the framework markers can be reduced if these markers are arranged according to the order in the clone map. We made the same observation in all eight cases examined in detail (see Supplementary Information). In general, it appears that the conflicts are caused by local inversions owing to a few (typically one or two) suboptimally located framework markers in the RH map. This in turn causes the order of all other markers previously placed in the RH map relative to that framework marker to be in conflict with their order in the clone map.

We carried out an additional check of contig assembly by comparing ‘virtual’ fingerprints calculated from finished mouse

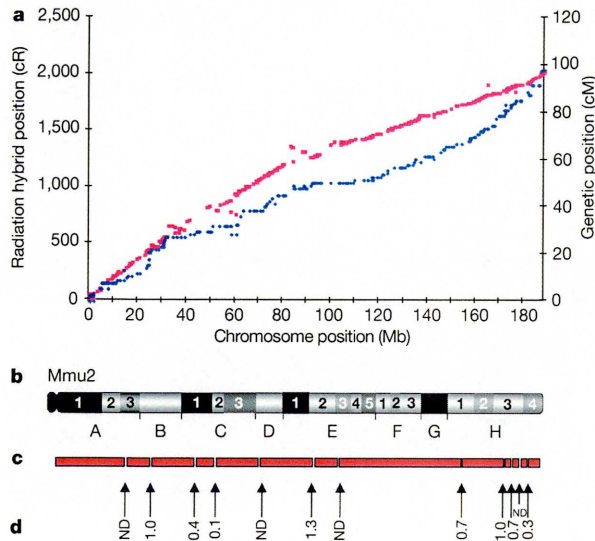


Figure 2 Comparison of radiation hybrid and genetic maps to the physical map of mouse chromosome 2. **a**, Radiation hybrid (pink) and genetic (dark blue) markers are plotted against their respective positions in the physical map of chromosome 2. **b**, Mouse chromosome 2 ideogram. **c**, **d**, Mouse BAC contigs (**c**) and gap sizes (**d**), estimated from bridging human sequence as described in the text. cR, centiRays; cM, centimorgans; ND, not determined.

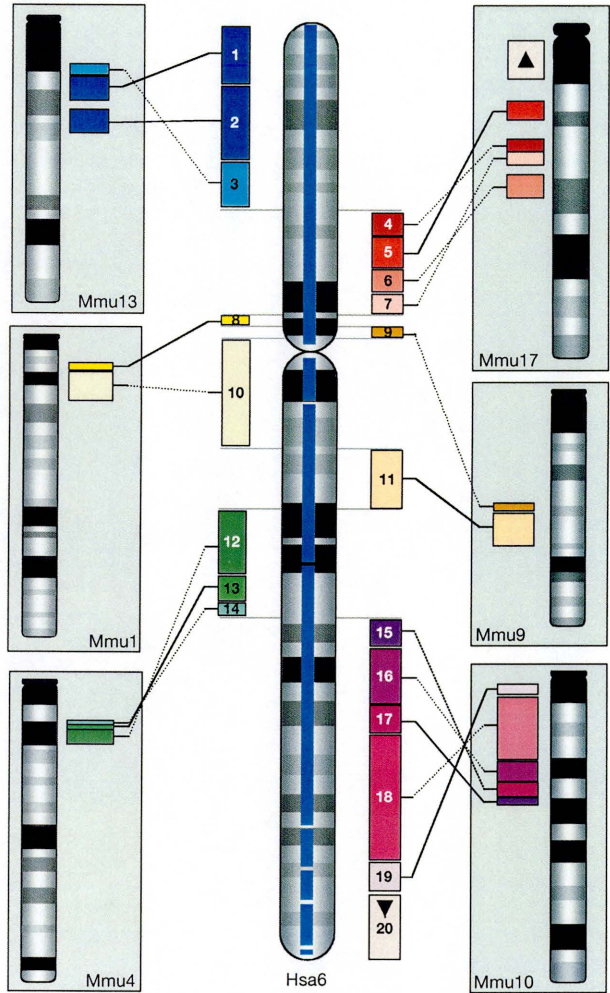


Figure 3 Conserved segments between human chromosome 6 (Hsa6) and the mouse genome. Blue bars in the centre of the chromosome ideogram represent the current extent of contig coverage in the human map. Numbered accession blocks correspond to Table 3 and denote conserved synteny with the mouse chromosomes. Dotted lines joining coloured blocks between the two species indicate conserved syntenic blocks inverted with respect to each other relative to the orientation of each chromosome as drawn.

Table 3 Conserved segments between human chromosome 6 and mouse

Segment	Human ptel-qtel number*	GenBank accession numbers	Human segment size (Mb)	Human-mouse homology hits	Hits per Mb	Mouse chromosome number	Mouse segment size (Mb)
6.1	3-97	AL365272-AL031785	9.0	220	24	13	9.9
6.2	99-207	AL031904-AL022726	10.3	303	29	13	9.0
6.3	209-302	AL008627-AL049543	9.5	146	15	13	9.9
6.4	310-374	AL022727-297183	5.6	89	16	17	3.4
6.5	376-432	AL161903-AL035690	5.1	116	23	17	4.4
6.6	434-453	AL136087-AL031778	1.8	37	21	17	1.9
6.7	458-537	AL139331-AL390247	6.5	178	27	17	6.6
6.8	560-582	AL360175-AL109918	2.7	70	26	1	3.1
6.9	582-613	AL109918-AL589796	3.1	57	18	9	2.9
6.10	620-771	AL031779-AL365232	12.4	204	16	1	13.2
6.11	773-900	AL603910-AL136082	11.1	257	23	9	10.9
6.12	918-998	AL096817-AL513186	7.0	174	25	4	7.5
6.13	1,005-1,031	AL607077-AL589740	2.9	45	16	4	2.7
6.14	1,033-1,044	Z84482-AL390959	1.1	24	22	4	1.7
6.15	1,048-1,120	AL080285-AL645528	6.8	120	18	10	8.3
6.16	1,121-1,227	AL355586-AL121953	9.2	157	17	10	10.4
6.17	1,229-1,297	AL354716-AL512283	6.2	141	23	10	7.0
6.18	1,301-1,579	AL591428-AL078581	26.1	616	24	10	27.7
6.19	1,584-1,637	AL355497-AL591419	3.9	65	17	10	4.1
6.20	1,639-1,797	AL591499-AL031259	15.0	246	16	17	11.4
Total			155.3	3,265	21		156.0

*Numbered arbitrarily from 1 (nearest the telomere of the short arm) to 1,800 (nearest the long-arm telomere).

sequence with the experimental fingerprints in the database. This was possible for 762 clones, each with more than 100 kb of finished sequence available. All virtual fingerprints were matched with high confidence to an experimentally derived fingerprint in the database, thus confirming the accuracy of the fingerprint data. Some 97% of them also matched to the expected position in contigs, confirming the assembled BAC map. The remaining 3% (20 clones) matched to other unique locations. These can be attributed to errors in tracking clone names during the project, and are generally resolved later by checking the overlaps between clones using sequence information as it becomes available.

Assuming the mouse genome is about 2.8Gb in total (see Methods), coverage of the mouse genome in mapped BACs is virtually complete: 296 contigs of average size 9.3 Mb cover an estimated 2,739 Mb. The estimated coverage of each mouse chromosome by BAC contigs is listed in Table 2. Four contigs were placed on the mouse Y chromosome. The low coverage is partly due to the lack of previously mapped markers, and partly because only part of the fingerprinted BAC collection was derived from a male mouse. A number of the unplaced contigs contain clones derived solely from the male mouse BAC library, and may also map to the mouse Y chromosome when more data is available. The map continues to be updated, and the current version can be viewed at <http://www.ncbi.nlm.nih.gov/genome/guide/mouse> (choose 'MapView') or at http://www.ensembl.org/Mus_musculus/cytoview (use the 'Jump to chr.' box to select chromosome; if searching specific features, select 'cytoview' option to view the map). The archive of the map at the time of publication is available as Supplementary Information. The level of continuity of the mouse clone map is similar to that of the current human genome map, which comprises 279 contigs covering approximately 2,928 Mb (as of March 2002; International Human Genome Sequencing Consortium, I. Vastrik, personal communication).

There are 275 gaps in the mouse clone map. Many of these gaps occur where there is a break in synteny between the two genomes. No direct measurement of the existing gaps has yet been attempted (for example by fluorescent *in situ* hybridization to chromosomes or DNA fibres). However, 83 gaps in the mouse map are bridged by human contigs. The total length of human sequence across these gaps is 51.9 Mb. If we assume collinearity between the mouse and human genomes across these gaps, then the average size of each gap in the mouse map is 0.63 Mb. On mouse chromosome 2, for example, 9 of the 12 gaps between contigs are bridged by segments of the human sequence ranging from 0.3 to 1.3 Mb (see Fig. 2). More

practically, the tracts of human sequence that bridge gaps in the mouse map may provide a source of probes (for example, selected from annotated exons in the human sequence) to screen for new mouse clones and thus assist in closing the gaps. Conversely, mouse clones that are collinear with gaps in the human tile path may be used to assist closure of the human map. Our study indicates that 132 of the 244 gaps in the human map (March 2002 release) are bridged by mouse contigs and might be closed in this way.

Human-mouse homology maps

Alignment of the human and mouse clone maps using 51,486 homology crosslinks allowed us to define the segments that are conserved in both genomes at a new level of resolution. In many cases we were able to locate the boundary between adjacent segments to within one or a few clones. For example, the sequence of human chromosome 6 contains 1,800 sections that overlap to form eight contigs. We numbered each section arbitrarily from 1 (nearest the telomere of the short arm) to 1,800 (nearest the long-arm telomere) for the purpose of this analysis (Table 3, 'ptel-qtel' numbers). We detected 220 high or medium stringency matches between a 9-Mb region of human 6p25.3 (segment 6.1, represented by accessions 3-97) and a region of about 9.9 Mb in a mouse BAC contig mapped to Mmu13A3 (Table 3 and Fig. 3). In addition, we found that the order of all 220 matches is consistent between the two maps, supporting the possibility that this is a conserved segment. The next segment (segment 6.2) starts in human accession 99 and extends as far as accession 207. This segment is defined by 303 matches of consistent order with a contig on Mmu13. Segments 6.1 and 6.2 are discontinuous in the mouse. The next segment (6.3) is aligned to another discontinuous region of Mmu13, whereas the fourth block (6.4) on human 6p is syntenic with a different mouse chromosome, Mmu17 (Table 3 and Fig. 3). In total, 20 conserved segments were identified along human chromosome 6, which subdivide the nine regions of conserved synteny (Fig. 3; see also Supplementary Information and updated views at http://www.ensembl.org/Homo_sapiens/syntenymap). The results of this analysis can also be viewed with respect to the mouse chromosomes. For example, mouse chromosome 11 contains five regions of conserved synteny with the human genome, which are subdivided into 21 conserved segments (Fig. 4; see also Supplementary Information and updated views at http://www.ensembl.org/Mus_musculus/syntenymap).

Overall, we defined 288 conserved segments contained within 167 regions of conserved synteny (Fig. 5). This compares with a previous

analysis using 2,997 markers, in which 183 conserved segments were detected⁶. The existence of multiple adjacent (but discontinuous) segments within the same syntenic region (for example segments 6.1–6.3 and 6.15–6.19 in Table 2 and Fig. 3) supports the hypothesis that a significant number of intrachromosomal inversions, in addition to interchromosomal rearrangements, contributed to formation of the present-day structures from the chromosomes of a common ancestor. Our results are consistent with previous observations for several chromosomal regions^{34–37}, including the recent high-resolution studies on human chromosomes 19 (refs 21, 38), 21 (ref. 39) and 7 (ref. 20). In the latter study, for example, comparative analysis using a high density of markers resulted in detection of 20 conserved segments within 16 regions of conserved synteny (compared with 25 and 15, respectively, in the present study). Small conserved segments will inevitably escape detection in the absence of sufficient homology crosslinks. For example, the Mmu2–Hsa7 segment reported in the previous study was estimated to be probably less than 100 kb (ref. 20), and was not detected in our study here. Anecdotal evidence from detailed comparisons of finished sequence between the mouse and human chromosomes indicates the presence of very small regions (as little as 1 kb) where conserved order is disrupted, either by recent duplications

or insertion of unrelated sequence^{23,34,39,40}. Ultimately, the alignment of finished sequences of the two genomes will be required to define the exact number and boundaries of every conserved segment.

Future work

Physical clone maps of complex genomes provide an essential framework to produce complete genome sequences. The clones also provide a source of well-characterized material for experimental studies. In the absence of large-scale sequencing programmes (and these may not be expected for a number of genomes in the foreseeable future), the availability of an accurate clone map will allow targeted sequencing of regions of specific interest. The alignment of maps of multiple genomes will also permit rapid investigation of orthologous gene sequences for structural and functional comparisons.

The first genomes to be mapped and sequenced in their entirety have been the result of enormous and expensive efforts. A hallmark of these studies has been the quality of the product, which has benefited from cross-validation between independently constructed maps for long-range information, and from the high accuracy of finished sequence. In our study, the availability of the human genome sequence has been exploited for faster characterization of the mouse genome. This approach will be applicable to many other mammals, and may also work for more distantly related vertebrates. Three factors contribute to the success of the mapping strategy: (1) good coverage of the genome in large contigs after the initial fingerprinting; (2) high-quality sequence cross-matches between most of these contigs and the reference sequence; and (3) sufficient independently mapped markers to order and orient all the contigs in the new map. Future projects would benefit from a similar depth of coverage in BACs (at least 15-fold) to ensure good representation of the genome in long contigs. Some savings might be made in the number of BESs required for the mapping alignment. One way to reduce the cost of the project would be to select clones from pre-existing contigs before sequencing the insert ends. However, this would reduce the number of sequence anchor points in the final map with consequent disadvantages (see below). For genomes more closely related than human and mouse, a higher proportion of the BESs would be expected to match the reference sequence (compared with 16% for the human–mouse study), which would allow reduction in the number of BESs generated without reduction of cross-matches.

The physical clone map of the mouse has provided 98% coverage of the genome in BAC contigs of average size more than 9 Mb. From the more than 300,000 BACs in the map, a complete tiling path of clones is being selected for production of the finished sequence. So

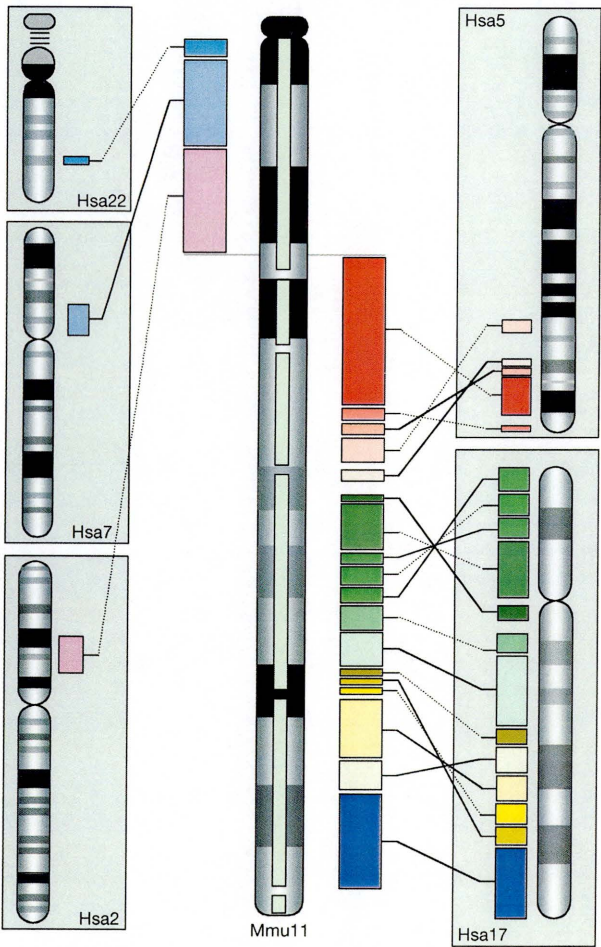


Figure 4 Conserved segments between mouse chromosome 11 and the human genome. The pale green bars in the centre of the chromosome ideogram represent the current extent of contig coverage in the mouse map. Dotted lines between the two species of same coloured blocks indicate conserved syntenic blocks inverted with respect to each other relative to the orientation of each chromosome as drawn.

Figure 5 Homology maps of the mouse and human genomes. **a**, The mouse–human homology map. Bars in the centre of each mouse chromosome ideogram denote the ordered and oriented mouse contigs determined by this study. The coloured blocks adjacent to each mouse chromosome indicate discrete regions where marker order is conserved between the two genomes. Colours correspond to specific human chromosomes in **b**. Positions of human telomeres are located within mouse contigs by arrows in the colour of their corresponding chromosome: up arrow indicates the p telomere and down arrow indicates the q telomere. The X-chromosome relationship is represented by arrows drawn in the direction Xp to Xq from the human. **b**, The human–mouse homology map. Bars in the centre of human chromosome ideograms denote clone contigs in the human genome. Adjacent coloured blocks indicate discrete regions where marker order is conserved with the mouse. Colours correspond to specific mouse chromosomes as in **a**. An interactive display of these figures is available (http://www.sanger.ac.uk/Projects/M_musculus/publications/fpcmap-2002). Regularly updated synteny information is also available (http://www.ensembl.org/Mus_musculus/syntenyview and http://www.ensembl.org/Homo_sapiens/syntenyview).

far, about 2.8% of the mouse genome sequence is available in this form (<http://www.ncbi.nlm.nih.gov>), and completion is scheduled for 2005. The mouse map contains more than 450,000 BESs (covering 220 Mb, or 7.8%, of the mouse genome), most of which contain sufficient unique sequence to anchor the current mouse whole genome sequence assemblies of 40 million reads ($\sim 6 \times$ coverage; <http://trace.ensembl.org>). This combined resource will provide a comprehensive working draft of the mouse genome in the public domain for immediate use. For example, the January 2002 release of this product included 20,652 annotated transcripts (http://www.ensembl.org/Mus_musculus/stats). The same sequence is also assisting the identification of genes on the basis of sequence conservation⁴¹ where no human cDNA is available. Detailed comparison between human and mouse sequences will therefore provide a comprehensive catalogue of genes (and orthologous-pair relationships where they exist) for comparative functional and genetic studies. It will also be possible to identify the evolutionary events at the sequence level that have occurred since divergence of the two species. □

Methods

Map construction

Fingerprints of RPCI-23 and RPCI-24 mouse BAC clones²² were generated by separation of *Hind*III restriction-enzyme digest fragments on 1.2% agarose gels⁴². Gel images were acquired with Image software (<http://www.sanger.ac.uk/Software/Image>) and restriction fragments identified using BANDLEADER software (D. Fuhrmann *et al.*, unpublished). Fingerprints were assembled within the program FPC⁴³ under high stringency conditions at a probability of 1×10^{-16} and a match tolerance of seven. The BESs⁴⁴ from clones within the fingerprint database were then matched to the tile path of human sequence clones. Human tile path accessions and mouse BESs were repeat masked and then aligned by BLASTN version 2.0a13MP-WashU, 10 June 1997 (<http://blast.wustl.edu>; W. Gish, personal communication)⁴⁵. All matches longer than 100 bp, and with a significance value above 0.01, were clustered using the initial fingerprint assembly. A 'high score' blast match (that is, with a blast score >700) was required to anchor each mouse map contig to the human tile path, supported by at least one other BLAST match (Fig. 1). Only matches with unique locations in the human tile path were used. Matches between the mouse BESs and human accessions had an average score of 627.29 and an average identity of 72.3%. Contigs that were adjacent to each other on the basis of their alignment to the human sequence were inspected manually and joined if fingerprints of the end clones overlapped with probability scores of better than 1×10^{-12} . Markers were added to the map either by electronic PCR³¹, or by hybridization using overgo probes³⁵. Markers were incorporated into the physical map only if they were uniquely placed within the map. Additional joins were made between contigs that were adjacent according to consistent mouse marker data if supported additionally by fingerprint overlaps with probability scores of better than 1×10^{-10} .

Coverage estimates

The exact length of 125 mouse clones, for which finished sequence was available (totalling 25,349 kb) was divided by the number of *Hind*III fragments (5,597) observed as single bands in the fingerprints of these clones. This provided a conversion factor of 4.5 kb per observed fragment, which was used to calculate all contig sizes in the consensus map as listed in Table 2. An estimate of 2.8 Gb for the size of the mouse genome was obtained as follows. Assembled mouse whole-genome shotgun data (November release, covering a total of 2.41 Gb) contained 91% coverage of 41 Mb of finished mouse genomic sequence. On this basis, the mouse genome is estimated to cover ~ 2.8 Gb (2.65 Gb euchromatin plus heterochromatin). Length estimates for individual mouse chromosomes were taken from refs 46 and 47, adjusted using the estimate of whole genome size described above (see Table 2). This result suggests that the mouse genome is shorter than the human genome. Support for this was obtained by comparing contiguous and finished mouse and human genomic sequence in 13 regions that could be aligned. The combined total lengths were 6.29 Mb (mouse) and 7.78 Mb (human) (ratio 0.8), although values for individual segments varied between 0.73 and 1.06. These results are in line with previous observations^{34,35,39,48–50}.

Received 15 April; accepted 4 July 2002; doi:10.1038/nature00957.
Published online 4 August 2002.

1. Fleischmann, R. D. *et al.* Whole-genome random sequencing and assembly of *Haemophilus influenzae* Rd. *Science* **269**, 496–512 (1995).
2. Churcher, C. *et al.* The nucleotide sequence of *Saccharomyces cerevisiae* chromosome IX. *Nature* **387**, 84–87 (1997).
3. The yeast genome directory. *Nature* **387** (Suppl.), 5 (1997).
4. The *C. elegans* Sequencing Consortium Genome sequence of the nematode *C. elegans*: a platform for investigating biology. *Science* **282**, 2012–2018 (1998).
5. Adams, M. D. *et al.* The genome sequence of *Drosophila melanogaster*. *Science* **287**, 2185–2195 (2000).
6. Lander, E. S. *et al.* Initial sequencing and analysis of the human genome. *Nature* **409**, 860–921 (2001).

7. Venter, J. C. *et al.* The sequence of the human genome. *Science* **291**, 1304–1351 (2001).
8. Collins, J. & Hohn, B. Cosmids: a type of plasmid gene-cloning vector that is packageable in vitro in bacteriophage lambda heads. *Proc. Natl Acad. Sci. USA* **75**, 4242–4246 (1978).
9. Shizuya, H. *et al.* Cloning and stable maintenance of 300-kilobase-pair fragments of human DNA in *Escherichia coli* using an F-factor-based vector. *Proc. Natl Acad. Sci. USA* **89**, 8794–8797 (1992).
10. Coulson, A., Sulston, J., Brenner, S. & Karn, J. Towards a physical map of the genome of the nematode *Caenorhabditis elegans*. *Proc. Natl Acad. Sci. USA* **83**, 7821–7825 (1986).
11. Olson, M. V. *et al.* Random-clone strategy for genomic restriction mapping in yeast. *Proc. Natl Acad. Sci. USA* **83**, 7826–7830 (1986).
12. Bentley, D. R. *et al.* The physical maps for sequencing human chromosomes 1, 6, 9, 10, 13, 20 and X. *Nature* **409**, 942–943 (2001).
13. McPherson, J. D. *et al.* A physical map of the human genome. *Nature* **409**, 934–941 (2001).
14. Green, E. D. Strategies for the systematic sequencing of complex genomes. *Nature Rev. Genet.* **2**, 573–583 (2001).
15. Dunham, I. *et al.* The DNA sequence of human chromosome 22. *Nature* **402**, 489–495 (1999).
16. Waterston, R. & Sulston, J. E. The Human Genome Project: reaching the finish line. *Science* **282**, 53–54 (1998).
17. Nadeau, J. H. & Taylor, B. A. Lengths of chromosomal segments conserved since divergence of man and mouse. *Proc. Natl Acad. Sci. USA* **81**, 814–818 (1984).
18. DeBry, R. W. & Seldin, M. F. Human/mouse homology relationships. *Genomics* **33**, 337–351 (1996).
19. Nadeau, J. H. & Sankoff, D. Counting on comparative maps. *Trends Genet.* **14**, 495–501 (1998).
20. Thomas, J. W. *et al.* Comparative genome mapping in the sequence-based era: early experience with human chromosome 7. *Genome Res.* **10**, 624–633 (2000).
21. Kim, J. *et al.* Homology-driven assembly of a sequence-ready mouse BAC contig map spanning regions related to the 46-Mb gene-rich euchromatic segments of human chromosome 19. *Genomics* **74**, 129–141 (2001).
22. Osogawa, K. *et al.* Bacterial artificial chromosome libraries for mouse sequencing and functional analysis. *Genome Res.* **10**, 116–128 (2000).
23. Hardison, R. C., Oeltjen, J. & Miller, W. Long human–mouse sequence alignments reveal novel regulatory elements: a reason to sequence the mouse genome. *Genome Res.* **7**, 959–966 (1997).
24. Koop, B. F. *et al.* The human T-cell receptor TCRAC/TCRCD (Ca/C δ) region: organization, sequence, and evolution of 97.6 kb of DNA. *Genomics* **19**, 478–493 (1994).
25. Ashworth, L. K. *et al.* An integrated metric physical map of human chromosome 19. *Nature Genet.* **11**, 422–427 (1995).
26. Kent, W. J. The BLAST-like alignment tool. *Genome Res.* **12**, 656–664 (2002).
27. Copeland, N. G. *et al.* A genetic linkage map of the mouse: current applications and future prospects. *Science* **262**, 57–66 (1993).
28. Dietrich, W. F. *et al.* A comprehensive genetic map of the mouse genome. *Nature* **380**, 149–152 (1996).
29. Cai, W. W. *et al.* An SSLP marker-anchored BAC framework map of the mouse genome. *Nature Genet.* **29**, 133–134 (2001).
30. Hudson, T. J. *et al.* A radiation hybrid map of mouse genes. *Nature Genet.* **29**, 201–205 (2001).
31. Schuler, G. D. Sequence mapping by electronic PCR. *Genome Res.* **7**, 541–550 (1997).
32. Altschul, S. F., Gish, W., Miller, W., Myers, E. W. & Lipman, D. J. Basic local alignment search tool. *J. Mol. Biol.* **215**, 403–410 (1990).
33. Ross, M. T., LaBrie, S., McPherson, J. P. & Stanton, V. P. In *Current Protocols in Human Genetics* (eds Dracopoli, N. C. *et al.*) 5.6.1–5.6.5 (Wiley, New York, 1999).
34. Pattagunta, R. *et al.* Comparative maps of human 19p13.3 and mouse chromosome 10 allow identification of sequences at evolutionary breakpoints. *Genome Res.* **10**, 1369–1380 (2000).
35. Carver, E. A. & Stubbs, L. Zooming in on the human–mouse comparative map: genome conservation re-examined on a high-resolution scale. *Genome Res.* **7**, 1123–1137 (1997).
36. Watkins-Chow, D. E. *et al.* Genetic mapping of 21 genes on mouse chromosome 11 reveals disruptions in linkage conservation with human chromosome 5. *Genomics* **40**, 114–122 (1997).
37. Stubbs, L. *et al.* Detailed comparative map of human chromosome 19q and related regions of the mouse genome. *Genomics* **35**, 499–508 (1996).
38. Dehal, P. *et al.* Human chromosome 19 and related regions in mouse: conservative and lineage-specific evolution. *Science* **293**, 104–111 (2001).
39. Fletcher, M. T., Wiltshire, T., Cabin, D. E., Villanueva, M. & Reeves, R. H. Use of comparative physical and sequence mapping to annotate mouse chromosome 16 and human chromosome 21. *Genomics* **74**, 45–54 (2001).
40. Oeltjen, J. C. *et al.* Large-scale comparative sequence analysis of the human and murine Bruton's tyrosine kinase loci reveals conserved regulatory domains. *Genome Res.* **7**, 315–329 (1997).
41. Batzoglu, S., Pachter, L., Mesirov, J. P., Berger, B. & Lander, E. S. Human and mouse gene structure: comparative analysis and application to exon prediction. *Genome Res.* **10**, 950–958 (2000).
42. Marra, M. A. *et al.* High throughput fingerprint analysis of large-insert clones. *Genome Res.* **7**, 1072–1084 (1997).
43. Soderlund, C., Humphray, S., Dunham, A. & French, L. Contigs built with fingerprints, markers, and FPC V4. *Genome Res.* **10**, 1772–1787 (2000).
44. Zhao, S. *et al.* Mouse BAC ends quality assessment and sequence analyses. *Genome Res.* **11**, 1736–1745 (2001).
45. Altschul, S. F. & Gish, W. Local alignment statistics. *Methods Enzymol.* **266**, 460–480 (1996).
46. Nusbaum, C. *et al.* A YAC-based physical map of the mouse genome. *Nature Genet.* **22**, 388–393 (1999).
47. Evans, E. P. In *Genetic Variants of the Laboratory Mouse* (eds Lyon, M. F., Rastan, S. & Brown, S. D. M.) 1446 (Oxford Univ. Press, New York, 1996).
48. Fletcher, M. T. *et al.* Chromosome evolution: the junction of mammalian chromosomes in the formation of mouse chromosome 10. *Genome Res.* **10**, 1463–1467 (2000).
49. Martindale, D. W. *et al.* Comparative genomic sequence analysis of the Williams syndrome region (LIMK1-RFC2) of human chromosome 7q11.23. *Manag. Genome* **11**, 890–898 (2000).
50. DeSilva, U. *et al.* Generation and comparative analysis of approximately 3.3 Mb of mouse genomic sequence orthologous to the region of human chromosome 7q11.23 implicated in Williams syndrome. *Genome Res.* **12**, 3–15 (2002).

Supplementary Information accompanies the paper on *Nature's* website (<http://www.nature.com/nature>). Updated views of the map are available from the authors' websites (http://www.ensembl.org/Mus_musculus/cytoview and <http://www.ncbi.nlm.nih.gov/genome/guide/mouse>), as is an archive version for this publication, plus comparisons and discussion of genetic, RH and clone maps, and an interactive version of the synteny displays of Fig. 5 (http://www.sanger.ac.uk/Projects/M_musculus/publications/fpcmap-2002).

Acknowledgements

The authors acknowledge the support of the Wellcome Trust, the National Institutes of Health and the US Department of Energy. We are grateful to the web team at the Sanger

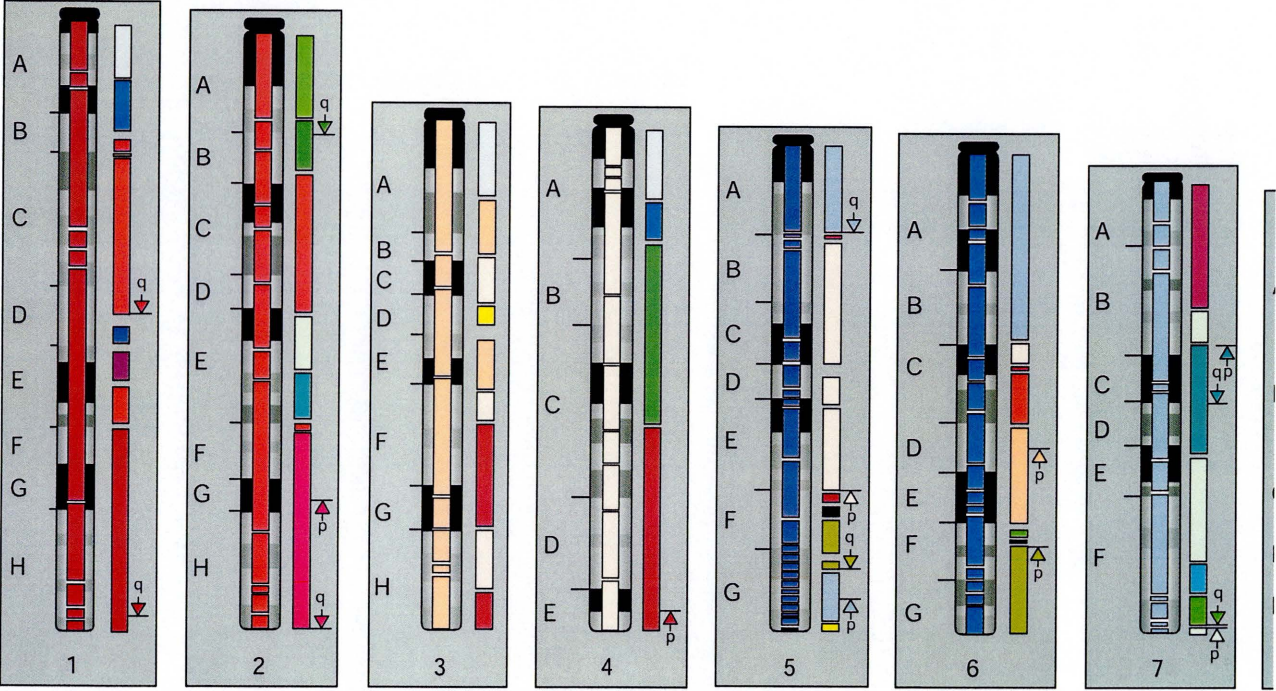
Institute for assistance with developing map displays, to P. Deloukas for RH map analysis, and E. Arnold-Berkowits, S. Lo, J. Gill and all present and past members of the Institute for Genomic Research BAC end sequencing team for the sequencing work.

Competing interests statement

The authors declare that they have no competing financial interests.

Correspondence and requests for materials should be addressed to D.R.B. (e-mail: drb@sanger.ac.uk).

a Mouse-human homology map



b Human-mouse homology map

